University of Kentucky

UKnowledge

Theses and Dissertations--Biology | Biology

2014

Targeted Knockout of Beclin-1 Reveals an Essential Function in Ovary and Testis

Thomas R. Gawriluk
University of Kentucky, tgawriluk@uky.edu

Right click to open a feedback form in a new tab to let us know how this document benefits you.

Recommended Citation

Gawriluk, Thomas R., "Targeted Knockout of Beclin-1 Reveals an Essential Function in Ovary and Testis" (2014). *Theses and Dissertations--Biology*. 19.
https://uknowledge.uky.edu/biology_etds/19

This Doctoral Dissertation is brought to you for free and open access by the Biology at UKnowledge. It has been accepted for inclusion in Theses and Dissertations--Biology by an authorized administrator of UKnowledge. For more information, please contact UKnowledge@lsv.uky.edu.

STUDENT AGREEMENT:

I represent that my thesis or dissertation and abstract are my original work. Proper attribution has been given to all outside sources. I understand that I am solely responsible for obtaining any needed copyright permissions. I have obtained needed written permission statement(s) from the owner(s) of each third-party copyrighted matter to be included in my work, allowing electronic distribution (if such use is not permitted by the fair use doctrine) which will be submitted to UKnowledge as Additional File.

I hereby grant to The University of Kentucky and its agents the irrevocable, non-exclusive, and royalty-free license to archive and make accessible my work in whole or in part in all forms of media, now or hereafter known. I agree that the document mentioned above may be made available immediately for worldwide access unless an embargo applies.

I retain all other ownership rights to the copyright of my work. I also retain the right to use in future works (such as articles or books) all or part of my work. I understand that I am free to register the copyright to my work.

REVIEW, APPROVAL AND ACCEPTANCE

The document mentioned above has been reviewed and accepted by the student's advisor, on behalf of the advisory committee, and by the Director of Graduate Studies (DGS), on behalf of the program; we verify that this is the final, approved version of the student's thesis including all changes required by the advisory committee. The undersigned agree to abide by the statements above.

Thomas R. Gawriluk, Student

Dr. Edmund B. Rucker III, Major Professor

Dr. David F. Westneat, Director of Graduate Studies

TARGETED KNOCKOUT OF BECLIN-1 REVEALS AN ESSENTIAL FUNCTION IN OVARY AND TESTIS

DISSERTATION

A dissertation submitted in partial fulfillment of the requirements for the degree of Doctor of Philosophy in the College of Arts and Sciences at the University of Kentucky

By

Thomas Raymond Gawriluk

Lexington, Kentucky

Co-Director: Dr. Edmund B. Rucker III, Associate Professor of Biology
Co-Director: Dr. Vincent M. Cassone, Professor of Biology

Lexington, Kentucky

Copyright © Thomas Raymond Gawriluk 2014

ABSTRACT OF DISSERTATION

TARGETED KNOCKOUT OF BECLIN-1 REVEALS AN ESSENTIAL FUNCTION IN OVARY AND TESTIS

An estimated 12% of couples worldwide are infertile. The contributing factor is approximately equal between men and women with nearly 25% diagnosed as idiopathic. Despite the increasing numbers of couples seeking assistance from infertility clinics, few molecular mechanisms have been identified for treatment. Autophagy is an evolutionarily conserved cellular process for bulk degradation and recycling of cytosolic components through the lysosome to maintain homeostasis. Several studies have observed increased levels of autophagy during ovarian folliculogenesis and gonadal steroidogenesis; however, no genetic studies to determine the significance of autophagy exist.

To investigate the function of autophagy in the ovary and testis, a directed genetic knockout approach was used to independently knockout two key autophagy genes, *Becn1* and *Atg7*. Chapter 2 reports that deficiency of *Becn1* results in 56% fewer primordial follicles at postnatal day 1. In addition, *Atg7* knockout mice do not have identifiable primordial follicles, suggesting that autophagy is necessary for survival of female germ cells during embryogenesis. Chapter 3 presents that *Becn1* is necessary to sustain pregnancy and the deficiency of *Becn1* in granulosa cells is a novel genetic model to study preterm labor due to impaired corpora lutea function. The results indicate that *Becn1* is necessary for lipid droplet formation and subsequent progesterone production in luteal cells. In contrast, *Atg7* is not necessary and deficiency results in overproduction of progesterone throughout pregnancy, suggesting that the defect in *Becn1* conditional knockout mice is additional to autophagy. Chapter 4 presents that Sertoli cell expression of *Becn1* is required for spermatogenesis after 8 weeks of age. Beyond 9-weeks-old, *Becn1* conditional knockout mice are unable to sire a litter due to a failure of spermatogenesis and a Sertoli-cell-only phenotype in a majority of the seminiferous tubules. *Atg7* was also identified as a necessary factor for spermatogenesis beyond 26-weeks-old. Together the data presented in Chapter 4 suggests that autophagy is necessary for adult Sertoli cell function. Primarily, this dissertation presents data from the first functional studies on autophagy in the reproductive tract. The results demonstrate an understanding of the functional significance for *Becn1* and *Atg7* in both the ovary and testis.

KEYWORDS: Autophagy, Reproductive Biology, Oocyte Attrition, Corpus Luteum, Sertoli Cell

Thomas Raymond Gawriluk
Student's Signature

April 30, 2014
Date

TARGETED KNOCKOUT OF BECLIN-1 REVEALS AN ESSENTIAL FUNCTION IN OVARY AND TESTIS

By

Thomas Raymond Gawriluk

Edmund B. Rucker III
Co-Director of Dissertation

Vincent M. Cassone
Co-Director of Dissertation

David F. Westneat
Director of Graduate Studies

April 30, 2014
Date

To Mom and Dad

“Somewhere, something incredible is waiting to be known” – Carl Sagan

"...there is in truth, no past, only a memory of the past. Blink your eyes, and the world you see next did not exist when you closed them. Therefore, the only appropriate state of the mind is surprise. The only appropriate state of the heart is joy. The sky you see now, you have never seen before. The perfect moment is now. Be glad of it." – Terry Pratchett, *Thief of Time*

ACKNOWLEDGEMENTS

Sitting down to think about all of the people who given their time to help me develop the ideas in this dissertation has humbled me, and truly, I must be lucky. Everyone who has helped me along the way whether it be discussing my data, letting me borrow reagents, helping me keep on track with the rest of my life or discovering new bourbons, you are my friends, family and colleagues. No words that I know can express my gratitude to all of you. I only hope that I can emulate your patience and kindness, to help my friends and future students realize their own potential.

I would first like to acknowledge my parents, grandparents, aunt Susie and sister Tegan who have nurtured my love for science since before I can remember. I attribute my curiosity, intelligence, imagination and the mindset that hard work pays off from you. You have fostered me with trips to museums and aquariums and have allowed me to work through my own confusing data over the phone. All of the heartache that I caused was worth it.

To Matt Stewart, who let me into his lab when no one else would and taught me the ropes of molecular biology, I say, cheers! To Ed Rucker, who has given me space in his lab, which I have called home for the last seven years, you have always supported my good ideas by steering me away from the bad ones, thank you for everything you have taught me. To my fellow “Ruckerites”, Amber and Dan, you have been my family, good luck in your own endeavors and thank you. To my committee members, Vinnie, Tom, Jay, Randal and Ashley, you have provided me expertise to which I aspire. I will always remember your well-timed patience with me. You have all taught me to be a better person and fueled my scientific fire, thank you.

To all of my friends in I have made during this journey: Jiffin and Alka P, Jason C., Seth T., Dustin and Tina P., Bruce O., Mike A., Elyse H., Clifford H., Tsten and Phuntsok Y., Stephen and Hillary H., Chuck G., Kory and Lauren D., Jeff O., Pete M., Andy B., Deep B., Swagata G., Nathan K., Brandon F., Jim S., Stacey G., Ye L., Deanna M., Dave K., Nayeem M., Johnny C., Brad H., Tyler and Karen F., Megan S., Travis and Sam S., Curt S., Evan and Sheila H., Ginger M., Matt M., and Scarlet P. Without you, I would not be sane right now, thank you.

To Maggie Murphy, I thank you for your continued support and understanding my passion for science.

To Leeloo, my pup, who kept me company many late nights and will always enjoy chasing the rabbits around the Thomas Hunt Morgan building, you are the best.

To all those mentioned, and the many more I did not, live long and prosper.

TABLE OF CONTENTS

LIST OF TABLES

LIST OF FIGURES

CHAPTER 1: SELF-EATING, FROM EGGS TO NUTS: A BASIS TO STUDY AUTOPHAGY IN THE MAMMALIAN REPRODUCTIVE SYSTEM

Keywords: autophagy, fertility, maternal-to-zygote transition, mitochondrial inheritance, gonadogenesis, folliculogenesis, atresia, steroidogenesis, Leydig cell, Sertoli cell, corpus luteum

Abbreviations used:
Atg, autophagy-related; ACD, autophagic cell death; ER, endoplasmic reticulum; mTOR, mammalian target of rapamycin; LH, luteinizing hormone; FSH, follicle stimulating hormone; CL, corpus luteum; PtdIns3p, phosphatidylinositol 3-phosphate; 3-MA, 3-methyl-adenine; mtDNA, mitochondrial DNA; TUNEL, terminal deoxynucleotidyl transferase dUTP nick end labeling; PGC, primordial germ cell; GnRH, gonadotropin releasing hormone; E, embryonic day; P, post-natal day; EsR, estrogen receptor; PgR, progesterone receptor; AVPV, antero ventral periventricular nucleus; AMP, adenosine monophosphate; cAMP, cyclic adenosine monophosphate

1.1 Introduction

The ability to reproduce and survive are the two most important factors with respect to evolutionary fitness. Thus, it makes sense that there is evolutionary conservation for many of the mechanisms controlling the functions of reproductive biology. Encompassing sex-specific endocrinology *and* development, gamete development *and* fertilization, reproductive behavior, mammary-gland development *and* function in mammals and placenta-mediated development for eutherian mammals, reproductive biology is essential for the persistence of a species.

Human interest in reproduction has existed for at least 24,000 years as evidenced in sculptures; for example “The Venus of Willendorf”, honoring fertility gods (Colman 1998). Teachings from the Greek physician Herophilus on human reproductive biology demonstrate one of mankind’s’ earliest scientific interest with reproduction beginning around 300 BC (Pierson and Stephanson 2010). In the last 200 years, through comparative, molecular and genetic approaches, reproductive biologists have realized the conserved development of reproductive systems, by the sequence identity and function of necessary transcription factors, proteins and endocrine/paracrine interactions. However, there remain a considerable number of questions regarding the reproductive system. By exploring the significance of a universal process such as autophagy in reproductive tissues, I believe that otherwise overlooked protein pathways can be uncovered. The role of autophagy in reproductive biology is a relatively new concept with a limited number of publications, yet nevertheless, deserves consideration.

Christen de Duve, winner of the 1974 Nobel Prize in Physiology for the discovery of lysosomes and peroxisomes, coined the term “autophagy” in 1963 at the *Ciba Foundation Symposium on Lysosomes* (Klionsky 2008). Literally meaning, “to eat oneself” (Greek roots: *auto* “self”, *phagein* “to eat”), de Duve was describing a cellular process where organelles are delivered to lysosomes via double-membrane vesicles that he and his colleagues observed from analyzing electron microscopic images. Autophagy was first reported by Keith Porter and Thomas Ashford who observed an increase in lysosome biogenesis and mitochondria destruction in hepatocytes after treatment with glucagon (Ashford and Porter 1962). However, Porter and Ashford misinterpreted their results, describing the formation lysosomes containing mitochondria, rather than delivering mitochondria to lysosomes by the autophagy-dependent vesicle, the autophagosome. Christen de Duve’s lab published the first autophagy papers in 1967 to describe the potent induction of autophagy in rat hepatocytes following glucagon injection and the subsequent trafficking and fusion of the autophagosome with lysosomes (Deter et al. 1967; Deter and De Duve 1967). Autophagy research has grown popular, with just over 10,000 “autophagy” papers resulting from a PubMed query over the past five years due to autophagy’s indispensable involvement in eukaryotic development and disease, particularly in tumor development (see Hale et al. 2013; Choi et al. 2013; Jiang and Mizushima 2013 for reviews). The intimacy between autophagy and lysosomes remains today where, as of 2014, the autophagy community recognizes three primary flavors of autophagy: macroautophagy, microautophagy and chaperone-mediated autophagy, which all conclude with degrading cytosolic components in a lysosome (see Parzych and Klionsky 2013 for review). De Duve and colleagues originally observed macroautophagy, and not-coincidentally, macroautophagy is the most studied, and will be solely discussed and referred to as autophagy for the remainder of this review. This review will primarily focus on data collected from mammals, specifically the mouse where possible, but occasionally will draw on data from other animals to formulate broad conclusions.

It is the goal of this review is to give an overview of the research to date that links autophagy to reproductive biology and to discuss the implications and possible directions of future research.

1.2 An Overview of the Functions and Process of Autophagy

1.2.1 Primer on the Functions of Autophagy

Autophagy is an evolutionarily conserved eukaryotic process that occurs at low constitutive levels in all cell types to sequester cytosolic material in a double membrane structure, termed the autophagosome, and to deliver the material to a lysosome for its breakdown and recycling into basic components (**Figure 1.1**). Using genetic screens in yeast, over 34 autophagy-related (*Atg*) genes have been identified with most having clear homologs in higher eukaryotes through protein-sequence identity (Nakatogawa et al. 2009; Tsukada and Ohsumi 1993; Thumm et al. 1994). Autophagy can be either ‘selective’ or ‘non-selective’, and is the only other process that degrades cytosolic components besides the ubiquitin-proteasome system. The specific delivery of cytosolic components and subsequent inclusion into an autophagosome through cytosolic receptors is selective autophagy. In contrast, non-selective autophagy is the arbitrary inclusion of cytosolic components found in close proximity to where the autophagosome forms.

Autophagy is a highly orchestrated requisite for eukaryotes to adapt to nutrient conditions and regulate cellular energy homeostasis; thus, autophagy is widely considered a pro-survival process. As the obvious cellular response to nutrient starvation, this was the major function of autophagy studied throughout the 1990s. However, over the last twenty years many labs have identified other survival-specific functions for autophagy, including (with recent reviews): mitochondria maintenance (Youle and Narendra 2011), lipid droplet metabolism (Liu and Czaja 2013; Christian et al. 2013), pathogen elimination (Levine et al. 2011), maintenance of unfolded proteins (Cebollero et al. 2012), endosome turnover (Lamb et al. 2013), protein secretion (Brooks et al. 2012) and trafficking proteins to the plasma membrane (Deretic et al. 2012).

Alongside the pro-survival functions, there are limited *in vivo* studies where autophagy has been established as a cause of cell death (Zhu et al. 2007; Denton et al. 2009; Berry and Baehrecke 2007; Koike et al. 2008; Nezis et al. 2010; Piras et al. 2011; Schwarze and Seglen 1985). In these studies there is an observed accumulation of autophagosomes prior to or concurrent with cell death, a morphology originally termed autophagic cell death (ACD) (Maiuri et al. 2007). However, how autophagy causes cell death is controversial. There are independent data concluding that autophagy can induce and mediate apoptosis, as well as be the sole cause of cell death (Kroemer and Levine 2008). The definition of ACD has been recently challenged to include a functional component beyond simple morphology, declaring that ACD should be ameliorated through chemical or genetic inhibition of autophagy and be independent from apoptosis or necrosis (Galluzzi et al. 2012; Klionsky et al. 2012). This more stringent definition makes ACD a very rare event (Shen and Codogno 2011) and argues against its occurrence in cancer cell lines screened for mutations in *Atg* genes (Shen et al. 2012). In this fashion, it is my stance to require both the results from functional experiments and distinction from apoptosis or necrosis to affirm ACD.

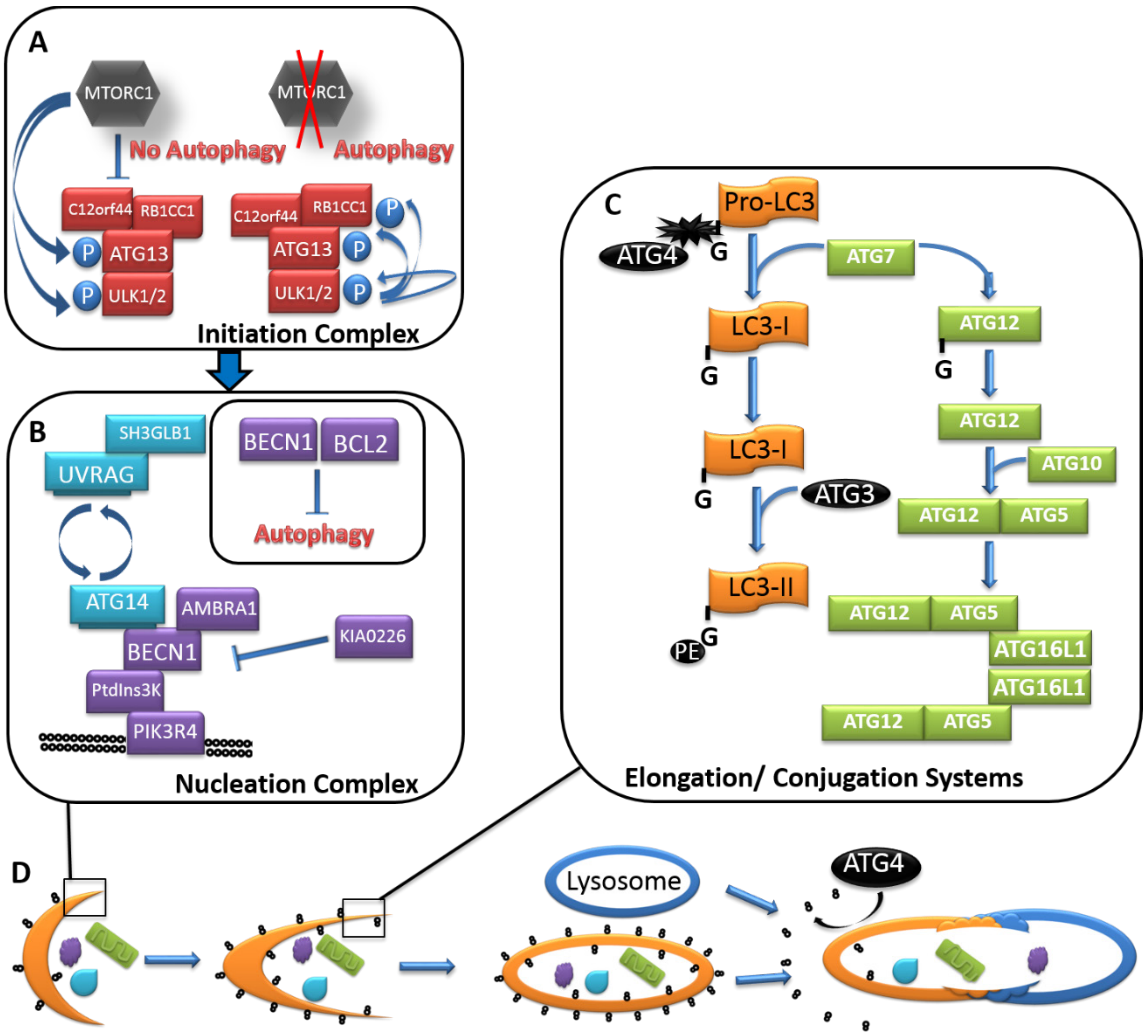

Figure 1.1 Molecular mechanism of autophagy in mammals.
(**A**) When mTOR is inhibited, the ULK complex dissociates from mTOR and ULK1 phosphorylates itself, ATG13 and RB1CC1, to induce the nucleation phase. (**B**) The nucleation complex is assembled at the site of isolation membrane and activated by the ULK complex. UVRAG and ATG14L bind to BECN1 in a mutually exclusive manner and the complex with ATG14L is necessary for nucleation. BECN1 is inhibited when bound by anti-apoptotic BCL2, which inhibits nucleation. (**C**) The two ubiquitin-like conjugation systems essential for membrane elongation that conjugate ATG8-like proteins to PE on the expanding membrane. (**D**) The progression of an autophagosome membrane (orange crescent) is dependent on ATG8-like proteins (stylized in black). Once completed the autophagosome is trafficked to and fuses with a lysosome. ATG8-like proteins bound to the outer membrane are cleaved by ATG4 while ATG8-like proteins on the inner-membrane are degraded by lysosomal enzymes along with the cargo of the autophagosome. Figure adapted from (Hale et al. 2013).

1.2.2 Primer on the Process of Autophagy

Several excellent reviews discuss the molecular machinery (Feng et al. 2014), transcriptional (He and Klionsky 2009), posttranscriptional (McEwan and Dikic 2011) and extracellular regulation (Lock and Debnath 2008; Boya et al. 2013) of autophagy elsewhere, and are beyond the scope of this review.

Briefly, autophagy is comprised of five sequential stages: 1) induction, 2) membrane nucleation, 3) membrane elongation, 4) trafficking and fusion of the autophagosome with a lysosome, and 5) degradation followed by transport of molecules back into the cytosol (**Figure 1.1**). This is distinct from other vesicle-producing processes (e.g. secretory pathway) because autophagosome membranes are produced *de novo* and not budding from pre-existing membranes (Noda et al. 2002; Kovács et al. 2007).

Numerous studies have begun to understand the hierarchical nature of proteins needed for autophagosome formation. In mammals, autophagy is induced as an outcome of several signaling pathways, of which mechanistic target of rapamycin (MTOR) and adenosine monophosphate (AMP) activated protein kinase (AMPK) are the best studied. MTOR and AMPK regulate the unc-51-like kinase family (either ULK1 or ULK2) complexes by direct phosphorylation (Kim et al. 2011; Lee et al. 2010; Mizushima et al. 2010). Activated ULK1/2 complex recruits the class III phosphatidylinositol 3-kinase (PtdIns3K) 'nucleation' complex, containing PtdIns3k, catalytic subunit type 3 (PIK3C3, also known as VPS34), PtdIns3k, regulatory subunit 4 (PIK3R4, also known as VPS15), Beclin-1 (BECN1), ultraviolet radiation associated (UVRAG) and ATG14L to an induction site (Itakura and Mizushima 2010), which occurs at endoplasmic reticulum (ER)-associated structures called omegasomes (Hayashi-Nishino et al. 2009). The production of the signaling lipid, phosphatidylinositol 3-phosphate (PtdIns3P), by the nucleation complex is required for the nucleation of the membrane, called the phagophore, and the progression of autophagy (Burman and Ktistakis 2010; Noda et al. 2010). PtdIns3P is a signaling molecule that recruits two ubiquitin-like conjugation systems (e.g. ATG5-ATG12 and ATG7) that work together to covalently conjugate ATG8-like proteins (e.g. microtubule associated 1A/1B-light chain 3 (LC3) and GABA receptor-associated protein (GABARAP) families) to phosphatidylethanolamine (PE) in the expanding phagophore (Geng and Klionsky 2008). While the exact function of the ATG8-like conjugates is unclear, they are indispensable for prolonged phagophore elongation (Xie et al. 2008) and trafficking of the finished autophagosome (Weidberg et al. 2010). The lipid sources for membrane expansion seem to be non-specific as the ER (Hayashi-Nishino et al. 2009), Golgi complex (Yen et al. 2010; Takahashi et al. 2011), mitochondria membrane (Hailey et al. 2010) and plasma membrane (Ravikumar et al. 2010) have all been observed to contribute.

Once completed, the autophagosome goes through a maturation process where the induction and elongation complexes are removed and interactions with both microtubules and actin filaments facilitate the delivery of the autophagosome to the lysosome (Monastyrska et al. 2009). Autophagosome-to-lysosome fusion proceeds in an ATG9-dependent manner that is regulated by soluble N-ethylmaleimide-sensitive fusion attachment protein receptors (SNAREs) (Nair et al. 2011). It is suggested that autophagosomes obtain SNAREs by first fusing with late endosomes before fusing with a lysosome; however, the mechanism of how autophagosomes fuse to endosomes remains to be elucidated (reviewed in Moreau et al. 2013). Once fusion has taken place, lysosome hydrolases and proteases catabolize the autophagosome contents into basic building blocks (e.g. amino acids, fatty acids and carbohydrates) and these are transported back into the cytoplasm for anabolic reactions.

1.3 Autophagy in pre-implantation embryo development

Fertilization of an egg by sperm marks the beginning of a myriad of developmental changes in the embryo. These changes include both cytoplasmic and genomic reprogramming that are necessary for development beyond the blastocyst. Upon fertilization, sequential waves of Ca^{2+} released into the cytoplasm signal the re-initiation of meiosis in the maternal pronucleus, protamine-histone exchange in the paternal pronucleus, followed by fusion of the maternal and paternal pronuclei and progression into mitosis (reviewed in Whitaker 2008). Fertilization also initiates the translation of several proteins essential for the progression into meiosis and mitosis along with the ubiquitination and destruction of several maternally inherited proteins (e.g. Cyclin B1) (Vasudevan et al. 2006; Huo et al. 2004). In order to drive this progression without the need for transcription from the condensed chromosomes, several translationally-delayed maternally-derived transcripts become activated (Conti 2011; Chen et al. 2011; Medvedev et al. 2011). The ubiquitin-proteasome system degrades many oocyte-derived proteins, which serves to cull the 3,699 different proteins found in metaphase II oocytes down to approximately 2,000 different proteins after fertilization (Pfeiffer et al. 2011; Wang et al. 2010). Protein degradation is essential for meiosis resumption, spindle assembly, polar body emission and pronucleus formation (Huo et al. 2004, 2005, 2006). Also during this time, both the maternal and paternal genomes undergo epigenetic reprogramming, which effectively removes nearly all methylation marks inherited from the parents and resets epigenetic marks, such as imprinting (Li 2002; Cantone and Fisher 2013). At the 2-cell stage in mice, embryos undergo a maternal-to-zygote transition where nearly all maternally inherited proteins and mRNA are destroyed, and transcription and translation begins from the zygotic genome (Pikó and Clegg 1982; Merz et al. 1981; De Leon et al. 1983). A combination of RNA-binding proteins and endo-siRNAs attach to the 3’ UTRs of maternally inherited RNAs resulting in their destabilization and degradation (Alizadeh et al. 2005; Suh et al. 2010). Maternal proteins are poly-ubiquitinated during the maternal-to-zygote transition followed by their elimination by the 4-cell stage. This process is stunted by treatment with MG-132, a potent and reversible proteasome inhibitor, and regulated by a proteasome assembly chaperone ZPAC, suggesting that the proteasome is involved (Shin et al. 2010, 2013). However, it seems unlikely that the proteasome system would be sufficient for the rapid turnover observed. An additional hypothesis is that early embryo induces autophagy to assist with the protein turnover.

Tsukamoto et al. found that within 4 hours after egg activation, by fertilization or parthenogenesis, the mouse zygote shows a massive induction of autophagy as shown by an increase in GFP-LC3 puncta (Tsukamoto et al. 2008b, 2008a). GFP-LC3 is a fusion protein used to monitor autophagosome flux due to the incorporation of GFP-LC3 into autophagosome membranes (Mizushima 2009). This induction is postulated to occur since mTOR, an upstream inhibitor of autophagy, is inhibited after Ca^{2+} wave initiation (Tsukamoto et al. 2008a). Autophagy is transiently suppressed from the late one-cell to late two-cell stage in mice that coincides with the maternal-to-zygote transition which is hypothesized to occur to protect the released nuclear factors during metaphase (Tsukamoto et al. 2008a). Additionally, zygotes generated from egg and sperm both devoid of ATG5, an essential protein of the autophagosome membrane conjugation system, do not develop beyond the 8-cell stage; furthermore, they have reduced protein synthesis after the 2-cell stage (Tsukamoto et al. 2008b). This suggests that ATG5 positively regulates protein synthesis necessary for embryogenesis. Data presented by Xu et al. using porcine parthanotes treated with autophagy modulators has demonstrated that degradation of the maternal transcripts *Gdf9*, *Bmp15*, *c-mos* and *cyclin B* are autophagy-dependent as pharmacological autophagy inhibition resulted in transcript accumulation and reduced development to blastocyst (Xu et al. 2012). These results suggest that autophagy is required for the maternal-to-zygote transition; however, we must take into consideration that the pharmacological modulators, 3-methyladenine (3-MA) and rapamycin exhibit off-target effects, beyond inhibiting autophagy (Yang et al. 2013). Data from *C. elegans* corroborates the observation that autophagic flux is increased after fertilization and additionally, several maternal proteins have been identified whose degradation is dependent on autophagy (reviewed in Sato and Sato 2013). These experiments establish that the activation of autophagy after fertilization is not specific to mammals, suggesting a deep evolutionarily conserved function for this pathway during embryogenesis. Furthermore, several *in vivo* and *in vitro* experiments have demonstrated the autophagy-dependent degradation of poly-ubiquitinated proteins in several somatic cell types through selective receptors such as SQSTM1 (reviewed by Shaid et al. 2013). A future direction will be to test whether poly-ubiquitinated proteins are delivered to autophagosomes after fertilization and during the maternal-to-zygote transition. There are two possibilities for the function of autophagy in the early embryo. One, autophagy degrades proteins and RNA that otherwise would halt development. Two, autophagy provides the basic components that the early embryo needs (e.g. nucleosides and amino acids). The latter is a possibility as zygotes cannot transport or synthesize amino acids or nucleosides at an appreciable rate until after the maternal-to-zygote transition (Rudraraju and Baltz 2009; Li et al. 2006b). While the exact function of autophagy after fertilization remains unclear, it will be necessary to use genetic and pharmacological approaches to distinguish between the contributions of autophagy and the ubiquitin-proteasome system.

1.4 Autophagy in paternal mitochondrial elimination

It is widely accepted that offspring inherit their mitochondrial genomes (mtDNA) from one parent, which in most animals studied is from the mother (Hutchison et al. 1974; Birky 1995). The timing of when the paternal mtDNA elimination occurs is controversial, as data exists for both pre- and post-fertilization, depending on the species studied. As a result, hypotheses for both active and passive mechanisms of paternal mtDNA elimination exist. One passive hypothesis states that only the head of the sperm enters the egg, leaving the tail containing paternal mitochondria outside of the embryo (Ankel-Simons and Cummins 1996). However, this cannot be true in humans, as the zygotic centrosome is paternally inherited and the sperm midpiece, which contains mitochondria, is evident inside the zygote hours after fertilization (Sathananthan et al. 1986, 1996). Another hypothesis for passive removal is that cell division dilutes the paternal mtDNA beyond the range of detection. An egg is several thousand times larger than a sperm and can contain at least one-thousand fold more mitochondria. Corroborating this viewpoint, mtDNA heterogeneity (i.e. heteroplasmy) is present in human tissues; however, it remains to be determined if these are truly paternally-generated mitochondrial DNAs or tissue-specific polymorphisms (He et al. 2010).

Two hypotheses for active elimination exist. The first contends that the sperm can digest and eliminate mtDNA prior to fertilization (DeLuca and O'Farrell 2012; Nishimura et al. 2006). Alternatively, another hypothesis argues that the embryo eliminates paternal mitochondria and mtDNA through a mechanism such as autophagy (Sutovsky et al. 1999; Al Rawi et al. 2011; Sato and Sato 2011). While passive elimination is still a possibility, the evidence for active elimination is accumulating.

Recently, *Drosophila* was identified as an organism that eliminates paternal mtDNA prior to the completion of spermatogenesis (DeLuca and O'Farrell 2012). Sperm mtDNA is enzymatically digested by endonuclease G and any remaining mtDNAs are targeted for transport into waste bags and removed from the maturing sperm (DeLuca and O'Farrell 2012). Similarly, mtDNA, as detected by PCR, declines in sperm throughout spermatogenesis in human, rat, and mouse (Rantanen et al. 2001; Larsson et al. 1997). Along these lines, May-Panloup et al. quantified 1.4 copies of mtDNA per sperm from purified samples of normal human sperm (May-Panloup et al. 2003). Together these data suggests that mammals do participate in pre-fertilization elimination of paternal mtDNA. Whether enzymatic digestion is involved in mammals is yet to be determined. However, the low amounts of mtDNA present in sperm prior to fertilization suggests that there must be post-fertilization elimination.

Early mouse studies demonstrated the loss of microinjected, labeled mitochondria and sperm-derived mtDNA into zygotes before the 8-cell stage (Cummins et al. 1997). Analogous results have been observed in bovine (Sutovsky et al. 1996) and the medaka fish, *O. latipes* (Nishimura et al. 2006) suggesting that post-fertilization destruction of mitochondria is evolutionarily conserved. Furthermore, hepatocyte-mitochondria microinjected into zygotes, can be detected in newborn mice; however, injected sperm-mitochondria are eliminated, suggesting that sperm mtDNA are labeled with specific degradation factors (Shitara et al. 2000). Observations from primate and bovine studies have indicated that paternal mitochondria are quickly poly-ubiquitinated after fertilization and that their degradation is dependent on lysosomes (Sutovsky et al. 2000). In a follow up study, Thompson et al. identified Prohibitin, an inner mitochondrial protein, as one of the more prominent paternal mitochondria substrates to be poly-ubiquitinated in bull and rhesus sperm (Thompson et al. 2003). To our knowledge, no study exists directly testing if Prohibitin poly-ubiquitination leads to mitochondrial destruction; however, knockdown of *Prohibitin-1* (human protein homologous to *Prohibitin*) in human cells induces autophagy of mitochondria (i.e. mitophagy) (Kathiria et al. 2012). The hypothesis that poly-ubiquitination of Prohibitin inhibits its function similar to the knockdown approach needs to be tested.

Three studies in *Caenorhabditis elegans* have suggested that autophagy is the mechanism for the elimination of paternal mitochondria by the 64-cell stage (Zhou et al. 2011a; Al Rawi et al. 2011; Sato and Sato 2011). Surprisingly, Luo et al. recently reported that despite the induction of autophagy after fertilization, paternal mitochondria are not eliminated from mouse embryos by autophagy (Luo et al. 2013). Sperm mitochondria congregated with the autophagy proteins SQSTM1 and LC3 immediately after fertilization and this co-localization persisted to the morula stage, yet never co-localized with lysosome markers (Luo et al. 2013). As a possible explanation, the authors detected an average of 1.29 copies of mtDNA in motile sperm and only 11% of sperm in the oviduct had detectable mtDNA providing evidence that mouse sperm actively destroy mtDNA prior to fertilization. Furthermore, embryos formed from sperm with multiple copies of mtDNA had detectable paternal mtDNA after birth. The authors concluded that pre-fertilization elimination of paternal mtDNA drives maternal inheritance in the mouse. It will be important to determine if other mammals, like humans, depend on pre-fertilization elimination, especially when mitochondria quality appear to contribute to the success of *in vitro* fertilization (Reynier et al. 2001; Yi et al. 2007). The increase in autophagic flux at fertilization and evidence that mitochondria are solely degraded through autophagy, a process termed ‘mitophagy’ (reviewed by Youle and Narendra 2011), provide a motive for studying the function of autophagy during this time. Live cell imaging of zygotes injected with mitochondrial and autophagosome markers generated by *in vitro* fertilization (IVF) across several species will be necessary experiments to determine the extent that autophagy-dependent paternal mitochondria elimination occurs.

1.5 Autophagy in prenatal gonad/gamete development

Embryonic reproductive tissues are dynamic in structure, physiology and gene expression. Relatively few studies have explored the significance of autophagy during reproductive development, and here I provide a background of reproductive development and speculate on potential functions for autophagy.

1.5.1 Migration of Primordial Germ Cells and Formation of the Bipotential Gonad

The development of gonads is well conserved, as many of the same signaling pathways and structures participate in *Drosophila*, zebrafish and mouse (Richardson and Lehmann 2010). Murine gonad development begins around embryonic day (E) 6.25 with the differentiation of a small group of approximately 6 cells found in the proximal epiblast, or outermost layer of the embryo proper that will differentiate to ectoderm and mesoderm, into primordial germ cell (PGC) precursors (Ohinata et al. 2005). PGC precursors will eventually give rise to the gametes in the adult. Differentiation occurs in response to bone morphogenetic protein (BMP) signaling and the PGC precursors begin expressing the necessary and functionally independent transcriptional repressors PRDM1 (PR domain zinc finger protein 1; also known as, B lymphocyte-induced maturation protein 1; Blimp1) and PRDM14 (Ohinata et al. 2005; Yamaji et al. 2008). Over the next 48 hours, the PGCs precursors proliferate to a population of roughly 100 cells as they begin to migrate through the primitive streak into the extra-embryonic endoderm and allantois (Anderson et al. 2000; Ginsburg et al. 1990). The PGC migration is in response to the chemoattractants expressed and released by somatic cells; mainly, kit ligand (KITL also known as stem cell factor (SCF) or Steel) and C-X-C motif ligand 12 (CXCL12, also known as Sdf1), which bind to the PGC membrane receptors kit receptor (KIT) and chemokine (C-X-C motif) receptor 4 (CXCR4) (Ara et al. 2003; Doitsidou et al. 2002; Molyneaux et al. 2003). These somatic and germ cell paracrine interactions remain essential for the remainder of PGC development into gametes.

Chromatin and epigenetic remodeling globally erases methylation marks and transitions the PCGs precursors into PGCs, manifesting in the expression of the stem cell markers *Oct4*, *Stella* and *Nanos3* (Saitou et al. 2002; Tsuda et al. 2003; Sato et al. 2002; Schöler et al. 1990). At some point during the migration between E7.0 and E9.0, the PCGs become transcriptionally silent and enter a transient G_2 phase cell cycle arrest (Seki et al. 2007). PGCs migrate into the embryo along the hindgut through the dorsal mesentery until they arrive in the dorsal mesoderm where they sort bilaterally and colonize the urogenital ridges at approximately E10.5. A single gonad forms on the surface of each mesonephros, or embryonic kidney, within the urogenital ridge. When PGCs arrive at the urogenital ridge, no mRNA expression or histological difference between male and female has taken place and the PGCs are bi-potential, meaning they can develop into ovaries or testes. PGCs lose motility as they associate with somatic cells expressing the highest amounts of HMG-CoA reductase (HMGCR) and SDF1A in *Drosophila* and zebrafish, respectively, but it is unknown if the same occurs in mammals (Van Doren et al. 1998; Reichman-Fried et al. 2004). Between E9.0 and E11.0, PGCs re-enter the cell cycle and upon arrival at the genital ridge actively proliferate, maintaining intercellular bridges, forming cell clusters, or cysts, of about 25,000 cells between the two gonads by E12.5 (Tam and Snow 1981; Lei and Spradling 2013; Pepling and Spradling 1998). After colonization of the gonads, male PGCs are called gonocytes and female PGCs are called oogonia.

Although it is currently unknown if migrating primordial germs cells actively undergo autophagy, multiple studies have shown that autophagy facilitates migration in tumor cells (Galavotti et al. 2013; Tuloup-Minguez et al. 2013; Macintosh et al. 2012). KIT signaling in migrating PGCs activates AKT which is necessary for PGC survival (De Miguel et al. 2002). Activated AKT both directly and indirectly inhibits autophagy in tumor cells (Wang et al. 2012b; Degtyarev et al. 2008), suggesting that autophagy is inhibited during PCG migration. However, a recent study in chicken shows that expression of a constitutively-active AKT retards PGC migration and prevents gonad colonization (Glover et al. 2013). This suggests that a specific amount of AKT activity exists for regulation PCG migration. The hypothesis that the levels of autophagic flux regulated by AKT is necessary for PGC migration remains untested. Several knockout mice for key autophagy genes are embryonic lethal before and during migration, making it difficult to study the significance of autophagy. Additionally, there is not a reliable conditional knockout paradigm to target PGCs during migration, further complicating the experiment. The use of a ligand inducible Cre-recombinase or pharmacological autophagy inhibitors would be possible but the results would be difficult to interpret from possible non-PGC effects in the mother's uterus or somatic cells in the embryo.

1.5.2 Testes Differentiation

While no histological differences occur until E12.5 in either XX or XY bipotential gonad, several genetic changes occur in the somatic tissue surrounding PGCs as early as E10.5. In mammals, the Y chromosome determines if the bipotential gonads will differentiate into a testis (XY individual) or ovary (XX individual), in an otherwise normal genetic background (Jost et al. 1973). The Y chromosome gene sex-determining gene, Y (*Sry*) is transiently expressed between E10.5 and E12.5 with a peak at E11.5, in the somatic cells, which later develop into Sertoli cells (Hacker et al. 1995; Bullejos and

Koopman 2001). The differentiation of these somatic cells into Sertoli cells drives the formation and function of the testis. SRY activity causes the increased expression of SRY-Related HMG-box, gene 9 (*Sox9*) in the somatic cells (Sekido et al. 2004; Bullejos and Koopman 2005). It is important to note that *Sox9* is present in both XX and XY gonads, but that *Sox9* is upregulated several-fold in the XY gonad. Subsequent expression of extracellular signaling peptides, such as fibroblast growth factor 9 (*Fgf9*), maintain *Sox9* expression and orchestrate the differentiation of these cells into Sertoli cells, organization of the testis cords, and formation of the coelomic vessel by E12.5 (DiNapoli et al. 2006; Kim et al. 2006). The latter two events are obvious morphologies of the early stage testes that persist to form the seminiferous tubules and the blood supply in the adult testes, respectively (Schmahl et al. 2004). While SRY is mammal-specific, the amino acid sequence and function of SOX9 is conserved across all tetrapods studied (Bagheri-Fam et al. 2010). Beginning at E12.5, gonocytes exit the cell cycle and enter a prolonged G_1/G_0 mitotic arrest until shortly after birth enforced by growth factors and paracrine signaling from Sertoli cells (reviewed by Payne 2013). Endocrine molecules produced by the somatic cells of the embryonic testes act as signals for the rest of the body to shift development to male secondary characteristics.

From E13.5 through E17.5 male gonocytes initiate apoptosis mediated by a BCL-X_L / BAX rheostat (Rucker et al. 2000; Coucouvanis et al. 1993). In particular, *Bax*-deficient males exhibit an excess of gonocyte clusters and disordered seminiferous tubules suggesting that cell death is necessary during embryogenesis for both gonocyte cyst breakdown and testicular development (Knudson et al. 1995). While the exact function for apoptosis is unknown, the dominant hypothesis is that there exists a fundamental gamete-to-somatic cell ratio for proper signaling in the adult testis. However, another hypothesis comes from observations during tissue regeneration, which demonstrate the release of paracrine factors from apoptotic cells at injury sites that leads to immunosuppression in the wounded area, which is necessary for matrix remodeling (Boland et al. 2013). Additionally, recent studies using *C. elegans* have indicated that autophagy regulates the clearance of apoptotic corpses and matrix remodeling during organogenesis (Li et al. 2012; Huang et al. 2013b). It is possible that autophagy participates in testis development by regulating cellular remodeling of gonocyte cysts and clearance of dying cells, implicating that misregulation of autophagy could result in male infertility.

1.5.3 Ovary Differentiation

In the absence of the expression of SRY the bipotential gonad develops into an ovary. The discovery of SRY led to several mammalian sex determination models. The correct model in Eutherian mammals states that a SRY-like factor, the “Z” locus, must exist for ovarian development that also suppresses the function of SRY, negatively regulates testes development and SRY must suppress the function of “Z” (McElreavey et al. 1993b). This model developed from familial studies on XX individuals that displayed sex-reversal with and without SRY (McElreavey et al. 1993a). Identification of the mutated genes in these individuals led to the discovery of r-spondin homolog 1 (*Rspo1*) as the first female-specific gene upregulated in XX gonads (Parma et al. 2006). Knockout mouse models for *Rspo1* duplicated the sex-reversal seen in humans and identified RSPO1 as an extracellular co-activator for wingless-type MMTV integration site family, member 4 (WNT4) that induces the activity of β-catenin to drive a positive feedback loop for *Wnt4* expression and subsequent ovary differentiation (Binnerts et al. 2007; Wei et al. 2007; Chassot et al. 2008; Tomizuka et al. 2008). The WNT pathway is a well understood and conserved pathway that starts with the binding of the extracellular WNT ligand to a Frizzled family of plasma membrane receptors. In canonical WNT signaling, the activated Frizzled receptor recruits a soluble Disheveled family protein that releases the transcriptional co-regulator β-catenin from the plasma membrane. It stands to reason that β-catenin would be factor "Z", as SRY directly inhibits β-catenin-mediated transcription (Bernard et al. 2008) and SOX9 interacts with β-catenin to cause their mutual degradation by the proteasome (Akiyama et al. 2004).

The expression of *Rspo1* begins around E11 with an increased synthesis and secretion of WNT4 observed shortly afterwards by the somatic cells surrounding the oogonia. The activation of the WNT-β-catenin pathway in oogonia, allows for the expression of stimulated by retinoic acid gene 8 (*Stra8*) in response to retinoic acid secreted by the mesonephros beginning on E12.5 (Chassot et al. 2011). STRA8 is a transcription factor that promotes the entry into meiosis and as such, oogonia enter meiosis, or begin oogenesis, on E13.5 in a rostral to caudal wave that takes up to 4 days to complete in the mouse (Menke et al. 2003). Nearly half of the oogonia are lost during this time through apoptotic cell death controlled by the interplay between BCL-X, an anti-apoptotic factor, and BAX, a pro-apoptotic factor (Rucker et al. 2000). The onset of oogenesis varies among mammals with cats, rabbits and golden hamsters occurring after birth (Lemon and Morton 1968; Peters et al. 1965; Winiwarter 1920). However, human oogenesis begins in the second month of pregnancy and which validates the mouse as a model for embryonic ovary differentiation (Kurilo 1981). At E16.5, only a few mitotic oogonia remain and the now primary oocytes have all entered a prolonged arrest in the diplotene stage of prophase I, or dictyotene, where they will remain until stimulated by pituitary luteinizing hormone (LH) after puberty (Vagner-Capodano et al. 1987; Singh et al. 1993).

Autophagy and the WNT-β-catenin pathway are antagonistic of each other. In mouse intestinal epithelium, β-catenin directly downregulates P62/SQSTM1 expression and reduces autophagosome formation through an unknown mechanism (Petherick et al. 2013). Conversely, both β-catenin and Disheveled are selectively degraded by autophagy through binding to LC3 and GABARAP proteins (Petherick et al. 2013; Gao et al. 2010; Zhang et al. 2011). The interplay between WNT and autophagy could be important in timing the proliferative window of both the somatic tissue and oogonia. Before oogonia enter meiosis, proliferation must cease, which could be dependent upon β-catenin degradation. Interestingly, a minimal amount of β-catenin is required for centrosome separation during mitosis, but it is unknown if the same is true during meiosis (Kaplan et al. 2004). Thus, the regulation of β-catenin by autophagy during oogenesis is important to determine. Little is currently known about autophagy prior to dictyotene; however, autophagy mediates the degradation of MutS homolog 4 (MSH4) in some human cell lines (Xu and Her 2013). The complex of MSH4 and MSH5 are necessary to stabilize Holiday junctions and the single stranded invasion intermediates to promote homologous recombination during meiosis (Snowden et al. 2004). Homologous recombination is orchestrated through the presence and degradation of several protein complexes, and it would make sense that the degradation of MSH4 is necessary to continue meiosis after homologous recombination, but this remains to be tested.

1.6 Autophagy in ovarian folliculogenesis

The ovarian follicle is the basic structure found within an adult ovary. Containing the oocyte and somatic cells, the follicle synthesizes endocrine hormones and is essential for producing the mature female gamete. The somatic cells include: 1) the granulosa that function as “nurse” cells providing proteins, mitochondria and substrates to the oocytes, and 2) theca cells that function to supply the granulosa with androstenedione so that they may produce estrogens. The autocrine, paracrine and endocrine signaling that occurs within the follicle determines oocyte development, physiology and survival. Folliculogenesis refers to the sequential developmental process that begins with oogonia-nest breakdown through ovulation and formation of a corpus luteum (**Figure 1.2**). A comprehensive review of the molecular pathways regulating follicle progression can be found elsewhere (Edson et al. 2009). In the following sections, I briefly describe the progression through folliculogenesis and discuss a potential role for autophagy.

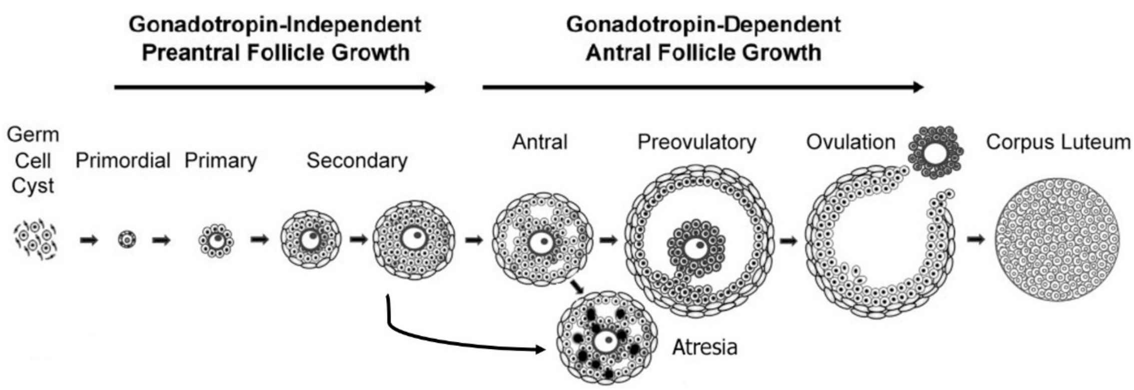

Figure 1.2 Ovarian folliculogenesis
Diagram depicting the developmental process of folliculogenesis. First, somatic pre-granulosa cells invade germ cell cysts and surround oocytes forming primordial follicles. Activation of primordial follicles occurs throughout life and they will progress to secondary follicles regulated by inter-follicle signaling between granulosa and the oocyte. During follicle progression, granulosa cells proliferate forming several cell layers that beginning producing estrogens and recruit an outer layer of androgen producing theca cells. Secondary follicles that become FSH-responsive develop into antral follicles after which progression is dependent on gonadotropins. Two populations of granulosa cells develop due to differential gradients from the oocyte and the blood. The *mural granulosa* are found next to the follicle wall and the *cumulus* are the population that surround the oocyte. After the LH surge, ovulation occurs and drives terminal differentiation of the remaining cells into luteal cells. After extensive tissue remodeling the corpus luteum is formed. At any time following activation, inadequate signals will induce apoptosis, depicted as blackened pyknotic nuclei, and the follicle dies through the process of atresia. Figure modified from (Edson et al. 2009).

1.6.1 Oocyte Attrition and Germ Cell Nest Breakdown

Prior to follicle formation, oocytes exist as clusters connected by cytoplasmic bridges or germ cell nests. Beginning hours after birth in mice, and during the 2nd trimester in humans, the nests begin breaking down and pre-granulosa cells begin surrounding individual oocytes to form primordial follicles (Pepling and Spradling 2001; Konishi et al. 1986). Between 40 and 70% of meiotic oocytes are lost during germ cell nest breakdown, which is known as 'oocyte attrition' (Baker 1966; Coucouvanis et al. 1993; Ratts et al. 1995; McClellan et al. 2003; Rodrigues et al. 2009; Pepling and Spradling 2001; Bristol-Gould et al. 2006a). Oocyte attrition may result from mechanisms devoted to reducing the amount of defective chromosome crossovers, and hence the propagation of mutations, while maximizing the limited number of pre-granulosa cells in the ovary. Thus, this restricts the number of primordial follicles that can form, while the remaining oocytes are removed. Indeed, mice with targeted mutations in genes resulting in crossover defects reduce the primordial follicle pool (Barlow et al. 1998; de Vries et al. 1999; Edelmann et al. 1999; Kneitz et al. 2000; Yoshida et al. 1998). Furthermore, mouse and human females with a single X chromosome (XO) (i.e. Turner syndrome), which leads to failed chromosome pairing are accompanied with increased oocyte attrition from massive apoptosis in the fetal ovary (Burgoyne and Baker 1985; Modi et al. 2003). Supporting that there is a limited numbers of pre-granulosa cells, adequate signaling from growth factors (e.g. KitL, LIF, IGF-I, interleukin-1-α and β) which are secreted by the pre-granulosa cells are necessary to exert anti-apoptotic control on oocytes in culture conditions to prevent oocyte attrition (see De Felici et al. 2005 for review). There is evidence for increased apoptosis and autophagy in ovaries during germ cell nest breakdown suggesting roles for both during oocyte attrition (Gawriluk et al 2011; Perez et al 1999).

Initiation of apoptosis occurs through either an extrinsic or an intrinsic pathway. Extrinsic activation is initiated by death receptors, such as TRAIL and FAS, which belong to the Tumor Necrosis Factor (TNF) and Nerve Growth Factor (NGF) superfamilies (Guicciardi and Gores 2009). These receptors are characterized by containing a death domain that, upon ligand binding, recruits the death-inducing signaling complex which cleaves pro-Caspase 8 to generate active-Caspase 8 (Medema et al. 1997). Active-Caspase 8 activates effector caspases (e.g. Caspase 3, Caspase 7) that trigger downstream apoptotic endpoints such as DNA fragmentation, nuclear degeneration, exposure of phosphatidylserine (PS), and plasma membrane blebbing (reviewed by Guicciardi and Gores 2009). Active-Caspase 8 can also initiate the intrinsic pathway by cleavage of BID (Li et al. 1998). Alternatively, the intrinsic pathway can be activated in response to toxins, growth factor withdrawal or DNA damage (reviewed by Elmore 2007). The intrinsic pathway is characterized as the functional depletion of the anti-apoptotic factors that inhibit pore-forming complexes (e.g. BAX, BAK), which allow the release of Cytochrome C from the inner mitochondria into the cytoplasm. Cytosolic Cytochrome C, APAF-1 and pro-Caspase 9 form the apoptosome, which initiates a Caspase 9 cascade leading to apoptosis. Ultimately, the balance between the pro-apoptotic factors (e.g. BAX, BAK, BAD, BIK) and the anti-apoptotic factors (e.g. BCL2, BCL2L1, MCL1) determine if a cell will survive or undergo apoptosis (reviewed by Czabotar et al. 2014).

It has been long thought that apoptosis is responsible for oocyte cell death during germ cell nest breakdown because prior to attrition oocytes exhibit multiple characteristics of apoptosis including nuclear condensation, cell blebbing, DNA laddering with TUNEL positive staining, and PARP1 immunoreactivity (Ghafari et al. 2007; Pepling and Spradling 2001; Pesce and De Felici 1994; Lobascio et al. 2007a, 2007b). However, the role of apoptosis during oocyte attrition is unclear. The extrinsic pathway is likely not important as the death receptors and their ligands are not expressed by oocytes during the perinatal period (Sakamaki et al. 1997). Examination of the contribution of the intrinsic pathway has given ambiguous results. First, the germ cell specific deletion of BCL2L1 (anti-apoptotic) was found to not affect the primordial germ cell pool (Riedlinger et al. 2002). This result is surprising as BCL2L1 is responsible for survival of oogonia (Rucker et al. 2000). Second, mice with a global deletion of BCL2 (anti-apoptotic) have normal endowment of primordial follicles at P1, 4 and 7 (Jones and Pepling 2013). However, following BCL2 knockout mice or mice overexpressing BCL2 out to P42 results in a decline and increase in the number of primordial follicles, respectively (Ratts et al. 1995; Flaws et al. 2001). This suggests that either: 1) BCL2 regulates cell death after P7, 2) the failure to see a difference at P7 is the result of different primordial follicle counting techniques, or 3) the mice in the 2013 report no longer harbor the phenotype. Third, the use of an MCL-1 (anti-apoptotic) antibody to disrupt its anti-apoptotic ability in oocyte cultures from E18 results in enhanced apoptosis but does not inhibit oocyte attrition (Jones and Pepling 2013). Fourth, the global deletion of BAX (pro-apoptotic) causes an increase in the follicle pool; however, it was concluded to be attributed to cell death that occurs during germ cell migration (Greenfeld et al. 2007). Fifth, global knockout of BAK (pro-apoptotic), BOK (pro-apoptotic) or the double knockouts of BAK/BOK and BAX/BOK have no phenotype for oocyte attrition (Lindsten et al. 2000; Ke et al. 2013). Sixth, staining for apoptotic markers in the perinatal ovary suggest that apoptosis is not responsible for clearing all of the oocytes that undergo attrition (Rodrigues et al. 2009). Overall, these data suggest that alternative cell death mechanisms beside apoptosis exist, or alternatively, the correct combination of apoptotic factors has not been identified. Given that autophagy can mitigate the effects of apoptosis, a block in autophagy may result in an increase in apoptosis and a decrease in the oocyte pool size.

Evidence that autophagy contributes to cell death during oocyte attrition comes from a single study by Rodrigues et al. using perinatal wild-type mice. The results of their analysis demonstrate increased autophagic flux and lysosome amplification in oocytes during germ cell nest breakdown. Additionally, the use of an autophagy inhibitor, 3-methyl-adenine, reduces the cell death in cultured perinatal ovaries placed into starvation media (Rodrigues et al. 2009). While the reduction in cell death was moderate (about 30% less), the use of a Caspase inhibitor to prevent apoptosis did not alleviate acidification (Rodrigues et al. 2009). This is not surprising since starvation induces autophagy and lysosome biogenesis to maintain energy homeostasis, which also occurs in every tissue tested upon parturition (Kuma et al. 2004). The authors of Rodrigues et al. suggest that autophagy participates in cell death during oocyte attrition; however, there is an alternative explanation.

Cell turnover is quick with nearly 8,000 oocytes removed in a matter of 48 hours (Pepling and Spradling 2001). Additionally, the attrition does not induce inflammation or the migration of lymphocytes. Moreover, the dying oocyte bodies must be eliminated yet the engulfing cell, presumed to be resident macrophages, but the cell has not been identified. Autophagy and lysosome biogenesis are processes that are upregulated in tissues actively removing dying cells, such as the testis or retina (Johnson et al. 2008; Deguchi et al. 1994). It is therefore possible that the increased acidification seen during germ cell nest breakdown can be attributed to the phagocytosis of dying cells. Furthermore, apoptotic spermatocytes in the testis are numerous but are removed during the early stages of apoptosis, perhaps to prevent inflammation in the tissue (Nakanishi and Shiratsuchi 2004). As such, many of the endpoints of apoptosis are not observed. I therefore, propose the hypothesis that autophagy is necessary for germ cell nest breakdown to occur normally without an inflammatory response and furthermore, that autophagy is necessary for the survival of oocytes exposed to the parturition related starvation. Using a mouse model with the conditional deletion of autophagy genes in embryonic oocytes should determine if autophagy is a regulator of oocyte attrition.

1.6.2 Primordial Follicle Activation

Once primordial follicles are born, they follow a sequential growth and differentiation until ovulation occurs. Recruitment into the growing follicle pool occurs in two stages. First, the activation of primordial follicles is continual process throughout life. Second, the cyclical recruitment of a limited number of primary follicles from the activated cohort is regulated through gonadotropin signaling which ‘selects’ a subset of follicles for ovulation. As primordial follicles are activated, there is a morphological transition in granulosa cells from a squamous to a cuboidal cell type. Additionally, the diameter of the oocyte increases slightly. The newly differentiated granulosa cells begin making cell-to-cell contacts between themselves and the oocyte via gap junctions that later serve to transport ions, metabolites, small molecules and organelles. Several growth factors and their receptors including follicle stimulating hormone receptor (FSHR), TGFβ superfamily, and insulin receptors begin to be expressed in the granulosa cells and oocyte that have numerous roles in the downstream stages (McLaughlin and McIver 2009). Many of the factors expressed by granulosa cells are also responsible for recruiting stromal cells that later become the theca. While no single factors has been identified, it appears that a combination of several including KITL, Growth Differentiation Factor 9 (GDF-9), Insulin-like Growth Factor (IGF) and BMPs are necessary for theca recruitment and differentiation (Young and McNeilly 2010). Additionally, the oocyte begins expressing many of the genes that regulate the formation of the zona pellucida, which is an essential structure for fertilization (Wassarman and Litscher 2012). The molecular mechanisms that govern the activation are poorly understood, although several necessary factors have been identified in mice that demonstrate crosstalk between the oocyte and granulosa cells (McLaughlin and McIver 2009).

Factors that positively regulate activation include newborn ovary homeobox (NOBOX), spermatogenesis and oogenesis helix-loop-helix 1 (SOHLH1), SOHLH2, folliculogenesis-specific basic helix-loop-helix (Figla), LIM homeobox protein 8 (Lhx8), Forkhead bOX L2 (FOXL2) (see Edson et al. 2009 for review). It is currently unknown what triggers the expression of these transcription factors; however, evidence suggests that increased signaling through KIT may be an early event. KIT is expressed in the oocyte and KIT ligand in granulosa cells throughout folliculogenesis (Horie et al. 1991; Joyce et al. 1999; Manova et al. 1993; Yoshida et al. 1997). As mentioned previously, KIT/KITL interactions mitigate migration of germ cells and recruitment of pre-granulosa around oocytes during germ cell nest breakdown. Thus, it would make sense functionally, that the interaction would continue to control the development of oocytes. KIT induces the AKT/PI3K signaling cascade that, in turn, inhibits FOXO3 (Accili and Arden 2004). Knockout mice for FOXO3 have premature activation of the primordial pool and early depletion of follicles, while inhibitors of AKT/PI3K signaling suppress follicle activation (Castrillon et al. 2003). Moreover, mice constitutively expressing FOXO3 in oocytes are infertile with a marked decline in the progression of folliculogenesis beyond primary follicles (Liu et al. 2007). The role of PI3K in activation is further demonstrated with the oocyte specific deletion of Phosphatase and TENsin homolog deleted on chromosome 10 (PTEN), which inhibits PI3K by catalyzing the reverse reaction. PTEN conditional knockout mice have premature activation of primordial follicles similar to the FOXO3a knockouts (Reddy et al. 2008).

PI3K activity activates AKT which in turn inhibits autophagy by activating mTOR and directly phosphorylating BECN1 (Degtyarev et al. 2008; Wang et al. 2012b). Conversely, FOXO3 acts as a positive regulator of autophagy by directly upregulating the expression of autophagy genes such as LC3 and Bnip3 (Mammucari et al. 2007; Sengupta et al. 2009). Therefore, I would expect that autophagy is downregulated during follicle activation. This would make sense as the follicle is beginning to produces large amounts of protein without a need for degradation. As an alternate hypothesis, autophagy is a positive regulator of mitotic senescence and would need to be inhibited in the soon to be proliferating granulosa cells (Young et al. 2009). Important questions remain to be addressed. Does autophagy negatively regulate follicle activation? Is autophagy necessary for primordial follicle survival?

1.6.3 From Primary to Secondary

As a primary follicle grows, the oocyte expands in size and granulosa cells enter the cell cycle beginning to proliferate to create several layers surrounding the oocyte. Additionally, somatic cells recruited to the primary follicle begin differentiating and morphologically flatten surrounding the granulosa. This outer layer of cells are the theca, responsible for recruiting endothelial cells and smooth muscle to feed the growing follicle and assist in follicle rupture, respectively. A follicle that has two layers of granulosa cells and a complete layer of theca is classified as a secondary follicle. The crosstalk between the granulosa and oocyte is even more apparent during this transition. The oocyte relies on the granulosa and theca to support its growth and development; however, the rate at which follicles develop are dependent on oocyte-derived factors. Eppig et al. completed experiments in which oocytes from secondary follicles were re-aggregated with granulosa cells from newborn mice, which do not have secondary follicles, and placed under a kidney capsule of an immune-suppressed mouse. The oocytes from secondary follicles supported the development of numerous antral follicles 9 days later; whereas control re-aggregation of newborn oocytes with newborn granulosa only had secondary follicles present (Eppig et al. 2002). This experiment demonstrates that the oocyte regulates the growth and progression of activated follicles.

The granulosa cells proliferate in response to oocyte-specific factors (e.g. GDF9 and BMP15) that are stimulated from KIT/KITL signaling, as described earlier. However, as the oocyte grows it produces increased amounts of GDF9 and BMP15, which both negatively regulate the expression of KITL in granulosa cells (Carabatsos et al. 1998; Elvin et al. 1999; Yan et al. 2001). Therefore, a negative feedback loop is activated that slows the growth of the oocyte. Without gonadotropin signaling of FSH and LH released from the pituitary, secondary follicles cease growth and granulosa cells initiate apoptosis to terminate the follicle (Kumar et al. 1997).

A small number of studies support that autophagy is significant during primary and secondary follicle development. A study by Choi et al. revealed that protein expression of LC3 increases as follicles progress through folliculogenesis with the highest immunoreactivity in granulosa cells of secondary and early antral follicles (Choi et al. 2010). While this study did not observe evidence for autophagy in the oocytes, Escobar et al. demonstrated both LC3 immunoreactivity and autophagosome formation in oocytes isolated from 1- through 28-day-old rats after 24 hours of culture (Escobar et al. 2010). As secondary follicles are present as early as P9, there must have been oocytes from secondary follicles in their study. Together these data support that both granulosa and oocytes from rats undergo autophagy during the developmental time when secondary follicles are forming. Electron micrographs of human primordial follicles collected from adults clearly show evidence of autophagosomes (Hertig and Adams

1967, figures 13, 30 and 35), supporting that induction of autophagy in oocytes is conserved between humans and rats. It is untested whether autophagosomes accumulate from failure to fuse with lysosomes or if there is an overall increase in autophagosome formation. Curiously, *Drosophila*, mouse and human follicles cultured in the presence of rapamycin, which inhibits MTOR, induces oocyte loss and follicle degeneration without signs of apoptosis (Thomson and Johnson 2010; McLaughlin et al. 2011). Experiments ablating tuberous sclerosis complex 1 (*Tsc1*) or *Tsc2* in mouse oocytes leads to the premature activation of primordial follicles and early depletion of the primordial follicle reserve (Adhikari et al. 2010, 2009). Additionally, a granulosa specific conditional knockout of *Tsc1* in granulosa cells of secondary follicles enhances follicle survival and results in increased numbers of ovulated oocytes (Huang et al. 2013a). The knockout experiments demonstrate that TSC1/2 act to inhibit MTOR activity, which suggests that mTOR positively regulates follicle survival and progression. It remains to be tested if the modulation of MTOR in the above experiments alters autophagy in the granulosa or the oocyte and furthermore, if autophagy is detrimental to follicles.

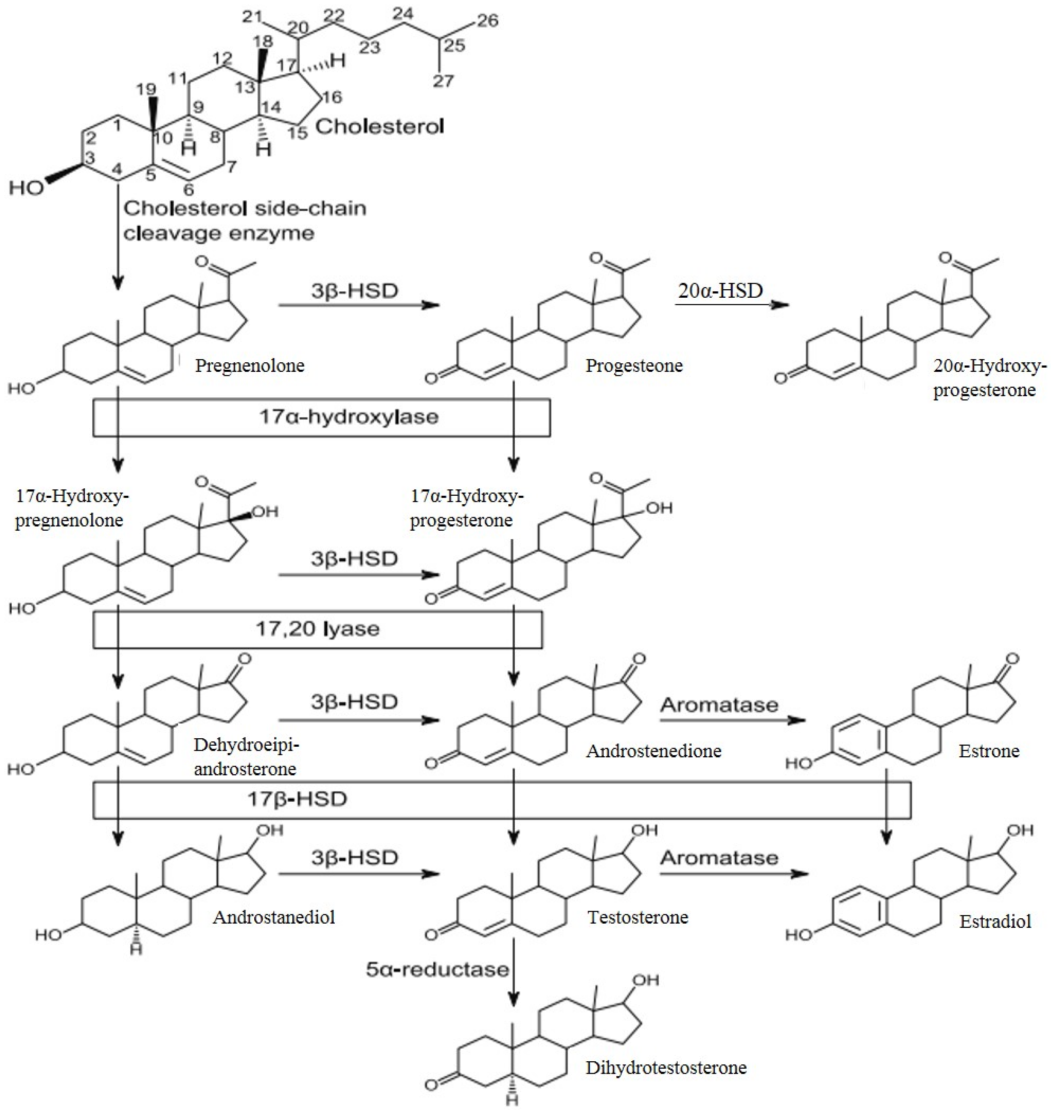

Figure 1.3 Progression of steroidogenesis
The diagram gives an overview of the structural progression of steroidogenesis with associated enzymes. All steroids are products produced from cholesterol in the following order: progestins, androgens and lastly estrogens. Not depicted are additional reactions, for example, the synthesis of corticosteroids. Carbon atoms in the cholesterol skeleton have been added as a reference for downstream transitions. All enzymes are indicated by their abbreviated names. Adapted from creative commons image by Mikael Häggström.

1.6.4 Primer of Steroidogenesis and GPCR Signalling

Physiologically, the secondary follicle begins steroidogenesis due to the expression of the full repertoire of enzymes by the granulosa and theca cells. The best-known hormone produced by the follicle is estrogen. The progression of steroid synthesis can be followed in **Figure 1.3**. Theca cells express steroidogenic acute regulatory protein (StAR), cytochrome P450 side-chain cleavage enzyme (CYP11A1), 3β-hydroxysteroid dehydrogenase (HSD3B1) and 17α-hydroxylase/17,20-lyase cytochrome P450 (CYP17A1). On the other hand, granulosa cells express cytochrome P450 aromatase (CYP19A1) and 17β-hydroxysteroid dehydrogenase (HSD17B1). StAR regulates the transport of cholesterol into mitochondria where CYP11A1 cleaves cholesterol to create pregnenolone, the substrate for all other reproductive steroids. HSD3B1 creates progesterone, while HSD17A1 creates dehydroepiandrosterone (DHEA) from pregnenolone. Both progesterone and DHEA are substrates for andostenedione via HSD17A1 and HSD3B1, respectively. CYP19A1 can then finally convert androstenedione into estrogen. An apparent cooperation must occur between granulosa and theca in order to produce estrogen. Granulosa cells do not express CYP17A1 and thus cannot produce the estradiol precursor, androstenedione. Alternatively, theca cells express CYP17A1 and produce androstenedione but are deficient in CYP19A1. Thus, a two-cell Theory exists where theca cells produce androstenedione, which is delivered to the granulosa cells for the synthesis of estrogens (Young and McNeilly 2010). The differential expression and downstream signaling of follicle stimulating hormone receptor (FSHR) and luteinizing hormone / choriogonadotropin receptor (LHCGR) in granulosa and theca, respectively, is partly responsible for the distinction in steroid enzyme expression.

Both FSHR and LHCGR are members of the of the G-protein coupled receptors (GPCRs) superfamily. GPCRs are seven-transmembrane proteins expressed throughout the body that mediate cellular responses to a variety of extracellular signals (e.g. photons, small molecules, peptides). GPCRs come in five functional flavors, of which FSHR and LHGCR belong to the Rhodopsin sub-family, or Class A GPCRs

(Katritch et al. 2013). The amino acid similarity between human FSHR and LHCGR is moderate with approximately 72% shared in the transmembrane domain, about 45% in the ligand binding extracellular domain and about 25% in the intracellular signal transduction domain (Dias et al. 2002; Vassart et al. 2004). The variation between the FSHR and LHCGR extracellular binding pockets accounts for the specificity to bind and respond to the different beta-subunits of FSH and LH or choriogonadotropin, respectively. Although it should be noted that there are species-specific differences as equine choriogonadotropin (eCG), also called pregnant mare serum gonadotropin (PMSG), binds preferentially to rodent FSHR and human choriogonadotropin (hCG) preferentially binds to rodent LHCGR (Mukumoto et al. 1995). As their name implies, FSHR and LHCGR are coupled to G-proteins found on the intracellular side of the plasma membrane and it is the G-protein that is responsible for transducing the intracellular signaling cascades that occur in response to ligand binding. Ligand binding to either FSHR or LHCGR causes the activation of heterotrimeric G_s proteins, followed by dissociation of two molecules, the α-subunit and the β/γ heterodimer. The α-subunit triggers the subsequent activation of adenylyl cyclase to produce cyclic adenosine monophosphate (cAMP) (Rajagopalan-Gupta et al. 1998). In turn, cAMP results in the release of protein kinase A (PKA) from its regulatory subunits to activate cAMP response element binding protein (CREB) and contribute to increased gene transcription by binding at cAMP Response Elements (CREs) (Salvador et al. 2002; Richards et al. 2002). CREs can be found in the promoters of the steroidogenesis genes mentioned above, in addition to, several genes involved with proliferation, differentiation and angiogenesis distinctly within granulosa and theca. Meanwhile, the β/γ heterodimer mainly activates phospholipase C (PLC) that cleaves phospholipid phosphatidylinositol 4,5-bisphophate to diacyl glycerol and inositol 1,4,5-triphosphate that in turn, activates protein kinase C (PKC). Activated PKC concordantly activates many of the same pathways as PKA. How then do FSHR and LHCGR cause different responses if they activate the same transduction pathways? Three independent but intertwined findings help answer this question. First, FSHR and LHCGR produce different amounts of cAMP when ligand/receptor ratio is held constant, demonstrating that the receptor response is not the same (Tobin et al. 2008). Second, the developmental time is important as the receptor density present on the plasma membrane is important for what downstream pathways are activated (Andric and Ascoli 2008). Lastly, other G-proteins that have different properties can specifically bind to either the FSHR or LHCGR leading to different cellular responses to ligand binding (Breen et al. 2013). Overall, the binding of signaling through FSHR and LHCGR in granulosa and theca, respectively, transduce similar intracellular signals, but regulate different processes due to the combination of intracellular environment and receptor activity.

1.6.5 Antral follicle selection

Once a secondary follicle responds to FSH and LH, the growth of the oocyte and proliferation of the granulosa and theca continues to form an antral follicle, which depend on gonadotropins for continued growth and ovulation. Supporting this conclusion, immature or hypophysectomized animals that have low levels of gonadotropins do not have observable antral follicles, while addition of exogenous gonadotropin rescues follicle progression (Braw and Tsafriri 1980; Braw et al. 1981). The gonadotropins FSH and LH are glycoproteins released in biphasic cyclic waves from gonadotrophs in the pituitary, which are stimulated by gonadotropin releasing hormone (GnRH) pulses that are released from GnRH neurons in the hypothalamus which in turn, are stimulated by several forms of the neuropeptide Kisspeptin (mRNA is *Kiss1*), that are released from *Kiss1*-expressing neurons (Kiss neurons) residing in the arcuate nucleus of the brain (reviewed by Popa et al. 2008).

The antral follicle is named for the fluid filled antrum that forms in the middle of the follicle that creates a functional diffusion barrier resulting in two populations of granulosa cells: mural and cumulus (Diaz et al. 2007). Because the vasculature that feeds follicles is in the theca layer, diffusion of opposing factors from the blood and the oocyte set up gradients that play a large role in the differentiation of these two granulosa-cell populations that are both essential for ovulation. Mural granulosa cells are found near the outside wall of the follicle and receive high amounts of FSH because they are the first to receive factors diffused from capillaries. As such, the mural granulosa are responsible for steroidogenesis. The cumulus granulosa population are the three to four layers of granulosa that surround the oocyte and intrinsically, receive high amounts of oocyte-secreted factors (e.g. BMP15, GDF9) (Diaz et al. 2007; Su et al. 2004; Hussein et al. 2005). The cumulus promote the growth and maturation of the oocyte and are essential for fertilization *and* its development into an embryo (i.e. developmental competence).

Secondary follicles are 'recruited' into the growing follicle pool by their ability to respond to FSH. This recruitment and subsequent growth and ovulation occurs in waves controlled by positive and negative feedback loops. As stated earlier, FSH promotes steroidogenesis, in addition to, granulosa cell proliferation. As a follicle grows, the amount of estrogen and progestins it can produce increases. Both estrogen and progestins have numerous roles throughout the body, but for the sake of this review, act as inhibitors of FSH and LH release early in the estrus cycle (see Zhu and Conney 1998; Deroo and Korach 2006 for reviews). Estrogens bind to estrogen-receptors (EsRs) in the arcuate nucleus, hypothalamus, and pituitary, which indirectly decrease the release of Kisspeptin, GnRH, FSH and LH. Progestins indirectly inhibit the release of GnRH, FSH and LH by binding to progesterone-receptors (PgRs) in the hypothalamus and pituitary. Additionally, a gonadotropin responsive follicle begins producing the peptide Inhibin, which acts directly on gonadotrophs to inhibit FSH synthesis and secretion. Thus, as an antral follicle grows, it exerts ‘dominance’ by suppressing the recruitment of other follicles through decreasing the available FSH. This establishes a negative selection against antral follicles that are not in the correct developmental window. Moreover, the dominant follicle(s) have extensive angiogenesis in the theca layer providing a larger amount of blood to itself.

Estrogens also act locally by regulating androgen production from the theca by inhibiting *Cyp17a1* expression, increasing the ratio of estrogen to androgen. Furthermore, FSH signaling results in the synthesis of insulin-like growth factor 1 (IGF-1) that acts as an additional paracrine signal with FSH on neighboring granulosa cells to phosphorylate and inhibit FOXO1 (Nakae et al. 2000). This promotes granulosa cell proliferation by stabilizing D- and E-type cyclins and increasing the expression of *Fshr* and *Cyp19a1* to escalate estrogen production (Robker and Richards 1998; Rosenfeld et al. 2001). In addition to regulating proliferation, FSH, IGF-1 and estrogen signaling synergistically result in the high expression of LHCGR in the mural granulosa cells.

To my knowledge, there are no experiments addressing the significance of autophagy in antral follicle development. However, drawing from studies stated in earlier sections, there is evidence that autophagy occurs in the granulosa cells and the oocyte of developing follicles. A candidate function of autophagy during antral follicle growth is the regulation of steroidogenesis. Experiments culturing rat Leydig cells, the steroidogenic cells of the testis, have demonstrated that autophagy activity is linearly associated to steroidogeneic output (Li et al. 2011). It remains unknown if autophagy regulates steroidogenesis in other cells, such as granulosa or theca.

1.6.6 3… 2… 1… Ovulation!

Ovulation is a coordinated effort from the entire follicle to release a competent oocyte that will traverse into the oviduct for fertilization. As the dominant follicles continue to outgrow all of the other follicles, becoming pre-ovulatory follicles, they will eventually produces a peak output of estrogen during proestrus in mice. Estrogens bind to E2Rs on a second population of Kiss neurons in the antero ventral periventricular nucleus (AVPV) that results in the increased expression of *Kiss1* and synthesis of Kisspeptins. With stimulation from neurons projecting from the suprachiasmatic nucleus, the AVPV Kiss neurons release Kisspeptins that in turn, stimulate a maximal release of GnRH from GnRH neurons and thus, a 'surge' of LH (and FSH) is released into the bloodstream from the gonadotrophs. The LH binds to LHCGRs on the theca and mural granulosa cells enabling several downstream events summarized below, all of which are dependent on LH/LHGCR interaction (Ma et al. 2004; Zhang et al. 2001; Lei et al. 2001):

1) Changes in steroidogenic capacity to progesterone production
2) activation of the EGF pathway
3) cumulus expansion
4) oocyte meiotic resumption
5) extracellular matrix degradation
6) inflammation and increase in follicular fluid pressure
7) endothelin-2 production and follicle contraction
8) follicle rupture & release of cumulus-oocyte complex
9) terminal differentiation of remaining cells and formation of corpus luteum

The LHCGR/G_S/cAMP/PKA transduction (as described earlier), activates actin modifying complexes that result in a change in granulosa cell morphology from rounded to spindle shaped cells after LH exposure (Ben-Ze'ev and Amsterdam 1989). Because neither cumulus granulosa nor oocytes express LHCGR, at least in mice, paracrine and intercellular signaling must exist to mediate the signal from the LH surge (Eppig et al. 1997). LH binds to LHCGR on mural granulosa resulting in the rapid induction in transcription and translation of epidermal growth factor (EGF)-like family members (e.g. Amphiregulin, Epiregulin and Betacellulin) (reviewed in Conti et al. 2012) and a disintegrin and metalloprotease 17 (ADAM17) (reviewed in Yamashita and Shimada 2012). The EGF-like transmembrane proteins are trafficked to the plasma membrane where ADAM17 cleaves and releases a soluble extracellular domain into the antrum. The extracellular domain acts as a ligand for EGF-receptors (EGFRs) present on cumulus granulosa cells and results in the activation of the MAPK pathway. Active MAPK activates the transcription factor, CCAAT/enhancer-binding protein β (C/EBPβ) that regulates the expression of prostaglandin synthase 2 (COX2) which synthesizes prostaglandin E2 (PGE2). PGE2 is a soluble ligand for prostaglandin receptors found on mural granulosa cells that in turn, also activate adenylyl cyclase, generating increased cAMP and a positive feedback loop. Additionally, PGE2 acts to induce many genes associated with inflammation and causes the increased secretion of follicular fluid (Ricciotti and FitzGerald 2011). Activated C/EBPβ is also responsible for the expression of genes responsible for the synthesis of the hyaluronan-rich cumulus matrix, which is termed the 'cumulus expansion' (Richards 2005). Similarly, the oocyte-derived factors GDF9 and BMP15 are also necessary for cumulus expansion, demonstrating a further role in how the oocyte regulates its own fate.

Prior to the LH surge, oocytes remain in meiotic arrest due to elevated cAMP levels inside the oocyte, which is upheld by cAMP produced by the surrounding granulosa cells that enters through gap junctions. In addition to gene regulation, activated MAPK in the cumulus inactivates connexin-43, a prominent protein in gap junctions connecting granulosa cells (Hsieh et al. 2011). This results in a reduction in cAMP transported into the oocyte and along with the increased activity of phosphodiesterase 3A (PDE3) the subsequent resumption of meiosis (Sun et al. 2009 and references within).

The synthesis of the hyaluronan-rich cumulus matrix and the large amount of prostaglandins during cumulus expansion supports the infiltration of leukocytes, making the follicle prior to ovulation comparable to inflammatory sites. In fact, blocking inflammation or cumulus expansion has negative effects on ovulation, attributing to the well-tested hypothesis that ovulation is an inflammatory reaction (Oakley et al. 2011). The LH surge induces several transcriptional regulators in the mural granulosa that are necessary for ovulation. Of these, the expression of *Pgr* in mural granulosa appears to be most important. After the LH surge, activated PKA also activates extracellular signal-regulated kinase 1 (ERK1) and ERK2 which mediate inhibition of *Lhcgr*, *Fshr*, and *Cyp19a1* mRNA expression while activating *Cyp11a1*, *StAR* and *Pgr* mRNA expression (Fan et al. 2009). This change in gene expression effectively makes the mural granulosa produce and respond to progesterone, in addition, to driving terminal differentiation of the granulosa to luteal cells. The requirement for progesterone signaling in the progression to ovulation is well established. Inhibition of progesterone synthesis, treatment with a progesterone receptor antagonist or ablation of *Pgr* in knockout mice all result in ovulation failure (Snyder et al. 1984; Lydon et al. 1995, 1996; Loutradis et al. 1991). One indication for these results is the PGR-dependent expression of several extracellular matrix-modifying proteases that begin degrading the extracellular matrix at the apex of the follicle, the future site of follicle rupture (Curry 2010 and references within). Approximately two hours before ovulation occurs in rodents and humans, the mural granulosa cells have a marked induction in endothelin-2 (*Et2*) expression (Ko et al. 2006; Palanisamy et al. 2006). The mechanism controlling *Et2* expression is debatable; however, *Pgr* knockout mice fail to induce *Et2* and hypoxia exaggerates *Et2* expression, *in vitro*, suggesting that both progesterone and hypoxia are required for *Et2* expression (Palanisamy et al. 2006; Na et al. 2008). As ET2 diffuses out of the follicle, it binds to endothelin type A receptors (ET_A) present on the smooth-muscle found in the outer layer of theca and induces contraction (Bridges et al. 2010). Activity of extracellular matrix modifying proteins weakens the follicle wall, while inflammation causes a rush of cells and fluid into the follicle, increasing follicle pressure. Finally, ET2 binding results in the contraction of follicle wall followed by follicle rupture and the oocyte is released.

The role of autophagy during ovulation is relatively unexplored. To my knowledge, there have been no experiments published directly testing the function of autophagy during ovulation. In particular, mice with an oocyte-specific deletion of *Atg5*, discussed earlier in pre-implantation development, ovulate wild-type numbers of oocytes, suggesting that autophagy in the oocyte is not essential for ovulation (Tsukamoto et al. 2008b). On the other hand, granulosa cell specific MTOR activity regulates ovulation. The granulosa cell specific deletion of *Tsc1*, a negative regulator of MTOR, results in increased MTOR activity and an increased number of ovulated oocytes resulting in larger litters (Huang et al. 2013a). Similarly, premenopausal woman taking Sirolimus (rapamycin) for immunosuppression after receiving clinical islet transplantation to treat type 1 diabetes have a high incidence of ovarian cysts, suggesting failed ovulation (Alfadhli et al. 2009; Cure et al. 2004). MTOR also regulates the onset of puberty by inducing *Kiss1* expression in the hypothalamus of mice and positively regulates steroidogenesis in rabbit ovary slices in response to LH and FSH (Roa et al. 2009; Kádasi et al. 2012). Thus, it cannot be concluded that mTOR directly regulates ovulation, but the data suggest that mTOR modulates the endocrine signaling triggering ovulation. The rate of autophagy was not explored in these studies; however, I will speculate that the increased mTOR activity, that promotes ovulation, would inhibit autophagy in pre-ovulatory follicles, therefore making autophagy a negative regulator of ovulation. Experiments utilizing conditional knockout alleles for autophagy genes in granulosa cells of growing follicles would be useful to examine.

1.6.7 Atresia

In the previous sections, I have described successful folliculogenesis through ovulation, but this fate only accounts for less than 1% of follicles in most mammals studied (Hirshfield 1991). A human female, for example, is estimated to be born with between one and two-million follicles, and by puberty only 400,000 remain (Baker 1963; Forabosco et al. 1991). When it is considered that approximately 400 ovulations occur in a lifetime, (one ovulation every 28 days equals 13 ovulations per year and with approximately 30 years between puberty and menopause, we arrive at 391 ovulations in a female that does not get pregnant), it is easily appreciated that over 99.9% of follicles fail to reach ovulation. The default program of a majority of the follicles is a process called atresia, which is Greek for “closure of hollow space”. Two types of atresia with different initiation points have been described (Hsueh et al. 1994). In primordial and primary follicles, oocyte-derived factors determine survival and as such, the oocyte is the first cell to die. In post-secondary follicles, the granulosa cells are critical for follicle survival and are initiators of atresia. A majority of follicles that undergo atresia are at the antral/preovulatory stage, consistent with the dependency on FSH to promote follicular development, as discussed earlier (Hsueh et al. 1994). In general, any follicle not receiving adequate signaling to develop will initiate atresia.

Elimination of pre-antral staged follicles is rare to observe in adult animals. Studies following rodents throughout reproductive life indicate that the majority of small follicle atresia occurs prior to puberty (Hirshfield and Midgley 1978; Faddy et al. 1987, 1976; Bristol-Gould et al. 2006b). Conversely, an ultrastructural analysis of ovary slices from adult pre-menopausal women support that primordial follicles undergo atresia throughout life, although at a low rate (de Bruin et al. 2002). Nonetheless, small follicle atresia is associated with cytoplasmic changes initiated in the oocyte including: mitochondrial decay, increased vacuolation of the cytoplasm, ruptured nuclear membranes, accumulation of lipid droplets and shrinkage of the oocyte. Using the prepubescent mouse, experiments have suggested that apoptosis is not a driving factor for small follicle atresia. Granulosa cells and oocytes of small follicles are refractory for apoptosis markers (e.g. BAX, active Caspases, PARP1, TUNEL, pyknotic nuclei and DNA fragmentation) (Vaskivuo et al. 2001; Hurst et al. 2006; Tingen et al. 2009; Rodrigues et al. 2009; Escobar et al. 2008, 2010). In spite of the results that mice overexpressing *Bcl2* specifically in oocytes have 30% fewer atretic small follicles compared to controls, demonstrating that apoptosis is a factor in small follicle atresia (Morita et al. 1999), autophagy has been suggested as an alternative cell-death pathway in small atretic follicles (Tingen et al. 2009; Rodrigues et al. 2009; Escobar et al. 2008, 2010).

The argument stems from two observations: 1) autophagy markers are increased in the ovaries of prepubescent rodents (Escobar et al. 2010, 2013, 2008; Rodrigues et al. 2009) and 2) only a few small follicles are positive for apoptotic markers at the time points studied (Tingen et al. 2009). Additionally, only 37 follicles were positive for apoptosis out of an estimated 155 that would be eliminated on P10, suggesting that these apoptotic small follicles are negligible to the total atresia (Tingen et al. 2009). Although, it should be noted that depending on the mouse strain and counting method there is discrepancy in the number of primordial follicles that are lost between P6 and P16. It is entirely plausible that the 37 positive follicles make up all of the atretic follicles in the ovaries studied at P10. Furthermore, the ultrastructure of the oocytes presented have extreme vacuolation, as stated by the authors; however, those vacuoles are not all autophagosomes as many do not have a double membrane, which was possibly misinterpreted by the authors. The autophagy markers used in these studies, LC3 and lysosomal-associated membrane protein 1 (LAMP1), which is actually a late endosome/lysosome marker, suggest that there is an increase in LC3 labeled membranes and biogenesis of lysosomes. Recent findings demonstrate that LC3 can associate with non-autophagosomal membranes, which brings into question the membrane that LC3 is associated with in small follicles (Martinez et al. 2011). A recently published mouse with GFP-labeled germ cells would be ideal to cross with apoptosis, autophagy and necrosis markers to observe atresia live in pre-pubertal ovaries to conclusively estimate atresia (Lin et al. 2014). Furthermore, the field needs a new method of counting follicles to circumvent the inaccuracy associated with the analysis of histological sections. It might be possible to disassociate ovaries and count GFP-tagged oocytes by flow cytometry or through confocal slices of cleared ovaries. Lastly, to determine if autophagic cell death is mediating atresia of pre-antral follicles, genetic experiments need to be performed that test whether the ablation of autophagy genes affect follicular atresia.

In contrast to small follicles, apoptosis of the granulosa cells identified by pyknotic nuclei is the most prominent feature of an atretic antral follicle. Early-atretic antral follicles are identified by 10-20% of granulosa cells with pyknotic nuclei. This progresses to the loss of nearly 50% of the mural granulosa and invasion of leukocytes due to the loss in integrity of the basement membrane. Next, the entire follicle shrinks, the theca undergo hypertrophy and the oocyte misshapens. In the final stage of degeneration, the granulosa, theca and oocyte are missing and fibroblasts have invaded the antrum. Considering that antral granulosa cells express the death receptors FAS and DcR1 in addition to the death ligands TRAIL and FASL, granulosa cells are primed to undergo apoptosis (Hakuno et al. 1996; Kaipia et al. 1996; Kim et al. 1999; Quirk et al. 1995; Hu et al. 2001). This means that granulosa cells can activate the extrinsic pathway of apoptosis in a paracrine fashion. Demonstrating this idea, mice overexpressing *Bcl2* specifically in granulosa cells have fewer atretic follicles and increased litter sizes compared to controls (Hsu et al. 1996). Thus, granulosa cells dictate a delicate balance between pro-apoptotic and anti-apoptotic signals. Furthermore, when the scale tips toward apoptosis, the result is quick and death is extensive throughout the follicle.

The same factors that promote granulosa cell proliferation and differentiation also inhibit apoptosis (Yu et al. 2004; Billig et al. 1993; Chun et al. 1996, 1994). A series of experiments from Aaron Hsueh's lab developed an understanding of the regulatory factors by experimenting with cultured mouse pre-ovulatory follicles. Fibroblast growth factor 2 (FGF2), transforming growth factor alpha (TGFα) and EGF all inhibit apoptosis in cultured granulosa cells (Tilly et al. 1992). The use of FSH or the downstream mediators, cAMP and IGF-1, prevent apoptosis of cultured antral and pre-ovulatory follicles (Chun et al. 1994, 1996). We now know that in the absence of FSH or IGF-I, FOXO1 induces expression of the death ligand *Fasl* and the apoptosis mediator *Bcl2l11* to promote apoptosis (Matsuda et al. 2011). Interleukin-1 beta (IL-1 beta), produced by the follicle in response to gonadotropin, induces nitric oxide production that triggers an increase in anti-apoptotic intracellular cyclic guanine monophosphate (cGMP) (Chun et al. 1995). Additionally, estrogen withdrawal or androgen administration which antagonizes the effect of estrogens can induce apoptosis and atresia of antral follicles in hypophysectomized rats (Billig et al. 1993). Consequently, estrogen inhibits the expression of the pro-apoptotic factors *p53* and *Bax*, as evidenced in aromatase knockout mice by their increased expression and the observation that folliculogenesis is stalled at the antral stage with abundant atretic follicles (Britt et al. 2001). Other stressors that induce atresia include: oxidative stress (Matsuda et al. 2011; Tilly and Tilly 1995), lithium treatment (Mirakhori et al. 2013), angiotensin II (Kotani et al. 1999) and inadequate angiogenesis (Rosales-Torres et al. 2010). I have not discussed the implications of reducing apoptosis and atresia here, but there is evidence that in the failure to undergo apoptosis, granulosa cells can contribute to tumor formation (reviewed by Jamieson and Fuller 2012). Overall, this body of work demonstrates that multiple factors produced by the follicle in response to gonadotropins can all effect the onset of apoptosis and atresia.

A recent interest in autophagy during pre-ovulatory development and atresia has implicated autophagy as a mediator of granulosa cell death during atresia. Characterization of rat follicles for the autophagy marker LC3 identified an increased expression of LC3, which paralleled the expression of Active-Caspase 3 in granulosa cells deprived of gonadotropin (Choi et al. 2010; Escobar et al. 2013). In a follow-up study, Choi et al. demonstrated increased apoptosis in cultured granulosa cells after Bafilomycin A1 treatment, which causes the accumulation of autophagosomes, suggesting that autophagosomes trigger apoptosis (Choi et al. 2011). These experiments do not test if the failure of autophagosome fusion and subsequent accumulation is the result of the pathways leading to apoptosis induction. In fact, inhibition of autophagy through RNAi or pharmacological inhibition induces apoptosis in human cell lines (Boya et al. 2005). Clearly, granulosa cells from pre-antral follicles have high levels of basal autophagy as autophagosomes can be identified in healthy or atretic conditions (Choi et al. 2010), suggesting that autophagy provides a function separate from apoptosis. A recent study using zebrafish, identified that nutritional supplementation of probiotics decrease apoptosis and atresia while increasing autophagic flux, or the rate of autophagosome formation and clearance (Gioacchini et al. 2013). A genetic study testing the function of autophagy during follicle development and atresia would be beneficial in understanding any role autophagosomes have during atresia. Furthermore, as with pre-antral atresia, functional experiments need to be completed demonstrating a role of autophagy in cell death before calling this autophagic cell death.

1.6.8 Formation and function of the corpus luteum

The corpus luteum (CL) is a dynamic, transient endocrine gland that rapidly forms from the remains of the ovulated follicle, a process called ‘luteinization’. The first drawings and description of CLs come from the work of Regneir de Graaf in 1668 characterizing rabbit ovaries, but he called them ‘globules’ (translated by Jocelyn & Setchell, 1972). The word corpus luteum literally means ‘yellow body’ and was first used by Marcello Malpighi in a 1681 letter to describe the yellow structures found on bovine ovaries (Malpighi 1685). The function of the CL eluded researchers until 1901, where in two independent studies ovariectomy or the destruction of the CLs of mated rabbits demonstrated the loss of pregnancy (Fraenkel 1901; Magnus 1901). After a series of studies in which a hormone was crystallized from the CL that demonstrated its action on maintaining pregnancy, the name progesterone was adopted (Allen 1935). This work allows me to say today that the CL is a professional progesterone producing and secreting gland that synthesizes upwards of 40 mg of progesterone per day in humans (Carr et al. 1982). Progesterone is a C-21 derived hormone essential for 1) development of the endometrium for implantation of the embryo, 2) the maintenance of pregnancy through quiescence of the myometrium 3) inhibiting the LH surge and 4) the development of the mammary glands (reviewed in Conneely et al. 2002, 2007). A comprehensive review of the molecular pathways regulating CL formation, function and regression can be found elsewhere (Stocco et al. 2007; Diaz et al. 2002). Here I will highlight CL formation, synthesis of progesterone by the CL during pregnancy and discuss roles for autophagy. As with the previous sections of this review, we will focus primarily on the mouse. It should be further noted that while there are differences in the formation, lifespan and regression of the CL between species, the function of the CL to produce progesterone in conserved.

The functional CL contains four main cell types: steroidogenic luteal cells (luteal cells), vascular cells, immune cells and fibroblasts. The luteal cells produce progesterone. Vasculature cells, which include pericytes and endothelial cells, allow for the transport of cholesterol to the CL, and progesterone away from the CL to the rest of the body. Immune cells regulate the lifespan of the CL. The activation of LHGCR after the LH surge in mural granulosa induces cell cycle arrest, changes in gene expression, induces the synthesis of progesterone (as described earlier) and regulates the terminal differentiation into luteal cells including hypertrophy (Carletti and Christenson 2009). There are two populations of luteal cells, large (30-35 μM) and small (15-17 μM), of which their cell diameter is the distinguishing characteristic, accounting for a 10-fold difference in volume (reviewed in Murphy 2000). Large luteal cells compared to small luteal cells produce on average 40-fold more progesterone, have more rough ER, and are more responsive to the regression stimulus, $PGF_{2\alpha}$ (reviewed by Diaz et al. 2002). It is well established that the theca also contribute to the steroidogenic population in ruminants and primates (Meidan et al. 1990; Fritz and Fitz 1991), but similar results are not observed in rodents (Nelson et al. 1992b, 1992a). In rodents, both large and small luteal cells appear to have a granulosa cell origin with both cell-types producing progesterone in response to LH (Nelson et al. 1992a). Whether or not the theca contribute to the rodent CL remains unknown.

In most mammals studied, ovulation is accompanied with 1) the folding of the follicular wall, granulosa cell layers and theca layers, 2) the destruction of the basement membrane and 3) the dilation of the blood vessels in the theca layer that results in extravasation of erythrocytes, followed by vascular injury and angiogenesis (Smith, McIntush, & Smith, 1994 and references within). Within minutes after ovulation, pericytes and endothelial cells begin invading the future CL that will become one of the most vascularized structures in the body (Bruce and Moor 1976; Reynolds et al. 1994). This amazing undertaking happens so rapidly that CL formation is only comparable to tumor growth (Reynolds et al. 2002). The microvasculature is so extensive that every luteal cells borders at least one capillary, and in the mature gland more than 50% of the cells are vascular-related endothelial cells and pericytes (Lei et al. 1991; Tamanini and De Ambrogi 2004). With the LH surge, granulosa cells begin expressing multiple angiogenic factors including VEGFA, FGF2, and endocrine gland VEGF (EG-VEGF) (Tamanini and De Ambrogi 2004). The high levels of the angiogenic factors along with the vascular injury promote the invasion of pericytes derived from the theca into the future CL. Pericytes play a role in recruiting migrating endothelial cells and then both cell populations undergo extensive proliferation creating dense networks of blood vessels throughout the CL (Goede et al. 1998). These extensive networks are necessary for the delivery of cholesterol (in the form of lipoproteins) to the luteal cells and the subsequent delivery of progesterone to the blood.

Production of progesterone is an overwhelming function of luteal cells. In rodents, luteal cells continue to produce androstenedione and estrogen, but the ratio compared to progesterone is minor. As shown previously in **Figure 1.3**, progesterone synthesis requires the substrate cholesterol and has two enzymatic steps requiring CYP11A1 and 3β-HSD. As such, luteal cells express several key proteins for the uptake, transport and synthesis of cholesterol and in processing cholesterol to progesterone. Several factors have been identified that regulate the expression of these proteins in the CL, called luteotropic factors, including LH, prolactin (PRL), placental lactogen (PL) and estrogen.

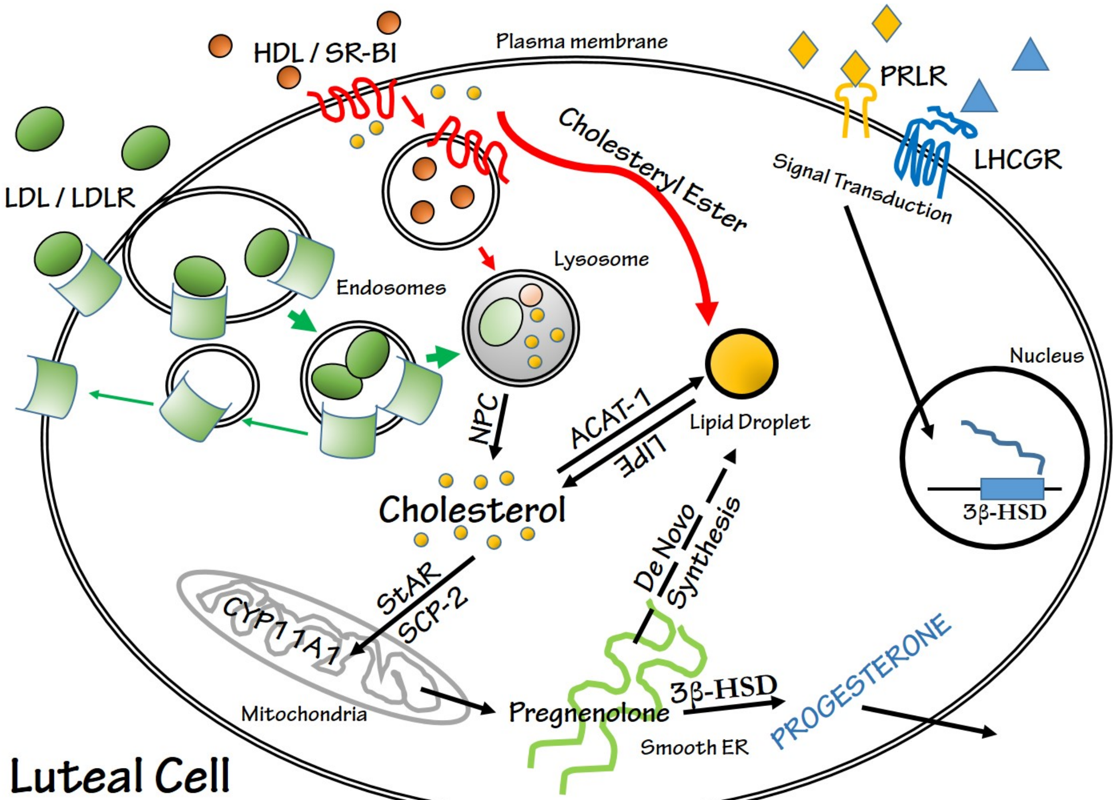

Figure 1.4 Progesterone synthesis pathway in a luteal cell.
Stimulation through PRLR and/or LHCGR initiates signal transduction upregulates the expression of progesterone synthesis enzymes (e.g. CYP11A1, StAR, 3β-HSD, etc.). There are three sources of cholesterol that can be used as a substrate for progesterone synthesis: LDL, HDL and de novo biosynthesis of cholesterol in the ER. LDL is endocytosed and cholesteryl ester is hydrolyzed to cholesterol in the lysosome, while LDLRs are recycled to the plasma membrane. NPC1/2 transport cholesterol out of the lysosome. HDL can be endocytosed, as well, but more frequently, cholesteryl ester is

directly transported to the plasma membrane where it is included into lipid droplets or hydrolyzed by LIPE. Cholesterol is directly used for steroidogenesis or stored into lipid droplets by action of ACAT-1. StAR and SCP-2 facilitate the transport of cholesterol into

Figure 1.4 Continued
the mitochondria, where CYP11A1 converts cholesterol to pregnenolone. Pregnenolone is in turn converted to progesterone by 3β-HSD in the ER.

Cholesterol is the substrate for steroidogenesis, and must be in constant supply to luteal cells to generate such high levels of progesterone. See **Figure 1.4** to illustrate the process detailed in the following paragraphs. The "cholesterol accumulation" network of genes regulate the biosynthesis, transport and storage of cholesterol within luteal cells. Cholesterol can come from three sources: intracellular biosynthesis, high-density lipoprotein (HDL) and low-density lipoprotein (LDL). Biosynthesis of cholesterol takes place within the ER using acetyl-CoA as a substrate. The multi-step synthesis is regulated by the rate-limiting enzyme 3-hydroxy-3-methylglutaryl coenzyme A (HMG-CoA) reductase (HMGCR) (Brown and Goldstein 1980). In order to facilitate storage or transport, cholesterol is dehydrated to cholesteryl ester. Acyl-CoA: cholesterol acetyltransferase 1 (ACAT1) catalyzes the dehydration of cholesterol to form cholesteryl ester in the ER (Chang et al. 1997). Cholesteryl can be then transported to other membranes by sterol carrier protein-2 (SCP-2) or stored in perilipin-associated lipid droplets, which are thought to bud off the endoplasmic reticulum (Gallegos et al. 2001; Walther and Farese 2009). It well established that luteal cells cannot support acute steroidogenesis through de novo biosynthesis, at least in part due to low expression of HMGCR, and that an extracellular source is necessary (Gwynne and Strauss 1982).

The lipoproteins HDL and LDL are biochemical assemblies of apolipoproteins and lipids (e.g. cholesterol, cholesteryl ester and triacylglycerides) formed in the liver to deliver lipids throughout the body (Hegele 2009). Characterized by their protein-to-lipid ratio, HDL has a high protein-to-lipid ratio, while LDL has a low ratio. Circulating LDL and HDL bind to the membrane receptors, scavenger receptor B1 (SCARB1) and LDL-receptor (LDLR) found on luteal cells. The primary lipoprotein utilized by cell types varies depending on species studied and is tissue-specific within a species. Several studies around 1980 demonstrated that the rat CL can bind and utilize both HDL and LDL, but in early pregnancy HDL is preferentially utilized to synthesize progesterone (Gwynne and Strauss 1982). Endocytosis of receptor-ligand complexes and subsequent delivery of the endosome to a lysosome allows for the release of the lipoprotein from the receptor followed by hydrolysis of cholesteryl to cholesterol by acidic cholesteryl ester hydrolase (aCEH) (HDL reviewed in Röhrl and Stangl 2013; LDL recounted in Goldstein and Brown 2009). Niemann-Pick C1 and C2 (NPC1 & NPC2) are necessary to transport cholesterol out of the lysosome to form free cholesterol pools that can be transported to other membranes or used for steroidogenesis (Watari et al. 1999; Ko et al. 2003). Functional LDLRs are the products of several post-translational modifications that are energy and time consuming steps. To circumvent the constant need to generate LDLRs, the cell recycles them back to the plasma membrane where they can perform the transport upwards of thousands of times before degradation (Goldstein and Brown 2009).

Alternatively, cholesteryl can be directly or bi-directionally transported between either LDL and HDL via SCARB1 and the plasma membrane (Connelly et al. 2003). Any extralysosomal cholesteryl can be hydrolyzed by a neutral cholesteryl hydrolase, mainly hormone-sensitive lipase (LIPE) in luteal cells, to form free cholesterol pools (Kraemer and Shen 2002). The amount of free cholesterol is regulated through a negative feedback loop in the endoplasmic reticulum by insulin-induced gene 1 (INSIG1). Under high sterol concentrations, INSIG1 is expressed to negatively regulate HMGCR transcription and directly increase the degradation of HMGCR and NPC1 (Yang et al. 2002). ACAT1 can also catalyze the dehydration of free cholesterol outside of the endoplasmic reticulum to form cholesteryl ester, which can be transported to lipid droplets for storage.

Once the luteal cell has cholesterol, the hydrophobic cholesterol must be transported to the site of steroidogenesis. The “progesterone synthesis” network includes genes involved in the synthesis of progesterone from cholesterol. SCP-2 and steroidogenic acute regulatory protein (StAR) regulate the transportation of free cholesterol to the mitochondria and then from the outer to the inner mitochondrial membrane, respectively. Located in the inner mitochondrial membrane is the enzyme cytochrome P450 side chain cleavage (CYP11a1), which catalyzes the oxidation of the side-chain to form pregnenolone (Stocco and Clark 1996; Gallegos et al. 2000). The action of StAR is considered the rate-limiting step of pregnenolone synthesis as cholesterol cannot diffuse across the aqueous intermembrane space fast enough to support acute steroidogenesis (Black et al. 1994). Pregnenolone then exits the mitochondria and is converted to progesterone by 3β-hydroxysteroid dehydrogenase (3β-HSD) in the microsomal compartment of the endoplasmic reticulum. In the event of high quantities of progesterone and during parturition, progesterone is metabolized to 20α-hydroxy-progesterone, a biologically inactive progestin, by 20α-hydroxysteroid dehydrogenase (20α-HSD). Low quantities of other steroidogenic enzymes are expressed in luteal cells and therefore, mainly progesterone is produced which freely diffuses into microvasculature that encompasses luteal cells.

The expression of the “cholesterol accumulation” and “progesterone synthesis” network, mainly CYP11a1, 3βHSD and StAR, are regulated through signaling initiated through the membrane receptors: LHCGR and the prolactin receptor (PRLR). Upon cervical stimulation during coitus, prolactin (PRL) secreted from the anterior pituitary and along with FSH and LH form a luteogenic complex that signals through PRLR and LHCGR on the luteinizing granulosa cells to promote corpus luteum formation and progesterone synthesis. Two forms of PRLR are found in CLs, the short and long forms activate many kinases including: SRC, PI3K, mitogen activated protein kinase (MAPK) and Nek3-vav2-Rac1; however, only the long form of PRLR (PRLR-L) is shown to activate JAK2/STAT5 (reviewed in Binart et al. 2010). These downstream signals indirectly and directly regulate gene expression of all components of the progesterone network, including PRLR and LHCGR. Beginning on pregnancy day (P) 6, a placenta-derived homolog, placental-lactogen I (PL-I) is produced with concentrations peaking at P10 then rapidly declines. PL-I functionally complements the mother's pituitary PRL (Colosi et al. 1988; Ogren et al. 1989). On P9, PL-II begins to be secreted and remains high until parturition (Soares et al. 1982). By P11, the mother no longer secretes PRL, and PL-I and PL-II are solely responsible for signaling through PRLR-L. The positive feedback initiated through activation of these receptors maintains the mother's body in a progesterone bath that is necessary for fetal development.

The role of autophagy in corpus luteum development and luteal cell steroidogenesis is unknown. However, the regulation of lipid droplets, mitochondria and endosomes by autophagy is of particular interest in luteal cells. As a luteal cell accumulates cholesterol, there is a simultaneous increase in lipid droplet formation. A balance of lipid droplet formation and metabolism is maintained throughout the pregnancy to generate a stable quantity of progesterone. One can imagine how progesterone synthesis would be severely hindered when autophagy is inhibited, if lipophagy regulates any part of lipid droplet metabolism in luteal cells. One mechanism to regulate steroidogenesis is to modulate the number of mitochondria, as shown in adrenal cortex and testis (Jing and Tang 1995). Along these lines, mitochondrial dynamics of fusion also regulates the production of progesterone in cultured MA-10 cells (Duarte et al. 2012). Seeing that autophagy is the only mechanism to degrade mitochondria, an increase in autophagy could remove mitochondria inhibiting steroidogenesis. In contrast, inhibiting autophagy could increase steroidogenesis by increasing the number of mitochondria or allow the accumulation of damaged mitochondria increasing reactive oxygen species (ROS) and ultimately kill the cell.

1.7 Autophagy in the adult testes

The adult testis is the site of testosterone production and male gamete formation through the active process of spermatogenesis. This is in contrast to the female that have dormant oocytes at the time of birth, as discussed earlier. The testis is an organ filled with many tubules wrapped and coiled on each other. The cords of germ and somatic cells that form during embryogenesis develop into these seminiferous tubules. In between the tubules is the testicular interstitium, a cellular compartment that houses the vasculature and the testosterone-producing Leydig cells. As sperm are produced, they are released into the lumens of the seminiferous tubules and exit through a collection duct, called the rete testis where they enter the epididymis to mature. Three cells types populate the seminiferous tubules: spermatogonia and their descendants, peritubular myoid cells, and Sertoli cells. Looking at a cross section of a mouse tubule (**Figure 1.5**), one will find one layer of peritubular myoid cells around the perimeter, which contain several actin filaments to provide structural integrity to the tubule. Additionally, peritubular myoid cells secrete a number of extracellular matrix components (e.g. fibronectin, type IV collagen and proteoglycans) and growth factors (e.g. TGFβ, IFG-I, and Activin) known to regulate Sertoli cell polarity and spermatogenesis (reviewed in

Mayerhofer 2013). On the inside of the tubule, is an organization of spermatogonia anchored to the basal lamina, a barrier between the peritubular myoid cells and the tubule, sitting in a stem-cell niche created by adjacent Sertoli cells. Spermatogonia proliferation and differentiation relies on interactions with and growth factors secreted by the Sertoli cells. Spermatogenesis occurs in 12 developmental stages, which ranges from 30 to 78 days in mammals to complete, and the stages are found heterogeneously in the adult testis (Hess and Renato de Franca 2008). It is now appreciated that spermatogenesis occurs in waves throughout the seminiferous tubules, which allows for the continual production of mature sperm throughout life (Hess and Renato de Franca 2008). Testosterone produced by the Leydig cells binds to androgen receptors in Sertoli cells that regulates the progression of spermatogenesis. Thus, both Sertoli and Leydig cells are necessary for sperm production. The following sections provide a discussion for the individual roles of Sertoli and Leydig cells in conjunction with possible roles for autophagy.

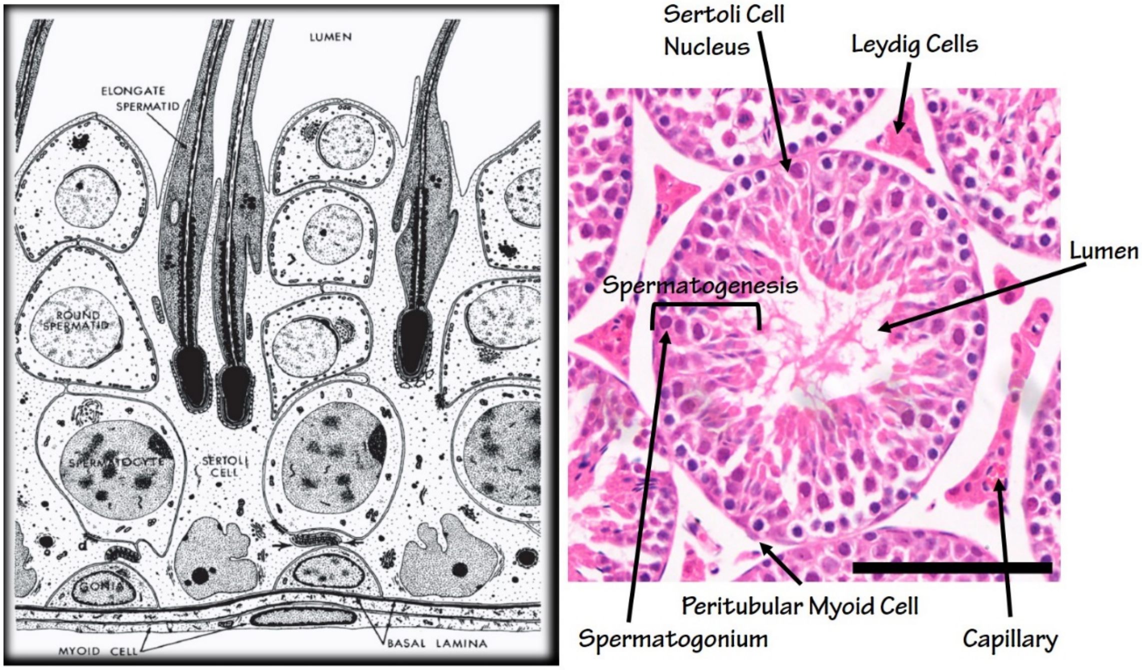

Figure 1.5 Seminiferous epithelium
(Left) Diagram showing a small area of a cross-section through a seminiferous tubule. Spermatogenesis progresses in a basal to adluminal direction terminating with elongated spermatid release. On the basal side of the tubule, in contact with the basal lamina, are the spermatogonia, which proliferate and begin meiosis as they migrate toward the lumen. A gap junction (arrows) between two Sertoli cells creates a blood-testis-barrier to allow the “non-self” haploid spermatids to evade the immune system. The columnar-shaped Sertoli cell are always interacting with developing spermatocytes and spermatids regulating their development. Figure adapted from (Morales and Clermont 1993). (Right) Cross-section of a seminiferous tubule from a 10-week old mouse testis stained with hematoxylin (blue=nuclei) and eosin (pink=cytoplasm). The beginnings of spermiogenesis are observed in this cross section. Here, Sertoli cells are difficult to observe except by the distinct-shaped nucleus, indicated. Groups of Leydig cells surrounding vasculature are present in the interstitial space between tubules as indicated. Scale bar equals 100 µM.

1.7.1 Autophagy and adult Leydig cells

Leydig cells get their name after Franz Leydig who was the first to describe the presence of cells between seminiferous tubules that had been overlooked by other researchers. Franz made his observation during a comparative study of the male reproductive tracts from nonhuman primates, bats, insectivores, carnivores, marsupials, rodents, rabbits, pigs, horses, artiodactyls and a dolphin (Leydig 1850). In his conclusion, Franz states: “From the comparative histology of the testis it is clear that, in addition to seminiferous tubules, blood vessels, and nerves, one find an additional constant component in the mammalian testis. Its main constituents are small granules of fatty appearance" (translated by Christensen 2007). We now know that Franz was describing lipid droplets inside the steroid producing cells of the testis. The adult Leydig cell is not present until after birth when a population of mesenchyme-like fibroblasts begin differentiating. There is a population of fetal Leydig cells that are eliminated by programmed cell death shortly after birth that the adult population entirely replaces, and a review can be found elsewhere (reviewed by Huhtaniemi and Pelliniemi 1992). In the rat, the progression to mature Leydig cells has been divided into three stages (Hardy et al. 1989). Each stage is characterized in depth elsewhere (reviewed by Haider 2004). In the 'progenitor' stage (P10-28), newly differentiated Leydig cells resemble fibroblasts, produce androstenedione (see **figure 1.3** for clarification) and begin to express LHCGR. The little androgen they do produce acts in a paracrine manner inducing proliferation in neighboring Leydig cell progenitors. Leydig cell progenitors proliferate to create homogenous populations around the seminiferous tubules and form colonies in close association with the interstitial capillaries. In the 'immature' stage (beginning P30-P56), which is around the same time as the onset of puberty (FSH and LH secretion), Leydig cells produce a small amount of testosterone. This is a synergistic response to both LH and androgen, but a majority of the testosterone is metabolized to a non-biologically active form. Additionally, signaling through LHCGR inhibits proliferation and downregulates the expression of the androgen receptor. Interestingly, in rodents the first wave of spermatogenesis does not require androgens, while androgen receptor signaling is required in all subsequent waves (Yoshida et al. 2006). In the final stage of Leydig cell development, 'mature' Leydig cells (P60 and beyond) express high levels of LHCGR that regulates the expression of the full complement of testosterone synthesizing enzymes, giving them a high capacity for testosterone synthesis.

Throughout adult Leydig cell differentiation, the cell morphology changes from spindle-shaped to large and spherical. Numerous lipid droplets and mitochondria are present in mature Leydig cells, evidence that they are steroid producing cells. As in theca and luteal cells, LHCGR activity in Leydig cells causes the transduction of a cAMP/PKA/CREB cascade that induces expression of lipoprotein receptors, cholesterol transporters and testosterone synthesizing enzymes (O'Shaughnessy et al. 2014; Ge et al. 2005; Sanz et al. 2013). Additionally, Leydig cells express low levels of CYP19A1 and do synthesize small amounts of estrogens that mainly acts on Sertoli cells and spermatogonia, but high levels of estrogen inhibit androgen synthesis (Abney 1999). There are several age-related changes in Leydig cells of rodents and humans. Common among these is a decrease in testosterone that is also associated with a decrease in LH (Bethea and Walker 1979). However, LH treatment does not reverse testosterone levels completely, suggesting that there are age-related changes in Leydig cells that diminish their ability to produce testosterone (Chen et al. 2002).

Several of the intermediate pathways of autophagy and its intimate connection to the endosome pathway were originally worked out in rat Leydig cells by Xue-Ming Tang (Jing and Tang 1999; Tang et al. 1992). In the introduction of the 1999 paper is stated, "We found that the relative frequency of autophagy in Leydig cells is much higher than in any [of the other 32 tested] cell types". It was later hypothesized that autophagy modulates steroid production through degradation of mitochondria within Leydig cells (Jing and Tang 1995). This interaction went untested until recently where in a study by Li et al., a comparison of young versus old rat Leydig cells revealed that autophagy activity, in parallel to testosterone production, is reduced in the Leydig cells from old rats (24 months old) compared to young cells (3 months old) (Li et al. 2011). Furthermore, the authors demonstrated that Leydig cells from young animals are induced to produce lower levels of testosterone, similar to the levels produced by older cells, by knockdown of key autophagy genes or pharmacological inhibition of autophagy. Moreover, the overexpression of key autophagy genes in Leydig cells from old animals restored testosterone production to levels seen in young cells. This experiment validates that autophagy regulates steroid production in Leydig cells. Furthermore, the age-related decline in testosterone production is at least, in part, caused by an age-related decline in autophagy activity. Interestingly, caloric restriction, which is a potent inducer of autophagy throughout the body, can attenuate the age-related decline in testosterone and circulating lipoproteins seen in rodents (Chen et al. 2005). Similar studies in humans are difficult, but initial observations suggest that humans' testosterone response to caloric restriction mimics rodents (Cangemi et al. 2010). Whether or not autophagy modulates mitochondria numbers and therefore regulates steroidogenesis is still untested, but the insights for autophagy-dependent role in steroidogenesis are intriguing. In addition, whether lipid metabolism is dependent on autophagy in steroidogenic cells to modulate steroidogenesis is unknown. Studying a mouse with the conditional deletion of autophagy genes in adult Leydig cells is possible, and would provide models to test these hypotheses in an *in vivo* scenario.

1.7.2 Autophagy and Sertoli cells

The Sertoli cell was first described as a 'mother' cell by Enrico Sertoli in 1865, from whom the cell gets its name (Sertoli 1865). Enrico was working in a medical school at the time, and, perhaps luckily, was looking at human testes samples, which have much larger Sertoli cells, occupying 37% of the epithelium compared to the 12% in rodents (Hess and Renato de Franca 2005). Enrico's intuition to call the Sertoli cell a 'mother' cell is remarkable because he implied its function in poorly fixed tissues. A testament to the Sertoli cell function, many researchers today refer to the Sertoli cell as a 'nurse' cell for the developing sperm (Petersen and Soder 2006). Unlike the adult Leydig cell, which develops after testis formation, the Sertoli cell is present from the very beginning of cord formation (as described earlier) throughout life, providing a niche for the development and maintenance of male germ cells. In the adult testis, the Sertoli cell has numerous functions, all of which are necessary to maintain spermatogenesis (reviewed by Tsai 2005). As a summary, the Sertoli cell: 1) maintains the architecture of the seminiferous epithelium by extending cellular processes around differentiating germ cells; 2) metabolizes and delivers nutrients by metabolic exchange with germ cells and secretes tubular fluid into the lumen; 3) produces growth factors to inhibit spermatogonia to enter meiosis; 4) forms Sertoli-Sertoli junctions (tight, adherens and gap) that maintain the blood-testis-barrier; 5) produces growth factors to support germ cell differentiation; 6) forms complex networks of cellular junctions with individual germ cell populations physically moving them in a basal to adluminal direction; and 7) is responsible for the phagocytosis of dying germ cells and residual bodies formed during germ cell differentiation. Due to the intimacy between the Sertoli cell and sperm production, the number of functional Sertoli cells determines both testicular size and daily sperm production (Johnson et al. 2008).

The Sertoli cell goes through a terminal differentiation from an immature to functional Sertoli cell around the onset of puberty, marked by the increased secretion of FSH from the pituitary. Pronounced transitions in Sertoli cell morphology, biochemistry and the structure of the seminiferous tubule are associated with the Sertoli cell differentiation. Upon FSHR binding, immature Sertoli cells enter the cell cycle, become elongated and begin polarizing their membranes. Numerous genes are regulated by FSH that provide mechanistic explanations (McLean et al. 2002). The formation of tight junctions between adjacent Sertoli cells begins with the expression of claudins. Tight junctions inhibit further mitosis of Sertoli cells, as suggested by a reduction of their proliferative capacity unless they are disassociated (Steinberger and Steinberger 1971). Cell-contact inhibition and contribution of non-hormonal factors provide evidence for the general acceptance that functional Sertoli cells do not proliferate (Schlatt et al. 1996; Jégou 1992). These tight junctions form the 'blood-testis-barrier' that separates diploid cells from haploid cells (Smith and Braun 2012). As the adaptive immune system develops before the onset of spermatogenesis, the haploid spermatocytes are targeted and destroyed by leukocytes that infiltrate the tubule in the absence of the blood-testis-barrier, which are recognized as "non-self". FSH also induces Sertoli cells to begin producing seminiferous fluid, which transforms the immature tubule from solid testis cords to lumen-filled tubules. The formation of the blood-testis-barrier also seals off the tubule for direct access for many nutrients, and as such, the differentiating germ cells become dependent on the secretion of factors by the Sertoli cells. As the Leydig cells respond to LH, the concentration of testosterone increases, which bind to androgen receptors in Sertoli cells. The gene targets of androgen receptor has proven to be a complicated task, but the identification of extracellular matrix proteins, growth factors, a series of reproductive homeobox on the X chromosome (Rhox) genes and phagocytosis-promoting machinery are among the most influential on spermatogenesis (Maclean et al. 2005; Zhou et al. 2011b; MacLean et al. 2013).

Throughout spermatogenesis, the differentiating germ cells undergo blatant morphology transformations from round spermatocytes to spermatids that possess a rounded head and elongated tail. This requires cellular remodeling where much of the cytoplasm is packaged into cytoplasmic residual bodies that get removed during spermiogenesis via the phagocytosis of the material by Sertoli cells (Chemes 1986). Additionally, there is extensive apoptosis of differentiating germ cells that has been estimated to occur in upwards of 60% of germ cells in contact with Sertoli cells (Shaha et al. 2010). Both intrinsic and extrinsic initiation of apoptosis are observed, suggesting that a combination of factors regulate this loss. While it remains uncertain why high amounts of apoptosis occur, removal of these dying cells is done exclusively by the Sertoli cell via phagocytosis (Chemes 1986). Thus, it should be appreciated that the functional Sertoli cell must have a pronounced ability to metabolize phagocytized material.

The process of phagocytosis involves binding of the substrate, ingestion and subsequent degradation. The signal recognized by Sertoli cells on dying apoptotic germ cells is the "eat-me" signal, phosphatidylserine (PS), as demonstrated by the apparent increase in apoptosis after administering Annexin V, which binds to PS (Maeda et al. 2002). Further analysis revealed that the scavenger receptors SR-BI and CD-36 are expressed by Sertoli cells and responsible for binding PS found on residual bodies and dying cells (Nakanishi and Shiratsuchi 2004; Gillot et al. 2005). The co-receptors of tyrosine kinase receptor (MERTK), GAS6 and protein S (PROS1) are both implicated in the ingestion of PS associated bodies by macrophages and are produced by Sertoli cells (Xiong et al. 2008). After GAS6 and PROS1 bind to PS, they are coupled to MERTK and ingestion occurs. Studies on *mertk,* knockout mice show a reduced ability for Sertoli cell phagocytosis, suggesting that this pathway is conserved from macrophages (Xiong et al. 2008). Once ingested the phagocytized material enters the endosome pathway and ends, similar to autophagy, with the fusion to a lysosome (Oczypok et al. 2013). There is a body of evidence suggesting that autophagy is associated with this process. Recently, a phenomenon called "LC3-Associated Phagocytosis" was observed in macrophages and found to be responsible for the clearance of phagocytic vesicles containing *Listeria monocytogenes* (Lam et al. 2013). Recent studies using Sertoli cells and retinal pigmented epithelial cells, both "non-professional" phagocytes (Rabinovitch

1995), have characterized increased levels of autophagy that coincide with phagocytosis, suggesting that autophagy is utilized in the processing of phagocytized material (Yefimova et al. 2013; Kim et al. 2013). Furthermore, using microglia cells, considered to be another "non-professional" phagocyte, Lucin et al. demonstrated that depletion of BECN1 severely abrogates retromer trafficking and phagocytosis (Lucin et al. 2013). Additionally, a role for autophagy in regulating the expression of scavenger receptors on the surface of macrophages was observed, further linking autophagy and phagocytosis (Bonilla et al. 2013). The functional role of autophagy in phagocytosis is yet to be tested *in vivo*, but this groundwork provides evidence for the involvement of autophagy. Furthermore, the data includes both professional (macrophages) and non-professional phagocytes, suggesting that autophagy has a conserved function in phagocytosis. The use of conditional knockout alleles of key autophagy genes specifically in Sertoli cells is possible and would provide good models for testing these hypotheses.

1.8 Conclusions

I have highlighted several studies characterizing the activity of autophagy in the ovary and testis throughout development. Among these, the fertilized embryo, developing ovarian follicle and functions in steroidogenesis and phagocytosis provide developmental models to test the significance of autophagy in reproductive tissues. I have presented ample evidence that autophagy is a cellular mechanism to maintain homeostasis. Along this line, I propose that autophagy is a necessary cellular function within the developing reproductive tract. Furthermore, the abrogation of autophagic activity will inhibit the development and function of the tissues discussed. Moreover, I hypothesize that modulation of autophagy will provide useful models of reproductive disease.

While a subset of these studies discussed suggest that autophagic cell death is a mechanism of cell regulation, the evidence does not fully support such conclusions. However, the findings do warrant further investigation into the role of autophagy in the ovary and testis during cell death. The reproductive field is poised at a wonderful time to begin answering these questions utilizing conditional knockout and comparative approaches.

Copyright © Thomas Raymond Gawriluk 2014

AIMS OF THE DISSERTATION

Autophagy is an evolutionarily conserved process that is essential for energy homeostasis and the destruction of specific cytosolic components within individual cells. The overall aim of this thesis is to determine the function of autophagy during perinatal gonad development and folliculogenesis. The focus is the hypothesis that autophagy is a survival mechanism for germ cells. It became apparent early on, that this would not be feasible with my methods, but I uncovered several other phenotypes. In the following chapters of this dissertation, I present methodology to test the following hypotheses, listed below, and present the data obtained from these experiments. In chapter 5, I discuss how the results of each chapter demonstrates a conserved function, in addition to autophagy, for *Becn1* in testes and ovaries. Furthermore, I discuss the implications of this work in the field of reproductive biology and how these results will shape future experiments.

Specific Aims

In Chapter 2, the hypothesis tested is that autophagy is necessary for prenatal germ cell development and survival of oocytes. The specific aims were to:

- Characterize ovaries from *Becn1*-decficient and *Atg7*-knockout mice at postnatal day 1.
- Investigate the role of autophagy in primordial follicle formation by quantifying follicles.
- Determine whether autophagy mediates oocyte attrition or survival

In Chapter 3, the hypothesis tested is that autophagy is necessary for folliculogenesis and corpus luteum formation *and* steroidogenesis. The specific aims were to:

- Characterize Cyp19-iCre for use in deletion of *Becn1* and *Atg7* in the follicle and corpus luteum.
- Investigate the role of autophagy on corpus luteum formation and luteal cell steroidogenesis by quantifying progesterone production from pregnant mice.
- Determine the involvement of *Becn1* on cholesterol metabolism in luteal cells.

In Chapter 4, the hypothesis tested is that autophagy is necessary for Sertoli cell phagocytosis and thus, regulates spermatogenesis. The specific aims were to:

- Characterize the knockout of *Becn1* and *Atg7* specifically in adult Sertoli cells.
- Determine the role of autophagy on Sertoli cell function as mice age.

Copyright © Thomas Raymond Gawriluk 2014

CHAPTER 2: AUTOPHAGY IS A CELL SURVIVAL PROGRAM FOR FEMALE GERM CELLS IN THE MURINE OVARY.

Keywords: autophagy, fertility, beclin-1, atg7

Abbreviations used: PGC, primordial germ cell; PCD, programmed cell death; P, post-natal day; TUNEL, terminal deoxynucleotidyl transferase dUTP nick end labeling

Previously published:
Reproduction. 2011. 141(6): 759-765

Abstract

It is estimated that infertility affects 15-20% of couples and can arise from female or male reproductive defects. Mouse models have ascribed roles to over 100 genes in the maintenance of female fertility. Although previous models have determined roles for apoptosis in male and female fertility, we find that compromised autophagy within the perinatal ovary, through the loss of Becn1 or Atg7, results in the premature loss of female germ cells. Becn1(+/-) ovaries have a 56% reduction of germ cells compared with control ovaries at post-natal day 1, whereas Atg7(-/-) ovaries lack discernable germ cells at this stage. Thus autophagy appears to be a cell survival mechanism to maintain the endowment of female germ cells prior to establishing primordial follicle pools in the ovary.

2.1 Introduction

Oocyte development can be classically split into six broad steps: 1) colonization of the indifferent gonad by primordial germ cells (PGCs), 2) formation of oogonia, 3) meiotic arrest at prophase I, 4) primordial follicle formation, 5) follicle maturation, and 6) ovulation (Edson et al. 2009). Early female germ cell development encompasses the first 4 stages and occurs during fetal and peri-natal development. The fetal ovary is endowed with the greatest number of germ cells prior to entering meiotic arrest. After this stage, most female germ cell loss occurs either during the fetal/peri-natal window or from post-natal follicular atresia. Ovarian follicular atresia is a cell death event that occurs in more than 99% of mature follicles (Byskov 1978), and excessive follicular atresia is associated with premature ovarian failure, one of the most common causes of infertility in women (Matzuk and Lamb 2008; Anasti 1998). The loss of germ cells has been attributed, in part, to genes devoted to programmed cell death.

Programmed cell death (PCD), an important physiological process required for development, is classified as either: Type I (apoptosis), Type II (autophagy), or Type III (non-lysosomal vesiculate degradation). Autophagy is a conserved mechanism, from yeast to mammals, for bulk recycling of proteins and organelles (Klionsky 2000). This process is important for normal development, tissue/organ remodeling, and cell death/survival, and can be triggered under stress conditions such as nutrient deprivation. A wide array of diseases manifest from altered autophagy including: neurodegenerative disorders (e.g. Alzheimer's, Parkinson's, Huntington's diseases), liver disease, myodegenerative disorders, heart disease, inflammatory diseases, and cancer (Levine and Kroemer 2008). Initially, the proteins/organelles are sequestered by lipids called 'isolation membranes', which then encapsulate the targets with a double-membrane structure called the autophagosome. These autophagosomes then fuse with liposomes to degrade the internal components. The yeast autophagy (Atg) proteins responsible for this process are classified into 4 groups: 1) induction of autophagy (ATG1 protein kinase complex), 2) vesicle nucleation (phosphatidylinositol 3-kinases class III ‘PI3KC3’ lipid kinase complex), 3) vesicle expansion (ATG7-ATG12-ATG5 and ATG8 pathways), and 4) the Atg protein retrieval system (Maiuri et al. 2007). Beclin 1 (BECN1), the mammalian counterpart of the yeast ATG6 protein, is integral in the vesicle nucleation phase for autophagosome formation. BECN1 forms a complex with UVRAG (UV radiation resistance-associated gene) and BIF-1 (BAX-interacting factor-1) to regulate the PI3KC3 kinase complex and promote autophagosome formation (Takahashi et al. 2007; Liang et al. 2006). ATG7 is an E1-like protein that is required for the conjugation of ATG5-ATG12 and the addition of phosphatidylethanolamine to LC3/ATG8 (microtubule-associated protein light chain 3).

Previous genetic mouse models have revealed the importance of more than 20 genes that impact the germ cell populations or the establishment of primordial follicles in the murine ovary (Matzuk and Lamb 2002, 2008). Of these, three apoptosis-associated genes are known to impact germ cell numbers in the fetal-neonatal ovary: *Bcl-*x_L, *Bax*, and *Caspase-2* (Rucker et al. 2000; Greenfeld et al. 2007; Bergeron et al. 1998). BCL-X_L and BAX have been shown to govern primordial germ cell numbers after colonization of the fetal gonads, around E11.5- E13.5, when a wave of apoptosis reduces the gonocyte populations. In contrast, the developmental window of germ cell loss at the time of parturition may be dependent upon mechanisms other than apoptosis. Ablation of *Bcl-*x_L in the fetal ovaries after this initial wave of germ cell loss does not impact the primordial follicle pool in the murine ovary (Riedlinger et al. 2002). Several additional reports suggest that the ovary may rely upon alternative pathways of cell survival and cell death. Analysis of the mouse ovary between E19.5 and P2 revealed a 44%

reduction in the number of follicles during this window (Rodrigues et al. 2009). At this stage few germ cells or somatic cells were found to be apoptotic, whereas lysosome amplification and increased LAMP1 (lysosomal-associated membrane protein 1) expression occurred, suggesting a role for autophagy. During the germ nest breakdown and establishment of the primordial follicle pool, the germ cells may need to maintain energy homeostasis through autophagy. Autophagy can promote cell survival or lead to cell death, depending upon the context (Codogno and Meijer 2005). Therefore, we wanted to determine the effect of autophagy, through the genetic loss of Becn1 or Atg7, on the endowment of the peri-natal ovary as a pro-survival or pro-death mechanism.

2.2 Materials and Methods

2.2.1 Gene targeting and generation of Becn1 conditional knockout mouse

For the targeting vector, a 3 loxP plasmid vector (ploxP3-NeoTK) with PGK (phosphoglycerol kinase)-neomycin and PGK-thymidine kinase cassettes for positive-negative selection was used. Genomic DNA isolated from 129SvEv mice was used to amplify three regions of homology for the targeting arms: a 2.7 kb *Becn1* arm #1 (*Becn1* promoter sequence), a 3.0 kb *Becn1* arm #2 (promoter, exon 1, intron 1, exon 2, and a portion of intron 2), and a 2.0 kb *Becn1* arm #3 (intron 2 sequence). For the amplification, the AccuPrime Pfx was used according to manufacturer's directions to generate blunt PCR fragments that were gel purified (Gel extraction kit, Qiagen) and cloned into pBlunt vector (Invitrogen). For the electroporations, 25 µg of *NotI*-linearized DNA was resuspended in 25 µl Electroporation Buffer (Chemicon) and electroporated into 1 x 10^7 129SvEv ES cells using the GenePulser II (250 V and 500 µFd; BioRad) with 0.4 cm cuvettes. G418 selection (200 ng/ml) was started on day 1 after electroporation and continued thereafter; gancyclovir selection (2 µM) was performed on days 4-7 after electroporation. On day 12, 3 x 96-well plates were picked and expanded for cell stocks and DNA isolation. Clones were initially screened by pooled PCRs using LaTaq (Takara) with a 5' flanking reverse primer (5' CCC TAG CTG GCC TGG AAC TCA GAA ATC T 3') and neomycin-specific reverse primer (5' TAC CGG TGG ATG TGG AAT GTG TGC GA 3') set. The presence of the third loxP site was confirmed using flanking PCR primers (forward: 5' CAG GAG AAG TGC CAT GGT GCA TCC TCT T 3'; reverse: 5' CAA AGC CAA GGT TTC CAT GCT AAT GCC 3'). Individual clones were subjected to PCR confirmation from positive pools. Positive clones were confirmed by Southern blot diagnostics with an external 5' probe. Targeted ES cells were expanded and used for blastocyst injections at the Transgenic Animal Core facility at Texas A & M University.

2.2.2 Generation of mice for ovary collections

Beclin 'floxed' mice were generated by gene targeting in 129SvEv ES cells and will be detailed elsewhere. *Becn1* null alleles were generated through heterozygous breedings of *Becn1*$^{fln/+}$ and *MMTV-CreA* mice. Mice carrying homozygous floxed alleles and neomycin cassettes were confirmed by PCR of tail-snipped DNA. True floxed alleles were generated by crossing *Becn1*$^{fln/+}$ and *Ella-CreA* mice. *CreA*$^{+/-}$ *Becn1*$^{+/-}$ transgenic mice were generated through breeding of homozygous *MMTV-CreA* (Jackson Labs, 003551) and heterozygous *Becn1*$^{+/-}$ mice, or those heterozygous for a "null" Cre generated locus. *CreA* strain genotypes were confirmed using Jackson Labs Protocol for *Tg(MMTV-cre)1Mam*. ATG7$^{-/-}$ ovaries were provided by Dr Doug Green. All animal work was conducted using protocols approved by the Institutional Animal Care and Use Committee at the University of Kentucky.

2.2.3 Histological Follicle Counts

To assess follicle numbers, whole ovaries including oviduct and approximately 1cm uterus were collected from control (n=3), Becn1$^{+/-}$ (n=6), and Atg7$^{-/-}$ (n=4) ovaries and fixed in 4% (w/v) paraformaldehyde for at least 24 hours. After fixation, tissues were dehydrated, embedded in Paraplast (VWR International, West Chester PA), serially sectioned (8 μm), mounted on glass slides, and stained with Weigert's hematoxylin-picric acid methylene blue. A stratified sample consisting of every tenth section was used to estimate total number of primordial and naked germ cells (germ cells not surrounded by somatic cells) per ovary. Only oocytes with a visible nucleus were counted to avoid double counting. In addition, all follicles were counted without knowledge of the genotype of the animal.

2.2.4 Immunohistochemistry

Whole ovaries including oviduct and a small portion of the uterus were fixed in 4% (w/v) paraformaldehyde for at least 24 hours. After fixation, tissues were cryo-protected by washing for 1 hour in 10% sucrose, 1 hour in 20% (w/v) sucrose and at least 12 hours in 30% (w/v) sucrose at 4 ^{o}C. Ovaries were then embedded in O.C.T. Compound (Sakura, Tokyo, Japan), frozen using a liquid-nitrogen-isopentane bath, serially sectioned (15μm) and mounted on glass slides. Slides were then washed for 5 minutes with PBS and stained using ImmPRESS Reagent Kit – Anti-Rabbit IgG (Vector Labs, MP-7401) in combination with primary antibody (anti-BECN1 at 1:80 dilution (Santa Cruz, sc-11427)) overnight at 4^{o}C. We confirmed the specificity of the antibody in control and BECN1-deficient mammary glands (WAP-Cre; *Becn1*$^{fl/-}$) at lactation day 1. All sections were counterstained with Hematoxylin QS (Vector Labs, H-3404) and visualized using a Nikon Eclipse E400. Total Rabbit-IgG 1:200 dilution (Santa Cruz, sc-2027) was used as a primary antibody negative control.

2.2.5 Statistical Analysis

Differences in germ cell numbers were evaluated by one-way analysis of variance, with statistical significance assigned at $p < 0.05$. When a significant p value was obtained, Scheffe's test was used in the post hoc analysis. The SPSS (version 10) program was used to compile statistics from the obtained data. For microarray data, statistical analysis, ANOVA and Holm-Sidak pairwise tests were completed with Sigma Plot (Systat).

2.2.6 Microarray Data

Becn1 mRNA expression data was obtained from microarray experiments of oocytes from primordial, primary, secondary, small and large antral follicles obtained from B6SJLF1 animals. Data represents four replicates and bars = standard error, * $p<0.05$

vs Primordial, ** $p<0.05$ vs Secondary/Large Antral. Data comes from previously published microarray experiments found in NCBI GEO (GDS1266 and GDS1265) (Pan et al. 2005).

2.3 Results

Characterization of mRNA from different oocyte stages was possible due to the efforts of Pan et al, 2005. They isolated oocytes from different follicle stages (primordial, primary, secondary, small antral, and large antral), extracted total RNA from each set, generated biotinylated cRNA, and hybridized probes to the "Mouse Expression Set 430" MOE430A and MOE430B Affymetrix GeneChips (Pan et al. 2005). These arrays, which contain mouse maintenance genes as normalization controls, interrogate the expression levels of over 39,000 transcripts from the mouse transcriptome. From this data set, *Becn1* mRNA was found to be expressed at highest levels in the murine ovary within the primordial oocyte (**Figure 2.1**). With respect to stage, the highest relative expression levels were found in the primordial oocyte population (3200 avg) compared to primary (1500 avg), secondary (1500 avg), small antral (2000 avg), and large antral oocytes (1500 avg). *Becn1* mRNA expression did not differ between 1 month ovaries (4500 avg) compared to 2 month (5000 avg) and 7 month ovaries (5000 avg). *Atg7* mRNA expression was present at all oocyte stages from the primordial to the large antral stage but did not vary statistically (not shown). Protein analysis by immunohistochemistry revealed that BECN1 is localized to the follicle (**Figure 2.1**). BECN1 expression is not found in the cortex or medulla, but throughout the follicle (oocyte, granulosa cells, and theca cells). Since homozygous *Becn1* null mice (-/-) are embryonic lethal at E9.5 (Yue et al. 2003; Qu et al. 2003), we decided to examine hemizygous *Becn1* ovaries (+/-) to compare them with *Atg7*-deficient ovaries at post-natal day 1 (P1). Analysis at this timepoint was chosen because of the peri-natal lethality of ATG5- and ATG7-deficient neonates at P1 (Kuma et al. 2004; Komatsu et al. 2005). For analysis of Becn1, we generated a floxed beclin mouse model by gene targeting in embryonic stem cells, which harbor loxP sites around exons 1 and 2. A null allele for Becn1 was generated by crossing with the *MMTV-CreA* line, a Cre transgenic which is expressed in the ovary for germline-specific deletions (Wagner et al. 1997). Although this transgene is 'leaky', we previously used the *MMTV-CreA* model to perform an oocyte-specific deletion of a floxed *bcl-*x_L gene because of its extremely high efficiency of recombination (Riedlinger et al. 2002).

Compromised autophagy, through loss of ATG7 or a dose-dependent reduction of BECN1, reduces female germ cell populations in the post-natal day 1 (P1) ovaries. Morphometric analyses were performed to quantitate germ cells, similar to methods from our previous studies (Rucker et al. 2000; Riedlinger et al. 2002; Greenfeld et al. 2007; Borgeest et al. 2002). Quantitative analysis of germ cells in the P1 ovary revealed a BECN1-dependent reduction of germ cells (**Table 2.1**). Wild-type, control P1 ovaries had an average of 8870 germ cells (SEM=962; n=3), compared to an average of 4065 germ cells (SEM=476; n=6) in *Becn1*$^{+/-}$ hemizygous ovaries (*Becn1*$^{+/-}$, *MMTV-CreA; Becn1*$^{+/-}$, or *MMTV-CreA*; *Becn1*$^{fl/+}$). There was a high loss of fetuses with the *MMTV-CreA*; *Becn1*$^{fl/-}$ genotype associated with heart and brain defects at embryonic day 11.5-12.5. This was confirmed in subsequent breedings with the *EIIa-Cre* line as well, which have mosaic Cre expression beginning at the 8-cell stage of development. From over 100 collected neonates, only 2 survived to the P1 stage (expected 1:4 ratio). Histological examination of the mutant P1 ovaries showed an altered distribution and a reduction in primordial follicles compared to the control ovaries (*Figure 2.2*). Wild-type ovaries had a more uniform distribution of follicles, and were larger due to the presence of more germ cells and primordial follicles. To substantiate the role of BECN1 and autophagy in the maintenance of female germ cell pools, we also collected P1 ovaries from *Atg7*$^{-/-}$ neonates (n=4). ATG7-deficient ovaries had a loss of germ cells, and moreover, the altered appearance of the germ cells within the ovary made them impossible to quantitate (**Figure 2.3**).

2.4 Discussion

In the context of autophagy, there are 6 major steps associated with the process: 1) regulation of induction, 2) isolation membrane recruitment and vesicle nucleation, 3) vesicle elongation, 4) protein retrieval, 5) docking and fusion of autophagosome and lysosome, and 6) vesicle breakdown and degradation (Maiuri et al. 2007). BECN1 is involved with both nucleation and autophagosome maturation, whereas ATG7 is needed for vesicle elongation. Although autophagy can proceed through either ATG7-dependent or ATG7-independent pathways, these results demonstrate that female germ cells utilize both ATG7 and BECN1 for induction of autophagy for cell survival. Determination of germ cell numbers in ATG7/BECN1-deficient ovaries would clarify if alternative pathways are utilized. This study demonstrates that autophagy may be an important regulator of germ cell survival prior to formation of the primordial follicular pool.

In addition to this early window of germ cell loss, evidence is mounting that the atresia within the pre-pubertal murine ovary is dependent upon autophagy. Two recent studies highlight a non-apoptotic mechanism for loss of primordial follicle pools. Atretic oocytes from P1 to P28 wild-type rat ovaries were described has having apoptotic markers of active caspase-3 and positive staining for TUNEL as well as the autophagic markers of increased numbers of autophagosomes (Escobar et al. 2008). Of particular interest was that hallmark apoptotic characteristics, pyknotic nuclei and membrane blebbing, were never observed. In the pre-pubertal mouse ovary, apoptotic characteristics (nuclear condensation, caspase 3 activation, PARP1 'poly [ADP-ribose] polymerase 1' cleavage, and DNA fragmentation) were not correlated with primordial follicles that were lost from atresia (Tingen et al. 2009). *In vitro* analyses of murine pre-pubertal oocytes showed that both apoptotic and autophagic processes were involved in the cell death of the oocytes (Escobar et al. 2008; Lobascio et al. 2007b). The importance of autophagy in follicular atresia has been demonstrated across multiple species including: Drosophila, telostei, caecilians, stingray, dove, quail, sheep, rats, and humans (Gaytán et al. 2008; Santos et al. 2008; Rosales-Torres et al. 2000; Velentzas et al. 2007; Zarnescu 2004).

Autophagy has been demonstrated to have a crucial function immediately after parturition within hours of birth, when neonates experience a starvation period. This is a crucial timepoint at which the neonate must utilize its energy reserves before the suckling response triggers milk ejection from the mother for sustenance. Knockout studies from $Atg5^{-/-}$ and $Atg7^{-/-}$ mice have shown a perinatal lethality (die within 1 day of birth) associated with a loss of autophagy during this early starvation period (Komatsu et al. 2005; Kuma et al. 2004). A burst of autophagy occurs upon parturition, peaks in tissues within 12 hours, then returns to basal levels within 1-2 days. *In utero*, the autophagy-deficient fetuses are able to obtain metabolites through the placenta; however, amino acid levels within tissues and plasma from the neonates are reduced compared to control siblings. Thus, autophagy appears to be a requisite mechanism to maintain energy homeostasis within the neonate.

In the context of the fetal and neonatal ovary, regulation of autophagy may occur through the Kit ligand/c-Kit signaling pathway. Naturally occurring mutations of Kit ligand, *Steel Panda* (Sl^{pan}) and *Steel Contrasted* (Sl^{con}), have been shown to result in reduced germ cell levels and fewer oocytes in the murine ovary (Bedell et al. 1995; Huang et al. 1993). Addition of anti-Kit antibody to fetal or neonatal oocytes *in vitro* caused a dramatic reduction in their growth (Packer et al. 1994). C-kit has been localized by immunohistochemistry to female germ cells at 14 dpc (days post coitum) and 16 dpc, and in the oocyte in the P2 and P7 murine ovary (Kang et al. 2003). C-kit signaling traditionally is known to activate the PI3K-Akt-mTOR signaling pathway to promote cell survival, and suppression of this survival pathway leads to premature follicle activation and infertility as revealed in knockout studies (Reddy et al. 2009; Adhikari et al. 2010; Reddy et al. 2008). Since mTOR acts to suppress autophagy, the question then becomes: how can cells concomitantly activate Akt and autophagy pathways? This apparent contradiction may be reconciled by the notion that signaling can occur through two, distinct isoforms of the PI3K p110-beta catalytic subunit. For Akt activation, signaling primarily occurs through the PI3K p110-beta catalytic subunit; however, it has been recently demonstrated that the PI3K p110-beta catalytic subunit triggers autophagy through activation of the PI3K class III complex (Dou et al. 2011). A recently developed floxed PI3K p110-beta mouse model could be used to address the activation mechanism for autophagy in the developing ovary (Jia et al. 2008).

Regulation of autophagy also may occur through crosstalk with apoptosis proteins, since BECN1 contains a BH3-region that serves as a BCL-2 binding domain (Oberstein et al. 2007; Maiuri et al. 2007; Shimizu et al. 2004). *In vitro* abrogation of the BECN1-BCL-2/BCL-X_L interaction with the pharmacological mimetic ABT737 triggers autophagy by reducing available BCL-2/BCL-X_L (Maiuri et al. 2007). Similarly, *Bcl-2* siRNA in MCF-7 cells induces autophagy, whereas overexpression of BCL-X_L in CHO cells suppressed both apoptosis and autophagy (Akar et al. 2008; Kim et al. 2009). However, BECN1 and BCL-2 co-expression in HeLa cells did not demonstrate an effect of BECN1 on inhibiting the anti-apoptotic effects of BCL-2 (Ciechomska et al. 2009). Thus, while it is clear that BCL-2 and BCL-X_L can regulate autophagy, there is some discrepancy as to the role the BECN1 has on the integration of apoptotic signaling. Therefore, the susceptibility of cells to undergo apoptosis and autophagy can be linked to the free, unbound levels of the anti-apoptotic BCL-2 family members. Within the developing ovary, this regulatory mechanism does not seem to be relevant. The reduction of

BECN1 in the $BECN1^{+/-}$ ovary would result in an increase in the unbound BCL-2/BCL-X_L fraction, leading to a surfeit of germ cells. Since the opposite is occurring with the loss of germ cells, this suggests that autophagy is not functioning in an autophagic cell death role, but rather in a pro-survival role in the ovary. This mislabeling of autophagy as a programmed cell death pathway seems to be a prevailing view in the scientific community. Currently we are using different Cre lines to perform cell-specific deletions of Becn1 in the murine ovary to determine its role in follicle maturation and atresia. In the future, *in vivo* and *in vitro* models of atresia and premature ovarian failure should take into consideration the combined effects of apoptosis and autophagy.

2.5 Acknowledgments

This work was supported by startup funds provided by the University of Kentucky to Edmund B. Rucker. Amber N. Hale, University of Kentucky, generated the *Becn1*-floxed mouse, Jodi A. Flaws, University of Illinois, completed the follicle quantification, Christopher P. Dillon and Douglas R. Green, St. Jude Children's Research Hospital, provided the *Atg7* knockout ovaries. The authors wish to thank Melissa Johnson, St. Jude Children's Research Hospital Animal Imaging Center, for assistance with tissue collections and CheMyong Ko, University of Illinos, for assistance with the *in silico* microarray analysis.

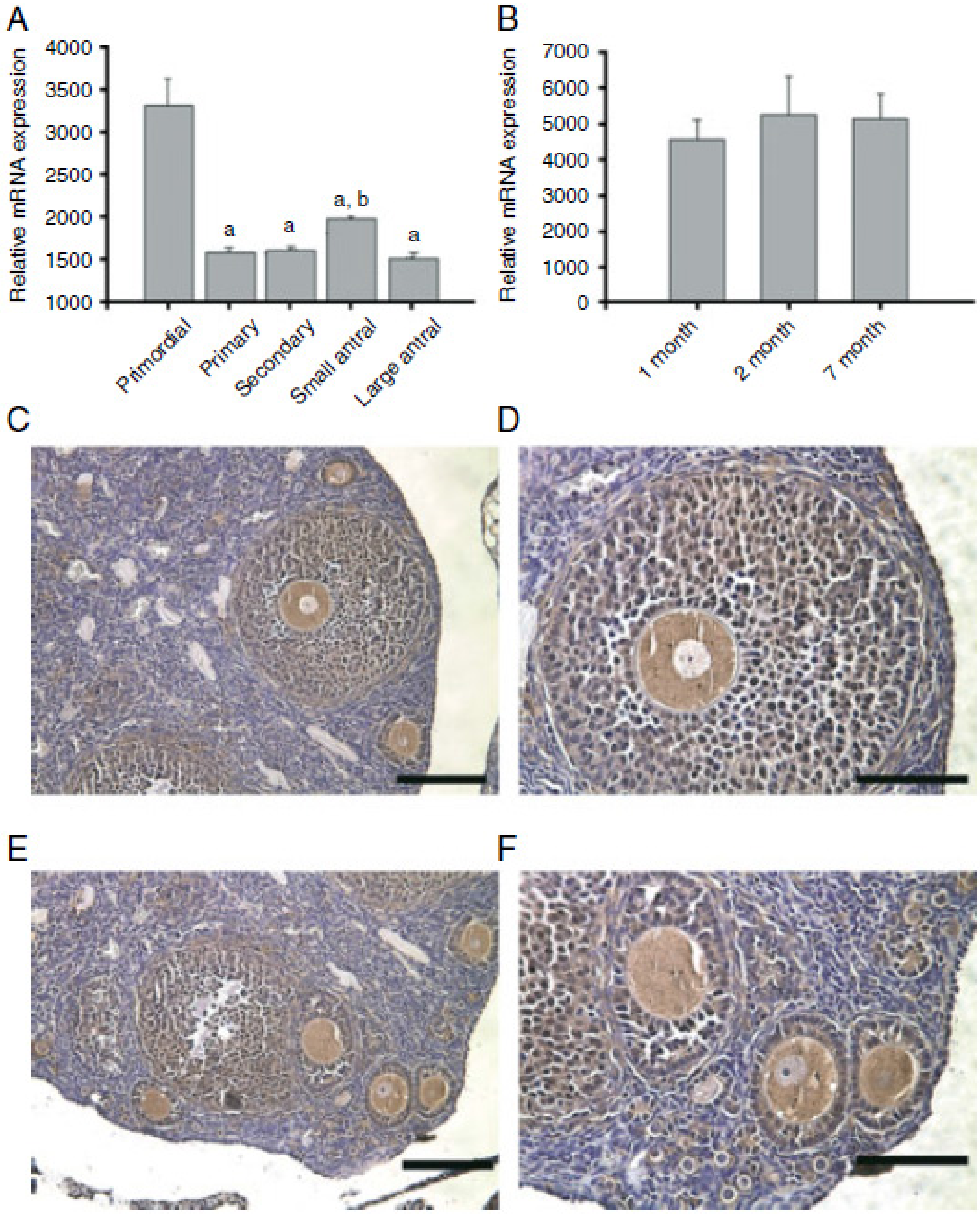

Figure 2.1 Expression profile of *Becn1* mRNA and protein in the murine ovary. (A) Oocyte Becn1 mRNA expression in different stages of follicles (n=3, error bar = S.E.M.; a, $p<0.05$ compared with primordial follicles; b, $p<0.05$ compared with primary, secondary, and antral staged follicles). (B) Ovarian *Becn1* mRNA expression at different stages of development from diestrus mice (n=2; error bars = S.E.M.). Figure was generated from a re-analysis of microarray data originally published by Pan et al. (2005). BECN1 immunolabeling in 3-month-old Sv129 ovary is present in all follicles (theca and granulosa cells) and oocytes, however absent from ovary epithelium. (C and E) 20X Magnification showing several follicles. (D) 40X Magnification of (B). (F) 40X Magnification of (E) showing several primordial and primary follicles. Graphs in (A) and (B) were generated by CheMyong Ko. Images were taken using Nikon E800, scale bar equals 100 μM.

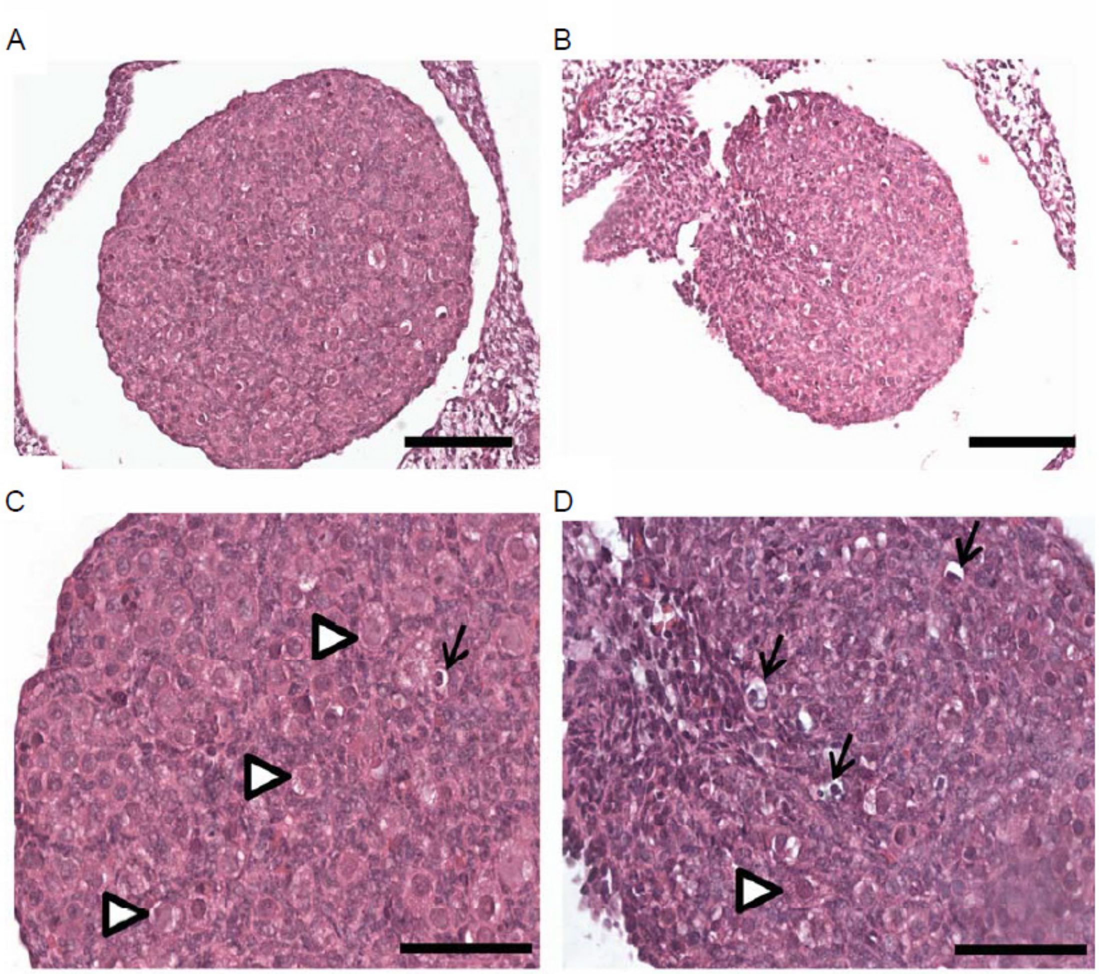

Figure 2.2. **Reduction of germ cells in *Becn1*-deficient ovaries**. Representative ovaries from *Becn1*$^{+/+}$ (a and c) and *Becn1*$^{+/-}$ females (b and d). Control ovary (a and c) shows a more uniform distribution of healthy germ cells than *Becn1*$^{+/-}$ ovary (b and d). Arrowheads: healthy germ cells; arrows: germ cells with 'pyknotic' nuclei. Images were taken using Nikon E800, scale bar equals 100 μM.

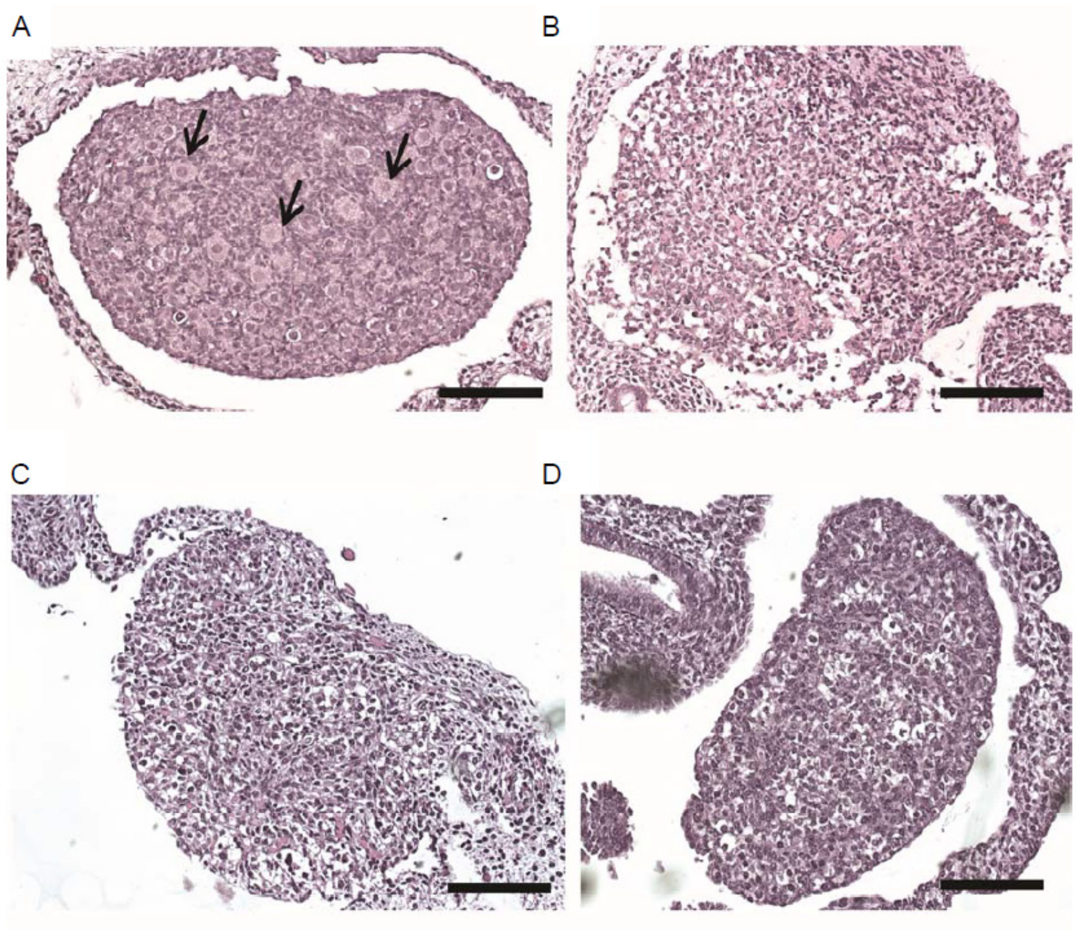

Figure 2.3. ***Atg7*-deficient ovaries demonstrate loss of germ cells**. (a) Postnatal day 1 (P1) control ovary contains healthy germ cells (marked by arrows). In contrast, P1 ovaries from three *Atg7*$^{-/-}$ females show loss of distinguishable germ cells (b–d). Images were taken using Nikon E800, scale bar equals 100 μM.

Table 2.1 Germ cell count in post-natal day 1 murine ovaries

Genotype of oocyte	Counts	Mean (S. E. M.)
Becn1$^{+/+}$	10,090	8870 (962)
	6970	
	9550	
Becn1$^{+/-}$	4680	4065 (476)
	2190	
	3610	
	3830	
	4430	
	5650	

$p<0.001$ between *Becn1*$^{+/+}$ and *Becn1*$^{+/-}$

Copyright © Thomas Raymond Gawriluk 2014

CHAPTER 3: BECLIN-1 DEFICIENCY PROMOTES PRETERM LABOR AND IS REQUIRED FOR PROGESTERONE SYNTHESIS IN THE CORPUS LUTEUM IN MICE

Keywords: corpus luteum, progesterone, autophagy, preterm birth, Beclin-1

Abbreviations Used: CL, corpus luteum; ER, endoplasmic reticulum; LH, luteinizing hormone; HDL, high-density lipoprotein; LDL, low-density lipoprotein; cKO, conditional knockout; P, pregnancy day; PBS, phosphate-buffered saline; TBST, Tris-buffered saline with Tween-20; HPG, hypothalamus-pituitary-gonadal; PFA/GLA, 4.0% paraformaldehyde / 3.5% glutaraldehyde; w/v, weight per volume; SDS-PAGE, sodium dodecyl sulfate polyacrylamide gel electrophoresis; cKO, conditional knockout

3.1 Introduction

The corpus luteum (CL) is an ephemeral endocrine gland responsible for the production of the pregnancy-maintaining hormone, progesterone (Gemmell 1995). After ovulation, the remainder of the ovarian follicle undergoes a rapid and remarkable amount of tissue remodeling and angiogenesis to form the CL. This developmental process, termed 'luteinization' is rivaled only by tumor growth (Reynolds et al. 2002). Steroid-producing cells, called luteal cells, terminally differentiate from the population of mural granulosa cells and theca cell in response to the luteinizing hormone (LH) surge, and in humans can produce upwards of 40 mg of progesterone per day during pregnancy (Carr et al. 1982; Deanesly 1930). Progesterone synthesized by luteal cells enters the female's circulation through the extensive microvasculature and binds to progesterone receptors throughout the body, regulating several pregnancy-related functions (e.g. endometrium activation, inhibition of myometrium, suppression of subsequent LH surges and mammary gland epithelium proliferation) (Conneely et al. 2002). In the mouse, the maintenance of pregnancy is entirely dependent on progesterone produced by the CL (Moor 1968). This is in contrast to humans who experience a transition to placenta-dependent progesterone production during mid-pregnancy (Malassiné et al. 2003). However, the mouse provides the ability to study progesterone synthesis throughout pregnancy in a single cell type.

Three enzymatic reactions synthesize progesterone from the substrate cholesterol. First, steroidogeneic acute regulatory protein (StAR) transfers cholesterol to the inner mitochondrial membrane (Lin et al. 1995). Second, cytochrome P450 side-chain cleavage (CYP11A1) cleaves cholesterol to generate pregnenolone (Stone and Hechter 1954). Third, pregnenolone exits the mitochondria and is then converted to progesterone by 3-beta hydroxysteroid dehydrogenase (3β-HSD) in the smooth endoplasmic reticulum (ER) (Rhéaume et al. 1991). Luteal cells have the ability to synthesize cholesterol from acetyl-coA, but it is generally accepted that acute steroidogenesis is dependent on the extracellular source from circulating low-density lipoprotein (LDL) and high-density lipoprotein (HDL) (Gwynne and Strauss 1982). Lipoproteins consist of a core of cholesteryl esters and triacylglycerides surrounded by a phospholipid monolayer and apolipoproteins (Alaupovic et al. 1972). A majority of the cholesterol obtained from LDL enters through receptor-mediated endocytosis by binding of apolipoprotein B to the LDL-receptor (LDLR) (Brown and Goldstein 1986). The subsequent hydrolysis of cholesteryl ester after endosome fusion to a lysosome, allows for the transport of cholesterol to cytosolic membranes by Niemann-Pick C1 (NPC1) and NPC2 (reviewed by Subramanian and Balch 2008). Alternatively, scavenger-receptor class B type I (SR-BI) specifically transports cholesteryl ester to the plasma membrane from HDL, which is then hydrolyzed to cholesterol by hormone-sensitive lipase (LIPE) (Acton et al. 1996; Cook et al. 1982). Intracellular free cholesterol can then be used directly for steroidogenesis or stored in lipid droplets after conversion to cholesteryl esters, a hallmark of luteal cells (Brown et al. 1979).

Autophagy is an evolutionarily conserved eukaryotic process that occurs at low constitutive levels in all cell types to sequester cytosolic material in a double membrane structure, termed the autophagosome, and to deliver the material to a lysosome for its breakdown and recycling into basic components (Klionsky and Emr 2000). In a recent study using rat Leydig cells, the testosterone-producing cell in the testis, the role of autophagy on age-related testosterone production decline was tested. Comparison of 3-month-old versus 24-month-old rat Leydig cells revealed that autophagy activity paralleled testosterone secretion (Li et al. 2011). Furthermore, the authors demonstrated that when they inhibited autophagy in young cells, lower levels of testosterone were secreted, and overexpression of an essential gene in autophagosome formation, Beclin-1 (*Becn1*), in old cells, restored testosterone secretion to that of young levels (Li et al. 2011).

Recent studies in multiple cell types have documented that autophagy can regulate free cholesterol stores by specifically targeting lipid droplets, a phenomenon called 'lipophagy' (Liu and Czaja 2013). Specifically, when mice are fasted for 24 hours, lipid droplets are observed within autophagosomes of hepatocytes (Singh et al. 2009a; Shibata et al. 2009). Additionally, the hepatocyte-specific, conditional-deletion of the essential gene in autophagosome membrane expansion, *Atg7*, resulted in the accumulation of lipid droplets and intracellular lipid concentrations (Singh et al. 2009a; Shibata et al. 2009). Lipophagy is yet to be explored in steroidogeneic cells. Furthermore, the mechanism linking testosterone production in Leydig cells to autophagy remains unknown.

I previously made the observation that BECN1 is present in corpora lutea of mice suggesting that it might also regulate steroidogenesis in luteal cells. In order to examine the significance of autophagy in the CL, I took advantage of the power of mouse genetics to generate mice with conditional knockout alleles for *Becn1* or *Atg7,* specifically in luteal cells. First, we wanted to determine if disruption of autophagy would decrease the amount of progesterone produced, as suggested by the Leydig cell study. Second, we wanted to determine if ablation of autophagy would abrogate lipid metabolism and subsequent progesterone production. These results suggest that BECN1 and ATG7 have different functions in luteal cells, and furthermore that BECN1 deficiency in luteal cells inhibits progesterone production resulting in preterm labor and abortion.

3.2 Materials and Methods

3.2.1 Mice

Becn1-floxed (Gawriluk et al. 2011), *Atg7*-floxed (kind gift from Q. Wang) (Komatsu et al. 2005), *CYP19A1-iCre* (kind gift from C. Ko) (Fan et al. 2008b), *GFP-LC3* (Riken #RBRC00806) (Mizushima and Yamamoto 2004), *CAG-CAT-EGFP* (kind gift from K. Wagner) (Kawamoto et al. 2000) mice were all on a 129/Sv and B57BL/6 mixed background. Conditional knockout females were generated by crossing $Becn1^{fl/\Delta}$; $CYP19A1\text{-}iCre^{+}$ or $Atg7^{fl/fl}$; $CYP19A1\text{-}iCre^{+}$ males to $Becn1^{fl/fl}$ or $Atg7^{fl/f}$ females, respectively. Controls females were littermates that did not carry the *CYP19A1-iCre* allele. The nucleotide sequence of *iCre* is homologous to the sequence for Cre-recombinase altered for mammalian codon bias, aka codon-improved Cre (Shimshek et al. 2002). All animals were genotyped using genomic DNA isolated from tail snips and alleles were detected by previously published PCR assays (see mouse strain references above). All mice were housed in a University of Kentucky DLAR facility, subjected to a 14:10 hour light:dark cycle and regular chow and water was available *ad libitum*. All animal procedures were compliant under the approved University of Kentucky IACUC protocol, 2008-0372.

3.2.2 Determination of Estrus Stage

All females involved were checked for stage of estrus cycle, by vaginal lavage technique (Caligioni 2009), at least 14 days prior to mating. Briefly, vaginal lavage was performed daily, between 0800 and 0900, by flushing the vagina with 0.9% sodium chloride. The samples were collected in a 24-well plate and examined, imaged and scored using a microscope with a 10x objective. Diestrus was determined by the presence of nucleated epithelial cells and the highest density of leukocytes. Proestrus was determined when the sample consisted predominately of nucleated epithelial cells. Estrus was determined by the presence of a high density of anucleated, cornified epithelial cells; whereas metestrus was identified by the presence all three cell-types: leukocytes, cornified and nucleated epithelial cells.

3.2.3 Fertility assays

Two to three females of ages 8 weeks to 6 months old were placed with a single proven wild type C57BL/6 male. Each morning females were checked for the presence of a seminal plug and, if present, were separated into a new cage (Pregnancy day 0.5). Every morning starting on P10.5 females were palpitated for fetuses and to determine if they were pregnant. The morning at which either a litter was present or the fetuses were no longer palpitated was considered the end of gestation. The ability to get pregnant, have a litter, size of litter born and last day of gestation were all recorded for analysis.

3.2.4 Exogenous progesterone administration

At 0900 each morning, pregnant females were subcutaneously injected with 1 mg progesterone (Sigma-Aldrich, P0130) dissolved in 100 µL sesame oil (Sigma-Aldrich, S3547). Alternatively, 100 µL of sesame oil (vehicle) was injected into separate females to serve as controls. These injections began on P10.5 and continued each morning until P16.5 for a total of 7 injections.

3.2.5 Collection of PMSG-primed granulosa cells

Granulosa cells were routinely collected from PMSG-primed animals as described (Mann et al. 1991). Briefly, 21-23 day old mice were injected IP with 5 IU PMSG (Calbiochem, 367222) at 1200 to stimulate folliculogenesis. Forty-eight hours later, ovaries were dissected, cleaned and incubated in sucrose/EGTA media for at least 10 minutes to facilitate separation into individual cells. Granulosa cells were released from follicles by poking follicles with 28-gauge needles. The cell suspension was filtered through 40 μM nylon mesh to remove oocytes. Granulosa cells were then pelleted, flash frozen in liquid nitrogen and stored at -80°C until analysis.

3.2.6 Tissue and blood collection

To control for any circadian controlled genes and/or proteins, all mice were euthanized between hours 1300 and 1500 on the developmental day indicated. Mice were euthanized by cardiac exsanguination via 18ga needle (see blood collection) after being anesthetized with Avertin (0.25 mg per g body weight) by IP injection. Reproductive tracts and number 4 inguinal mammary glands were removed and washed briefly in ice cold PBS and immediately processed as detailed in section 3.2.9. Reproductive tracts were trimmed of fat and ovaries were removed from their bursa, weighed, then either assigned into one of two groups: histology or molecular analysis. For routine histology, ovaries were placed into fresh, ice cold 4% (w/v) paraformaldehyde for 6 to 16 hours. However, for GFP-LC3 analysis immediate fixation was needed. Females were first transcardally perfused at a rate of 20 ml per minute with ice-cold 10% (w/v) sucrose for 3 minutes, followed by fresh 4% (w/v) paraformaldehyde for 5 minutes. Ovaries were dissected out and post-fixed for routine histology. For RNA, protein or lipid analysis, the corpora lutea were carefully dissected away from the ovary using #5 fine-tipped forceps under a stereoscope and flash frozen in liquid nitrogen.

For serum collections, blood collected during exsanguination was transferred to a 2 mL round-bottom tube, incubated for 90 minutes at room temperature to allow for clotting and centrifuged for 15 minutes at 1,000 x *g*. Serum was removed and transferred to a new 1.5 mL tube and stored at -20°C.

For plasma collections, approximately 50 μL of blood was collected every other day from alternating submandibular venous beds using a 5 mm lancet (Goldenrod, Medipoint, INC.). Blood was immediately mixed with EDTA, to a final concentration approximately 0.01M, to prevent clotting and then centrifuged for 15 minutes at 1,000 x *g*. Plasma was removed and transferred to a new 1.5 mL centrifuge tube and stored at -80°C.

3.2.7 Tissue preparation and histology

For frozen sections, ovaries and female reproductive tracts were washed with PBS (3 changes 15 minutes each) and cryo-protected by placing them into 10, 20 and 30% (w/v) sucrose solution until the tissues sunk. Cryo-protected tissues were blotted dry, transferred to a mold filled with Tissue-Tek O.C.T. Compound (Sakura Finetek USA, Inc.) and then immediately flash-frozen in an isopentane/dry-ice slurry. Frozen tissues were stored at -80°C until sectioned. Afterward, 5 µm sections were obtained using a high-profile blade (Leica 818) on a Leica CM1850 cryostat, with temperature set between -22 *and* -20°C and blade clearance angle of 5.5°.

For paraffin sections, fixed ovaries were washed with PBS (3 changes, 15 minutes each) and dehydrated by transferring them through an ethanol gradient: 50% (w/v) for overnight, 70% (w/v) for storage. Processing was done using a rapid microwave processor of 100% ethanol for 1 hour, 100% isopropanol for 1 hour, vacuum dried, and infiltrated with molten paraffin for 1 hour and finally embedded into molds. Sections (5 µM) were placed onto gelatin-subbed slides and stored at room temperature. Sections were deparaffinized with xylene, rehydrated and then either stained with hematoxylin and eosin for routine analysis or processed for immunohistology.

For immunofluorescence, sections were subjected to antigen retrieval by treatment with 10mM sodium citrate pH=6.0, incubated at 95°C for 20 minutes. Sections were washed three times with PBS, then incubated in PBS with 0.2% (w/v) Triton-X 100 for 20 minutes for membrane permeabilization, followed by three more washes in PBS. Slides were blocked with 10% BSA in PBS for one hour at room temperature and then incubated with primary antibody diluted with 3% (w/v) BSA in PBS overnight at 4°C. (see **Table 3.1** for dilutions). The following day, slides were washed with PBS three times, incubated with diluted secondary antibody for 1 hour at room temperature, washed with PBS three times and mounted with Prolong Gold anti-fade media containing 4',6-diamidino-2-phenylindole (Life Technologies, P-36931).

3.2.8 Oil Red-O staining

Paraformaldehyde-fixed tissue was cryoprotected by immersion into 30% (w/v) sucrose at 4°C until the tissue sunk, usually overnight. Tissue was blotted dry, flash frozen into OCT (Sakura, 4583) with a isopentane / dry ice bath, sectioned to 5µM using high-profile blades (Leica, 818) at -18 to -23°C, placed onto gelatin-subbed slides and allowed to air dry for at least one hour. Dried sections were washed in PBS to remove OCT, incubated in 60% isopropyl alcohol for 5 minutes, stained with freshly prepared 0.15% (w/v) Oil red-O for 10 minutes, washed in 60% isopropyl alcohol, counterstained with hematoxylin and mounted with glycerol jelly.

3.2.9 Mammary gland whole mounts

The number 4 mammary gland was carefully removed from euthanized females, washed several times in PBS and mounted onto Superfrost plus charged slides. Mounted glands were placed into Carnoy's fixative (60% ethanol, 30% chloroform, 10% acetic acid) for 12-18 hours at room temperature. Glands were washed in 70% ethanol (twice, 15 minutes each), 50% ethanol (twice, 15 minutes each), distilled water (three times, 15 minutes each) and stained in carmine alum overnight at 4 ^{0}C. Glands were dehydrated, cleared in xylenes and mounted with Permount until imaged.

3.2.10 Hormone profiling

All hormones were analyzed by the Ligand Assay and Analysis Core run by Center for Research in Reproduction at the University of Virginia, School of Medicine, which is funded by the National Institute of Child Health and Human Development through a U54 Center Grant (U54-HD28934). Estradiol was measured by ELISA (Calbiotech, INC.), progesterone by radio-immune-assay (Siemens) and FSH and LH together by Milliplex MAP (Millipore).

3.2.11 Immunoblotting

Tissue or cells were subjected to ice-cold RIPA buffer (with freshly added protease/phosphatase inhibitors, Santa Cruz, sc-24948), sonicated (3 to 5 cycles of 40% duty cycle, magnitude of 4, 10 seconds followed by 30 seconds on ice), rocked for 30 minutes at 4°C and centrifuged 10,000 rpm for 10 minutes at 4°C to pellet the insoluble fraction. The soluble fraction was collected and total protein quantified by bicinchoninic acid assay (Thermo, 23225).

Twenty-five µg of total protein per sample was denatured in Laemmli buffer for 10 minutes at 95°C and separated by SDS-PAGE on a 12% tris-acrylamide mini-gel. Granulosa cell extracts were first precipitated by 15% trichloroacetic acid / 0.02% sodium deoxychlorate to concentrate the lysate. Separated proteins were transferred to a PVDF membrane with 0.45 µM pores (GE Healthcare, RPN303F) overnight (~16 hours @ 70mV) at 4°C. Transferred proteins were visualized by staining with Ponceau-S and membranes trimmed.

The membrane was blocked using 5% (w/v) skim milk in TBST for 1 hour at room temperature. Primary antibody diluted in 5% (w/v) skim milk in TBST was added to membrane and allowed to incubate overnight (~16 hours) in a 4°C cold room on a rocker. The membrane was washed three times with TBST for 5 minutes each and then HRP-conjugated secondary antibody diluted in 5% (w/v) skim milk in TBST was added and allowed to incubate for 1 hour at room temperature with agitation. Membranes were washed 3 times with TBST for 5 minutes. Secondary antibody was detected using Pierce ECL Plus substrate (Thermo, 32132, 1:1 dilution) and detected by CCD camera and specific band intensities were digitally quantified. For multiple antigen detection, membranes were stripped with 0.2M Glycine, 1% Tween-20, 0.1% SDS, pH=2.2 and then re-probed with new antibodies. Antibodies and dilutions used can be found in **Table 3.1**.

3.2.12 Real-time PCR

RNA was extracted from snap frozen tissue using TRIzol reagent as per manufacturer's protocol for high proteoglycan samples (Life Technologies). Total RNA was subjected to DNase (Invitrogen), as per manufacturer specifications, to remove any genomic DNA that was co-precipitated and then cleaned up on RNeasy spin columns (Qiagen). Total RNA was quantified by nanodrop and analyzed by bioanalyzer (Agilent). Only RNA with a RNA Integrity Number (RIN) greater than 5 was used. Total RNA (500 ng) was used for first-strand synthesis to create cDNA (Quanta Biosciences). Detection of specific mRNA was then performed on samples in triplicate using SYBR-green PCR and quantified by ΔΔCt method. Primers for specific genes can be found in **Table 3.2**.

3.2.13 Electron Microscopy

Two ovaries from each P13.5 WT and Becn1 (fl/Δ) mice were collected and used for routine preparation of transmission electron microscopy under supervision from the University of Kentucky Imaging Facility. Briefly, tissues were quickly dissected out and washed several times in ice-cold PBS. Next, tissues were diced with a razorblade to ~1 mm^3 cubes while in a droplet of freshly prepared 4% (w/v) paraformaldehyde / 3.5% (v/v) glutaraldehyde in 0.1 M cacodylate buffer (PFA/GLA). Following, tissue pieces were incubated in PFA/GLA for 2 hours at 4°C until fixed. After the first fixation, tissue pieces were washed four times with 8% (w/v) sucrose before post-fixing with 1% (w/v) OsO_4 for 1.5 hours at 4°C. After dehydration through ethanol into propylene oxide, tissues pieces were infiltrated and embedded into Eponate 12 (PELCO). Embedded tissue pieces were sectioned to ultrathin slices of about 70 nm using a Reichert Ultracut E, mounted on copper grids, stained with uranyl acetate followed by lead citrate and observed by transmission electron microscopy (Philips Tecnai Biotwin 12).

3.2.14 Statistics

All statistics were performed in SigmaPlot 12 after consultation with the Applied Statistics Laboratory at the University of Kentucky. A two-way ANOVA was used with Holm-Sidak post-hoc testing between groups for comparisons with two variables. For all other comparisons, the statistical test used is indicated in the text. I was unable to run a repeated-measures ANOVA for the daily progesterone data due to missing data from several time points. During collections, if a mouse bled more than 4 drops of blood the next collection needed to be skipped to comply with IACUC; thus, a two-way ANOVA for genotype and day was used to analyze the data.

3.2.15 Imaging

All slides were imaged on an Olympus IX-71 microscope equipped with a DP72 CCD camera (Olympus). Images were edited in Photoshop (Adobe) to subtract background field.

Table 3.1 Antibodies Used

Antigen	Species Raised in	Manufacturer (Product No.)	Dilution Used	Application
GFP	Chicken	Aves Labs (GFP-1020)	1:500	IF
BECN1	Rabbit	Santa Cruz (sc-11427)	1:2,000	WB
LC3	Rabbit	MBL (PM036)	1:2,000	WB
SQSTM1	Rabbit	Enzo (PW9860)	1:2,000	WB
StAR	Rabbit	Dr. Buck Hales – UIUC	1:10,000	WB
Actin	Rabbit	Sigma (A2066)	1:10,000	WB
Secondary Antibodies				
Chicken IgY (H&L)	Goat	Invitrogen (A-11039)	1:1,000	IF
Rabbit IgG (H&L)	Donkey	Rockland (611-703-127)	1:10,000	WB

Table 3.2 Real-time PCR Primers**Target**	**NCBI Ascension**	**Fwd Primer (5'-3')** **Rev Primer (5'-3')**	**Amplicon Size (bp)**
Scarb1	NM_016741	TGC CCA TGC CGA GAG TCT CAG AGG CGC ACC AAA CCT	60
Ldlr	NM_010700	AGG CTG TCC CCC CAA GAC GGA GAT GCA CTT GCC ATC CT	64
Lipe	NM_010719	CGC TGG AGG AGT GTT TTT TTG CAG TTG AAC CAA GCA GGT CAC A	66
Hmgcr	NM_008255	TGT TCA CCG GCA ACA ACA AG TGC TCA GCA CGT CCT CTT CA	72
Inisg1	NM_153526	CGG CAG CGG CTG TTG GGT TCT CCC AGG TGA CTG TCA	58
Star	NM_011485	CCG GAG CAG AGT GGT GTC A GCC AGT GGA TGA AGC ACC AT	65
Cyp11a1	NM_019779	CCA GTG TCC CCA TGC TCA AC GCA TGG TCC TTC CAG GTC TTA G	73
Hsd3b1	NM_008293	CCA GGC AGA CCA TCC TAG ATG TGG CAC ACT GGC TTG GAT AC	
Akr1c18	NM_134066	TGA TTG CCC TTC GCT ACC A TCT CTG ATT CTC TCC TCA TTG AAA CTC	75
Lhcgr	NM_013582	GAC GCT AAT CTC GCT GGA GTT GTA GGA TGA CGT GGC GAT GA	172
Prlr (long)	NM_011169	GCG TTC TTT GCA AGA AGT GCT CCA GGT GGT GAC TGT CCA TT	243
Prlr (short)	NM_001253781	GGC TCT GAT AGA GCT CCC TG GCA ATA GAT CAG AGG CTC CCT TC	156
Becn1	NM_019584	TTT TCT GGA CTG TGT GCA GC GCT TTT GTC CAC TGC TCC TC	171
Atg7	NM_001253717	ATG CCA GGA CAC CCT GTG AAC TTC ACA TCA TTG CAG AAG TAG CAG CCA	349
Pecam1	NM_008816	CCA AGG CCA AAC AGA AAG GGA GCC TTC CGT TCT	300
Acat1	NM_144784	TGG GCG CAG GTT TAC CTA TT TTC CTG AAG CAC AAA CCT TGT TT	63
Scp2	NM_011327	CCC TCA GTC GGC CTT CTT TC ATG GCC AGT CCC ATG TTA CC	60
Npc1	NM_008720	TCA GTG TTG CGG TGG TGA AC ACG AAT CGT TTG GCA TTG AGA	69
Npc2	NM_023409	TCC CTG TCA GCT GCA CAA AG TGA GTG CCG CTG GTA AAG GT	63
Vegf	NM_001025250	CAT CTT CCA GGA GTA CCC CGA CAC TCC AGG GCT TCA TCG TT	81

3.3 Results

3.3.1 Disruption of Becn1 in mouse luteal cells

In order to analyze the role of autophagy in the corpus luteum (CL) I generated mice with conditional knockout (cKO) alleles for *Becn1* in luteal cells. Mice carrying one floxed and one null allele of *Becn1* (*Becn1*$^{fl/\Delta}$) were crossed with Tg(CYP19A1-cre)1Jri (*Cyp19-iCre*) mice to generate parental strains (Fan et al. 2008a; Gawriluk et al. 2011). Expression of *Cyp19-iCre* is restricted to granulosa cells of primary and secondary follicles that terminally differentiate into both large and small luteal cells after ovulation in rodents (Stocco et al. 2007). I bred the parents such that Cre was passed solely by the father to generate two experimental strains: 1) *Cyp19-iCre*; *Becn1*$^{fl/fl}$ (Becn1(fl/fl) cKO) and 2) *Cyp19-iCre*; *Becn1*$^{fl/\Delta}$ (Becn1(fl/Δ) cKO) (**Figure 3.1 A**). The siblings of the experimental strains that did not carry Cre were used as the control strain, or wild-type (WT), and unless otherwise specified, the data represent pooled WT genotypes. Mice were born at the expected Mendelian ratios and both males and females were otherwise healthy. I performed Western blot analysis to detect BECN1 protein and SQSTM1 in granulosa cells collected from PMSG-primed WT and cKO siblings as stated in the material and methods (**Figure 3.1 C**). BECN1 protein levels were decreased as expected in both Becn1(fl/fl) cKO and Becn1(fl/Δ) cKO with almost 75% depletion of BECN1 in Becn1(fl/Δ) cKO compared to WT (**Figure 3.1 D**). The decrease in BECN1 observed is greater than *Becn1*$^{fl/\Delta}$ control mice that only have a single allele, suggesting that both the Becn1(fl/fl) cKO and Becn1(fl/Δ) cKO have more than 50% allele recombination. The turnover of the protein SQSTM1, also known as p62, is autophagy-dependent and can be used to monitor autophagy, such that an accumulation of SQSTM1 indicates inhibition of autophagy and vice-versa (Bjørkøy et al. 2005; Ichimura et al. 2008). As expected, the deletion of *Becn1* caused an almost 3-fold increase in SQSTM1. Becn1(fl/fl) cKO and Becn1(fl/Δ) cKO have a similar increase in SQSTM1 protein compared to the wild-type strain, supporting that autophagy is equally inhibited in both strains after gene ablation (**Figure 3.1 D**). The data demonstrate that there is protein reduction and a functional response, providing evidence of gene deletion in PMSG-primed granulosa cells.

Previous reports using the *Cyp19-iCre* mouse have shown variable Cre expression in follicles of naturally cycling animals (Hsieh et al. 2011; Bennett et al. 2012). To determine if Cre expression is extensive enough in the CL of natural cycling animals, I independently crossed Becn1(fl/Δ) cKO onto a *CAG-CAT-EGFP* Cre-reporter background (Kawamoto et al. 2000). I chose to look at only Becn1(fl/Δ) cKO mice because of the more robust BECN1 depletion that occurs in granulosa cells compared to Becn1(fl/fl) cKO. In cells expressing Cre, a floxed chloramphenicol acetyltransferase (CAT) gene recombines allowing for enhanced green fluorescent protein (EGFP) gene expression. In addition, conditional deletion of *Becn1* also occurs and allows for the determination of cell viability, post gene ablation. Epi-fluorescent examination of ovaries from pregnancy day (P) 8.5 indicated prominent GFP expression in the CLs of *CAG-CAT-EGFP*$^{+}$*; Cyp19-iCre; Becn1*$^{fl/\Delta}$ but not in *CAG-CAT-EGFP*$^{+}$*; Becn1*$^{fl/\Delta}$ (**Figure 3.1 B**). Immunofluorescence for GFP on P8.5 tissue sections supports that recombination was robust throughout the CLs of Becn1(fl/Δ) cKO females (**Figure 3.1 G, H, J, K**). I detected GFP in both large and small diameter cells, indicating that recombination occurred in both large and small luteal cells. No recombination was detected in mammary glands, uterus or placenta, which is supported by previous reports using the *Cyp19-iCre* mouse (data not shown) (Fan et al. 2008b, 2008a). Thus, the conditional deletion paradigm is viable for examination of the function of *Becn1* in luteal cells.

3.3.2 Becn1 is necessary to maintain of pregnancy

I next sought to test the effectiveness of each knockout at impairing autophagy in the CL during pregnancy. I performed Western blot analysis for BECN1, SQSTM1, LC3 (~18 and 16 kDa), and StAR (~30 kDa) on CLs isolated from P8.5 ovaries (**Figure 3.2A**) and quantified the relative band intensity compared to ACTIN (**Figure 3.2B**). Both *Becn1* cKO strains had an approximate 50% reduction in BECN1 compared to WT. This amount of reduction is an expected result, because granulosa-derived luteal cells are only approximately 40% of total population and other cells in the CL express BECN1 (e.g. pericytes, endothelial cells, lymphocytes and theca contribution) (Lei et al. 1991). Both *Becn1* cKO strains had a nearly 5-fold increase in total SQSTM1 protein compared to WT. Microtubule associated protein 1B light chain 3 (LC3) is a protein that incorporates into the expanding autophagosome membrane. During expansion, the cytoplasmic form (LC3-I, ~16 kDa) is processed to the membrane form (LC3-II, ~14 kDa) by conjugation to phosphatidyl-ethanolamine (PE) found in the isolation membrane (Kabeya et al. 2000). This allows for an estimate of autophagosome quantity and autophagic flux within a tissue by Western blot. LC3-I was increased almost 3-fold in both *Becn1* cKOs compared to WT. No LC3-II was detected in any CL sample, suggesting that LC3-II does not accumulate. Taken together, the accumulation of SQSTM1 and LC3-I support that autophagosome formation is impaired in Becn1(fl/fl) cKO and Becn1(fl/Δ) cKO corpora lutea.

To determine if luteal cell differentiation occurs, I examined steroidogenic acute regulatory protein (StAR). StAR regulates the rate-limited step by transporting cholesterol from the outer to inner mitochondrial membrane (Black et al. 1994). Importantly, StAR expression was induced 5-fold upon luteinization and remained elevated throughout pregnancy (Pescador et al. 1996). StAR protein in both *Becn1* cKOs was comparable to WT. Thus, the data suggest that production of StAR is unaffected by gene ablation.

To establish that ovulation, fertilization and implantation are similar between the experimental strains, I examined litter size at P8.5. The number of implanted fetuses at P8.5 was equal for all strains, implying that all earlier steps are unaffected by gene ablation (**Figure 3.2 C**). The mass of ovaries at P8.5 was also unaffected by gene ablation, suggesting that cell composition is similar (**Figure 3.2 D**).

I next examined the effect of *Becn1* ablation on pregnancy success. 8- to 26-week-old female mice were mated with wild-type male mice to determine the length of gestation for each strain. The male studs carried non-floxed, wild-type alleles to eliminate any effect of recombination that might occur outside of the ovary, specifically in the placenta and uterus. All strains achieved pregnancy at similar rates, as detected at P5.5 (data not shown); however, Becn1(fl/fl) cKO and Becn1(fl/Δ) cKO mice cannot maintain pregnancy having early parturition and abortion, respectively. To determine the day of parturition in WT and Becn1(fl/fl) cKO, I observed pregnant mice daily for the presence of pups as described in the materials and methods (**Figure 3.2 E**). WT mice gave birth on P18.95 ± 0.12 and Becn1(fl/fl) cKO had a 10% reduced gestation length compared with WT to 17.08 ± 0.25 days ($p<0.001$, Dunn's multiple comparison test, data presented as mean ± s.e.m.). Furthermore, no litter born from a Becn1(fl/fl) cKO mother before P18.5 survived. Becn1(fl/Δ) cKO mothers had a more drastic phenotype and never give birth to litters, despite following females visibly pregnant at P10.5 (n = 28 pregnancies).

Following up on the Becn1(fl/Δ) cKO, I determined when pregnancy was lost by collecting reproductive tracts on P5.5, P8.5 and P13.5 to observe the presence of implanted fetuses. At P5.5, WT and Becn1(fl/Δ) cKO females had the same pregnancy rate (p=1.00, Fisher's exact test) (**Figure 3.2 F**). However, by P8.5, 46% fewer Becn1(fl/Δ) cKO females were pregnant compared to their WT siblings (p=0.03, Fisher's exact test). At P13.5, the observation was more pronounced with only 28% of Becn1(fl/Δ) cKO females pregnant compared to WT (p<0.001, Fisher's exact test). The data support that female Becn1(fl/Δ) cKO mice continuously lose their litters throughout pregnancy after implantation. Thus, the data suggests that *Becn1* is necessary to maintain pregnancy.

3.3.3 Becn1 is required for progesterone synthesis during mid-pregnancy

I next tested if *Becn1*-deficiency in luteal cells affects progesterone production during pregnancy. Pregnancy is a highly orchestrated process in which the mother must inhibit the estrous cycle, maintain quiescence of the myometrium, nourish the fetus and physiologically prepare for nursing. Progesterone is the steroid hormone that signals throughout the body to maintain pregnancy, and in rodents, the corpora lutea are solely responsible for synthesizing the progesterone necessary to maintain pregnancy (Rubinstein and Forbes 1963).

I collected plasma every other day from WT and Becn1(fl/fl) cKO females beginning at P1.5 until parturition to quantify progesterone. As 72% of Becn1(fl/Δ) cKOs lose their pregnancy by P13.5, I collected plasma every day from P1.5 to P8.5 to quantify progesterone from mice with established pregnancies at P10.5.

The WT data are comparable to that of published data with the largest amount of progesterone produced late in pregnancy at P15.5 with a mean of 55.9 ng/mL (Virgo and Bellward 1974) (**Figure 3.3 A**). Both Becn1(fl/fl) cKO and Becn1(fl/Δ) cKO were equivalent to WT through P7.5 (**Figure 3.3 A** and **Figure 3.5**). While there appears to be a decrease at P8.5 in the Becn1(fl/Δ) cKO, it is known that rodent progesterone levels are bimodal with a trough at P8.5 (Virgo and Bellward 1974) (**Figure 3.5**). Thus, I interpret that this decrease is likely normal. From P13.5 onward the Becn1(fl/fl) cKO profile is vastly different from WT. Becn1(fl/fl) cKO progesterone levels peak at P9.5 with a mean of 51.0 ng/mL. Every time-point after P11.5 had a drop in progesterone, whereas WT levels increased until P17.5. Thus, *Becn1* is required for increased progesterone serum concentrations during mid- and late- pregnancy, but is not required during in early-pregnancy.

Knowing that progesterone levels decline during mid-pregnancy in Becn1(fl/fl) cKOs, I sought to test if this reduced progesterone is sufficient to cause the reduced gestation length. I administered exogenous progesterone into WT, Becn1(fl/fl) cKO and Becn1(fl/Δ) cKO dams in attempt to rescue gestation length and pregnancy, respectively. I started the injections on P10.5 for two reasons. First, I wanted to administer progesterone during the time when progesterone is decreasing, and second, P10.5 is a stage when palpitation can be used to confirm pregnancy. I determined that seven, daily, sub-cutaneous injections of 1 mg progesterone diluted in 100 μL sesame oil starting on P10.5 until P16.5 did not affect gestation length in WT, and therefore, was the experimental paradigm (**Figure 3.3 B**).

Vehicle treated dams for all three groups gave birth similarly to the previously stated results (**Figure 3.3 C**). WT mice (n=4) had their litters on P19.0 ± 0.41 (**Figure 3.3 C**). Becn1(fl/fl) cKOs (n=6) gave birth on P17.2 ± 0.48 (figure 3C). All Becn1(fl/Δ) cKO (n=3) lost their pregnancy as determined by palpitation by P14.3 ± 0.67 (**Figure 3.3 C**). Exogenous progesterone had no effect on WT mice (n=6), as they gave birth on P18.5 ± 0.22 (p=0.8, Holm-Sidak post-hoc test) (**Figure 3.3 C**). However, progesterone-treated

Becn1(fl/fl) cKO (n=5) had an extended gestation length equivalent to WT giving birth on P18.8 ± 0.2 ($p<0.01$ vs. vehicle, $p=0.7$ vs. WT, Holm-Sidak posthoc test) (**Figure 3.3 C**). Moreover, progesterone-treated Becn1(fl/Δ) cKO mice (n=5) had increased gestation equivalent to WT, giving birth to live litters on P18.6 ± 0.25 ($p<0.001$ vs. vehicle, $p=0.8$ vs. WT, Holm-Sidak posthoc test) (**Figure 3.3 C**). Therefore, exogenous progesterone rescues the reduced gestation and abortion resulting after *Becn1* ablation. Thus, variable *Becn1* ablation in luteal cells results in significantly reduced circulating progesterone levels that in turn result in abortion and early parturition.

To test if the hypothalamus-pituitary-gonadal (HPG) axis is affected by *Becn1* deletion in luteal cells, I collected serum from WT and Becn1(fl/fl) cKO at diestrus, P13.5 and P16.5 to quantify estradiol, follicle-stimulating hormone (FSH) and luteinizing hormone (LH). No differences between WT and Becn1(fl/fl) cKO were detected at diestrus (**Figure 3.4 B, C, D, E**). Estradiol at P13.5 was increased in Becn1(fl/fl) cKO compared to WT ($p<0.05$, Holm-Sidak post-hoc test), but by P16.5 no difference was detected ($p=0.6$, Holm-Sidak post-hoc test) (**Figure 3.4 C**). FSH concentrations were inverse to estradiol with reduced concentration in Becn1(fl/fl) cKO at P13.5 and no difference at P16.5 (**Figure 3.4 D**). No difference was detected in LH at P13.5 or P16.5 (**Figure 3.4 E**). In addition, no difference in estrus cyclicity was found between WT and Becn1(fl/fl) cKO (**Figure 3.4 A**). This data indicates that the HPG axis is not affected by *Becn1* ablation and that progesterone reduction is not due to global, systemic effects.

3.3.4 Becn1 is required for lipid droplet formation within luteal cells

The reduction in circulating progesterone could result from reduced progesterone synthesis within luteal cells or an upregulation of progesterone metabolizing enzymes, such as 20α-HSD (Albarracin et al. 1994). Equally, the failure to transport progesterone to the vasculature could be limited (Pauli et al. 2005). Free cholesterol, the substrate of progesterone synthesis, is created through hydrolysis of intracellular cholestryl ester that is stored within lipid droplets, a common characteristic of luteal cells.

To determine if lipid stores are present in Becn1(fl/Δ) cKO luteal cells, I stained frozen ovary sections from P8.5 and P13.5 for neutral lipids using Oil Red-O. All ovaries, regardless of genotype, showed expected staining in the ovarian medulla and in the theca at both P8.5 and P13.5 (**Figure 3.6 A, B, E, F**). At low magnification, staining was evident in the CLs from WT females at both P8.5 and P13.5, (**Figure 3.6 C, G**). The CLs of Becn1(fl/Δ) cKOs never had intense staining at either time points, suggesting a reduction in neutral lipid storage (**Figure 3.6 B, F**). At higher magnification, numerous red staining puncta are apparent in luteal cells from WT ovaries indicating the presence of lipid droplets (**Figure 3.6 C, G**). Becn1(fl/Δ) cKO luteal cells are rarely positive for staining and when present, the staining appears less intense and the puncta appear smaller in diameter compared to WT (**Figure 3.6 D, H**, arrowheads). Furthermore, the qualitative increase in amount of neutral lipid staining observed from P8.5 to P13.5 in WT luteal cells does not occur in Becn1(fl/Δ) cKO luteal cells. The apparent patterns in Oil Red-O staining is similar between Becn1(fl/Δ) and Becn1(fl/fl) cKO luteal cells (data not shown). This data demonstrates that *Becn1* deletion causes a failure in neutral lipid storage. Thus, *Becn1* promotes neutral lipid storage in luteal cells.

3.3.5 Becn1 is required for endosome and LC3-positive vesicle clearance

To determine the level of autophagic flux occurring after ablation of *Becn1*, I crossed Becn1(fl/Δ) cKO mice with *GFP-LC3#53* (GFP-LC3) mice (Mizushima and Yamamoto 2004). GFP-LC3 is expressed ubiquitously by a CAG-promoter (Niwa et al. 1991) and the subsequent fusion protein incorporates into growing autophagosomes similar to

LC3B allowing for the observation of membrane-inclusion by increased density as GFP puncta. *GFP-LC3*$^{+}$; Becn1(fl/Δ) cKO and *GFP-LC3*$^{+}$; WT ovaries were collected at P8.5 and P13.5 and GFP was observed directly in tissue sections by epi-fluorescence.

Interestingly, qualitatively very few GFP-puncta are observed at either time point in WT luteal cells (**Figure 3.7 A, C, E, G**). Granulosa cells and oocytes appear to contain more GFP-puncta compared to luteal cells, and there is no marked observable difference from P8.5 and P13.5 (**Figure 3.7 A, E**). This implies that any LC3-incorporated structures, such as autophagosomes, are small, short-lived and do not accumulate within WT luteal cells. On the other hand, luteal cells from Becn1(fl/Δ) cKO ovaries have multiple large GFP-puncta (**Figure 3.7 B, D, F, H**). In several luteal cells, the GFP puncta take up the entirety of the cell (**Figure 3.7 D, H**). The data suggest that Becn1 ablation leads to the accumulation of multiple, large LC3-incorporated structures, presumably autophagosomes.

To determine if the increased number of LC3-incorporated structures are accumulated autophagosomes, I collected CLs from P13.5 ovaries from WT and Becn1(fl/Δ) cKO mice for transmission electron microscopy. This also allowed us to determine if the difference in Oil red-O staining is attributed to lipid droplets. Numerous differences exist between WT and Becn1(fl/Δ) cKO luteal cells (**Figure 3.8**). First, in corroboration with the neutral lipid staining, it appears that there are fewer observed lipid droplets present in Becn1(fl/Δ) cKO luteal cells compared to WT (**Figure 3.8 A, B**). Second, the cytoplasm of Becn1(fl/Δ) cKO luteal cells is extensively vacuolated compared to WT cells. A closer look at these vacuoles shows that they are large, electron-sparse, single-membrane vesicles (**Figure 3.8 D**). I suspect that these are endosomes that are created after endocytosis. In the WT luteal cell numerous multivesicular bodies can be identified

(**Figure 3.8 E**), that are not present in Becn1(fl/Δ) cKO cells. The data confirm that *Becn1* is required for lipid droplet formation and further suggest that *Becn1* is required for endosome clearance.

By P13, expansion of the smooth endoplasmic reticulum is the most prominent feature observable in luteal cells and is thought to be necessary for increased steroidogenesis. Endoplasmic reticulum membrane expansion is distinct in WT luteal cells observed as numerous small circular single membrane inclusions, or cross-sections of the endoplasmic reticulum tubules (**Figure 3.8 C, E**). Qualitatively, reduced ER expansion as evidence of the presence of whorls in Becn1(fl/Δ) cKO luteal cells suggest that ER-swelling is not occurring (**Figure 3.8 D**). The data support that less cholesterol is being utilized by Becn1(fl/Δ) cKO luteal cells.

I observe Becn1(fl/Δ) cKO luteal cells with autophagosomes containing what appears to be numerous organelles and cytoplasmic contents (**Figure 3.8 F**). Such structures are not observed in WT luteal cells. The presence of autophagosomes supports that autophagosomes are accumulating in accordance with the GFP-LC3 data. Few autophagosomes were identified in the WT luteal cells, which also corroborates the GFP-LC3 data. Overall, the transmission electron microscopy observations support the GFP-LC3 data suggesting autophagosome accumulation and decreased lipid droplets in Becn1(fl/fl) cKO compared to WT. Interestingly, there was a qualitative increase in the number of endosomes and a reduction in endoplasmic reticulum membrane expansion in Becn1(fl/fl) cKO luteal cells compared to WT. Thus, *Becn1* is required for autophagosome and endosome clearance in luteal cells.

3.3.6 Atg7 ablation results in normal gestation length and increased progesterone production

BECN1 functions as a scaffold for the class III phosphatidylinositol 3-kinase (PtdIns3K) 'nucleation' complex, which is necessary to generate phosphatidylinositol 3-phosphate (PtdIns3P) on the forming autophagosome membrane. PtdIns3P is a lipid that signals for the recruitment of subsequent complexes necessary for autophagosome membrane expansion, closure, trafficking and fusion to a lysosome. While the PtdIns3K complex is necessary for autophagosome formation it has recently been described in endosome fusion, phagocytosis and interacting with the exocyst complex. To determine if the additional functions of BECN1 are responsible for the phenotypes already described, I tested another autophagy gene required for conjugation of Atg8-like proteins to the expanding autophagosome membrane, *Atg7* (**Figure 3.9 A**). I crossed *Cyp19-iCre*$^{+}$*; Atg7*$^{fl/fl}$ (Atg7 cKO) to *CAG-CAT-EGFP* mice to determine the extent of recombination in corpora lutea, as previously described. The P8.5 CLs of *CAG-CAT-EGFP*$^{+}$*; Cyp19-iCre; Atg7*$^{fl/fl}$ indicate extensive Cre recombination in small and large luteal cells, that appear to be similar to the recombination observed in Becn1(fl/Δ) cKOs (**Figure 3.9 B, C**). I determined BECN1, SQSTM1, LC3 and StAR protein levels by immunoblot on P8.5 corpora lutea and quantified the bands relative to ACTIN (**Figure 3.9 D**). Atg7 cKO CLs have nearly twice as much BECN1 ($p<0.01$, t-test), potentially indicating a compensatory mechanism. Levels of SQSTM1 and LC3-I are increased several fold in Atg7 cKO compared to WT ($p<0.01$, t-test), suggesting that autophagy is inhibited. StAR is increased in Atg7 cKO by almost two-fold compared to WT ($p<0.05$, t-test), suggesting a higher potential for steroidogenesis. I also saw increased neutral lipid staining compared to WT at P8.5 (data not shown). These data indicate that loss of *Atg7* affects autophagy similar to the loss of *Becn1*, but that StAR quantity is not dependent upon *Becn1*.

I next performed a fertility assay on the Atg7 cKOs to determine if *Atg7* ablation affects pregnancy. WT and Atg7 cKO gestation lengths are the same, with parturition occurring on P18.95 ± 0.12 and P19.06 ± 0.15, respectively ($p=0.82$, Dunn's multiple comparison test, data presented as mean ± s.e.m) (**Figure 3.9 E**). I repeated the progesterone quantification with Atg7 cKO mice by collecting plasma every other day during pregnancy. Beginning on P3.5 and until P15.5, Atg7 cKOs have a nearly two-fold increase in progesterone concentration (**Figure 3.9 F**). These data indicate that *Atg7* ablation does not affect gestation time and suggest an increase in progesterone production. Thus, *Atg7* is not required for the maintenance of pregnancy and ablation causes increased progesterone production. This suggests that Becn1 and Atg7 have independent roles with regards to steroidogenesis in luteal cells.

3.3.7 Atg7 ablation causes upregulation of genes in the "progesterone synthesis" network

Several proteins, as described in Chapter 1, are involved in the accumulation of cholesterol and the synthesis of progesterone. As many of the genes are transcriptionally regulated, I chose to use real-time PCR to determine how subsets of the "cholesterol accumulation", "progesterone synthesis" and "signal regulation" networks are affected by *Becn1* and *Atg7* ablation. I did this to determine several ideas related to the difference between *Becn1* and *Atg7*, which is: 1) if luteal cell differentiation has occurred, 2) if steroidogenesis factors are differentially expressed, and 3) if cholesterol transport is differentially expressed. I isolated individual P8.5 corpora lutea from WT (n=4), Becn1(fl/fl) cKO (n=4), Becn1 (fl/Δ) cKO (n=5) and Atg7 cKO (n=4) females for RNA isolation. I chose P8.5 since lipid stores are already reduced in Becn1(fl/fl) cKO at this point and made it possible to test if luteal cell differentiation had occurred.

No differences were detected in any of the “cholesterol accumulation” genes of Becn1(fl/fl) or Becn1(fl/Δ) cKOs when compared to WT mice ($p>0.05$, Holm-Sidak post-hoc test) (**Figure 3.10 A**). However, there is increased expression of LIPE in the Atg7 cKO compared to WT ($p<0.01$, Holm-Sidak post-hoc test), and a trend for increased expression in all other genes in the “cholesterol accumulation” network (**Figure 3.10 A**). The data show that *Becn1* does not regulate cholesterol transport and biosynthesis in contrast to the negative regulation by *Atg7*.

I found no differences in any of the “progesterone synthesis” genes of Becn1(fl/fl) cKO or Becn1(fl/Δ) cKO mice when compared to WT mice ($p>0.05$, Holm-Sidak post-hoc test) (**Figure 3.10 B**). On the other hand, *Cyp11a1* and *3β-hsd* are increased in Atg7 cKO compared to WT ($p<0.01$, Holm-Sidak posthoc test) (**Figure 3.10 B**). Additionally, there are trends for increased *Star* and *20α-hsd* in Atg7 cKOs. The data show that *Becn1* does not regulate, whereas, *Atg7* negatively regulates the expression of progesterone synthesis genes.

I saw a reduction in PRLR-S in Becn1(fl/fl) and Becn1(fl/Δ) cKO mice compared to WT ($p<0.01$, Holm-Sidak post-hoc test) (**Figure 3.10 C**). There also appears to be a trend for reduced levels of LHGCR and PRLR-L, showing that *Becn1* positively regulates the expression of the regulatory network genes. I observed no difference in Atg7 cKOs compared to WT ($p>0.05$, Holm-Sidak post-hoc test), suggesting that *Atg7* does not regulate the expression of the regulatory network genes (**Figure 3.10 C**). To determine the extent of PRLR signaling in the Becn1(fl/ Δ) cKO I compared the epithelial ductal tree that forms in response to progesterone and prolactin receptor signaling to WT at P8.5 and P13.5 (Hennighausen et al. 1997). There was no observable difference in the lobuloalveolar growth between WT and Becn1(fl/Δ) cKO at either time, suggesting that circulating prolactin and placental lactogen are equivalent (data not shown).

To confirm that ablation of *Becn1* and *Atg7* reduces expression, I also quantified mRNA expression of *Becn1* and *Atg7* in the corpus luteum. *Becn1* is reduced in both Becn1 cKOs compared to WT ($p<0.01$, Holm-Sidak post-hoc test), demonstrating gene knockout (**Figure 3.10 C**). *Atg7* shows high variability in expression and is not significantly reduced in Atg7 cKOs compared to WT ($p=0.07$, Holm-Sidak test) (**Figure 3.10 C**). However, there is a trend for a reduction in the Atg7 cKO and there is reduced variance within the Atg7 cKO compared to the other genotypes. It is possible increasing sample size will make this reduction significant. Thus, transcription of *Becn1* is reduced and maybe *Atg7* after conditional deletion.

3.4 Discussion

The corpus luteum represents a dynamic endocrine gland during pregnancy which must undergo several developmental processes after ovulation to promote and maintain pregnancy including tissue remodeling (Liu et al. 1999), extensive angiogenesis (Reynolds et al. 2000), granulosa cell differentiation and increased steroid secretion (Stocco et al. 2007). I designed the experiments of this study to test the hypothesis that autophagy is necessary for corpus luteum cellular homeostasis. Specifically, I was interested in regulation of lipid droplets through autophagy, or lipophagy, and steroid synthesis. In the present study, I chose to knockout *Becn1* or *Atg7*, which both function in autophagosome formation, specifically in luteal precursor cells. The data presented here show that *Becn1* but not *Atg7* is necessary for progesterone synthesis within the corpus luteum to maintain pregnancy, and that luteal cell specific deletion of *Becn1* induces preterm labor in mice. Furthermore, the data show that autophagy is impaired by either *Becn1* or *Atg7* cKO through accumulated SQSTM1 and LC3, suggesting that *Becn1*'s role in progesterone synthesis is an additional function independent of autophagosome formation.

3.4.1 Role of Becn1 and Atg7 on luteal cell development and corpus luteum formation

Utilizing the *Cyp19-iCre* mouse, I found that recombination, which may have occurred in the granulosa cells prior to ovulation, is robust within both small and large luteal cells as evident from the Cre-mediated GFP-expression. This study is the first, to my knowledge, to use the *Cyp19-iCre* mouse to study gene function in the corpus luteum and furthermore, this represents the first genetic approach to study the function of autophagy in the corpus luteum. The ability to use a granulosa cell specific Cre to study the corpus luteum implies that the developmental steps from secondary follicle to corpus luteum formation must not be affected. As expected, the data showed that the deletion of either *Becn1* or *Atg7* in granulosa cells did not affect the presence of the CL during pregnancy. In regards to luteal cell differentiation, the data demonstrates that *Becn1* or *Atg7* deletion does not decrease progesterone production, the prominent function of luteal cells, during the first eight days of pregnancy. Moreover, the mRNA expression of the luteal-specific transcripts *Cyp11a1*, *3bHSD*, *SRBI*, *LIPE* and *StAR* , or the protein expression of StAR was not different in either *Becn1* or Atg7 cKO mice compared to wild-type siblings at P8.5. Together this supports that luteal cell differentiation and corpus luteum formation has occurred in all three experimental strains studied. The numbers of fetuses at P8.5 were also not different among the observed strains, suggesting that an equal numbers of oocytes were fertilized and implanted. Therefore, *Becn1* or *Atg7* is not necessary for folliculogenesis, ovulation or luteinization.

It is largely unknown how autophagy is related to normal cellular function in granulosa and luteal cells. Ryter et al, recently presented a hypothesis that autophagy is a critical regulator of metabolism and homeostasis within all cells (Ryter et al. 2013). Thus, I expected that ablation of autophagy-specific genes would result in dysregulation of homeostasis that could ultimately result in cell death. On the contrary, recent studies in rats have suggested that together with apoptosis, autophagy is responsible for granulosa cell attributed follicular atresia through *in vitro* studies (Choi et al. 2010, 2011). This idea is supported by the observation of autophagosomes in granulosa cells of atretic follicles in several species including: rat (Peluso et al. 1980), ewe (Rosales-Torres et al. 2000), bovine (Rodgers and Irving-Rodgers 2010), characiform fish (Santos et al. 2008), goose (Kovács et al. 1992), quail (D'Herde et al. 1996) and human (Duerrschmidt et al. 2006). In the present study, I did not directly study atresia; however, I did indirectly test the role of autophagy on atresia. Atresia is a mechanism to remove "weak" follicles that have insufficient FSH-mediated signaling and thus, oocytes are also removed from the ovulatory pool (Hsueh et al. 1994). I would have expected larger litters from both *Becn1* and *Atg7* conditional knockouts if autophagy mediates atresia, which we did not see. A weakness of this conclusion is that poor quality oocytes, which would have a low competence to form viable embryos through *in vitro* fertilization (IVF), are typically found in atretic follicles (Eppig and Schroeder 1989; Pavlok et al. 1992). Nevertheless, the developmental competence of oocytes ovulated from atretic follicles is not zero. While we cannot ignore the possibility that Becn1 cKO mice ovulate oocytes from atretic follicles that were not fertilized, these data suggests that autophagy does not contribute to granulosa cell attributed atresia. It would be worthwhile to use the strains described in this study to observe follicular atresia to test this hypothesis.

3.4.2 Becn1(fl/fl) cKO mice have spontaneous preterm labor

Preterm birth is a human-specific term, defined as parturition at less than 37 weeks of gestation (full term being 39 or more weeks) (Beck et al. 2010). Preterm birth occurs in an estimated 1 in 8 pregnancies and is the leading cause of neonatal deaths (Shapiro-Mendoza and Lackritz 2012). In addition, preterm birth is the direct cause of metabolic, heart and behavioral diseases later in life for the preterm infant (Behrman and Butler 2007). Few mouse models have been identified that have a similar preterm birth phenotype, or preterm labor. Lipopolysaccharide inflammatory response (Dudley et al. 1993), acute alcohol exposure in late pregnancy (Salo et al. 1996), progesterone-receptor antagonism (Dudley et al. 1996), *Stat5b* knockout mice (Udy et al. 1997; Teglund et al. 1998), inactivation of cannabinoid receptor CB1 (Wang et al. 2008) and *Trp53* deletion in progesterone receptor expressing cell linages (Hirota et al. 2010) are the more prominent preterm labor mouse models. The WT mice in this study gave birth on day 19 of gestation which is not different from previously published data for inbred mouse strains (Murray et al. 2010). The shortened gestation length of 17 days as seen in Becn1(fl/fl) cKO mice is not observed in any otherwise wild-type, inbred mouse strains. Furthermore, gestation length is shortened by a similar percent of total gestation time for a human categorized as preterm. Thus, the Becn1(fl/fl) cKO mouse can be used as a novel preterm labor model.

The Becn1 cKO mice gestation length is rescued by exogenous progesterone administration which is the only proven clinical treatment for women with a history of preterm birth (Conde-Agudelo et al. 2012; Rode et al. 2009; Hassan et al. 2011) . It is also worth reiterating that Becn1(fl/Δ) mice had 100% reabsorption of fetuses by P14 . Considering that recombination was extensive but not complete, as some cells were not positive for Cre-recombination, begs the question of how many *Becn1* alleles are necessary to maintain pregnancy. These data demonstrates that a 50% reduction has no effect; however, the data suggests a threshold exists.

Progesterone production in humans is different in that the syncytiotrophoblast of the placenta are the progesterone producing cells after the first eight weeks of gestation (Albrecht and Pepe 1990). Despite this difference, a BECN1 deficiency could be a major contributor to preterm birth in human. A recent study by Hung et al., reported steady mRNA and protein expression of *Becn1* in villous tissue (which contains synciotrophoblast and cytotrophoblast) collected from placenta from 7 weeks of gestation to full-term birth (Hung et al. 2013). Additionally, several studies report no change in LC3 immunostaining in placenta from several pregnancy outcomes including Caesarian section, intrauterine growth restriction, or preterm birth, suggesting that autophagy is not dynamic for placenta function, similar to this study (Oh et al. 2008; Avagliano et al. 2013; Hung et al. 2013; Signorelli et al. 2011). As the data provides the conclusion that *Becn1* is participating in functions in addition to autophagy in these mice, studying the function of *Becn1* in human placenta would be an opportunity to characterize a novel pathway that could be affected during preterm birth. Thus, the luteal cell specific deletion of *Becn1* offers an interesting model for future studies to help understand the regulation of preterm labor and gives insight to possible roles for *Becn1* in human pregnancy.

3.4.3 Becn1 and Atg7 differentially influence progesterone synthesis in luteal cells

The data presented here clearly show an unexpected, different response between *Becn1* and *Atg7* ablation. The first difference is demonstrated by the day of parturition. Becn1(fl/fl) cKO females have parturition an average of 2 days early compared to wild-type siblings and Becn1(fl/Δ) cKO females get visibly pregnant but never give birth. Atg7 cKO mice, on the contrary, have no trouble getting pregnant and the day or parturition is equivalent to wild-type siblings. The second result showing the difference is the synthesis of progesterone. The Becn1(fl/fl) cKO mice showed reduced progesterone levels after P9.5, down to pre-pregnancy levels by P17. This corroborates the preterm labor since progesterone is sufficient and necessary to maintain pregnancy in mice. On the other hand, I observed increased progesterone levels in the Atg7 cKO mice throughout pregnancy. The third result is neutral lipid storage within luteal cells. *Becn1* deletion reduces the amount of neutral lipid staining by Oil Red-O whereas *Atg7* deletion increases it. The increased lipids in the Atg7 cKO luteal cells would provide more available cholesterol for steroidogenesis to support an increase in progesterone synthesis. Lastly, the expression of genes involved with progesterone synthesis are different. *Becn1* deletion does not change the expression of any gene studied, with the exception of PRLR-S that was decreased in both *Becn1* cKOs. On the other hand, Atg7 cKO mice have an increased expression of progesterone synthesis genes compared to WT, providing additional evidence for the increased progesterone synthesis. Overall, the data conclude that *Becn1* function is required for adequate lipid storage and when expression is disrupted, the reduced lipid stores lead to hindered progesterone synthesis. Another conclusion that can be drawn is that *Atg7* provides negative feedback on lipid storage and the expression of steroidogenesis genes, such that, in its absence lipid storage is increased resulting in subsequent increase in enzyme expression and increased progesterone production.

Autophagy and the mobilization of lipids from lipid droplets are intimately linked. Autophagy facilitates a catabolic process termed lipophagy, where autophagosomes deliver small inclusions of lipid droplets to lysosomes (reviewed in Liu and Czaja 2013). On the contrary, autophagy is also suggested to positively regulate the growth and accumulation of lipid droplets in some tissues, including in adipose tissue of obese and diabetic individuals (Ost et al. 2010). The role of *Becn1* in lipid droplet regulation has only been recently explored. Knockout of the yeast homolog, *Atg6*, in *S. cervisae* inhibits the degradation of lipid droplet specific proteins Faa4-GFP and Egr6-GFP by the vacuole (van Zutphen et al. 2014), suggesting that *Atg6* participates in lipid droplet degradation. Three previous studies support that *Becn1* is required for lipid droplet growth. Knockdown of the *Becn1* homolog, *Atg6*, in *Drosophila* reduces the size of lipid droplets in the larval fat body (Wang et al. 2012a). *C. elegans* with a mutated Bec-1 (homologous to Becn1) have reduced numbers of lipid droplets throughout development regardless of diet (Lapierre et al. 2013). Similarly, knockdown of *Becn1* in cultured 3T3-L1 induced-adipocytes reduces lipid storage as detected by neutral lipid staining (Ro et al. 2013). Now, in the present study, I show that knockout of *Becn1* in mouse luteal cells reduces lipid storage. All of these studies demonstrate a conserved function for *Becn1* in lipid droplet regulation. Additionally, except for the yeast study, which did not address lipid droplet formation, these studies identify that the absence of *Becn1* negatively affects lipid droplet formation. In the present study, I did not quantify lipid droplet formation between the Becn1(fl/fl) cKO and Becn1(fl/Δ) cKO; however, qualitatively there was not a difference. This suggests that the loss of Becn1 results in cell catastrophe, like cell death, which was not studied. Whether lipid droplet formation is a direct or indirect function of Becn1, needs to be addressed by genetic rescue and overexpression experiments.

An equally interesting story on lipid droplet maintenance has been emerging for *Atg7*. The increased lipid metabolism and progesterone synthesis seen in the Atg7 cKO mice of the present study is similar to the increased lipid metabolism reported in *Atg7*-decificient adipocytes (Zhang et al. 2009; Singh et al. 2009b). *Fabp4-Cre*; *Atg7*$^{fl/fl}$ mice, which specifically ablate *Atg7* in brown and white adipose tissue, are more active and slimmer than controls with gonadal fat pads 20% the weight of controls despite no difference in food intake (Zhang et al. 2009; Singh et al. 2009b). Additionally, the adipocyte-specific deletion of *Atg7* causes a dramatic increase in the number of small lipid droplets present, but an overall decrease in the total amount of circulating lipid (Zhang et al. 2009; Singh et al. 2009b). Adipocytes can utilize lipid stores by releasing them into circulation during starvation or oxidize them for immediate ATP generation in the mitochondria. An increased number of mitochondria in *Atg7*-cKO adipose tissue, which results in increased β-oxidation, is the main indication as to why adipocyte-specific *Atg7* cKO mice have increased lipid metabolism. This suggests that *Atg7* negatively regulates fatty acid transport to mitochondria in the adipocyte. In the present study, I observed an increase in lipid stores by Oil Red-O staining and increased metabolism as determined by progesterone synthesis in Atg7 cKO mice. Clearly, these data also support that *Atg7* inhibits fatty acid metabolism.

An unanswered question is how lipid droplets form and grow (Ohsaki et al. 2014). A possible link between BECN1 and ATG7 and lipid droplet formation is LC3. LC3 is necessary for lipid droplet formation and is present on lipid droplet membranes (Shibata et al. 2010). Furthermore, both lipid droplets and autophagosomes are formed from lipid-rich membranes and are proposed to be formed from endoplasmic reticulum at the similar sites, near the mitochondrial-associated membrane (Jiang and Napoli 2013; Hamasaki et al. 2013). ATG7 is required to activate LC3 before it can be conjugated to an autophagosome. It is unknown if LC3 that is associated with lipid droplets is activated but this function of ATG7 could be conserved for conjugation of LC3 to a lipid droplet to target it for use or removal. It is also possible that as autophagosomes and lipid droplets potentially are synthesized at the same location, BECN1 participates in the formation of both autophagosome and lipid droplet formation.

I postulate that there are three possibilities for the decreased progesterone seen in pregnant *Becn1* cKO mice: 1) progesterone is not being synthesized, 2) progesterone is being degraded or 3) progesterone is not getting into the vasculature. The plasma analysis for progesterone throughout pregnancy demonstrates that progesterone is produced at wild-type levels for at least the first 11 days, but then precipitously drops to non-pregnancy levels concurrent with preterm labor. Additionally, the expression of all progesterone-related genes are not different from WT, including 20a-HSD, which is the dominant gene to metabolize progesterone to an inactive form. Although the expression of PRLR-S was decreased in both *Becn1* cKO CLs at P8.5, PRLR-S binds both PRL and PL but lacks the intracellular domain to activate Stat5. However, PRLR-S may promote angiogenesis by regulating the expression of vascular endothelial growth factor (VEGF) in luteal cells (Le et al. 2012). Furthermore, PRLR-S is found predominately on endothelial cells in the corpus luteum of bovine (Ricken et al. 2007). These data suggests that progesterone synthesis is reduced after P11.5 because of the reduced lipid availability in the luteal cells. Additionally, the data suggest that there is not an increase in the degradation of progesterone from the 20α-HSD expression. Beyond this conclusion, it is also possible that BECN1 function is necessary for *Prlr* and *Lhcgr* expression as their expression was reduced. However, I cannot discount that the vasculature is negatively affected by *Becn1* ablation.

3.4.4 Becn1 is required for autophagosome and endosome clearance

Extracellular cholesterol is required for acute steroidogenesis. Circulating HDL and LDL provide the predominant source of cholesterol to luteal cells. One of the modes for transport of HDL and LDL is receptor-mediated endocytosis. After endocytosis, endosomes mature and fuse with lysosomes where the cholesterol esters are hydrolyzed and transported out of the lysosome for use by the cell. LDL-Rs are recycled back to the plasma membrane to facilitate further transport approximately every 10 minutes allowing for maintained cholesterol influx (Brown et al. 1983). Receptor mediated endocytosis is primarily used to transport LDL particles but HDL has been observed in endosomes (Röhrl and Stangl 2013). Substantial evidence demonstrates a role for BECN1 in endosome maturation. BECN1 forms an evolutionarily-conserved complex with VPS15, VPS34, UVRAG and Bif-1 that is necessary for autophagosome and endosome to lysosome fusion in *Drosophila*, *C. elegans*, mouse and human cells (Thoresen et al. 2010; Liang et al. 2008; Juhász et al. 2008; Ruck et al. 2011). Furthermore, epithelial growth factor receptor (EGFR) undergoes endosome mediated membrane recycling and the process requires the BECN1 complex (Petiot et al. 2003; Johnson et al. 2006; Thoresen et al. 2010).

At P8.5 and P13.5, Becn1(fl/Δ) cKO luteal cells have increased numbers of GFP-LC3 puncta, which is indicative of autophagosome accumulation. To determine if these puncta were actually autophagosomes, I performed electron microscopy on P13.5 luteal cells. There was an increased number of large autophagosomes, as detected by GFP-LC3 in the Becn1(fl/Δ) cKO luteal cells but also, surprisingly, a dramatic increase in the number of endosomes. The observation supports the previously mentioned studies that the BECN1 complex mediates endosome maturation. It is possible that these endosomes are sequestering lipoprotein receptors, such as LDL-R, to dampen the transport of cholesterol into the cells. Thus, the cell cannot synthesize lipid droplets because of reduced lipid transport. It will be necessary to show lipoprotein transporters in these endosomes and to identify if these are retrograde endosomes or secretory vesicles.

3.4.5 Summary

The present study demonstrates that *Becn1* is required for progesterone synthesis in murine luteal cells and a threshold of BECN1 is necessary to maintain pregnancy, such that below that threshold, preterm labor and abortion occur. This is one of few genetic mouse models for preterm birth and supports the significance of *Becn1* in steroidogenesis. The data suggests that *Becn1* deletion decreases progesterone synthesis in two ways. First, *Becn1* deletion impedes endosome maturation, which in turn causes reduced cholesterol availability that reduces progesterone synthesis. Second, I showed that *Becn1* is required for lipid droplet formation. Whether the two functions is an example of pleiotropy in addition to autophagy or if all three are provided by the same function of *Becn1* is an important question for future studies. I also presented data showing that *Atg7* deletion results in mice producing more progesterone.

This suggests that the function of *Becn1* in lipid droplet formation and endosome maturation is in addition to its function in autophagy.

These results provide significance to study at *Becn1* in many lipid-dependent developmental pathways such as atherosclerosis and adrenal gland steroidogenesis. The continued research has identified multiple roles for lipid droplets in physiological functions. As such, a *Becn1* deficiency may participate in all of the same functions...

3.5 Acknowledgements

This work was completed in part, with funding from KSEF-2305-RDE-014 to Edmund Rucker and Gertrude Flora Ribble Graduate Student Fellowship to Thomas Gawriluk. I would like to thank CheMyong Ko (University of Illinois) for the *CYP19A-iCre* mouse, Kay-Uwe Wagner (University of Nebraska Medical Center) for the *CAG-CAT-EGFP* mouse, Qingjun Wang (University of Kentucky) for the *Atg7*-flox mouse, Buck Hales (Southern Illinois University) for the StAR antibody, Wendy Katz (University of Kentucky) for embedding tissues, Vincent Cassone (U. Kentucky) for reagents and use of his lab space, Ashley Seifert (U. Kentucky) for use of his tissue processing system, and Maggie Murphy (U. Kentucky) for help with histology. All of the real-time PCR was completed by Xiaoman Hong and assistance with analysis was done by Lane Christenson (University of Kansas Medical Center).

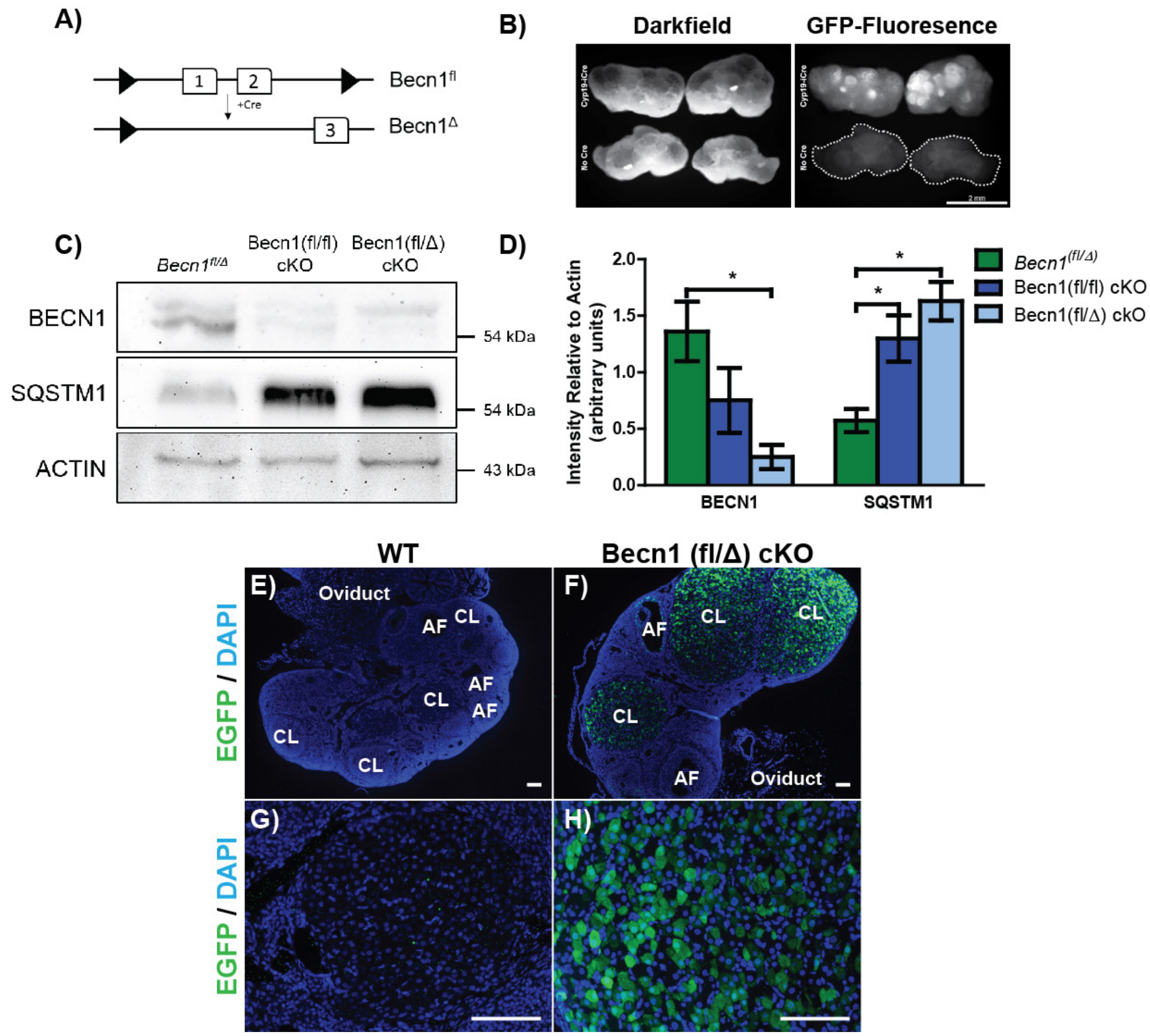

Figure 3.1. Cyp19-iCre leads to sufficient recombination in the corpus luteum. (**A**) Genetic strategy to conditionally knockout Becn1. Numbered boxes correspond to exons with dashed boxes representing engineered insertions and triangles represent LoxP sites. (**B**) Ovaries from P8.5 CAG-CAT-EGFP females on both WT and Cyp19-iCre backgrounds represented in darkfield and GFP-fluorescence with WT ovaries outlined. (**C**) Representative immunoblots from granulosa cells 48 hours after PMSG injection. (**D**) Quantified band intensity relative to Actin for BECN1 and SQSTM1, n=4 for each genotype. Data represents mean with standard error of the mean. (**E - H**) Representative images showing immunofluoresence for EGFP, indicating Cre recombination, co-stained with DAPI on tissue sections from P8.5 ovaries. Low magnification to see entire ovary (E and F). CL = corpus luteum, AF = antral follicle. High magnification of corpus luteum to demonstrate recombination in luteal cells. Bars equal 100 μM.

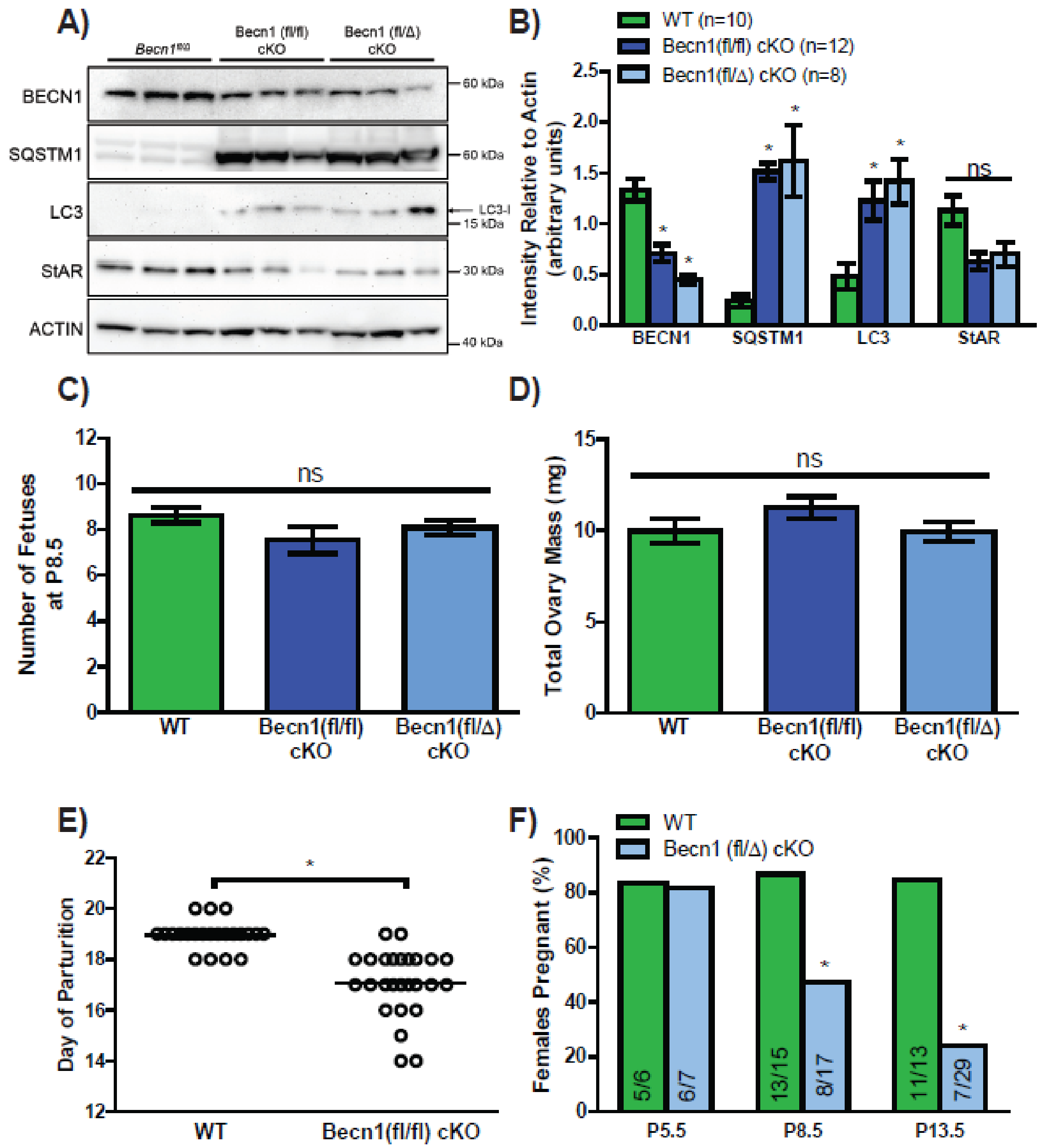

Figure 3.2. ***Becn1* is required to maintain pregnancy.** (**A and B**) Immunoblots for P8.5 pregnant corpora lutea (A) and relative quantification (B). * denotes p-value <0.05 for Holm-Sidak post-hoc test versus WT. (B) Day of pregnancy when mothers gave birth for WT (n=22), Becn1 (fl/fl) cKO (n=26) and Atg7 cKO (n=18). Each data point represents one individual and the horizontal line indicates the mean. ** denotes p-value <0.001 for Dunn's multiple comparison test versus WT. (**C and D**) Number of implanted fetuses observed (C) and wet mass of both ovaries on P8.5 for individual strains (D). Data represent mean with s.e.m. (E) Histogram representing the day of parturition observed for WT (n=22) and Becn1(fl/fl) cKO (n=26) females. Each data point represents a single pregnancy, bar is mean, * denotes p-value <0.01 for t-test.

Figure 3.2 continued. (**F**) Percent of Becn1(fl/Δ) cKO females that are pregnant on the designated day after mating. Observed number of pregnant females out of total females mated indicated vertically inside each bar. * denotes p-value <0.05 for fisher's exact test between the two genotypes.

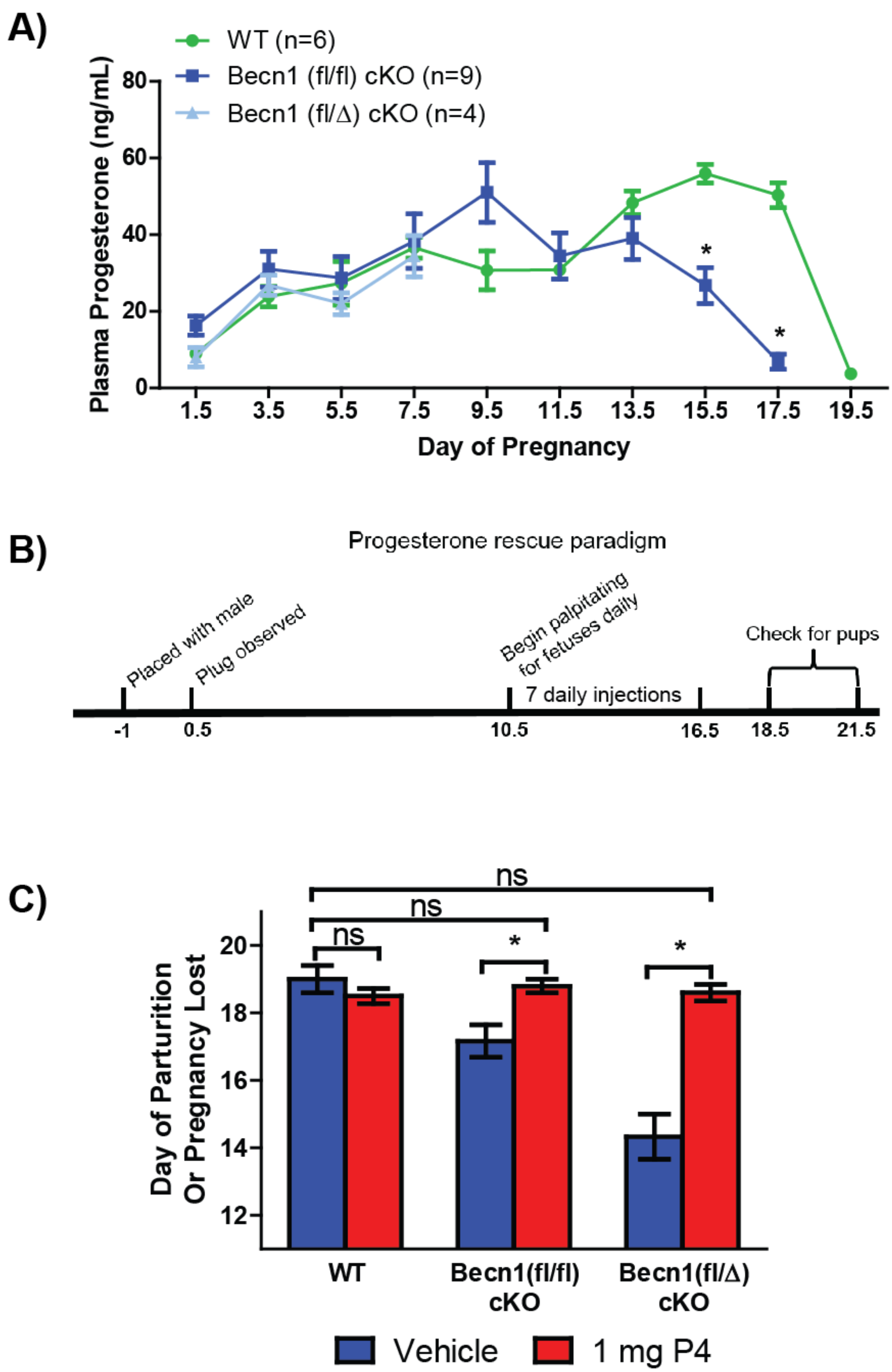

Figure 3.3. ***Becn1*** **cKO early parturition is progesterone-dependent.**

Figure 3.3. Continued. (**A**) Progesterone quantified from plasma every other day throughout pregnancy for WT, Becn1(fl/fl) cKO and Becn1(fl/Δ) cKO. Data represents mean with s.e.m. * denote a p-value <0.05 for Holm-Sidak post-hoc test versus WT for that day. (**B**) Diagram depicting dosing paradigm for exogenous progesterone administration. (**C**) Day of parturition for females that were given sesame oil (vehicle) or 1 mg progesterone daily (n ≥ 3 for each group). Data represents mean with standard error of the mean. * denotes p-value < 0.001 for Holm-Sidak post-hoc test for interaction indicated. ns = not significant

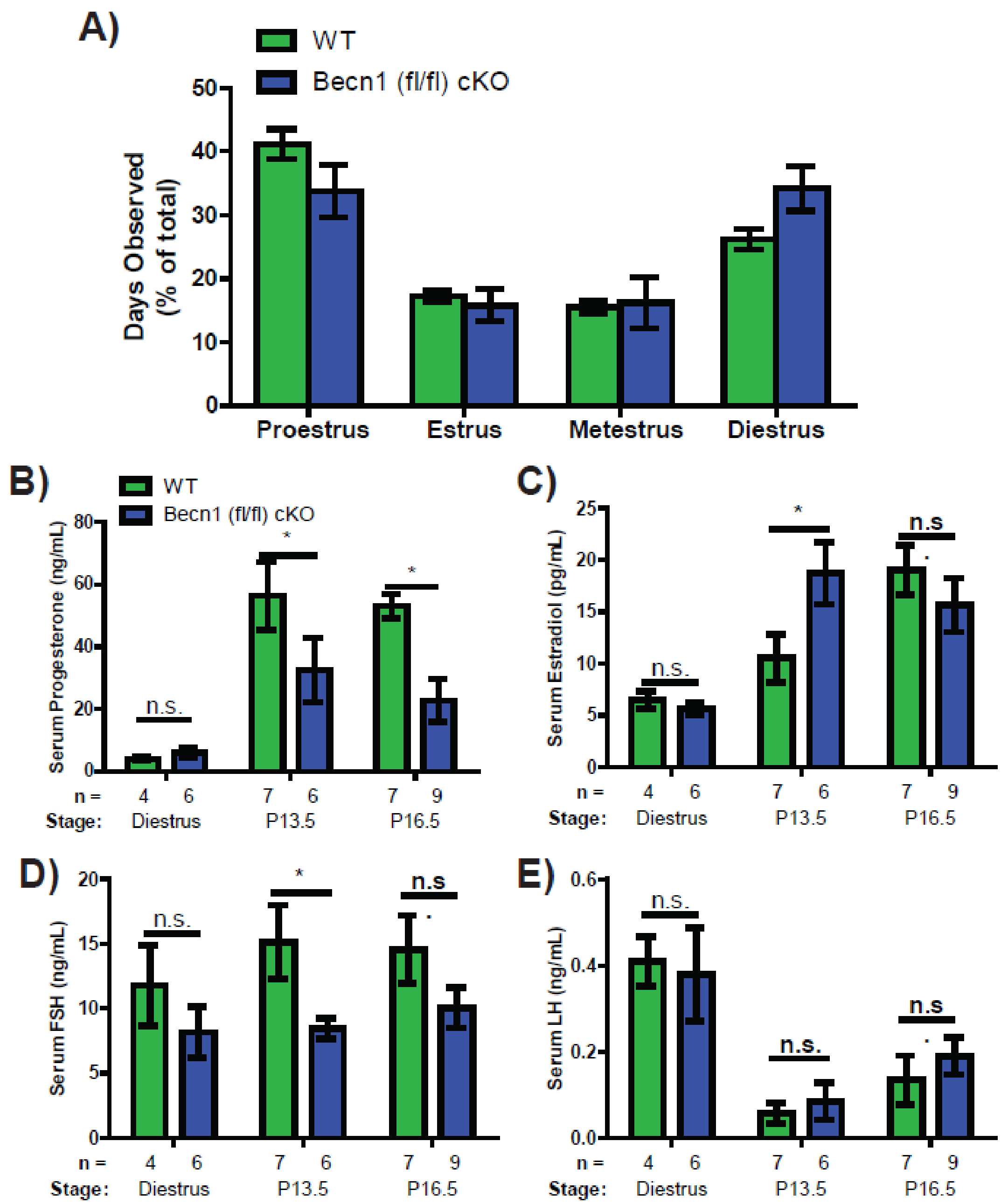

Figure 3.4. Becn1 (fl/fl) cKO hormone profile and estrus cyclicity are normal. (**A**) Percent of time that each estrus stage was observed for WT (n=20) and Becn1 (fl/fl) cKO (n=15) over 21 days. Data represents mean with standard error of the mean. p-value equals 0.09 for two-way ANOVA for genotype x stage interaction. (**B**, **C**, **D** and **E**) Reproductive hormones progesterone (B), estradiol (C), follicle-stimulating hormone (D) and luteinizing hormone (E) quantified from serum collected during euthanasia at the specified times. For all charts, data represents mean with standard error of mean. * denotes a p-value <0.05, respectively for Holm-Sidak post-hoc test versus WT. ns = not significant.

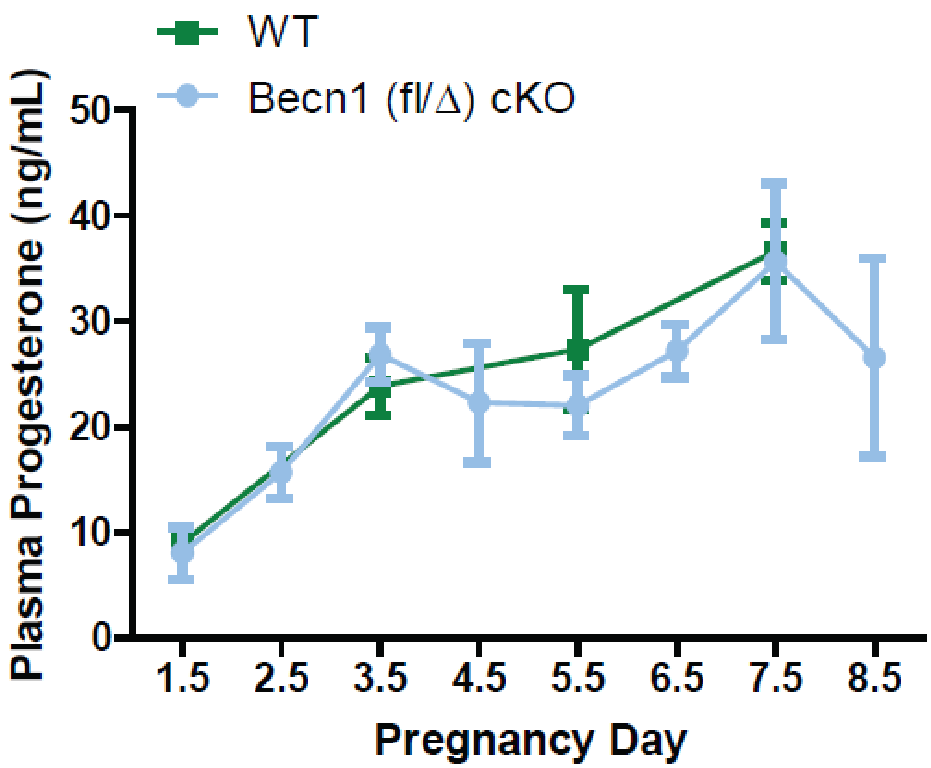

Figure 3.5. First eight days of pregnancy plasma progesterone in Becn1 (fl/Δ) cKO. Plasma concentrations of progesterone for Becn1 (fl/Δ) cKO (n=4) and WT (n=6) from P1.5 to P8.5. Data represent mean with standard error of the mean. No significant differences identified, two-tailed t-test for each day, $p>0.05$.

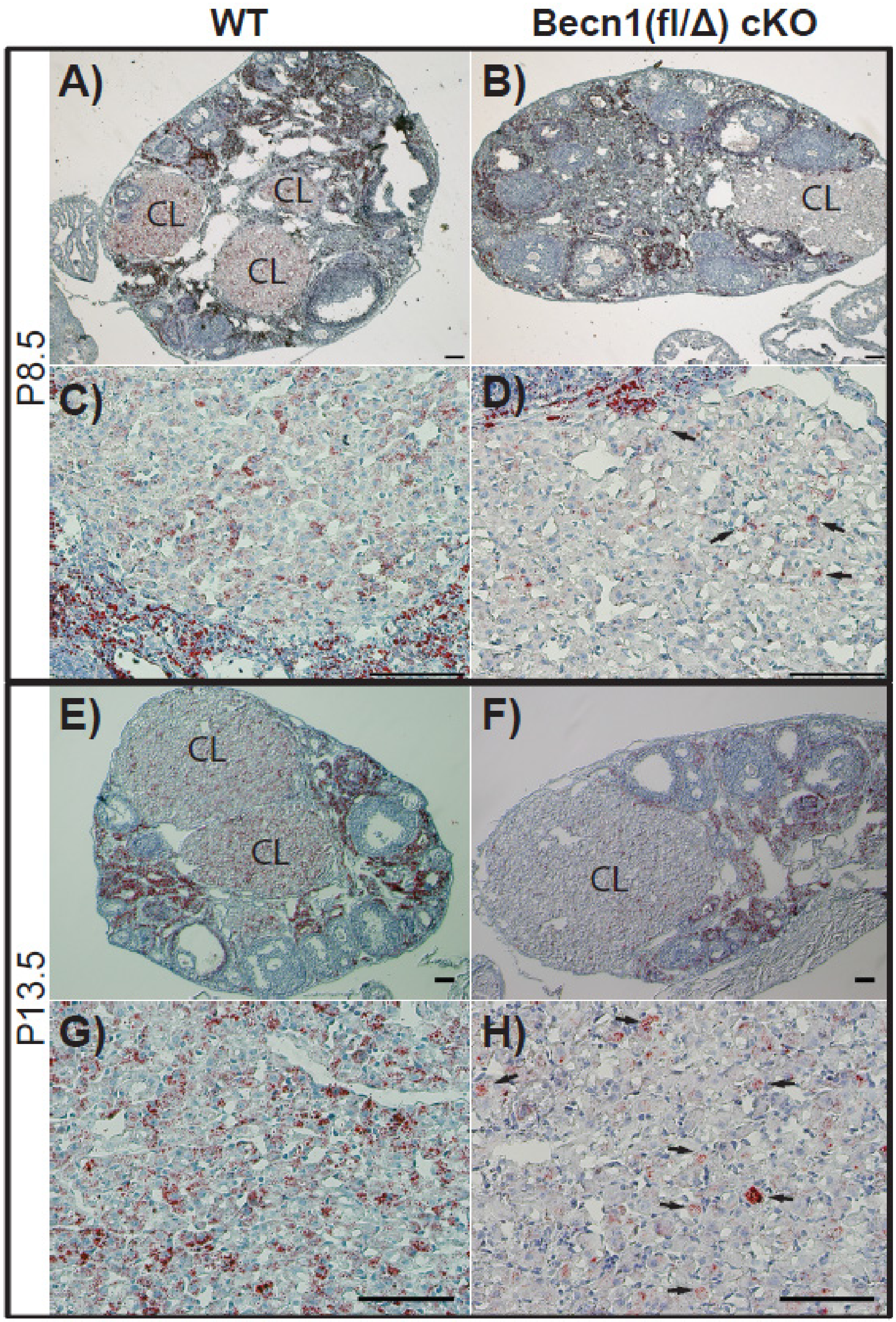

Figure 3.6. ***Becn1*** **promotes neutral lipid stores in luteal cells.** (**A – H**) Representative images of frozen tissue sections stained with oil red-O (red) and counterstained with hematoxylin (blue) at P8.5 (A-D) and P13.5 (E-H).

Figure 3.6. Continued. Low magnification indicates staining in medulla, theca and corpus lutea (A, B, E, F). Higher magnification of corpus luteum to highlight luteal cell staining (C, D, E, H). Oil red-O stains neutral lipids, mainly observed as lipid droplets (arrows). Bars equal 100 μM.

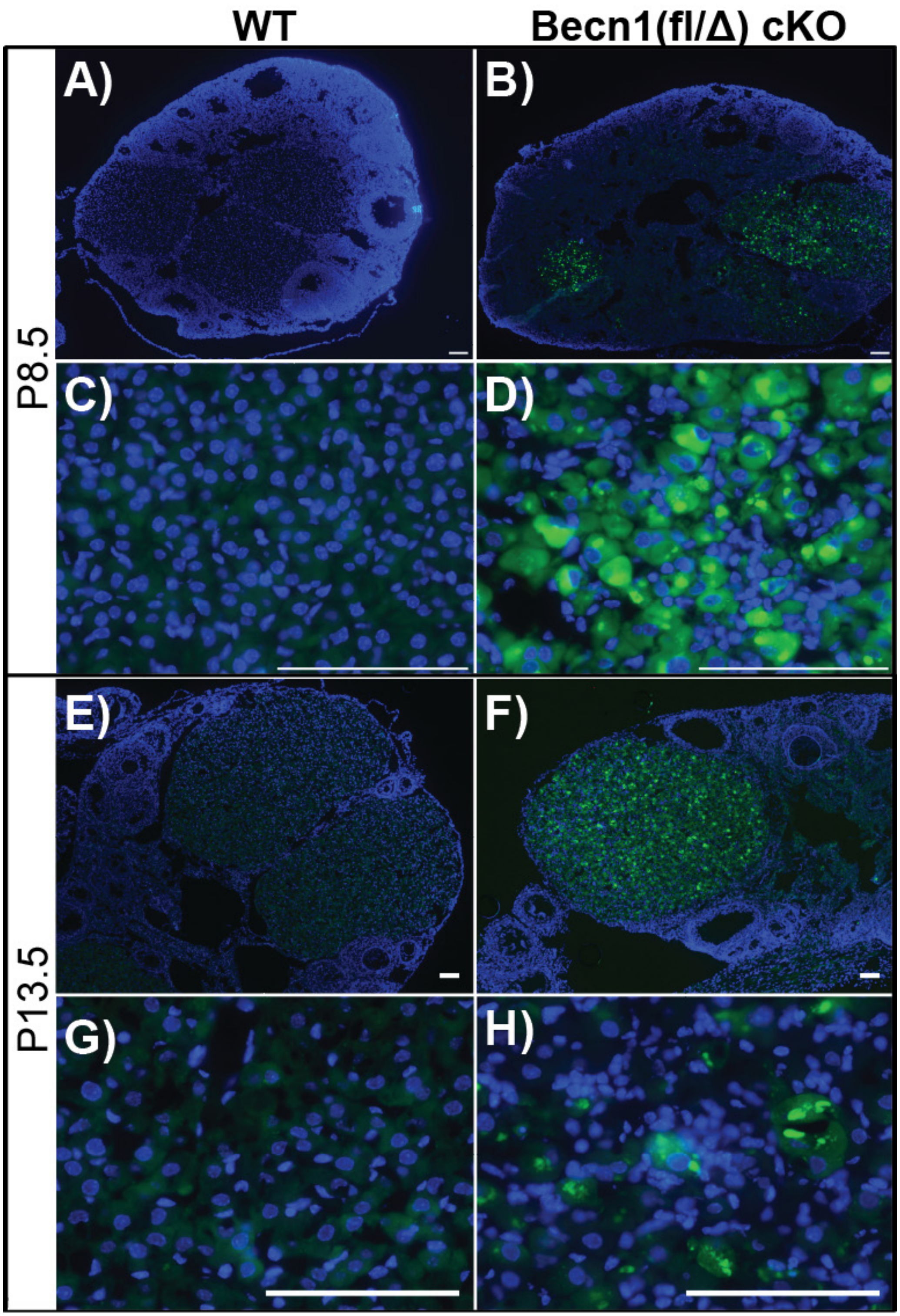

Figure 3.7. ***Becn1*** **is necessary for the clearance of GFP-positive vesicles**
Representative images of frozen tissue sections directly viewed for GFP-LC3. Low magnification (A, B, E and F) shows that only CLs of Becn1 (fl/Δ) cKO have intense GFP. GFP-LC3 puncta are present in Becn1 (fl/Δ) cKO (D and H) but not in WT luteal cells (C and G). Bars equal 100 μM.

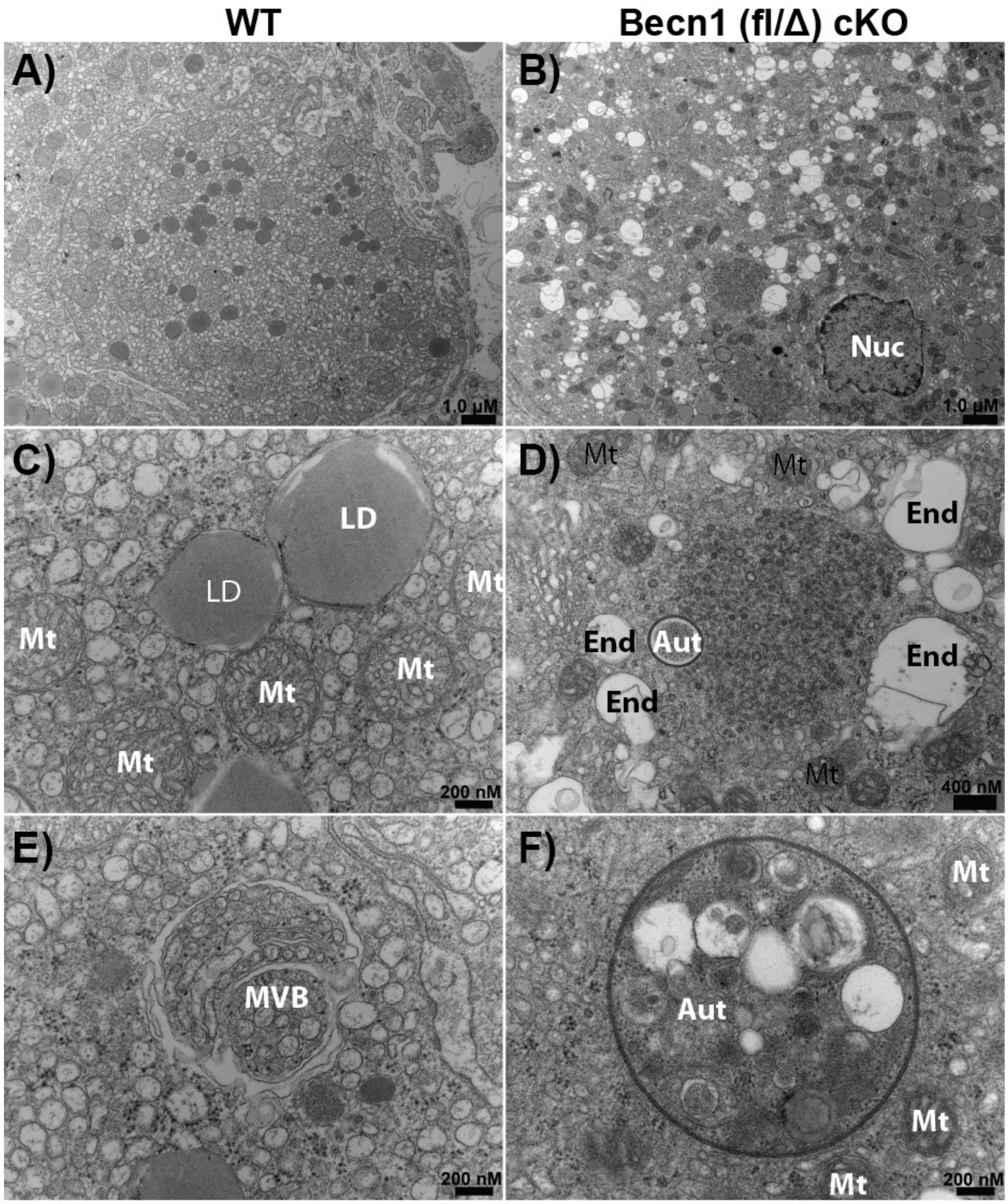

Figure 3.8. ***Becn1* is necessary for the clearance of autophagosomes and endosomes.**
Representative images from transmission electron microscopy of P13.5 large luteal cells from WT (A, C, E) and Becn1 (fl/Δ) cKO (B, D, F). An entire cells ultrastructure where lipid droplets mitochondria and nuclei are seen (A and B). High magnification images indicating mitochondria (Mt), lipid droplets (LD), multi-vesicular bodies (MVB), endosome (End), and autophagosomes (Aut) (C, D, E, F). Scale indicated on lower right corner of each image.

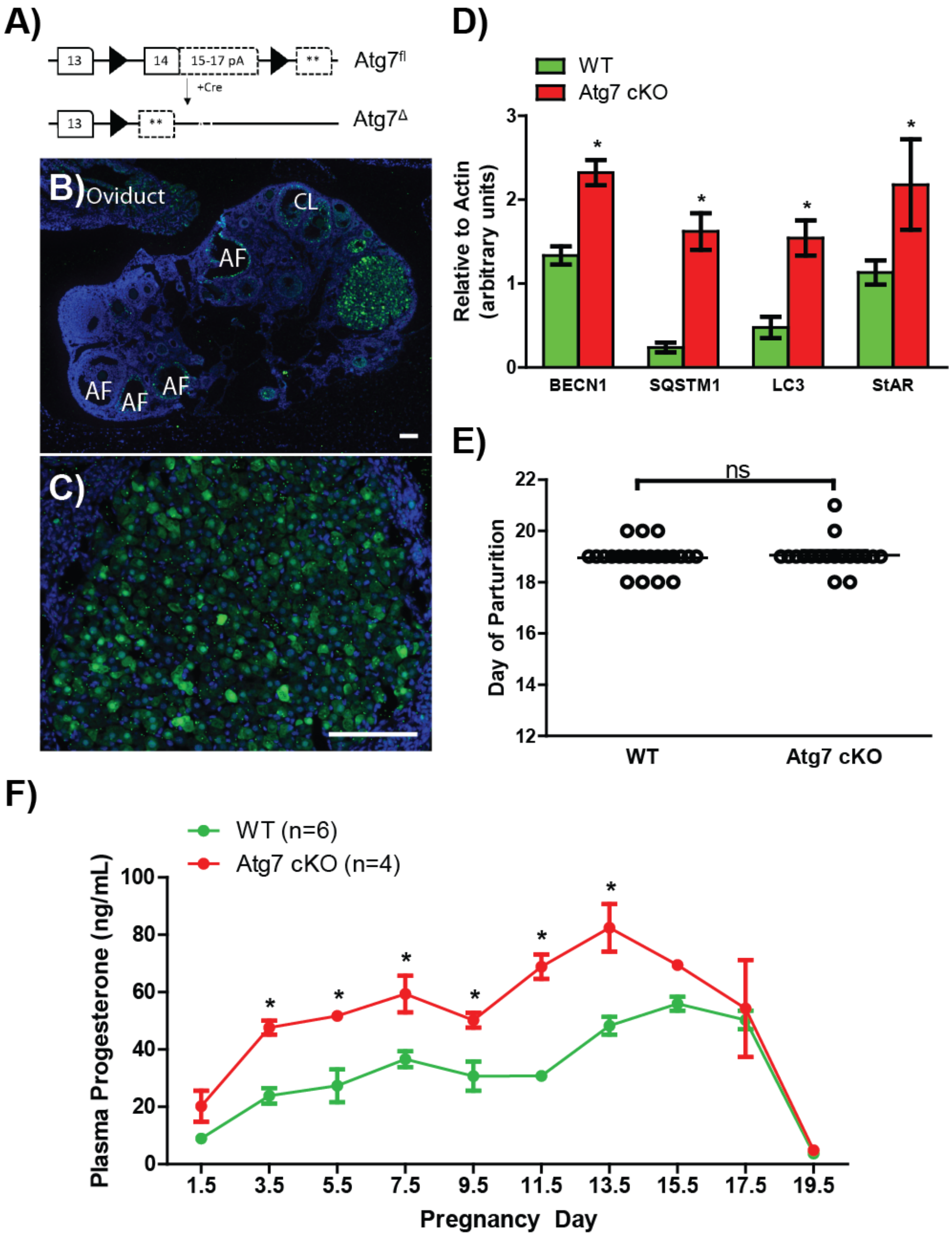

Figure 3.9. ***Atg7* ablation have normal gestation and have increased progesterone throughout pregnancy. (A)** Genetic strategy to conditionally knockout Atg7. Numbered boxes correspond to exons with dashed boxes representing engineered insertions, ** is a translational STOP and triangles represent LoxP sites. **(B and C)** Immunofluoresence for EGFP, indicating Cre-recombination in P8.5 ovaries (B) and CL (C). Bar equals 100 μM. (D) Relative quantification of indicated proteins from immunoblots. * denotes p<0.05 for t-test, data represents mean ± s.e.m. **(E)** Histogram depicting the day of parturition for WT (n=22) and Atg7 cKO (n=18) females. **(F)** Plasma concentrations for progesterone throughout pregnancy. * denotes p<0.05 for t-test, data represent mean ± s.e.m.

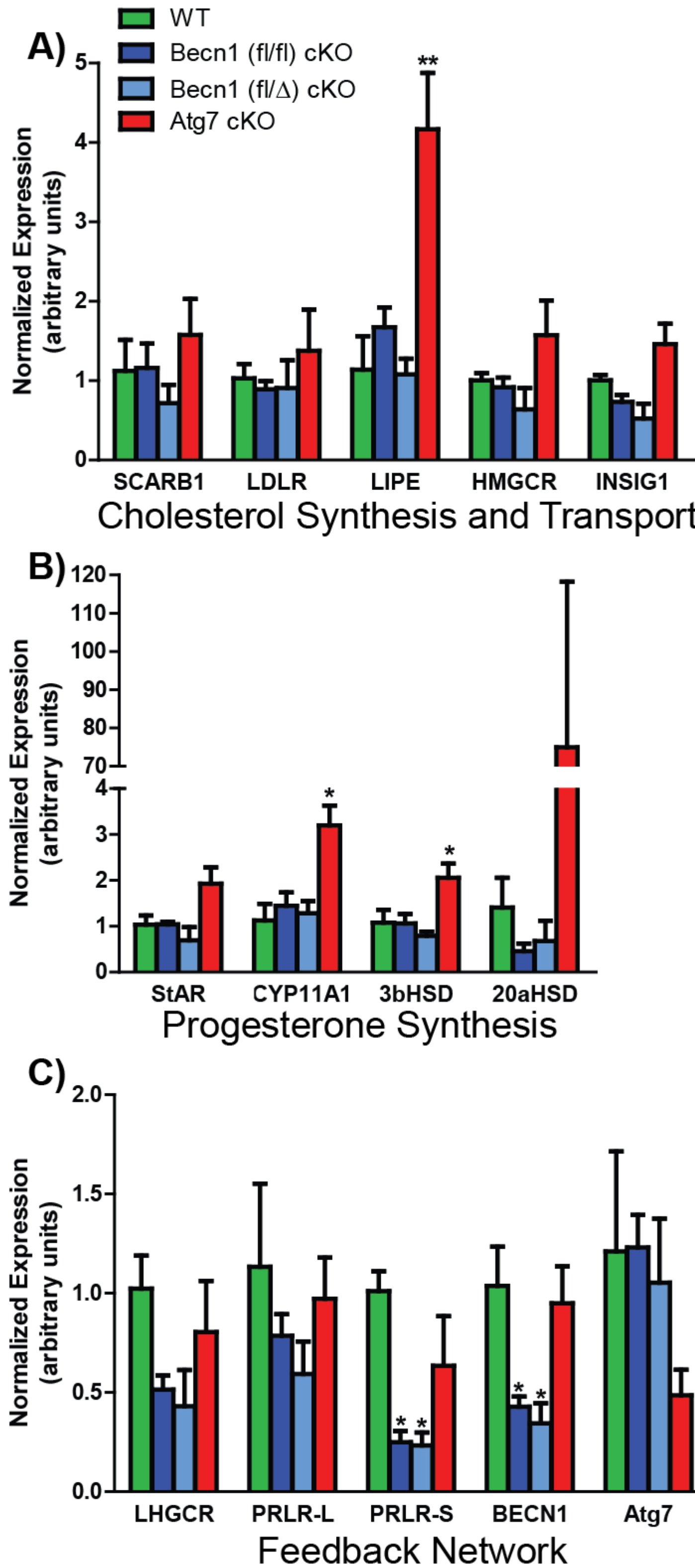

Figure 3.10 ***Becn1*** **cKO and** ***Atg7*** **cKO have different responses in the progesterone gene network.**

Figure 3.10. Continued. (**A**, **B** and **C**) mRNA expression relative to WT and normalized to *Beta-actin* and *Gapdh* for genes for progesterone synthesis (A), cholesterol transport and synthesis (B) and luteal cell signaling (C). Data represents mean with standard error of the mean for $n \geq 4$ for each group. * and ** denotes a p-value <0.05 and <0.001, respectively for Holm-Sidak post-hoc test versus WT individually for each gene.

Copyright © Thomas Raymond Gawriluk 2014

CHAPTER 4: AUTOPHAGY IS NECESSARY FOR ADULT SERTOLI CELL FUNCTION IN MICE

Keywords: Sertoli cell, autophagy, Beclin-1, Atg7

Abbreviations Used: PS, phosphatidylserine; PtdIns3k, class III phosphatidylinositol 3-kinase; PtdIns3P, phosphatidylinositol 3-phosphate; PBS, phosphate-buffered saline; TBST, tris-buffered saline; SDS-PAGE, sodium dodecyl sulfate polyacrylamide gel electrophoresis; PFA/GLA, 4.0% paraformaldehyde / 3.5% glutaraldehyde; w/v, weight per volume; cKO, conditional knockout

4.1 Introduction

Sertoli cells have been referred to as “mother” cells because of their distinguishing functions in the seminiferous tubule epithelium. The Sertoli cell fosters the growth and development of undifferentiated spermatogonia into elongated spermatids. Differentiating germ cells remain in contact with the Sertoli cell throughout this process, which in turn, provides growth factors, nutrition and protection from the immune system to the differentiating germ cells through the formation of the blood-testis-barrier. Therefore, understanding the processes that are required for Sertoli cell function may lead to novel mechanisms to treat male infertility.

Throughout spermatogenesis, the differentiating germ cells undergo a dramatic morphological transformation from round spermatocytes to spermatids, which have 1000-fold less cytoplasm, possess a rounded head and an elongated tail (Hess and Renato de Franca 2008). This requires cellular remodeling where much of the cytoplasm is packaged into cytoplasmic residual bodies that will be removed during spermiogenesis via the phagocytosis of the material by Sertoli cells (Chemes 1986; Nakagawa et al. 2005). Additionally, there is extensive apoptosis of differentiating germ cells that has been estimated to occur in upwards of 60% of germ cells in contact with Sertoli cells (Shaha et al. 2010). Both intrinsic and extrinsic initiation of apoptosis are observed, suggesting that a combination of factors regulate this loss. While it remains uncertain why such a high degree of apoptosis occurs, removal of these dying cells is completed by Sertoli cells via phagocytosis (Chemes 1986; Nakagawa et al. 2005). Thus, it should be appreciated that the functional Sertoli cell has a pronounced ability to metabolize phagocytized material.

The process of phagocytosis involves binding of the substrate, ingestion and subsequent degradation. Receptors on Sertoli cells bind to phosphatidylserine (PS) on the membranes of residual bodies and apoptotic cells as demonstrated by the apparent increase in apoptosis after administering Annexin V, which binds to PS (Maeda et al. 2002). Once ingested, the phagocytized material enters the endosome pathway and ends with the fusion to a lysosome, after which the contents are degraded and metabolized by the Sertoli cell (Oczypok et al. 2013). Autophagy is an evolutionarily conserved eukaryotic process that occurs at low constitutive levels in all cell types to sequester cytosolic material in a double membrane structure, termed the autophagosome, and to deliver the material to a lysosome for its breakdown and recycling into basic components. It should be realized that both autophagy and phagocytosis perform similar tasks, especially once a phagocytic vesicle has entered a cell.

There is a body of evidence suggesting that autophagy is associated with the process of phagocytosis. Recently, a phenomenon called "LC3-Associated Phagocytosis" was observed in macrophages, and is responsible for the clearance of phagocytic vesicles containing *Listeria monocytogenes* (Lam et al. 2013). Additional recent studies using Sertoli cells and retinal pigmented epithelial cells, both "non-professional" phagocytes (reviewed by Rabinovitch 1995), have characterized increased levels of autophagy that coincide with phagocytosis, suggesting that autophagy is utilized in the processing of phagocytized material (Yefimova et al. 2013; Kim et al. 2013). Furthermore, using microglia cells, considered to be another "non-professional" phagocyte, Lucin et al. demonstrated that depletion of BECN1 severely abrogates retromer trafficking (endosomes from plasma membrane to the Golgi apparatus) and phagocytosis (Lucin et al. 2013). The functional role of autophagy in phagocytosis is yet to be tested *in vivo*, but this groundwork provides evidence for the involvement of autophagy proteins.

In the present study, I utilized a conditional knockout mouse design to independently ablate two key autophagy genes specifically in adult Sertoli cells. The gene *Becn1* encodes a scaffold protein essential to the formation of the class III phosphatidylinositol 3-kinase (PtdIns3K) ‘nucleation’ complex, which is necessary to generate phosphatidylinositol 3-phosphate (PtdIns3P) on the forming autophagosome membrane. PtdIns3P is a lipid that signals for the recruitment of subsequent complexes necessary for autophagosome membrane expansion, closure, trafficking and fusion to a lysosome. The second gene, *Atg7*, is a key component of the enzyme system that conjugates Atg8-like proteins to the autophagosome membrane, and is essential for membrane expansion. I performed this study to address 1) if Becn1 has a similar function in phagocytosis in Sertoli cells as in glial cells, and 2) if the function of BECN1 in phagocytosis is an additional function to autophagy. These findings support that autophagy is necessary for the function of adult Sertoli cells, and that *Becn1* has a pleiotropic function in regulating phagocytosis.

4.2 Materials and Methods

4.2.1 Mice

Becn1-floxed (Gawriluk et al. 2011), *Atg7*-floxed (kind gift from Q. Wang) (Komatsu et al. 2005), *Amhr2*$^{tm3(cre)Bhr}$ (kind gift from C. Ko) (Jamin et al. 2002), *CAG-CAT-EGFP* (kind gift from K. Wagner) (Kawamoto et al. 2000) mice were all on a 129/Sv and B57BL/6 mixed background. *Becn1* conditional knockout males were generated by crossing *Becn1*$^{fl/fl}$; *Amhr2*$^{tm3(cre)Bhr/+}$ males to *Becn1*$^{fl/fl}$; *Amhr2*$^{+/+}$ females. The *Becn1*$^{fl/fl}$*; Amhr2*$^{tm3(cre)Bhr/+}$ males are infertile after 8-weeks old, so they were mated as early as five-weeks-old. Atg7 conditional knockout males were generated by crossing *Atg7*$^{fl/fl}$; *Amhr2*$^{tm3(cre)Bhr/+}$ males to *Atg7*$^{fl/fl}$; *Amhr2*$^{+/+}$ females. Controls males were littermates that did not carry the *Amhr2*$^{tm3(cre)Bhr}$ allele. All animals were genotyped using tail genomic DNA and alleles were detected by previously published PCR assays (see strain references above). All mice were housed in a University of Kentucky, Division of Laboratory Animal Resources facility, subjected to a 14:10 hour light:dark cycle and regular chow and water was available *ad libitum*. All animal procedures were compliant under the approved University of Kentucky IACUC protocol, 2008-0372.

4.2.2 Fertility assay

Males were placed into separate cages and housed with one or two females. Each morning after being setup, the females were checked for copulation plug and if present, placed into a separate cage to monitor for pregnancy and litter. Males were mated starting at 5-weeks-old to 26-weeks-old. The male's age when the plug was present, status of pregnancy and size of litter was collected for each mating.

4.2.3 Tissue collection and preparation

Males of correct age were euthanized by cardiac exsanguination via 18ga needle after being anesthetized by IP injection of Avertin (0.25 mg / g body weight). To control for any circadian controlled genes and/or proteins all mice were euthanized between 1300 and 1500 throughout the study. Reproductive tracts were quickly dissected out and washed several times in ice-cold PBS. The cauda epididymis was removed, placed into TYH media and sliced open to allow sperm to swim out for quantification by hemocytometer. Testes, seminal vesicles and prostate were carefully separated, as previously described, and weighed (Barclay and Cramer 2005).

For RNA and protein isolation, a testis was cut in half, flash frozen in liquid nitrogen and stored at -80°C. For histology and immunohistochemistry, the tunica was carefully cut in several places to facilitate fixative diffusion, and the whole testis was immersed in freshly-prepared, ice-cold 4% (w/v) paraformaldehyde for 12-24 hours with agitation at 4°C. Fixed testes were washed to remove paraformaldehyde, dehydrated through 25%, 50% and 70% ethanol and finally embedding in paraffin.

4.2.4 Histology

Paraffin embedded tissues were sectioned to 5 μM, adhered to gelatin subbed slides and air dried overnight at 37°C. Sections were deparaffinized with xylene, rehydrated and stained with Harris hematoxylin, followed by eosin, dehydrated and mounted with Permount.

For immunofluorescence, slides were blocked with 10% (w/v) BSA in PBS for one hour at room temperature and then incubated with primary antibody diluted with 3% (w/v) BSA in PBS overnight at 4°C. The following day, slides were washed with PBS three times, incubated with diluted secondary antibody for 1 hour at room temperature, washed with PBS three times and mounted with Prolong Gold anti-fade media containing 4',6-diamidino-2-phenylindole (Life Technologies, P-36931).

4.2.5 Real-time PCR

RNA was extracted from snap frozen tissue using TRIzol reagent as per manufacturer's protocol for high proteoglycan samples (Life Technologies). Total RNA was subjected to DNase (Invitrogen), as per manufacturer protocol, to remove any genomic DNA that was co-precipitated and then cleaned up on RNeasy Spin Columns (Qiagen). Total RNA was quantified by nanodrop. Total RNA (500 ng) was used for first-strand synthesis to create cDNA from a manufacturer kit (Quanta Biosciences). Detection of specific mRNA was then performed on samples in triplicate using SYBR-green PCR and quantified by ΔΔCt method. Primers for specific genes can be found in **Table 4.1**.

4.2.6 Immunoblotting

Tissue was subjected to ice-cold RIPA buffer (with freshly added protease/phosphatase inhibitors, Santa Cruz, sc-24948), homogenized (max speed for 45 seconds), sonicated (3 to 5 cycles of 40% duty cycle, magnitude of 4, 10 seconds followed by 30 seconds on ice), rocked for 30 minutes at 4°C and centrifuged 10,000 rpm for 10 minutes at 4°C to pellet the insoluble fraction. The soluble fraction was collected and total protein quantified by bicinchoninic acid assay (Thermo, 23225).

Twenty-five µg total protein per sample was denatured in Laemmli buffer for 10 minutes at 95°C and separated by SDS-PAGE on a 12% tris-acrylamide mini-gel. Separated proteins were transferred to a PVDF membrane with 0.45 µM pores (GE Healthcare, RPN303F) overnight (~16 hours @ 70mV) at 4°C. Transferred proteins were visualized by staining with Ponceau-S and membranes trimmed.

Membrane was blocked using 5% (w/v) skim milk in TBST for 1 hours at room temperature. Primary antibody (see **Table 4.2** for antibody concentrations) diluted in 5% (w/v) skim milk in TBST was added to membrane and allowed to incubate overnight (~16 hours) in a 4°C cold room. The membrane was washed three times with TBST for 5 minutes each and then HRP-conjugated secondary antibody diluted in 5% (w/v) skim milk in TBST was added and allowed to incubate for 1 hour at room temperature. Membranes were washed 3 times with TBST for 5 minutes. Secondary antibody was detected using Pierce ECL Plus substrate (Thermo, 32132, 1:1 dilution) and detected by CCD camera and specific band intensity was digitally quantified. For multiple antigen detection, membranes were stripped with 0.2M Glycine, 1% Tween-20, 0.1% SDS, pH=2.2 and then re-probed with new antibodies. Antibodies and dilutions used can be found in **Table 4.2**.

4.2.7 Electron Microscopy

Routine preparation for transmission electron microscopy was completed under supervision from the University of Kentucky Imaging Facility. Briefly, tissues were quickly dissected out and washed several times in ice-cold PBS. Next, tissues were diced with a razorblade to ~1 mm^3 cubes while in a droplet of freshly prepared 4% (w/v) paraformaldehyde / 3.5% (v/v) glutaraldehyde in 0.1 M cacodylate buffer (PFA/GLA). Following, tissue pieces were incubated in PFA/GLA for 2 hours at 4°C until fixed. After the first fixation, tissue pieces were washed four times with 8% (w/v) sucrose before post-fixing with 1% OsO_4 for 1.5 hours at 4°C. After dehydration through ethanol into propylene oxide, tissues pieces were infiltrated and embedded into Eponate 12 (PELCO). Embedded tissue pieces were sectioned to ultrathin slices of about 70 nm using a Reichert Ultracut E, mounted on copper grids, stained with uranyl acetate followed by lead citrate and observed by transmission electron microscopy (Philips Tecnai Biotwin 12).

4.2.8 Statistics

All statistics were performed in SigmaPlot 12 after consultation with the Applied Statistics Laboratory at the University of Kentucky. A two-way ANOVA was used with Holm-Sidak post-hoc testing between groups for comparisons with two variables. For all other comparisons, the statistical test used is indicated in the text.

Table 4.1
Real-time PCR Primers

Target	**NCBI Accession**	**Fwd Primer (5'-3')** **Rev Primer (5'-3')**	**Amplicon Size (bp)**
ApoJ	NM_013492	AGC AGG AGG TCT CTG ACA ATG GGC TTC CTC TAA ACT GTT GAG C	164
Beta-Actin	NM_007393	GCG TGA CAT CAA AGA GAA GC AGG ATT CCA TAC CCA AGA AGG	187
HSD17b3	NM_008291	AGG TTC TCG CAG CAC CTT TTT CAT CGC CTG CTC CGG TAA TC	100
Rhox5	NM_008818	GCA ACA CCA GTC CCT GAA CA CAA AAT CTC GGT GTC GCA AA	101
Stra8	NM_009292	GAA GGT GCA TGG TTC ACC GTG G GCT CGA TGG CGG GCC TGT G	161
TNF	NM_013693	CCC TCA CAC TCA GAT CAT CTT CT GCT ACG ACG TGG GCT ACA G	61
Tnp1	NM_009407	GGC GAT GAT GCA AGT CGC A CCA CTC TGA TAG GAT CTT TGG CTT TTG G	162

Table 4.2
Antibodies Used

Antigen	**Species Raised in**	**Manufacturer (Product No.)**	**Dilution Used**	**Application (kDa)**
GFP	Chicken	Aves Labs (GFP-1020)	1:500	IF
GCNA	Rat	George Enders	1:50	IF
BECN1	Rabbit	Santa Cruz (sc-11427)	1:2,000	WB (60)
ATG7	Rabbit	Cell Signaling (2631P)	1:1,000	WB (75)
LC3	Rabbit	MBL (PM036)	1:2,000	WB (16/18)
SQSTM1	Rabbit	Enzo (PW9860)	1:2,000	WB (62)
Actin	Rabbit	Sigma (A2066)	1:10,000	WB (42)
Secondary Antibodies				
Chicken IgY (H&L)	Goat	Invitrogen (A-11039)	1:1,000	IF
Rat IgM	Goat	Invitrogen (A-11044)	1:1,000	IF
Rabbit IgG (H&L)	Donkey	Rockland (611-703-127)	1:10,000	WB

4.3 Results

4.3.1 Becn1 is necessary for adult male fertility after 8 weeks of age

To study the function of autophagy in Sertoli cells I generated mice with conditional knockout (cKO) alleles for *Becn1* in adult Sertoli cells. *Becn1*$^{fl/fl}$ mice were crossed with anti-Müllerian hormone receptor 2-Cre (*Amhr2*$^{tm3(cre)Bhr}$) mice to generate male and female mice of genotype *Amhr2*$^{tm(cre)Bhr/+}$*; Becn1*$^{fl/fl}$ or Becn1 cKOs (Gawriluk et al. 2011; Jamin et al. 2002). The Amhr2-Cre allele is a knock-in to the *Amhr2* locus and thus, is expressed in cells that normally express *Amhr2*. This includes the Müllerian duct mesenchyme, embryonic Leydig and adult Sertoli cells in the male (Jamin et al. 2002; Tanwar et al. 2010; Jeyasuria et al. 2004). Wildtype (WT) mice were siblings of Becn1 cKO mice that did not carry Cre. Becn1 cKO mice were born at regular Mendelian frequencies and were healthy, with the exception of infertility in males and subfertility in females. The Becn1 cKO females had smaller litters and hypertrophy in the uterus and oviducts (data not shown). For the remainder of this chapter I will refer only to the males. Becn1 cKO males were mated to *CAG-CAT-EGFP* Cre-reporter mice to test the Sertoli cell deletion specificity (Kawamoto et al. 2000). In cells that have had Cre-recombinase expressed, the CAT cassette is removed and an EGFP cassette is expressed. EGFP was detected by epi-fluorescence in the seminiferous tubules of testis from *CAG-CAT-EGFP*$^{+}$; Becn1 cKO mice but not testis from *CAG-CAT-EGFP*$^{+}$; WT mice (**Figure 4.1 A, B**). Immunofluorescence for EGFP on fixed tissue sections indicates EGFP expression only in what appears to be the Sertoli cells of 6-week old Becn1 cKO testis (**Figure 4.1 C, D**). Previous studies have used the Amhr2-Cre mouse to study the Leydig cell population (Jeyasuria et al. 2004; Tanwar et al. 2010); however, I did not detect EGFP expression in the interstitial cells, suggesting that recombination does not occur in the Leydig cells. Thus, *Amhr2-Cre* expression is specific to the adult Sertoli cells in six-week-old testes.

To determine extent of knockout I performed immunoblotting to quantify the protein amount of BECN1 and SQSTM1 relative to ACTIN on whole testis from 6- and 10-week-old WT and Becn1 cKO mice. There was no difference in BECN1 quantity between 6-week-old WT and Becn1 cKO ($p=0.6$, Holm-Sidak post hoc test) (**Figure 4.7 A, B**). However, BECN1 was reduced by 2-fold in Becn1 cKO compared to WT at 10-weeks-old ($p<0.01$, Holm-Sidak post hoc test), demonstrating knockout (**Figure 4.7 A, B**). The 10-week-old Becn1 cKO group probably is a better reflection of deletion rate than the 6-week-old Becn1 cKO, which has a greater percentage of germ cells in the seminiferous tubules. The protein-turnover of SQSTM1, also known as p62, is autophagy-dependent and can be used to monitor autophagy, such that an accumulation of SQSTM1 indicates inhibition of autophagy and vice-versa (Bjørkøy et al. 2005). There was no difference in SQSTM1 at 6-weeks between WT and Becn1 cKO ($p=0.8$, Holm-Sidak post hoc test) (**Figure 4.7 A, B**). However, at 10-weeks, SQSTM1 was increased by 2-fold in Becn1 cKO compared to WT ($p<0.01$, Holm-Sidak post hoc test), demonstrating the accumulation of SQSTM1. Therefore, BECN1 is reduced and there is inhibition of autophagy due to the increase in SQSTM1 in Becn1 cKO testes.

To determine the effects of *Becn1* deletion on fertility I set up a fertility assay, as described in the materials and methods, to examine age-related reproductive performance. Five-week-old Becn1 cKO males showed evidence of mating with females within four days and 71% of the females got pregnant and had a litter (**Figure 4.1 J**). Six-week-old Becn1 cKO males had similar performance (**Figure 4.1 J**); however, 7- and 8-week-old Becn1 cKO males have reduced fertility where less than 50% of plugged females gave birth (**Figure 4.1 J**). No Becn1 cKO after 9 weeks of age or older sired a litter, despite presence of seminal plugs (**Figure 4.1 J**). The fertility assays were completed with a minimum of five Becn1 cKO males for each age tested, demonstrating a fully penetrant phenotype. In contrast, WT mice up to 1-year-old are regularly used in the colony for breeding purposes. Therefore, Becn1 cKO have reduced fertility that quickly diminishes to zero by 9-weeks of age. Thus, *Becn1* is required for male fertility after 9 weeks of age.

To determine the basis for reduced fertility, I analyzed reproductive tracts from Becn1 cKO and WT males at several time points from 6- to 17-weeks-old. The body weights of WT and Becn1 cKO showed similar increases with age and there was no difference between genotypes during this period ($p>0.5$, Holm-Sidak post hoc test) (**Figure 4.1 E**). On the other hand, as Becn1 cKO male mice age, their testes undergo regression such that they weigh less than 50% of WT testes by 10-weeks-old ($p<0.001$, Holm-Sidak post hoc test) (**Figure 4.1 F, I**). The weight of the seminal vesicles are directly proportional to testosterone production by the Leydig cells of the testes and as such, the weight of the seminal vesicles can be used to monitor testosterone signaling (Deanesly and Parkes 1933; Ayata et al. 1988). The seminal vesicle weights of WT and Becn1 cKO displayed similar increases and were not different between genotypes at any time observed ($p>0.2$, Holm-Sidak post hoc test) (**Figure 4.1 G**). This result suggests that *Becn1* ablation does not affect Leydig cell function prior to 17-weeks-old and that normal levels of inhibin are being produced by the Sertoli cells. The number of sperm collected from the cauda epididymis of Becn1 cKO mice was markedly reduced compared to WT mice beginning at 8 weeks of age, and this persisted until the end of the study ($p<0.001$, Holm-Sidak post hoc test) (**Figure 4.1 H**). At 12, 15 and 17 weeks of age spermatozoa were rarely witnessed in the collection dish, indicating a complete disruption of spermatogenesis. Moreover, at 6- and 8-week time points, there were sloughed germ cells and leukocytes in the Becn1 cKO collections that were not present in WT collections. Thus, *Becn1* is necessary for spermatogenesis and male fertility after 6-weeks-old.

4.3.2 Becn1 is required for spermatogenesis

The difference in testis weight, in addition to the difference in observed cauda sperm between WT and Becn1 cKO mice, suggested the dysregulation of spermatogenesis. I examined testis histology from 6-, 10- and 17-week-old WT and Becn1 cKO mice to determine the effect of *Becn1* ablation on spermatogenesis. Testes from WT mice have normal seminiferous tubules with all stages of spermatogenesis present, demonstrating typical spermatogenesis at each time point (**Figure 4.2 A-F**). At 6-weeks of age, Becn1 cKO seminiferous tubules are structurally different when compared to WT (**Figure 4.2 G, J**). There were numerous seminiferous tubules where sperm heads are closer to the basement membrane than primary spermatocytes. Another striking difference is the presence of large amounts of eosinophilic material released into the tubule lumens, most likely from sloughed spermatocyte cysts and residual bodies. At 10-weeks of age, large vacuoles were found in a majority of tubules (**Figure 4.2 H, K**, arrowheads). By 10 weeks of age, only the occasional sperm head was identified, and there was no evidence for spermatogenesis in any tubule. The ratio of Leydig cells is observably increasing, possibly due to hyperplasia. At 17-weeks of age, no evidence of sperm remained and many tubules had a Sertoli-cell only phenotype, suggesting a failure in the maintenance of spermatogonia (**Figure 4.2 I, L**). Large vacuoles were still present, which could be newly formed or persisting from earlier stages (**Figure 4.2 I, L**, arrowheads).

Histology of epididymides from 6-week old individuals showed a prevalence for leukocytes and sloughed cells (**Figure 4.2 N**, arrows). I only rarely observe leukocytes in WT tubules (**Figure 4.2 M**). Because no recombination was observed in the epididymides, this suggests that *Becn1* ablation in Sertoli cells disrupts the blood-testis-barrier or blood-epididymis-barrier, allowing infiltration of immune cells into the seminiferous and epididymal tubules.

4.3.3 Becn1 ablation increases Sertoli cell injury

To determine if the spermatogonial stem cell niche was negatively affected by *Becn1* ablation and thus, was responsible for loss of spermatogenesis, I measured the expression of several testis-specific cell markers by real-time PCR on RNA collected from whole testis. First, I examined markers corresponding to different stages of spermatogenesis and cell-types in the testis. Testosterone 17-beta-dehydrogenase 3 (*Hsd17b3*) is the enzyme expressed by Leydig cells that catalyzes the conversion of androstenedione to testosterone, and was used as a marker for Leydig cells. There was no detectable difference in *Hsd17b3* between WT and Becn1 cKO mice at 6-weeks-old ($p>0.3$, Holm-Sidak post-hoc test) (**Figure 4.3 A**). However, there was a 3-fold and 12-fold increase in *Hsd17b3* of Becn1 cKO testes compared to WT at 8- and 12-weeks-old ($p<0.01$, Holm-Sidak post-hoc test). This data supports the qualitative observation for the enrichment of Leydig cells in Becn1 cKO testes found by histology. The expression of *Rhox5*, a Sertoli-cell specific transcription factor, was not different between WT and Becn1 cKO at 6-weeks-old, but *Rhox5* was reduced by 2- and 5-fold in Becn1 cKO compared to WT at 8- and 12-weeks-old, respectively ($p<0.05$, Holm-Sidak test) (**Figure 4.3 A**). There was no difference detected between WT and Becn1 cKO at any time point, in the expression of *Stra8*, a marker for spermatogonia and pre-meiotic spermatocytes, suggesting that spermatogonia are present (**Figure 4.3 A**). Finally, the expression of *Tnp1*, a spermatid marker, was reduced 100-fold in 12-week-old Becn1 cKO testes compared to WT ($p<0.001$, Holm-Sidak post-hoc test), corroborating the histological and observational evidence for no spermatogenesis (**Figure 4.3 A**).

Due to the dramatic changes in morphology of the Becn1 cKO seminiferous tubules and the presence of immune cells in the epididymis, I next examined the injury markers tumor necrosis factor (*Tnf*) and clusterin (*Clu*). *Tnf* is expressed at low levels by both Sertoli cells and round spermatocytes in normal conditions and has been shown to regulate germ cell survival (reviwed in Lysiak, 2004). However, when Sertoli cells are injured (e.g. phthalate exposure, heat shock), *Tnf* expression is increased in Sertoli cells that induces *Fasl* expression in Sertoli cells, which in turn induces apoptosis and subsequent *Tnf* expression in spermatocytes (Yao et al. 2007; Mazaud-Guittot 2011). *Clu* is another gene upregulated by Sertoli cells in response to germ cell injury and in the presence of apoptotic bodies, is thought to act as a detergent to facilitate the removal of cellular material (Bailey et al. 2002; Bailey and Griswold 1999). Both *Tnf* and *Clu* were increased in Becn1 cKO testes compared to WT at 8- and 12-weeks-old, demonstrating that injury occurs after *Becn1* ablation ($p<0.001$, Holm-Sidak post hoc tests) (**Figure 4.3 B**).

To determine the location of spermatogonia, I next performed immunohistochemistry for germ cell nuclear antigen (GCNA). GCNA positive cells were located in their niche locations on the basal side of the tubule near the basement membrane between Sertoli cells in all WT tubules (**Figure 4.3 C, D, E**). GCNA positive cells were identified in Becn1 cKO tubules confirming the rt-PCR results for *Stra8,* up to the end of the experiment at 17-weeks-old (**Figure 4.3 F, G, H**). However, the GCNA positive cells were not in their niche locations and often present in clusters near the lumen of the tubule. The presence of GCNA positive cells in Becn1 cKO at 17-weeks-old suggests that spermatogonia persist for at least 8 weeks after infertility has occurred. Furthermore, this suggests that *Becn1*function in Sertoli cells is necessary for the differentiation of germ cells.

4.3.4 Becn1 is necessary for *endocytosis in Sertoli cells*

BECN1 functions as a scaffold for the PtdIns3K ‘nucleation’ complex, which generates PtdIns3P on the forming autophagosome membrane (Funderburk et al. 2010). While the PtdIns3K complex is necessary for autophagosome formation it has recently been described in endosome fusion, phagocytosis and regulating the exocyst complex (Liang et al. 2008; Bodemann et al. 2011; Lucin et al. 2013). To test if Becn1 ablation affects Sertoli cell autophagy or endocytosis, I performed transmission electron microscopy on 6-week-old testes. Six-week-old testes were looked at because beyond 6-weeks-old several vacuoles are present in a majority of tubules indicating Sertoli cell damage, and I predicted that there would be a difference prior to the phenotypes.

The wild-type Sertoli cells had numerous lysosomes, as evident by the electron dense vesicles and several smaller endosomes with diameters of about 500 nm (**Figure 4.4 A, C, E, G**). I also observed multiple autophagosomes within WT cells indicating that autophagy does occur at detectable levels.

The Becn1 cKO Sertoli cells, on the other hand, had numerous small vesicles in addition to large vacuoles, as seen by histology (**Figure 4.4 B, D, F, H**). No autophagosomes were observed in any Sertoli cell, indicating a block in autophagosome formation. Surprisingly, a sperm head was observed within a Sertoli cell (**Figure 4.4 D**, labeled), demonstrating that Becn1 cKO Sertoli cells were phagocytizing sperm. Additionally, endosomes with cellular debris are present without any indication of productive degradation (**Figure 4.4 H**, labeled). Most striking was the absence of electron dense lysosomes in the Becn1 cKO Sertoli cells. Therefore, *Becn1* is necessary for the clearance of phagocytic vesicles in Sertoli cells.

4.3.5 Atg7 is necessary for continued spermatogenesis

Because *Becn1* has an additional function in endocytosis and the data demonstrated that endocytosis is clearly abrogated in Becn1 cKO Sertoli cells, I wanted to determine the significance of another key autophagy gene, Atg7 for Sertoli cell function I observed that *Amhr2*$^{tm3(cre)Bhr/+}$; *Atg7*$^{fl/fl}$ (Atg7 cKO) also became infertile but not until 26-weeks old (data not shown). I performed immunoblot analysis to quantify ATG7 and SQSTM1 relative to ACTIN in 20- and 26-week-old WT and Atg7 cKO testes. There is a moderate 25% reduction in ATG7 in Atg7 cKO compared to WT at 20-weeks (p=0.03, Holm-Sidak post hoc test) (**Figure 4.7 C, D**). Comparing 20-week-old to 26-week-old samples there is a 4-fold decrease in ATG7 (p<0.01, Holm-Sidak post hoc test) and there is no difference between WT and Atg7 cKO at 26-weeks-old (p=0.6, Holm-Sidak post hoc test), suggesting that there is transition in ATG7 expression (**Figure 4.7 C, D**). At both 20- and 26-week-old I detected an expected 3-fold increase of SQSTM1 in Atg7 cKO samples compared to WT (p<0.001, Holm-Sidak post hoc test), suggesting inhibition of autophagy. Therefore, while the knockout of *Atg7* is not detected in 26-week-old mice, the increase in SQSTM suggests the expected inhibition of autophagy (**Figure 4.7 C, D**).

To determine if testosterone production was reduced in Atg7 cKO males, I compared the reproductive tracts of WT and Atg7 cKOs at 12-, 20- and 26-weeks-old. WT and Atg7 cKOs were not different for the first 20 weeks of age in terms of body, seminal vesicle and testis weight (p>0.5, t-test) (**Figure 4.5 A, B, C**). Furthermore, no difference in the number of epididymal sperm was observed at 12- or 20-weeks-old (p>0.4, Holm-Sidak post-hoc test) (**Figure 4.5 D**). Interestingly, at 26-weeks-old, testes weight and sperm count was decreased compared to WT ($p<0.01$, Holm-Sidak post-hoc test) (**Figure 4.5 B, D**). Additionally, three 26-week-old Atg7 cKO males were mated to two WT females each, but no litters were sired. Moreover, 26-week-old Atg7 cKO seminal vesicle weight was increased by 70% compared to WT ($p<0.01$, Holm-Sidak post-hoc test) (**Figure 4.5 C**). A similar increase was also seen in prostate weight (data not shown), together suggesting an increase in testosterone signaling in 26-weeks-old Atg7 cKO males.

To determine if *Atg7* ablation affect spermatogenesis I performed histology on 20- and 26-week-old testes. The histology indicates similarities between the Atg7 cKO and Becn1 cKO mice. At 20 weeks, Atg7 cKO seminiferous tubules had vacuolation in addition to eosinophilic contents present in the lumens (**Figure 4.6 C**). Moreover, there was evidence of leukocytes in the epididymis of Atg7 cKO mice (**Figure 4.6 G**). At 26 weeks, there was extensive vacuolation and many tubules represent Sertoli-cell only with no spermatogenesis observed (**Figure 4.6 D**, arrowheads). The Atg7 cKO epididymis was full of immune cells at 26-weeks-old, further indicating that the blood-testis-barrier or blood-epididymis-barrier had been compromised (**Figure 4.6 H**, arrows). Thus, *Atg7* is required for spermatogenesis and fertility.

4.4 Discussion

The Sertoli cell performs multiple diverse tasks within the seminiferous tubule that make it essential for arguably the most important aspect of testicular function, spermatogenesis. I undertook the experiments described here to determine a role for autophagy in the adult Sertoli cell by conditionally deleting *Becn1* or *Atg7,* specifically in the adult Sertoli cell population. I predicted that the relationship between phagocytosis and autophagy could be exploited in Sertoli cells and that dysregulation of autophagy would compromise Sertoli cell function. The data presented suggests that this prediction is correct and that autophagy is required for Sertoli cell function, as both Becn1 cKO and Atg7 cKO males have degenerative seminiferous tubules that eventually fail to produce sperm. However, the ablation of *Becn1* is more severe with males becoming infertile at least 12 weeks earlier than the deletion of *Atg7.* Thus, the data suggest that *Becn1*has an additional function besides autophagy in Sertoli cells.

4.4.1 Both Atg7 and Becn1 are necessary for Sertoli cell function

The deletion of either *Atg7* or *Becn1* leads to infertility due to failure of spermatogenesis. This was evident by counting sperm from the cauda epididymis, where 8-week-old Becn1 cKO males are devoid of sperm and 26-week-old Atg7 cKO males have dramatically reduced numbers. A fertility assay performed on Atg7 cKO and Becn1 cKO males corroborated the reduced sperm counts with the failure to sire litters after 26 weeks and 9 weeks of age, despite mating behavior evidenced by the presence of seminal plugs. Lastly, the testes histology from Atg7 cKO and Becn1 cKO mice demonstrates a lack of spermatogenesis and Sertoli-cell only tubules by 26- and 10-weeks-old, respectively. Since Sertoli cells are long-lived, prominent regulators of spermatogenesis, and autophagy is an essential cellular process, it is not surprising that dysregulation of autophagy would affect spermatogenesis. However, the dramatic difference in timing was not expected.

Both knockouts have similar phenotypes in that seminiferous tubules show vacuolation around Sertoli cells and the presence of cytoplasmic material and leukocytes in the epididymis. While the function of autophagy has not been tested in Sertoli cells, signaling pathways that regulate autophagy have been studied. The induction of autophagy occurs in response to the phosphorylation of the ULK1/2 complex. The ULK1/2 complex associates with and is a target of the active mTOR complex, which inhibits autophagy. The conditional deletion of the negative regulators of mTOR, TSC1 or TSC2, show vacuolation of tubules at 12 weeks, followed by complete loss of germ cells by 5 months of age (Tanwar et al. 2012). Similarly, the conditional deletion of an inhibitor of TSC1 and TSC2, LKB1, shows vacuolation of tubules and complete loss of germ cells by 5 months of age (Tanwar et al. 2012). Moreover, AMPK is also a target of LKB1, which can directly phosphorylate the ULK1/2 complex not associated with the mTOR complex, promoting autophagy (Kim et al. 2011). When the extracellular ligand Wnt binds its receptor, Frizzled, a signal transduction pathway leads to the stabilization of cytoplasmic β-catenin. In turn, β-catenin regulates several processes in the cytoplasm and can translocate in the nucleus and regulate transcription. Cytoplasmic and nuclear targets of β-catenin involve inhibiting autophagy (Petherick et al. 2013). Alternatively, autophagy inhibits the activation of β-catenin by directly degrading the Wnt receptor (Petherick et al. 2013; Gao et al. 2010; Zhang et al. 2011). The Wnt/β-catenin pathway is essential throughout development and was recently explored in Sertoli cells through the introduction of a constitutively active β-catenin, which causes the vacuolation of the seminiferous tubules and loss of germ cells by 12 weeks of age

(Tanwar et al. 2010; Boyer et al. 2008). In the above studies, autophagy was not tested but I could speculate that autophagy was inhibited in the Sertoli cells of all these mice.

Noticing that the LKB1, TSC1 and TSC2 cKOs all have gradual declines in seminiferous tubule morphology, which is similar to the Atg7 cKO, it is possible that the inhibition of ATG7-dependent autophagy is related in these phenotypes. Similarly, the Becn1 cKO has a rapid degeneration similar to the constitutively active β-catenin. Future characterization of β-catenin to determine if a higher level of β-catenin activity is present in the Becn1 cKO, would test if similar mechanisms are involved.

4.4.2 Becn1 is necessary for the clearance of phagocytized material

These results indicate that *Becn1* regulates the clearance of phagocytized differentiating germ cells. The Sertoli cell is a non-professional phagocyte within the seminiferous tubule and is responsible for the phagocytosis of apoptotic germ cells, in addition to, residual bodies. In H&E stained tissue, I observe the presence of sperm heads within Sertoli cells in close proximity to the basal lamina. Additionally, by ultrastructure analysis I observe the presence of elongated sperm heads and what appear to be spermatocytes within vesicles of the Becn1 cKO Sertoli cell. Moreover, these inclusions have a noticeable structure, with the ability to be identified, and are not present in WT Sertoli cells, indicating that they are not being degraded. These observations support my hypothesis that autophagy proteins are necessary for the clearance of phagocytic vesicles.

I propose a four-step model for Sertoli cell failure in Becn1 cKO mice. First, Sertoli cells begin phagocytizing apoptotic, differentiating germ cells and residual bodies, but cannot fuse these to lysosomes. The BECN1 complex that binds to UVRAG has been shown to be necessary for endosomes containing EGFR and Cathepsin D to fuse to lysosomes

(Zeng et al. 2006). One would expect an excess of lysosomes in Becn1 cKO Sertoli cells if this was the case, but the data showed the opposite. The lack of lysosomes could be due to decreased lysosome biogenesis that partly occurs from endosome-endosome fusion events (Nielsen et al. 2007), which I have implicated BECN1 in previously. Either way, phagocytized vesicles fail to fuse to lysosomes. Second, Sertoli cells undergo a stress response due to having an accumulation of phagocytic vesicles and drop in available ATP. While the true implication of an accumulation of phagocytic vesicles is largely unknown, the accumulation of autophagosomes, endosomes or lysosomes is attributed to cell death. Thus, I suspect that the accumulation of undigested phagocytic vesicles would be detrimental. Furthermore, Sertoli cells have a very high metabolism compared to other cells in the testis and obtain ATP from lipid metabolism or through the degradation of phagocytized material (Xiong et al. 2009). Third, since Sertoli cells cannot further support phagocytosis, management over the incredibly high amount of apoptosis that occurs in the seminiferous tubule is lost. The observation of particles that resemble residual bodies in the epididymides of both Becn1 cKO and Atg7 cKO mice suggest that there is a failure in Sertoli cells to support further phagocytosis. Additionally, a role for autophagy in regulating the expression of scavenger receptors on the surface of macrophages has been demonstrated (Bonilla et al. 2013). The specific scavenger receptor, scavenger-receptor, class B I (SR-BI) is partly responsible for the binding to and phagocytosis of membranes with exposed PS (e.g. apoptotic cells and residual bodies) (Nakanishi and Shiratsuchi 2004). Thus, loss of scavenger receptor trafficking by autophagy proteins in my conditional knockouts may be responsible for the apparent reduced phagocytosis. While SR-BI knockout males are fertile no study on the testis have been performed to determine what compensatory mechanisms exist (Rigotti et al. 1997). Fourth, with differentiating germ cells undergoing apoptosis there is an increase in inflammatory cytokines, such as TNFα, resulting in the degradation of the tubule and infiltration of leukocytes. Indeed, exposure of the seminiferous epithelium to TNFα disrupts the blood-testis-barrier leading to leukocyte infiltration (Li et al. 2006a). Additionally, recent insights have identified that TNFα downregulates the expression of Coxsackievirus and adenovirus receptor in Sertoli cells, which facilitates germ cell-to-Sertoli cell junctions and results in sloughing of material into the lumens (Gao and Lui 2014). I detected an inflammatory response in the Becn1 cKO as increased *Tnfa* and *ApoJ* expression, and leukocyte infiltration into the epididymides.

To determine if this model is correct, there are several experiments that need to be done. First, a molecular identification of the cytoplasmic material in the epipdymides to determine if these are residual bodies should be completed. Second, the characterization of an accumulation of phagocytized material needs to be performed. This could be done though feeding bacteria that block phagocytic vesicle fusion. Third, apoptotic indices of differentiating germ cells in mutant testes should be characterized to determine if increased apoptosis occurs with gene ablation. Fourth, to determine the apparent permeability of the blood-testis-barrier small molecule tracers could be injected into mutant testes. Characterization of the ability of mutant Sertoli cells to bind molecules like PS can determine the propensity to initiate phagocytosis. Lastly, the presence of GNCA positive cells in Becn1 cKO tubules, suggests that Sertoli cells are minimally functioning. If the Sertoli cells are simply stressed, then this should be reversible through reintroduction of the gene that was knocked out. This could be done with the use of an inducible gene system, such as a TET-on system, where a tetracycline-induced transcription factor induces the expression of a replacement transgene that is expressed only after Cre recombination, to limit the rescue to the original cells.

4.4.3 Summary

Amhr2-Cre has also been shown to be expressed in interstitial cells of the testis, and any confounding effects from that expression might be of concern (Teixeira et al. 1996; Jeyasuria et al. 2004; Tanwar et al. 2010). However, I did not observed recombination by GFP expression in Leydig cell and there was no phenotypic defect observed in Leydig cell steroidogenesis when comparing WT and Becn1 cKO mice. The dysregulation of *Becn1* in rat Leydig cells reduces testosterone production, and would have been an expected result if recombination occurred in Leydig cells. However, I did not detect a decrease in testosterone, as suggested by similar seminal vesicle weights. Moreover, comparison of the seminal vesicles and prostate from 26-week-old Atg7 cKO mice and WT, suggest that there are increasing amounts of testosterone produced. In Becn1 cKO testis, it appears that Leydig cell hyperplasia does occur. However, at 12-weeks-old Becn1 cKO testes are smaller than WT testes, and their weight is half of WT testes, suggesting the apparent increase in Leydig cells numbers in any given section is caused by the decrease in total volume of the adult mutant testis. Similar observations have been made in other mouse models with defective Sertoli and/or Sertoli-germ functions (Meng et al. 2000; Papaioannou et al. 2009; Tanwar et al. 2010).

The conclusions from this study support a role for *Becn1* in regulating Sertoli cell phagocytosis and function. Furthermore, the similar phenotype in Atg7 cKO mice demonstrate a role for autophagy in Sertoli cell function, although the ablation of *Atg7* is less severe when compared to the deletion of *Becn1*. The conclusions from any study where a crucial developmental pathway is perturbed should be carefully analyzed, and this is true for this study. Further experiments are needed for broad and mechanistic conclusions, but I provide novel evidence that of autophagy is a necessary process for Sertoli cells.

4.5 Ackowledgements

This work was completed in part with University of Kentucky funds to Edmund Rucker and Gertrude Flora Ribble Graduate Student fellowship to Thomas Gawriluk. I would like to thank CheMyong Ko (University of Illinois) for the $Amhr2^{tm3(cre)Bhr}$ mouse, Kay-Uwe Wagner (University of Nebraska Medical Center) for the *CAG-CAT-EGFP* mouse, Qingjun Wang (University of Kentucky) for the *Atg7*-flox mouse, George Enders (University of Kansas Medical Center), Wendy Katz (University of Kentucky) for embedding tissues, Vincent Cassone (U. Kentucky) for reagents, use of his lab space, and rt-PCR machine, Ashley Seifert (U. Kentucky) for use of his tissue processing system, and Maggie Murphy (U. Kentucky) for help with histology.

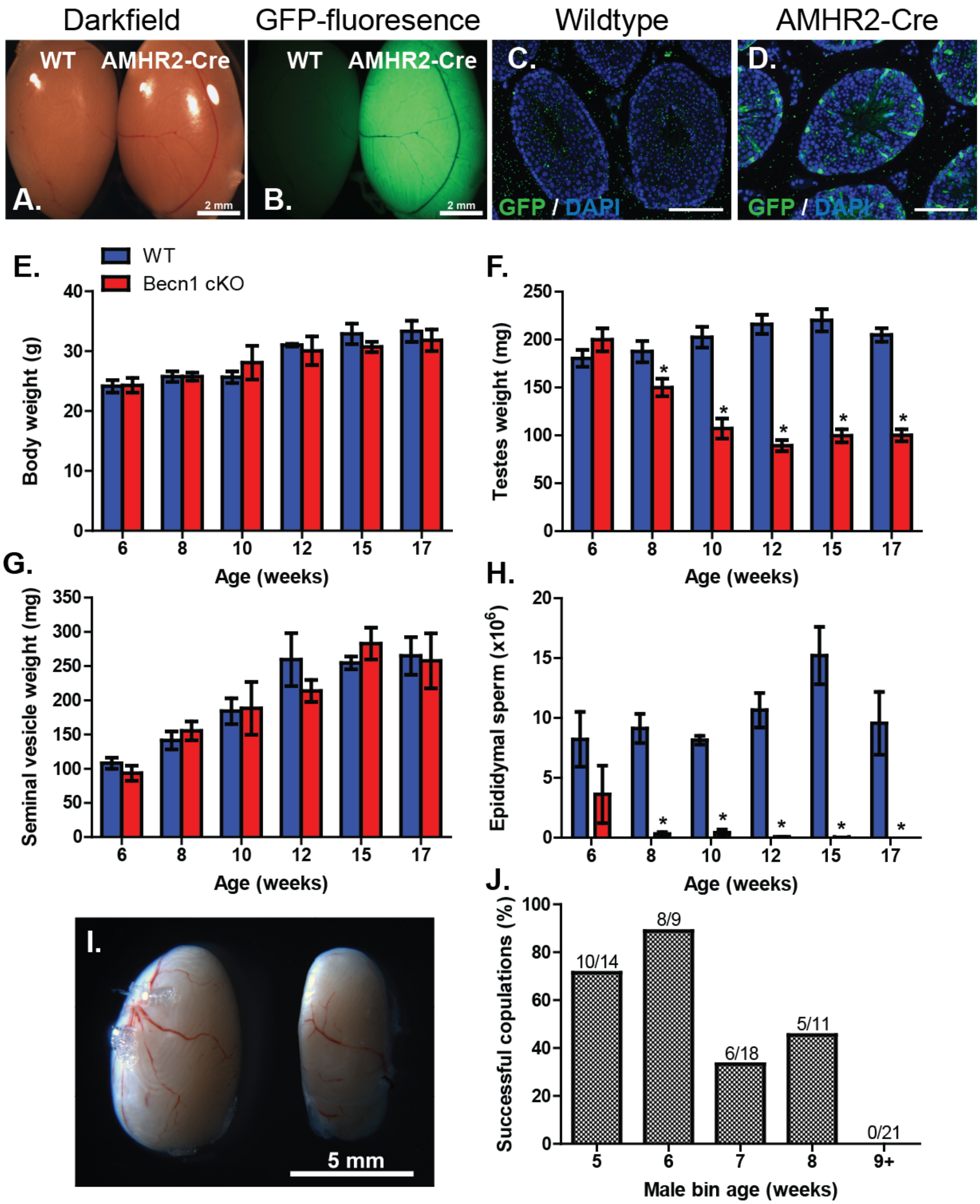

Figure 4.1. *Becn1* expression in Sertoli cells is necessary for fertility beyond 8 weeks. (**A through D**) Six-week-old testis and epididymis from *CAG-CAT-EGFP*$^{+}$ animals on either WT or Becn1 cKO backgrounds viewed under dark-field (A) and EGFP epi-fluoresence (B). Immunofluorescence for EGFP counterstained with DAPI to show cellular localization of GFP expression in WT (C) and Becn1 cKO backgrounds (D). Bar equals 100 µM.

Figure 4.1 Continued. (**E through H**) Body (E), testes (F), and seminal vesicle (G) masses at time of euthanasia, and estimated number of epididymal sperm (H). Bars indicate mean ± s.e.m. * indicates $p<0.05$ versus WT using Holm-Sidak post-hoc test. n ≥ 3 for each group. (**I**) Comparison of testis from WT (left) and Becn1 cKO (right) at 10 weeks of age. (**J**) Results from fertility assay, indicating the percent of successful mating for different aged Becn1 cKO males. Ratio above each bar indicate the number of litters per total mating attempts. Each bar represents attempts from at least five different Becn1 cKO males.

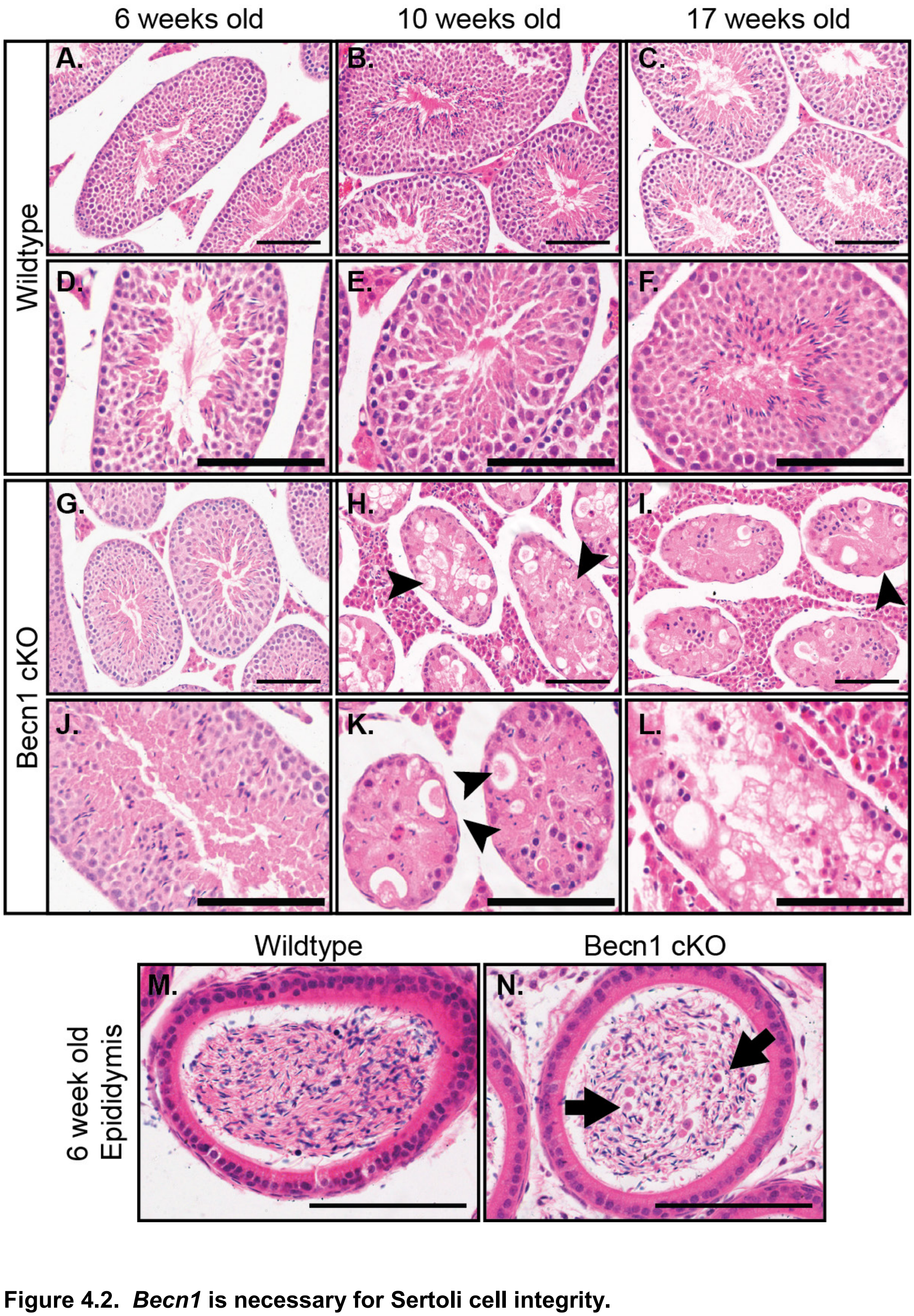

Figure 4.2. *Becn1* is necessary for Sertoli cell integrity.

Figure 4.2. Continued. (**A through H**) Representative images of H&E stained seminiferous tubules from males at 6- (A D, G and J), 10- (B, E, H and K) and 17- (C, F, I and L) week-old WT and Becn1 cKO males. Vacuolation of the tubules in Becn1 cKOs is evident (arrowheads). Bar equals 100 µM. (**M and N**) Representative images of H&E stained cross-sections of epididymal tubules from 6-week-old WT and Becn1 cKO males (M and N, respectively). Immune cells are present in the tubules of Becn1 cKO males (arrows). Bar equals 100 µM.

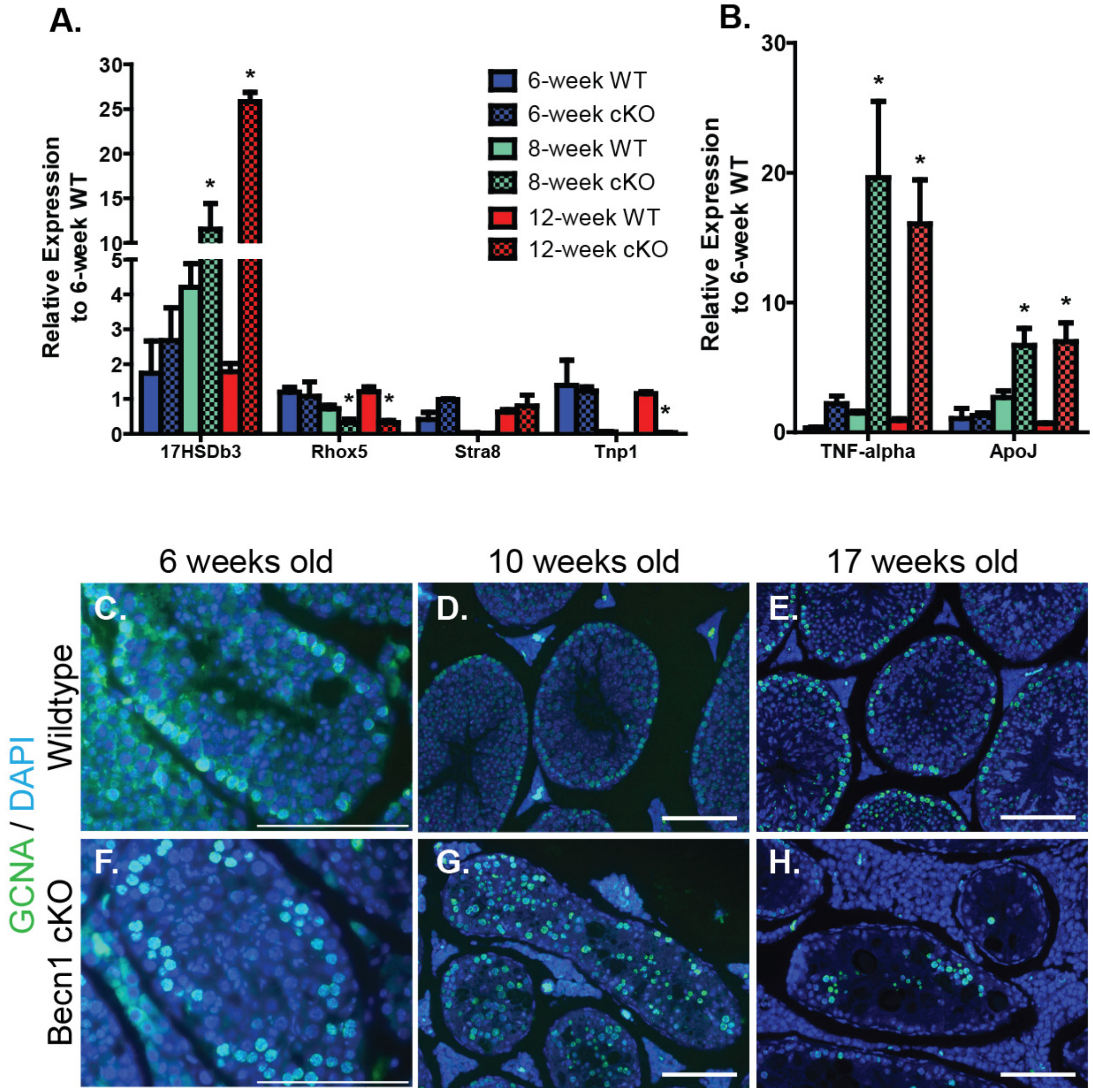

Figure 4.3. Spermatogonia are still present with evidence of Sertoli cell injury in Becn1 cKOs. (**A and B**) Real-time PCR analysis for germ cell development markers (A) and cell injury makers (B). Bars represent mean ± standard error of the mean. Data is expression normalized to Beta-actin. * indicates p-value <0.05 for Holm-Sidak posthoc test versus WT for that age, within each gene. (**C through H**) Representative images of seminiferous tubules immunostained for GCNA (green) and counterstained with DAPI (blue) from 6- (C and F), 10- (D and G) and 17- (E and H) week-old WT and Becn1 cKO males. Bar equals 100 μM.

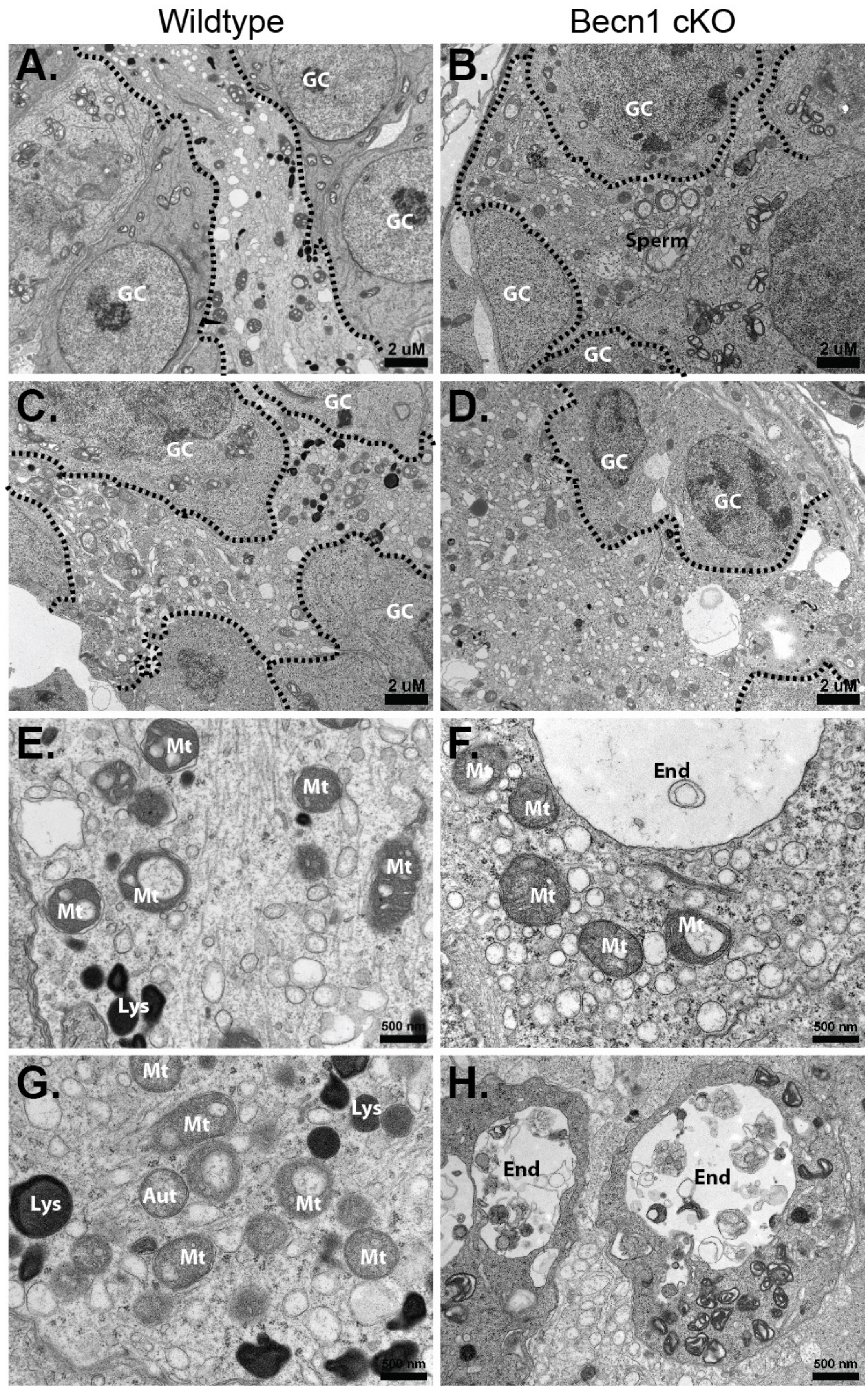

Figure 4.4. Endocytosis is abrogated after *Becn1* ablation.

Figure 4.4 Continued. (**A through H**) Lower magnification transmission electron microscopy images showing the basal side of single Sertoli cells from 6-week-old WT (A and C) and Becn1 cKO males (B and D) (dashed line is to outline Sertoli cell). Higher magnification indicating autophagosomes and lysosomes in WT (E and G) in contrast to extensive vacuolation and failed endocytosis in Becn1 cKO (F and H). Structures are labeled by abbreviations: GC, germ cell; Mt, mitochondria; Lys, lysosome; End, endosome.

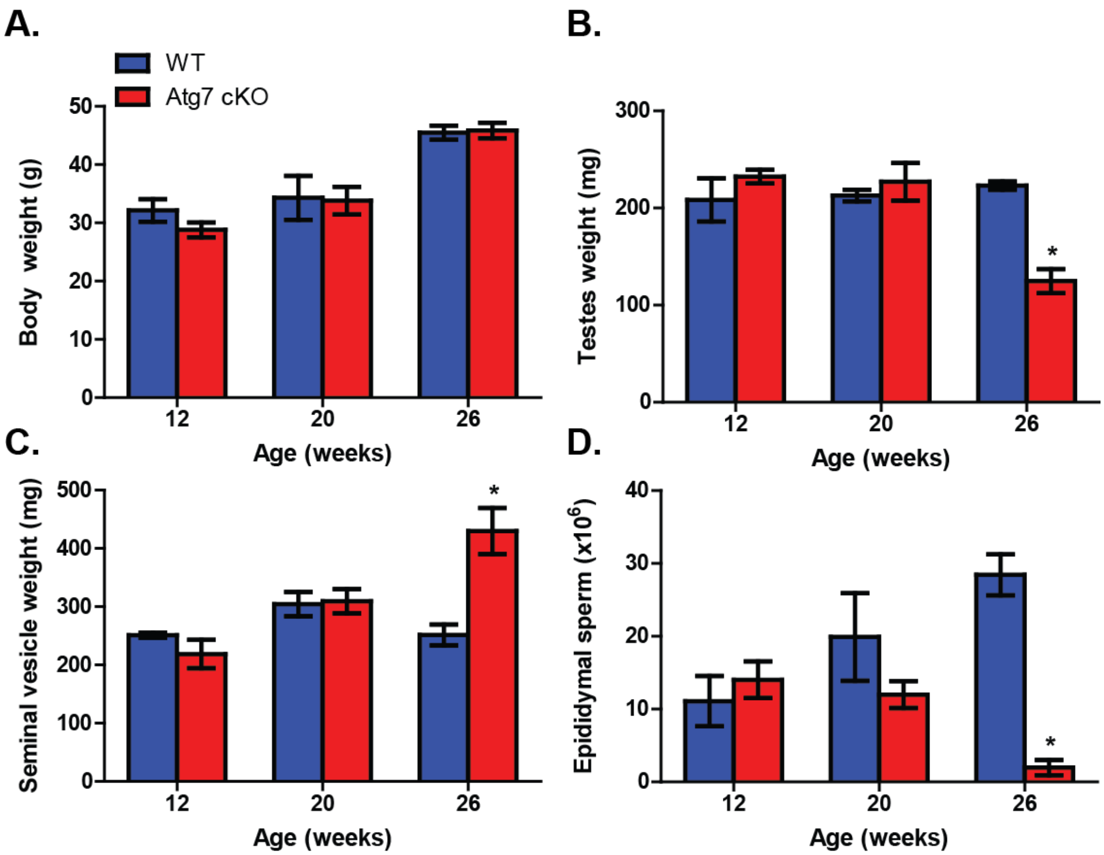

Figure 4.5. 26-week old Atg7 cKOs have reduced sperm. (**A through D**) Body, testes and seminal vesicle masses at time of euthanasia (E, F and G, respectively) and estimated number of epididymal sperm (H). Bars indicate mean ± standard error of the mean. * indicates $p<0.05$ for Holm-Sidak post-hoc test for age. $n \geq 3$ for each bar.

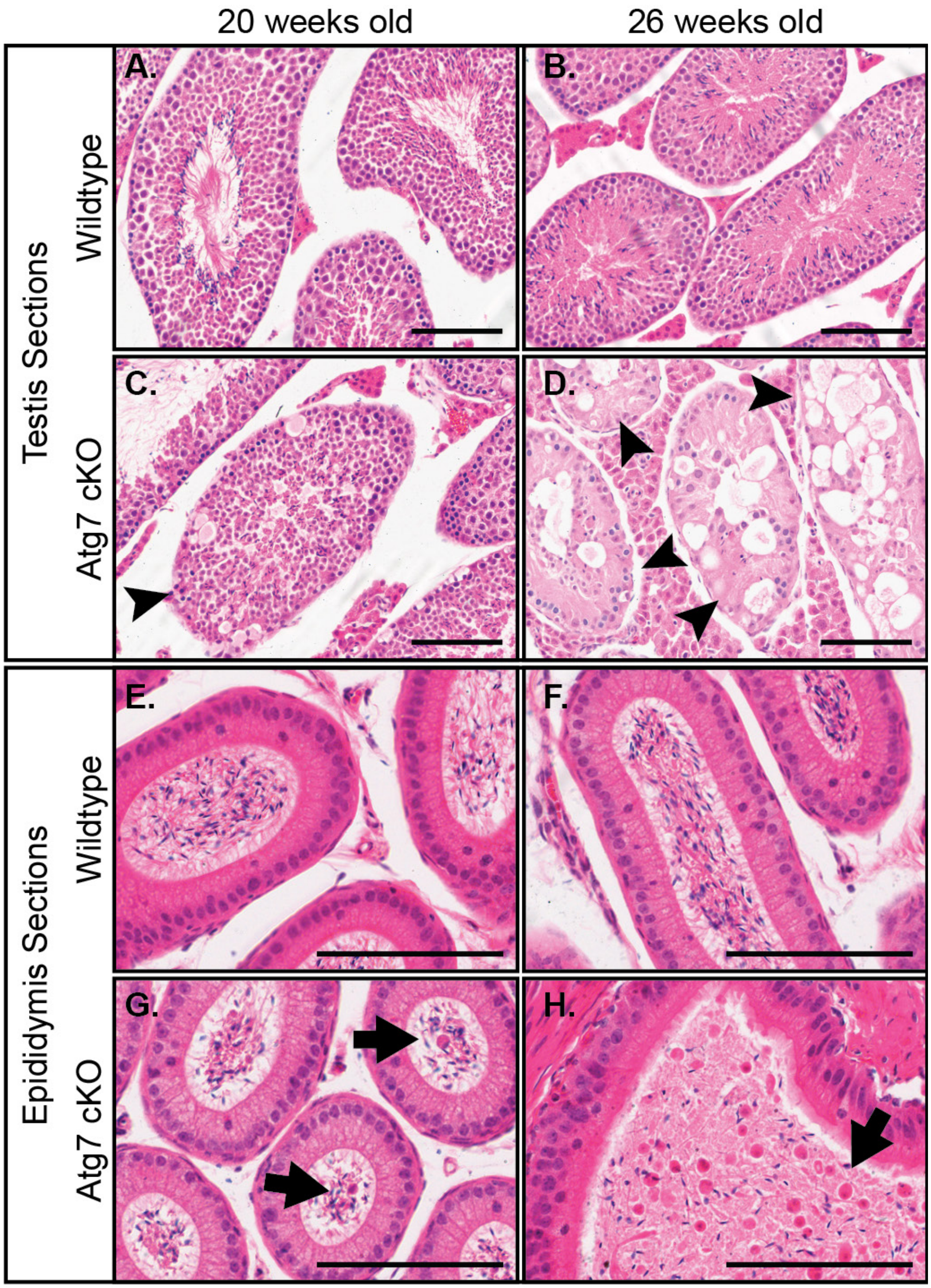

Figure 4.6. Atg7 is necessary for Sertoli cell integrity. (**A through D**) Representative images of hematoxylin and eosin stained seminiferous tubules from 20- (A and C) and 26- (B and D) week-old WT and Atg7 cKO males. Vacuolation of the tubules in Atg7 cKO is evident (arrowheads). Bar equals 100 μM. (**E through H**) Representative images of H&E stained cross-sections of epididymal tubules from 20- (E and G) and 26- (F and H) week-old WT and Atg7 cKO males. Immune cells are present in the tubules of Atg7 cKO males (arrows). Bar equals 100 μM.

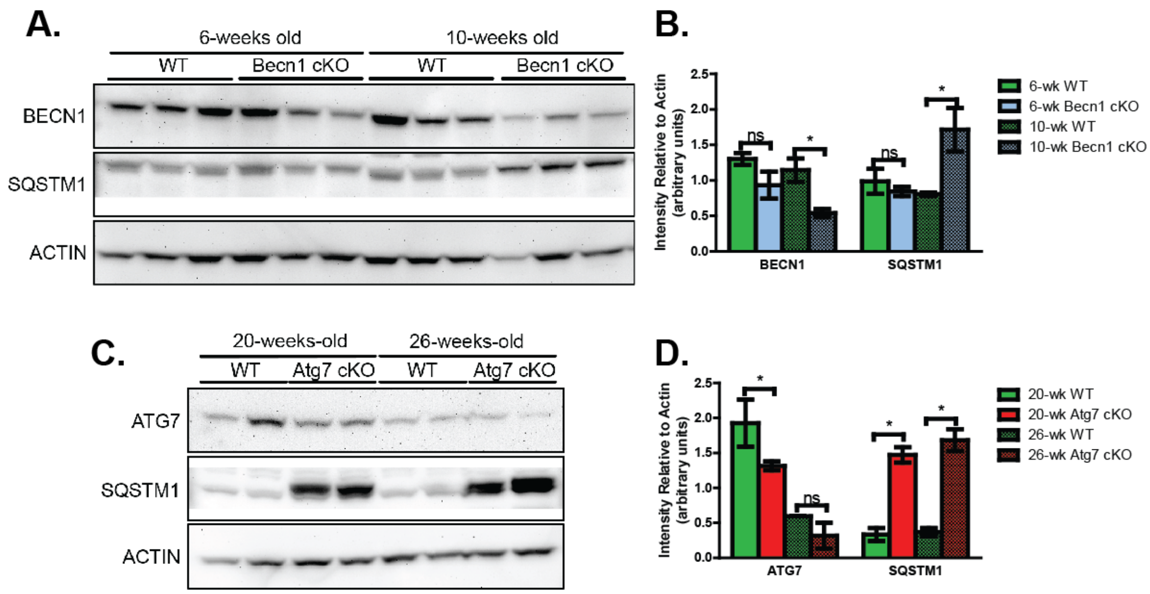

Figure 4.7 BECN1 and ATG7 proteins levels in testes.
(**A and B**) Representative immunoblot for BECN1, SQSTM1 and ACTIN at 6- and 10-weeks-old (A). Quantification of band density relative to ACTIN (B). Data represent mean with s.e.m. * denotes $p<0.05$ for indicated comparison by Holm-Sidak post-hoc test. n=5. (**C and D**) Representative immunoblot for ATG7, SQSTM1 and ACTIN at 20- and 26-weeks-old (C). Quantification of band density relative to ACTIN (B). Data represent mean with s.e.m. * denotes $p<0.05$ for indicated comparison by Holm-Sidak post-hoc test. n=4.

Copyright © Thomas Raymond Gawriluk 2014

CHAPTER 5: GENERAL CONCLUSIONS AND DISCUSSION

The data presented in this dissertation support that autophagy is required for embryonic oocyte survival and adult Sertoli cell function. Additionally, the data support that *Becn1* is necessary for luteal cell steroidogenesis. The goal of this dissertation was to determine the significance of autophagy in the ovary and testis though conditional deletion of two key autophagy genes, *Atg7* and *Becn1* in the mouse. The underlying hypothesis tested was that autophagy is necessary for cellular homeostasis and data presented in Chapters 2 and 4 data support this. Deficiency in either *Atg7* or *Becn1* resulted in a reduced oocyte endowment in females and the degeneration of the seminiferous tubule followed by infertility in males. However, in Chapter 3, the data support two contradictory conclusions, dependent on the gene studied. *Becn1* is required for progesterone synthesis during pregnancy and gene deficiency resulted in reduced circulating progesterone followed by abortion or preterm labor. In contrast, *Atg7* gene deficiency resulted in a 2-fold increased production of progesterone, and did not affect pregnancy outcome. Presented in this final chapter, is a discussion of how these findings relate to each other and possible future directions to take.

Dysregulation of an essential process such as autophagy is likely to have a detrimental phenotype. Indeed, knockout mice for several key regulators of autophagy cannot survive after birth or are embryonic lethal (reviewed by Hale et al. 2013). Additionally, many of the secondary and tertiary regulators of autophagy have been implicated in several human diseases (reviewed by Jiang and Mizushima 2014). For example, mutation of an Atg8-like protein that becomes conjugated to autophagosome membranes in neurons results in higher iron-ion accumulation and causes neuron damage leading to behavioral abnormalities (Haack et al. 2012). By obstructing autophagy through the ablation of *Atg7* or *Becn1,* I expected a negative effect on cellular homeostasis that would inhibit the normal function of that cell, as well as the revelation of any or non-autophagy related functions. In the case of embryonic oocytes and Sertoli cells this notion was supported. I observed fewer oocytes at birth and seminiferous tubules degenerated in autophagy deficient mice. However, we must also consider that key regulators of essential pathways are under strong selection pressure. Furthermore, this selection pressure supports the development of functionally redundant pathways and proteins. It should be appreciated that autophagy is not only an animal process, but that it is deeply rooted in the eukaryote lineage, with a well-supported hypothesis that autophagy was developed in the last-common ancestor to all eukaryotes that last existed approximately 2 billion years ago (Hughes and Rusten 2007). This makes sense as eukaryotes have organelles, and autophagy is the only process characterized to remove and degrade organelles at any appreciable rate. Thus, it is reasonable that throughout time gene duplication events would have allowed for redundant genes and pathways to develop. Many of the single genes identified in yeast that participate in many aspects of autophagy have expanded to gene families in mammals. For example, *Atg8* is represented in mammals by three gene families for a total of 10 different proteins (reviewed by Shpilka et al. 2011).

Now let us consider all of the processes in a cell. Many of these processes are unrelated, but occasionally we will find proteins that perform functions in several different pathways, also called pleiotropy. Additionally, proteins can develop new functional domains that can create dependence for that protein in an additional process. Furthermore, some of these proteins are key regulators of essential processes, forming interaction networks that are subject to high selection pressure. However, more often we will find that there are cellular processes that rely upon essential processes to function. Think about ATP synthesis, RNA transcription or fatty acid hydrolysis that all generate products that are necessary for downstream cellular processes. There are models that try to explain how selection drives these interactions networks elsewhere, but I will not elaborate (Nowak et al. 1997). It is here that I will leave you with the implied hypothesis of this dissertation. By ablating the key regulators of autophagy *Atg7* and *Becn1* we dysregulate autophagy allowing for the potential discovery of processes that depend on either the gene, autophagy or both.

This dissertation provides evidence that *Becn1* is necessary for endosome maturation, in addition, to its role in autophagy. The transmission electron micrographs presented in both Chapters 3 and 4 are great examples of this, demonstrating an accumulation of endosomes in *Becn1* cKO luteal cells and Sertoli cells. Endosomes are a diverse group of vesicles within a cell. They can originate from the Golgi apparatus to secrete soluble proteins, the endoplasmic reticulum to deliver transmembrane signaling molecules and transporters or the plasma membrane to internalize extracellular components (Huotari and Helenius 2011). Moreover, there is evidence that not all endosomes are created equal. Different functional families of endosomes have a distinct protein-profile associated with their membranes and contents.

Endocytosis or the process of internalizing extracellular components into endosomes, parallels autophagy in many aspects. First, cells can acquire energy and nutrients through endocytosis of macromolecules and proteins. Second, the end is the same, as a mature endosome fuses to a lysosome. An important function of endocytosis is the internalization of cell-surface receptors and their ligands, which is vital for a cell's growth and communication, and can provide an example for endosome maturation. Endocytosed material is internalized as endocytic vesicles that fuse together to form early endosomes. The function of the early endosome is to sort its contents for downstream processes. Cell-surface receptors inside can be recycled back to the plasma membrane, transferred to the Golgi network or remain in the endosome. The contents of an endosome can be directly recycled without digestion or can be transported to multivesicular bodies, also called late endosomes where the continued fusing with intraluminal vesicles and themselves cause them to grow in size and gather contents. Late endosomes then fuse with lysosomes and the contents are digested and provided for use by the cell.

There are a number of proteins involved in transporting and identifying the different classes of endosomes. Of these the Rab-GTPases, Rab5 and Rab7 are best studied. Once activated the Rab-proteins facilitate the binding to motor proteins to transport the endosome along microtubules. Additionally, the Rab-proteins recruit other proteins that facilitate endosome maturation including hydrogen ion pumps, which act to lower the pH inside a late endosome. Rab5 is found predominately on early endosomes and is necessary for early endosome fusion events, suggesting its role in sorting. On the other hand, Rab7 is predominately found on late endosomes and is necessary for multivesicular body and lysosome fusion. Thus an exchange of Rab5 for Rab7 occurs during this transition that can be modeled (Binder and Holzhütter 2012).

In the Becn1 cKO luteal cells, I found an increased number of endosomes with a concurrent decrease in progesterone production and neutral lipid storage. Cholesterol is the substrate for steroidogenesis and lipid droplet formation, and as discussed in Chapter 3, it is possible that a decrease in the ability to transport cholesterol is responsible for these phenotypes. I observed large endosomes that in many cases were empty, throughout a majority of the cytoplasm. There is no evidence that these endosomes fuse with multivesicular bodies and / or lysosomes because they are too big and are not electron dense structures. It is possible that these endosomes are early endosomes and their contents include the compliment of LDL and HDL cell-surface receptors. If we believe this, then receptors cannot be recycled back to the plasma membrane because early endosomes are not maturing. Therefore, the luteal cell cannot transport enough HDL and LDL to support progesterone production. If this is true, then there should be an accumulation of Rab5 on the endosomes in the luteal cells of Becn1 cKOs. I would also expect a phenotype in progesterone production when the receptor in question is inhibited. The LDLR knockout females have no apparent fertility defects (Ishibashi et al. 1993). As LDLR is the prominent lipoprotein receptor endocytosed and mice can compensate for its loss, this is not a likely candidate. In contrast, SR-BI females are infertile (Trigatti et al. 1999). This appears to be due to an increase of circulating HDL that in turn has a detrimental effect on oocyte competence (Miettinen et al. 2001). However, the SR-BI knockout females have been shown to produce 50% less progesterone during an induced pseudopregnancy (Jiménez et al. 2010) and knockdown of SR-BI in human differentiated granulosa cells results in reduced progesterone synthesis (Kolmakova et al. 2010). This suggests that SR-BI function could be affected in the Becn1 cKO. I did not observe a reduction in *Scarb1* mRNA in my study at P8.5 but it is possible the cellular distribution of SR-BI is not in the plasma membrane where it would be expected. While the relationship between SR-BI progesterone is suggestive of the interaction with BECN1, the endocytosis of SR-BI is not the primary function described and might be rare. It would be important to characterize SR-BI endocytosis in mouse luteal cells during pregnancy. Additionally, I do not know what the contents of the observed endosomes are. The endosomes may be full of LDLR and LDL or SR-BI contributing to reduced cholesterol transport. Alternatively, the increased number of endosomes may cause cell stress leading to decreased steroidogenesis. A necessary experiment would be to detect Rab5 and Rab7 in isolated endosome fractions to determine if these are early or late endosomes. In the same study, the presence of the cell-surface receptor candidates can be tested.

The phagocytosis block in Sertoli cells presented in Chapter 4 parallels the endosome story. I identified elongated spermatids and degenerating spermatocytes within the Sertoli cells of Becn1 cKO but not in controls. This supports that phagocytized material is not entering the endosome pathway for further maturation and degradation. Phagocytized vesicles are decorated with Rab-proteins and proceed to mature similar to early and late endosomes. A difference between endocytosis and phagocytosis being that cell-surface receptors are not recycled back to the plasma membrane but to the Golgi complex through the retromer complex. As introduced in Chapter 4, there is growing evidence that the Atg8-like protein, LC3, is recruited to phagocytic vesicles that contain *Listeria monocytogenes* (Lam et al. 2013), and this association is necessary for degradation. It is unknown if something similar occurs in Sertoli cells; however, cultured Sertoli cells have been shown to activate autophagy as recognized by LC3 conversion during phagocytosis (Yefimova et al. 2013). I attempted to look at this phenomenon by observing LC3 in the testes of GFP-LC3 mice; however, there was no detectable GFP puncta in WT or mutants (data not shown). This is surprising because autophagosomes have been observed by electron microcopy in Sertoli cells (Galdieri et al. 1981); however, GFP puncta were also not observed in WT luteal cells, but were seen in oocytes and theca cells. As both the Sertoli cell and luteal cells are highly metabolic, it is possible that any autophagosome that is formed is small and short lived, making it difficult to observe puncta. Alternatively, it could be possible that fixation quenched the GFP signal in the testes. However, I did observed GFP puncta in the epididymal clear cells (data not shown). Additionally, different amounts of fixation did not bring about signal, suggesting that no puncta exist in the testis. I quantified LC3 by Western blot from whole testis but detected no difference between either Atg7 cKO or Becn1 cKO and WT (data not shown). This result could be because there is no difference, or that the population of Sertoli cells is too small to detect a difference. A better experiment would be to detect LC3 in a purified population of Sertoli cells. Now if we believe the GFP-LC3 results in the testis, that there are no puncta, this must mean either Sertoli cells do not use LC3 for incorporation into membranes or the LC3 is quickly degraded. Treatment of cultured *GFP-LC3* Sertoli cells with bafilomycin A1, which blocks lysosome maturation, and thus causes an accumulation of autophagosomes, would be one way to test this. Regardless of these suggested experiments, the data demonstrate the phenotype.

The ablation of either *Becn1* or *Atg7* in the Sertoli cells appear to have the same phenotype. I performed no mechanistic analysis to prove this, but the phenotypes are similar. It is possible that dysregulation of autophagy is the cause of the phenotype in both mutants, but the delayed onset in Atg7 cKO mice casts doubt. It is possible that Atg7-independent autophagy occurs in Sertoli cells to compensate for the loss of *Atg7* and it merely takes longer for the phenotype to manifest itself. Alternatively, *Becn1* is involved with the endosome maturation and this is essential for Sertoli cell function while in the *Atg7* mutants the Sertoli cell succumbs to the loss of homeostasis. The latter is clearly the case in the luteal cells, where the loss of *Atg7* showed the opposite phenotype compared to the loss of *Becn1*. Not explored in this dissertation was the idea that compensation for the loss of *Becn1* could be happening through *Beclin-2*. It would be easy enough to look at mRNA expression of *Beclin-2* and protein expression of BECN2 in the *Becn1* knockouts.

So what is the evidence that BECN1 participates in endosome maturation? The receptor recycling of EGFR and the maturation of Cathepsin D are the best examples I currently know of. EGFR is a cell-surface receptor that binds to EGF and EGF-like ligands. Upon ligand binding, the receptor homodimerizes and results in the activation of multiple signaling pathways (e.g. MAPK, JAK/STAT, PI3K/AKT/mTOR, and PLC/PAG/PKC) (Sui et al. 2014). Many of which were discussed in relation to the activation of the cumulus granulosa during the LH surge in Chapter 1. Once bound to ligand, the EGFR-ligand complex remains active and in order to downregulate the transduction pathways, the EGFR-ligand complex undergoes receptor-meditated endocytosis to either degrade the receptor-ligand complex or to degrade the ligand and recycle the receptors back to the plasma membrane. The presence of PtdIns3P on early endosomes that contain EGFR-ligand complexes is responsible for maturation and sorting to late endosomes by recruiting Rab7 (Petiot et al. 2003). It was later shown the presence of PtdIns3P is not a function of the plasma membrane class I PtdIns3k, but of the class III PtdIns3k, which also regulates autophagosome formation (Thoresen et al. 2010). Moreover, the knockdown of individual components of the PtdIns3k complex (e.g. VPS34, VPS15, BECN1, UVRAG and BIF-1) results in inhibited EGFR sorting and recycling (Thoresen et al. 2010).

The evidence with Cathepsin D is similar, but from a different source of endosome. I have only described endocytosis, thus far, but endosomes can mature from the Golgi-network, as well. Cathepsin D is an aspartic protease that is a member of the milieu of lysosome proteases. To inhibit random protease activity, many lysosome proteases are translated in an inactive form that only become active after entering a lysosome. Cathepsin D is such a protein that must undergo maturation by cleavage after entering a lysosome. Thus, tracking of Cathepsin D through the endosome maturation is possible by detecting the different forms. Using experiments similar to what I just described, Cathepsin D was identified as another protein that did not translocate correctly in endosomes when trying to elucidate how EGFR is sorted in VPS34 deficient cells (Row et al. 2001). In the same experiments already discussed for EGFR, Cathepsin D maturation was equally, negatively affected, suggesting a similar mechanism (Thoresen et al. 2010). The identification of the Rab7 interacting protein, Rubicon, that also interacts with BECN1, demonstrated a mechanism for how the BECN/PtdIns3K complex could interact with endosomes (Liang et al. 2008). Later a "feed-forward loop" between UVRAG, Rubicon and C-VPS/HOPS (C vacuolar protein sorting complex / homotypic vacuole fusion and protein sorting) was found to exist in human cell culture that activates Rab7 and subsequent endosome maturation (Sun et al. 2010). Thus, the BECN1/PtdIns3k complex is present on endosomes during endosome maturation. However, this appears to only influence some endosomes, such as those containing Cathepsin D and EGFR, as other aspects of endosome maturation were reported to be normal in the referenced studies. So, is there a commonality between phagocytic vesicles, vesicles containing potential lipid substrate and the EGFR/Cathepsin D endosomes? I am not sure, but will speculate that the scavenger receptors involved with phagocytosis in Sertoli cells and endocytosis in luteal cells are similar to EGFR/Cathepsin D. It would be an attractive experiment to follow such receptors in the mutants described in this dissertation.

Within this dissertation, I have presented data supporting my hypotheses that autophagy is necessary for oocyte survival and Sertoli cell function. Additionally, the data provide evidence that *Becn1* has an essential role for steroidogenesis in luteal cells. A theme that *Becn1* has pleiotropic roles to autophagy is also prevalent in the data, further supporting that the BECN1/PtdIns3K complex plays a role in endosome maturation, regulating the degradation of phagocytic vesicles and perhaps lipoprotein-receptor mediated endocytosis. Overall, I have shown that autophagy is a process necessary for the function of the reproductive system and is an attractable model to study. The preterm labor mouse may provide insights into progesterone production in humans, and demonstrates that there is conservation of autophagy regulation on steroidogenesis between Leydig and luteal cells. This provides us with a hypothesis that *Becn1* deficiency in placenta will negatively impact steroidogenesis, and may lead to preterm birth. Additionally, this opens up the opportunity to test the autophagy-steroidogenesis interaction in other cell types, like the adrenal corticotrophs. The implications for the Sertoli cell work may be important for future study of phagocytosis, trafficking and degradation of the phagocytized material. Knowing that phagocytosis machinery such as BECN1 is conserved among several different phagocytes, allows for a comparative approach to studying disease models such as, macular degeneration. Regardless of these outcomes, the data within this dissertation provide a better understanding of the role of autophagy in oocytes, luteal cells and Sertoli cells and provides new evidence to ask new questions in the field of reproductive biology.

Copyright © Thomas Raymond Gawriluk 2014

Bibliography

Abney TO. 1999. The potential roles of estrogens in regulating Leydig cell development and function: a review. *Steroids* **64**: 610–7.

Accili D, Arden KC. 2004. FoxOs at the crossroads of cellular metabolism, differentiation, and transformation. *Cell* **117**: 421–6.

Acton S, Rigotti A, Landschulz KT, Xu S, Hobbs HH, Krieger M. 1996. Identification of scavenger receptor SR-BI as a high density lipoprotein receptor. *Science* **271**: 518–20.

Adhikari D, Flohr G, Gorre N, Shen Y, Yang H, Lundin E, Lan Z, Gambello MJ, Liu K. 2009. Disruption of Tsc2 in oocytes leads to overactivation of the entire pool of primordial follicles. *Mol Hum Reprod* **15**: 765–70.

Adhikari D, Zheng W, Shen Y, Gorre N, Hämäläinen T, Cooney AJ, Huhtaniemi I, Lan Z-J, Liu K. 2010. Tsc/mTORC1 signaling in oocytes governs the quiescence and activation of primordial follicles. *Hum Mol Genet* **19**: 397–410.

Akar U, Chaves-Reyez A, Barria M, Tari A, Sanguino A, Kondo Y, Kondo S, Arun B, Lopez-Berestein G, Ozpolat B. 2008. Silencing of Bcl-2 expression by small interfering RNA induces autophagic cell death in MCF-7 breast cancer cells. *Autophagy* **4**: 669–79.

Akiyama H, Lyons JP, Mori-Akiyama Y, Yang X, Zhang R, Zhang Z, Deng JM, Taketo MM, Nakamura T, Behringer RR, et al. 2004. Interactions between Sox9 and beta-catenin control chondrocyte differentiation. *Genes Dev* **18**: 1072–87.

Alaupovic P, Lee DM, McConathy WJ. 1972. Studies on the composition and structure of plasma lipoproteins. Distribution of lipoprotein families in major density classes of normal human plasma lipoproteins. *Biochim Biophys Acta* **260**: 689–707.

Albarracin CT, Parmer TG, Duan WR, Nelson SE, Gibori G. 1994. Identification of a major prolactin-regulated protein as 20 alpha-hydroxysteroid dehydrogenase: coordinate regulation of its activity, protein content, and messenger ribonucleic acid expression. *Endocrinology* **134**: 2453–60.

Albrecht ED, Pepe GJ. 1990. Placental steroid hormone biosynthesis in primate pregnancy. *Endocr Rev* **11**: 124–50.

Alfadhli E, Koh A, Albaker W, Bhargava R, Ackerman T, McDonald C, Ryan EA, Shapiro AMJ, Senior PA. 2009. High prevalence of ovarian cysts in premenopausal women receiving sirolimus and tacrolimus after clinical islet transplantation. *Transpl Int* **22**: 622–5.

Alizadeh Z, Kageyama S-I, Aoki F. 2005. Degradation of maternal mRNA in mouse embryos: selective degradation of specific mRNAs after fertilization. *Mol Reprod Dev* **72**: 281–90.

Allen WM. 1935. The isolation of crystalline progestin. *Science (80-)* 89–93.

Anasti JN. 1998. Premature ovarian failure: an update. *Fertil Steril* **70**: 1–15.

Anderson R, Copeland TK, Schöler H, Heasman J, Wylie C. 2000. The onset of germ cell migration in the mouse embryo. *Mech Dev* **91**: 61–8.

Andric N, Ascoli M. 2008. The luteinizing hormone receptor-activated extracellularly regulated kinase-1/2 cascade stimulates epiregulin release from granulosa cells. *Endocrinology* **149**: 5549–56.

Ankel-Simons F, Cummins JM. 1996. Misconceptions about mitochondria and mammalian fertilization: implications for theories on human evolution. *Proc Natl Acad Sci U S A* **93**: 13859–63.

Ara T, Nakamura Y, Egawa T, Sugiyama T, Abe K, Kishimoto T, Matsui Y, Nagasawa T. 2003. Impaired colonization of the gonads by primordial germ cells in mice lacking a chemokine, stromal cell-derived factor-1 (SDF-1). *Proc Natl Acad Sci U S A* **100**: 5319–23.

Ashford TP, Porter KR. 1962. Cytoplasmic components in hepatic cell lysosomes. *J Cell Biol* **12**: 198–202.

Avagliano L, Virgili E, Garò C, Quadrelli F, Doi P, Samaja M, Bulfamante G Pietro, Marconi AM. 2013. Autophagy and human parturition: evaluation of LC3 expression in placenta from spontaneous or medically induced onset of labor. *Biomed Res Int* **2013**: 689768.

Ayata M, Yamane T, Li W, Terada N, Kitamura Y, Matsumoto K. 1988. Proliferative response of seminal vesicle cells to androgen in mice castrated neonatally and pretreated with estrogen or androgen at adulthood. *Endocrinol Jpn* **35**: 511–5.

Bagheri-Fam S, Sinclair AH, Koopman P, Harley VR. 2010. Conserved regulatory modules in the Sox9 testis-specific enhancer predict roles for SOX, TCF/LEF, Forkhead, DMRT, and GATA proteins in vertebrate sex determination. *Int J Biochem Cell Biol* **42**: 472–7.

Bailey R, Griswold MD. 1999. Clusterin in the male reproductive system: localization and possible function. *Mol Cell Endocrinol* **151**: 17–23.

Bailey RW, Aronow B, Harmony JAK, Griswold MD. 2002. Heat shock-initiated apoptosis is accelerated and removal of damaged cells is delayed in the testis of clusterin/ApoJ knock-out mice. *Biol Reprod* **66**: 1042–53.

Baker TG. 1963. A quantitative and cytological study of germ cells in human ovaries. *Proc R Soc Lond B Biol Sci* **158**: 417–33.

Baker TG. 1966. A quantitative and cytological study of oogenesis in the rhesus monkey. *J Anat* **100**: 761–76.

Barclay WW, Cramer SD. 2005. Culture of mouse prostatic epithelial cells from genetically engineered mice. *Prostate* **63**: 291–8.

Barlow C, Liyanage M, Moens PB, Tarsounas M, Nagashima K, Brown K, Rottinghaus S, Jackson SP, Tagle D, Ried T, et al. 1998. Atm deficiency results in severe meiotic disruption as early as leptonema of prophase I. *Development* **125**: 4007–17.

Beck S, Wojdyla D, Say L, Betran AP, Merialdi M, Requejo JH, Rubens C, Menon R, Van Look PFA. 2010. The worldwide incidence of preterm birth: a systematic review of maternal mortality and morbidity. *Bull World Health Organ* **88**: 31–8.

Bedell MA, Brannan CI, Evans EP, Copeland NG, Jenkins NA, Donovan PJ. 1995. DNA rearrangements located over 100 kb 5' of the Steel (Sl)-coding region in Steel-panda and Steel-contrasted mice deregulate Sl expression and cause female sterility by disrupting ovarian follicle development. *Genes Dev* **9**: 455–70.

Behrman R, Butler A. 2007. *Preterm birth: causes, consequences, and prevention*.

Bennett J, Wu Y-G, Gossen J, Zhou P, Stocco C. 2012. Loss of GATA-6 and GATA-4 in granulosa cells blocks folliculogenesis, ovulation, and follicle stimulating hormone receptor expression leading to female infertility. *Endocrinology* **153**: 2474–85.

Ben-Ze'ev A, Amsterdam A. 1989. Regulation of cytoskeletal protein organization and expression in human granulosa cells in response to gonadotropin treatment. *Endocrinology* **124**: 1033–41.

Bergeron L, Perez G, Macdonald G. 1998. Defects in regulation of apoptosis in caspase-2-deficient mice. *Genes Dev* 1304–1314.

Bernard P, Sim H, Knower K, Vilain E, Harley V. 2008. Human SRY inhibits beta-catenin-mediated transcription. *Int J Biochem Cell Biol* **40**: 2889–900.

Berry DL, Baehrecke EH. 2007. Growth Arrest and Autophagy Are Required for Salivary Gland Cell Degradation in Drosophila. *Cell* **131**: 1137–1148.

Bethea CL, Walker RF. 1979. Age-related changes in reproductive hormones and in Leydig cell responsivity in the male Fischer 344 rat. *J Gerontol* **34**: 21–7.

Billig H, Furuta I, Hsueh AJ. 1993. Estrogens inhibit and androgens enhance ovarian granulosa cell apoptosis. *Endocrinology* **133**: 2204–12.

Binart N, Bachelot A, Bouilly J. 2010. Impact of prolactin receptor isoforms on reproduction. *Trends Endocrinol Metab* **21**: 362–8.

Binder B, Holzhütter H-G. 2012. A hypothetical model of cargo-selective rab recruitment during organelle maturation. *Cell Biochem Biophys* **63**: 59–71.

Binnerts ME, Kim K-A, Bright JM, Patel SM, Tran K, Zhou M, Leung JM, Liu Y, Lomas WE, Dixon M, et al. 2007. R-Spondin1 regulates Wnt signaling by inhibiting internalization of LRP6. *Proc Natl Acad Sci U S A* **104**: 14700–5.

Birky CW. 1995. Uniparental inheritance of mitochondrial and chloroplast genes: mechanisms and evolution. *Proc Natl Acad Sci U S A* **92**: 11331–8.

Bjørkøy G, Lamark T, Brech A, Outzen H, Perander M, Overvatn A, Stenmark H, Johansen T. 2005. p62/SQSTM1 forms protein aggregates degraded by autophagy and has a protective effect on huntingtin-induced cell death. *J Cell Biol* **171**: 603–14.

Black SM, Harikrishna JA, Szklarz GD, Miller WL. 1994. The mitochondrial environment is required for activity of the cholesterol side-chain cleavage enzyme, cytochrome P450scc. *Proc Natl Acad Sci U S A* **91**: 7247–51.

Bodemann BO, Orvedahl A, Cheng T, Ram RR, Ou Y-H, Formstecher E, Maiti M, Hazelett CC, Wauson EM, Balakireva M, et al. 2011. RalB and the exocyst mediate the cellular starvation response by direct activation of autophagosome assembly. *Cell* **144**: 253–67.

Boland K, Flanagan L, Prehn JHM. 2013. Paracrine control of tissue regeneration and cell proliferation by Caspase-3. *Cell Death Dis* **4**: e725.

Bonilla DL, Bhattacharya A, Sha Y, Xu Y, Xiang Q, Kan A, Jagannath C, Komatsu M, Eissa NT. 2013. Autophagy regulates phagocytosis by modulating the expression of scavenger receptors. *Immunity* **39**: 537–47.

Borgeest C, Symonds D, Mayer LP, Hoyer PB, Flaws JA. 2002. Methoxychlor may cause ovarian follicular atresia and proliferation of the ovarian epithelium in the mouse. *Toxicol Sci* **68**: 473–8.

Boya P, González-Polo R-A, Casares N, Perfettini J-L, Dessen P, Larochette N, Métivier D, Meley D, Souquere S, Yoshimori T, et al. 2005. Inhibition of macroautophagy triggers apoptosis. *Mol Cell Biol* **25**: 1025–40.

Boya P, Reggiori F, Codogno P. 2013. Emerging regulation and functions of autophagy. *Nat Cell Biol* **15**: 713–20.

Boyer A, Hermo L, Paquet M, Robaire B, Boerboom D. 2008. Seminiferous tubule degeneration and infertility in mice with sustained activation of WNT/CTNNB1 signaling in sertoli cells. *Biol Reprod* **79**: 475–85.

Braw RH, Bar-Ami S, Tsafriri A. 1981. Effect of hypophysectomy on atresia of rat preovulatory follicles. *Biol Reprod* **25**: 989–96.

Braw RH, Tsafriri A. 1980. Effect of PMSG on follicular atresia in the immature rat ovary. *J Reprod Fertil* **59**: 267–72.

Breen SM, Andric N, Ping T, Xie F, Offermans S, Gossen JA, Ascoli M. 2013. Ovulation involves the luteinizing hormone-dependent activation of G(q/11) in granulosa cells. *Mol Endocrinol* **27**: 1483–91.

Bridges PJ, Jo M, Al Alem L, Na G, Su W, Gong MC, Jeoung M, Ko C. 2010. Production and binding of endothelin-2 (EDN2) in the rat ovary: endothelin receptor subtype A (EDNRA)-mediated contraction. *Reprod Fertil Dev* **22**: 780–7.

Bristol-Gould SK, Kreeger PK, Selkirk CG, Kilen SM, Cook RW, Kipp JL, Shea LD, Mayo KE, Woodruff TK. 2006a. Postnatal regulation of germ cells by activin: the establishment of the initial follicle pool. *Dev Biol* **298**: 132–48.

Bristol-Gould SK, Kreeger PK, Selkirk CG, Kilen SM, Mayo KE, Shea LD, Woodruff TK. 2006b. Fate of the initial follicle pool: empirical and mathematical evidence supporting its sufficiency for adult fertility. *Dev Biol* **298**: 149–54.

Britt KL, Drummond AE, Dyson M, Wreford NG, Jones ME, Simpson ER, Findlay JK. 2001. The ovarian phenotype of the aromatase knockout (ArKO) mouse. *J Steroid Biochem Mol Biol* **79**: 181–5.

Brooks D, Bader C, Ng Y. 2012. At the intersection of the pathways for exocytosis and autophagy. *… Traffick Pathway …*.

Brown MS, Anderson RG, Goldstein JL. 1983. Recycling receptors: the round-trip itinerary of migrant membrane proteins. *Cell* **32**: 663–7.

Brown MS, Goldstein JL. 1986. A receptor-mediated pathway for cholesterol homeostasis. *Science* **232**: 34–47.

Brown MS, Goldstein JL. 1980. Multivalent feedback regulation of HMG CoA reductase, a control mechanism coordinating isoprenoid synthesis and cell growth. *J Lipid Res* **21**: 505–17.

Brown MS, Kovanen PT, Goldstein JL. 1979. Receptor-mediated uptake of lipoprotein-cholesterol and its utilization for steroid synthesis in the adrenal cortex. *Recent Prog Horm Res* **35**: 215–57.

Bruce NW, Moor RM. 1976. Capillary blood flow to ovarian follicles, stroma and corpora lutea of anaesthetized sheep. *J Reprod Fertil* **46**: 299–304.

De Bruin JP, Dorland M, Spek ER, Posthuma G, van Haaften M, Looman CWN, te Velde ER. 2002. Ultrastructure of the resting ovarian follicle pool in healthy young women. *Biol Reprod* **66**: 1151–60.

Bullejos M, Koopman P. 2005. Delayed Sry and Sox9 expression in developing mouse gonads underlies B6-Y(DOM) sex reversal. *Dev Biol* **278**: 473–81.

Bullejos M, Koopman P. 2001. Spatially dynamic expression of Sry in mouse genital ridges. *Dev Dyn* **221**: 201–5.

Burgoyne PS, Baker TG. 1985. Perinatal oocyte loss in XO mice and its implications for the aetiology of gonadal dysgenesis in XO women. *J Reprod Fertil* **75**: 633–45.

Burman C, Ktistakis NT. 2010. Regulation of autophagy by phosphatidylinositol 3-phosphate. *FEBS Lett* **584**: 1302–12.

Byskov AGS. 1978. *Follicular atresia. In the Vertebrate Ovary*. ed. R.E. Jones. Plenum Press, New York, NY.

Caligioni CS. 2009. Assessing reproductive status/stages in mice. *Curr Protoc Neurosci* **Appendix 4**: Appendix 4I.

Cangemi R, Friedmann AJ, Holloszy JO, Fontana L. 2010. Long-term effects of calorie restriction on serum sex-hormone concentrations in men. *Aging Cell* **9**: 236–42.

Cantone I, Fisher AG. 2013. Epigenetic programming and reprogramming during development. *Nat Struct Mol Biol* **20**: 282–9.

Carabatsos MJ, Elvin J, Matzuk MM, Albertini DF. 1998. Characterization of oocyte and follicle development in growth differentiation factor-9-deficient mice. *Dev Biol* **204**: 373–84.

Carletti MZ, Christenson LK. 2009. Rapid effects of LH on gene expression in the mural granulosa cells of mouse periovulatory follicles. *Reproduction* **137**: 843–55.

Carr BR, MacDonald PC, Simpson ER. 1982. The role of lipoproteins in the regulation of progesterone secretion by the human corpus luteum. *Fertil Steril* **38**: 303–11.

Castrillon DH, Miao L, Kollipara R, Horner JW, DePinho RA. 2003. Suppression of ovarian follicle activation in mice by the transcription factor Foxo3a. *Science* **301**: 215–8.

Cebollero E, Reggiori F, Kraft C. 2012. Reticulophagy and ribophagy: regulated degradation of protein production factories. *Int J Cell Biol* **2012**: 182834.

Chang TY, Chang CC, Cheng D. 1997. Acyl-coenzyme A:cholesterol acyltransferase. *Annu Rev Biochem* **66**: 613–38.

Chassot A-A, Gregoire EP, Lavery R, Taketo MM, de Rooij DG, Adams IR, Chaboissier M-C. 2011. RSPO1/β-catenin signaling pathway regulates oogonia differentiation and entry into meiosis in the mouse fetal ovary. *PLoS One* **6**: e25641.

Chassot A-A, Ranc F, Gregoire EP, Roepers-Gajadien HL, Taketo MM, Camerino G, de Rooij DG, Schedl A, Chaboissier M-C. 2008. Activation of beta-catenin signaling by Rspo1 controls differentiation of the mammalian ovary. *Hum Mol Genet* **17**: 1264–77.

Chemes H. 1986. The phagocytic function of Sertoli cells: a morphological, biochemical, and endocrinological study of lysosomes and acid phosphatase localization in the rat testis. *Endocrinology* **119**: 1673–81.

Chen H, Hardy MP, Zirkin BR. 2002. Age-related decreases in Leydig cell testosterone production are not restored by exposure to LH in vitro. *Endocrinology* **143**: 1637–42.

Chen H, Luo L, Liu J, Brown T, Zirkin BR. 2005. Aging and caloric restriction: effects on Leydig cell steroidogenesis. *Exp Gerontol* **40**: 498–505.

Chen J, Melton C, Suh N, Oh JS, Horner K, Xie F, Sette C, Blelloch R, Conti M. 2011. Genome-wide analysis of translation reveals a critical role for deleted in azoospermia-like (Dazl) at the oocyte-to-zygote transition. *Genes Dev* **25**: 755–66.

Choi AMK, Ryter SW, Levine B. 2013. Autophagy in human health and disease. *N Engl J Med* **368**: 651–62.

Choi J, Jo M, Lee E, Choi D. 2011. Induction of apoptotic cell death via accumulation of autophagosomes in rat granulosa cells. *Fertil Steril* **95**: 1482–6.

Choi JY, Jo MW, Lee EY, Yoon B-K, Choi DS. 2010. The role of autophagy in follicular development and atresia in rat granulosa cells. *Fertil Steril* **93**: 2532–7.

Christensen AK. 2007. A History of Leydig Cell Research. In *Contemporary Endocrinology: The Leydig Cell in Health and Diesease* (eds. A.H. Payne and M.P. Hardy), pp. 3–30, Humana Press, Totowa, NJ.

Christian P, Sacco J, Adeli K. 2013. Autophagy: Emerging roles in lipid homeostasis and metabolic control. *Biochim Biophys Acta* **1831**: 819–24.

Chun SY, Billig H, Tilly JL, Furuta I, Tsafriri A, Hsueh AJ. 1994. Gonadotropin suppression of apoptosis in cultured preovulatory follicles: mediatory role of endogenous insulin-like growth factor I. *Endocrinology* **135**: 1845–53.

Chun SY, Eisenhauer KM, Kubo M, Hsueh AJ. 1995. Interleukin-1 beta suppresses apoptosis in rat ovarian follicles by increasing nitric oxide production. *Endocrinology* **136**: 3120–7.

Chun SY, Eisenhauer KM, Minami S, Billig H, Perlas E, Hsueh AJ. 1996. Hormonal regulation of apoptosis in early antral follicles: follicle-stimulating hormone as a major survival factor. *Endocrinology* **137**: 1447–56.

Ciechomska I a, Goemans GC, Skepper JN, Tolkovsky a M. 2009. Bcl-2 complexed with Beclin-1 maintains full anti-apoptotic function. *Oncogene* **28**: 2128–41.

Codogno P, Meijer AJ. 2005. Autophagy and signaling: their role in cell survival and cell death. *Cell Death Differ* **12 Suppl 2**: 1509–18.

Colman E. 1998. Obesity in the Paleolithic era? The Venus of Willendorf. *Endocr Pract* **4**: 58–9.

Colosi P, Ogren L, Southard JN, Thordarson G, Linzer DI, Talamantes F. 1988. Biological, immunological, and binding properties of recombinant mouse placental lactogen-I. *Endocrinology* **123**: 2662–7.

Conde-Agudelo A, Romero R, Nicolaides K, Chaiworapongsa T, O'Brien JM, Cetingoz E, da Fonseca E, Creasy G, Soma-Pillay P, Fusey S, et al. 2012. Vaginal progesterone vs cervical cerclage for the prevention of preterm birth in women with a sonographic short cervix, previous preterm birth, and singleton gestation: a systematic review and indirect comparison metaanalysis. *Am J Obstet Gynecol* **null**.

Conneely OM, Mulac-Jericevic B, Arnett-Mansfield R. 2007. Progesterone signaling in mammary gland development. *Ernst Schering Found Symp Proc* 45–54.

Conneely OM, Mulac-Jericevic B, DeMayo F, Lydon JP, O'Malley BW. 2002. Reproductive functions of progesterone receptors. *Recent Prog Horm Res* **57**: 339–55.

Connelly MA, Kellner-Weibel G, Rothblat GH, Williams DL. 2003. SR-BI-directed HDL-cholesteryl ester hydrolysis. *J Lipid Res* **44**: 331–41.

Conti M. 2011. When an egg is not an egg: compromised maternal mRNA storage and stabilization. *Biol Reprod* **85**: 429–30.

Conti M, Hsieh M, Zamah AM, Oh JS. 2012. Novel signaling mechanisms in the ovary during oocyte maturation and ovulation. *Mol Cell Endocrinol* **356**: 65–73.

Cook KG, Yeaman SJ, Strålfors P, Fredrikson G, Belfrage P. 1982. Direct evidence that cholesterol ester hydrolase from adrenal cortex is the same enzyme as hormone-sensitive lipase from adipose tissue. *Eur J Biochem* **125**: 245–9.

Coucouvanis EC, Sherwood SW, Carswell-Crumpton C, Spack EG, Jones PP. 1993. Evidence that the mechanism of prenatal germ cell death in the mouse is apoptosis. *Exp Cell Res* **209**: 238–47.

Cummins JM, Wakayama T, Yanagimachi R. 1997. Fate of microinjected sperm components in the mouse oocyte and embryo. *Zygote* **5**: 301–8.

Cure P, Pileggi A, Froud T, Norris PM, Baidal DA, Cornejo A, Hafiz MM, Ponte G, Poggioli R, Yu J, et al. 2004. Alterations of the female reproductive system in recipients of islet grafts. *Transplantation* **78**: 1576–81.

Curry TE. 2010. ADAMTS1 and versican: partners in ovulation and fertilization. *Biol Reprod* **83**: 505–6.

Czabotar PE, Lessene G, Strasser A, Adams JM. 2014. Control of apoptosis by the BCL-2 protein family: implications for physiology and therapy. *Nat Rev Mol Cell Biol* **15**: 49–63.

D'Herde K, De Prest B, Roels F. 1996. Subtypes of active cell death in the granulosa of ovarian atretic follicles in the quail (Coturnix coturnix japonica). *Reprod Nutr Dev* **36**: 175–89.

Deanesly R. 1930. The corpora lutea of the mouse with special reference to fat accumulation during the oestrous cycle. *Proc R Soc B Biol Sci* **106**: 578.

Deanesly R, Parkes AS. 1933. Size changes in the seminal vesicles of the mouse during development and after castration. *J Physiol* **78**: 442–50.

Degtyarev M, De Mazière A, Orr C, Lin J, Lee BB, Tien JY, Prior WW, van Dijk S, Wu H, Gray DC, et al. 2008. Akt inhibition promotes autophagy and sensitizes PTEN-null tumors to lysosomotropic agents. *J Cell Biol* **183**: 101–16.

Deguchi J, Yamamoto A, Yoshimori T, Sugasawa K, Moriyama Y, Futai M, Suzuki T, Kato K, Uyama M, Tashiro Y. 1994. Acidification of phagosomes and degradation of rod outer segments in rat retinal pigment epithelium. *Invest Ophthalmol Vis Sci* **35**: 568–79.

DeLuca SZ, O'Farrell PH. 2012. Barriers to male transmission of mitochondrial DNA in sperm development. *Dev Cell* **22**: 660–8.

Denton D, Shravage B, Simin R, Mills K, Berry DL, Baehrecke EH, Kumar S. 2009. Autophagy, not apoptosis, is essential for midgut cell death in Drosophila. *Curr Biol* **19**: 1741–6.

Deretic V, Jiang S, Dupont N. 2012. Autophagy intersections with conventional and unconventional secretion in tissue development, remodeling and inflammation. *Trends Cell Biol* **22**: 397–406.

Deroo BJ, Korach KS. 2006. Estrogen receptors and human disease. *J Clin Invest* **116**: 561–70.

Deter RL, Baudhuin P, De Duve C. 1967. Participation of lysosomes in cellular autophagy induced in rat liver by glucagon. *J Cell Biol* **35**: C11–6.

Deter RL, De Duve C. 1967. Influence of glucagon, an inducer of cellular autophagy, on some physical properties of rat liver lysosomes. *J Cell Biol* **33**: 437–49.

Dias JA, Cohen BD, Lindau-Shepard B, Nechamen CA, Peterson AJ, Schmidt A. 2002. Molecular, structural, and cellular biology of follitropin and follitropin receptor. *Vitam Horm* **64**: 249–322.

Diaz FJ, Anderson LE, Wu YL, Rabot A, Tsai SJ, Wiltbank MC. 2002. Regulation of progesterone and prostaglandin F2alpha production in the CL. *Mol Cell Endocrinol* **191**: 65–80.

Diaz FJ, Wigglesworth K, Eppig JJ. 2007. Oocytes determine cumulus cell lineage in mouse ovarian follicles. *J Cell Sci* **120**: 1330–40.

DiNapoli L, Batchvarov J, Capel B. 2006. FGF9 promotes survival of germ cells in the fetal testis. *Development* **133**: 1519–27.

Doitsidou M, Reichman-Fried M, Stebler J, Köprunner M, Dörries J, Meyer D, Esguerra C V, Leung T, Raz E. 2002. Guidance of primordial germ cell migration by the chemokine SDF-1. *Cell* **111**: 647–59.

Van Doren M, Broihier HT, Moore LA, Lehmann R. 1998. HMG-CoA reductase guides migrating primordial germ cells. *Nature* **396**: 466–9.

Dou Z, Pan J-A, Lin RZ, Zong W-X. 2011. The beta identity of class I PtdIns3K: A positive role of p110β in autophagy revealed. *Autophagy* **7**: 246–7.

Duarte A, Poderoso C, Cooke M, Soria G, Cornejo Maciel F, Gottifredi V, Podestá EJ. 2012. Mitochondrial fusion is essential for steroid biosynthesis. *PLoS One* **7**: e45829.

Dudley DJ, Branch DW, Edwin SS, Mitchell MD. 1996. Induction of preterm birth in mice by RU486. *Biol Reprod* **55**: 992–5.

Dudley DJ, Chen CL, Branch DW, Hammond E, Mitchell MD. 1993. A murine model of preterm labor: inflammatory mediators regulate the production of prostaglandin E2 and interleukin-6 by murine decidua. *Biol Reprod* **48**: 33–9.

Duerrschmidt N, Zabirnyk O, Nowicki M, Ricken A, Hmeidan FA, Blumenauer V, Borlak J, Spanel-Borowski K. 2006. Lectin-like oxidized low-density lipoprotein receptor-1-mediated autophagy in human granulosa cells as an alternative of programmed cell death. *Endocrinology* **147**: 3851–60.

Edelmann W, Cohen PE, Kneitz B, Winand N, Lia M, Heyer J, Kolodner R, Pollard JW, Kucherlapati R. 1999. Mammalian MutS homologue 5 is required for chromosome pairing in meiosis. *Nat Genet* **21**: 123–7.

Edson M a, Nagaraja AK, Matzuk MM. 2009. The mammalian ovary from genesis to revelation. *Endocr Rev* **30**: 624–712.

Elmore S. 2007. Apoptosis: a review of programmed cell death. *Toxicol Pathol* **35**: 495–516.

Elvin JA, Yan C, Wang P, Nishimori K, Matzuk MM. 1999. Molecular characterization of the follicle defects in the growth differentiation factor 9-deficient ovary. *Mol Endocrinol* **13**: 1018–34.

Eppig JJ, Schroeder AC. 1989. Capacity of mouse oocytes from preantral follicles to undergo embryogenesis and development to live young after growth, maturation, and fertilization in vitro. *Biol Reprod* **41**: 268–76.

Eppig JJ, Wigglesworth K, Pendola F, Hirao Y. 1997. Murine oocytes suppress expression of luteinizing hormone receptor messenger ribonucleic acid by granulosa cells. *Biol Reprod* **56**: 976–84.

Eppig JJ, Wigglesworth K, Pendola FL. 2002. The mammalian oocyte orchestrates the rate of ovarian follicular development. *Proc Natl Acad Sci U S A* **99**: 2890–4.

Escobar ML, Echeverría OM, Casasa AS, García G, Aguilar SJ, Vázquez-Nin GH. 2013. Involvement of Pro-Apoptotic and Pro-Autophagic Proteins in Granulosa Cell Death. *Cell Biol* **1**: 9–17.

Escobar ML, Echeverría OM, Ortíz R, Vázquez-Nin GH. 2008. Combined apoptosis and autophagy, the process that eliminates the oocytes of atretic follicles in immature rats. *Apoptosis* **13**: 1253–66.

Escobar ML, Echeverría OM, Sánchez-Sánchez L, Méndez C, Pedernera E, Vázquez-Nin GH. 2010. Analysis of different cell death processes of prepubertal rat oocytes in vitro. *Apoptosis* **15**: 511–26.

Faddy MJ, Jones EC, Edwards RG. 1976. An analytical model for ovarian follicle dynamics. *J Exp Zool* **197**: 173–85.

Faddy MJ, Telfer E, Gosden RG. 1987. The kinetics of pre-antral follicle development in ovaries of CBA/Ca mice during the first 14 weeks of life. *Cell Tissue Kinet* **20**: 551–60.

Fan H-Y, Liu Z, Cahill N, Richards JS. 2008a. Targeted disruption of Pten in ovarian granulosa cells enhances ovulation and extends the life span of luteal cells. *Mol Endocrinol* **22**: 2128–40.

Fan H-Y, Liu Z, Shimada M, Sterneck E, Johnson PF, Hedrick SM, Richards JS. 2009. MAPK3/1 (ERK1/2) in ovarian granulosa cells are essential for female fertility. *Science* **324**: 938–41.

Fan H-Y, Shimada M, Liu Z, Cahill N, Noma N, Wu Y, Gossen J, Richards JS. 2008b. Selective expression of KrasG12D in granulosa cells of the mouse ovary causes defects in follicle development and ovulation. *Development* **135**: 2127–37.

De Felici M, Klinger FG, Farini D, Scaldaferri ML, Iona S, Lobascio M. 2005. Establishment of oocyte population in the fetal ovary: primordial germ cell proliferation and oocyte programmed cell death. *Reprod Biomed Online* **10**: 182–91.

Feng Y, He D, Yao Z, Klionsky DJ. 2014. The machinery of macroautophagy. *Cell Res* **24**: 24–41.

Flaws JA, Hirshfield AN, Hewitt JA, Babus JK, Furth PA. 2001. Effect of bcl-2 on the primordial follicle endowment in the mouse ovary. *Biol Reprod* **64**: 1153–9.

Forabosco A, Sforza C, De Pol A, Vizzotto L, Marzona L, Ferrario VF. 1991. Morphometric study of the human neonatal ovary. *Anat Rec* **231**: 201–8.

Fraenkel L. 1901. Experimentelle untersuchengen uber die function des corpus luteum (Theorie von Born). *Allg Med Cent* **70**: 1209.

Fritz MA, Fitz TA. 1991. The functional microscopic anatomy of the corpus luteum: the "small cell"-"large cell" controversy. *Clin Obstet Gynecol* **34**: 144–56.

Funderburk SF, Wang QJ, Yue Z. 2010. The Beclin 1-VPS34 complex--at the crossroads of autophagy and beyond. *Trends Cell Biol* **20**: 355–62.

Galavotti S, Bartesaghi S, Faccenda D, Shaked-Rabi M, Sanzone S, McEvoy A, Dinsdale D, Condorelli F, Brandner S, Campanella M, et al. 2013. The autophagy-associated factors DRAM1 and p62 regulate cell migration and invasion in glioblastoma stem cells. *Oncogene* **32**: 699–712.

Galdieri M, Ziparo E, Palombi F, Russo M, Stefanni M. 1981. Pure Sertoli Cell Cultures: A New Model for the Study of Somatic—Germ Cell Interactions. *J Androl* **2**: 249–254.

Gallegos AM, Atshaves BP, Storey SM, Starodub O, Petrescu AD, Huang H, McIntosh AL, Martin GG, Chao H, Kier AB, et al. 2001. Gene structure, intracellular localization, and functional roles of sterol carrier protein-2. *Prog Lipid Res* **40**: 498–563.

Gallegos AM, Schoer JK, Starodub O, Kier AB, Billheimer JT, Schroeder F. 2000. A potential role for sterol carrier protein-2 in cholesterol transfer to mitochondria. *Chem Phys Lipids* **105**: 9–29.

Galluzzi L, Vitale I, Abrams JM, Alnemri ES, Baehrecke EH, Blagosklonny M V, Dawson TM, Dawson VL, El-Deiry WS, Fulda S, et al. 2012. Molecular definitions of cell death subroutines: recommendations of the Nomenclature Committee on Cell Death 2012. *Cell Death Differ* **19**: 107–20.

Gao C, Cao W, Bao L, Zuo W, Xie G, Cai T, Fu W, Zhang J, Wu W, Zhang X, et al. 2010. Autophagy negatively regulates Wnt signalling by promoting Dishevelled degradation. *Nat Cell Biol* **12**: 781–90.

Gao Y, Lui W-Y. 2014. Synergistic effect of interferon-gamma and tumor necrosis factor-alpha on coxsackievirus and adenovirus receptor expression: an explanation of cell sloughing during testicular inflammation in mice. *Biol Reprod* **90**: 59.

Gawriluk TR, Hale AN, Flaws JA, Dillon CP, Green DR, Rucker EB. 2011. Autophagy is a cell survival program for female germ cells in the murine ovary. *Reproduction* **141**: 759–65.

Gaytán M, Morales C, Sánchez-Criado JE, Gaytán F. 2008. Immunolocalization of beclin 1, a bcl-2-binding, autophagy-related protein, in the human ovary: possible relation to life span of corpus luteum. *Cell Tissue Res* **331**: 509–17.

Ge R-S, Dong Q, Sottas CM, Chen H, Zirkin BR, Hardy MP. 2005. Gene expression in rat leydig cells during development from the progenitor to adult stage: a cluster analysis. *Biol Reprod* **72**: 1405–15.

Gemmell RT. 1995. A comparative study of the corpus luteum. *Reprod Fertil Dev* **7**: 303–12.

Geng J, Klionsky DJ. 2008. The Atg8 and Atg12 ubiquitin-like conjugation systems in macroautophagy. “Protein modifications: beyond the usual suspects” review series. *EMBO Rep* **9**: 859–64.

Ghafari F, Gutierrez CG, Hartshorne GM. 2007. Apoptosis in mouse fetal and neonatal oocytes during meiotic prophase one. *BMC Dev Biol* **7**: 87.

Gillot I, Jehl-Pietri C, Gounon P, Luquet S, Rassoulzadegan M, Grimaldi P, Vidal F. 2005. Germ cells and fatty acids induce translocation of CD36 scavenger receptor to the plasma membrane of Sertoli cells. *J Cell Sci* **118**: 3027–35.

Ginsburg M, Snow MH, McLaren A. 1990. Primordial germ cells in the mouse embryo during gastrulation. *Development* **110**: 521–8.

Gioacchini G, Valle LD, Benato F, Fimia GM, Nardacci R, Ciccosanti F, Piacentini M, Borini A, Carnevali O. 2013. Interplay between autophagy and apoptosis in the development of Danio rerio follicles and the effects of a probiotic. *Reprod Fertil Dev* **25**: 1115–25.

Glover JD, Taylor L, Sherman A, Zeiger-Poli C, Sang HM, McGrew MJ. 2013. A novel piggybac transposon inducible expression system identifies a role for akt signalling in primordial germ cell migration. *PLoS One* **8**: e77222.

Goede V, Schmidt T, Kimmina S, Kozian D, Augustin HG. 1998. Analysis of blood vessel maturation processes during cyclic ovarian angiogenesis. *Lab Invest* **78**: 1385–94.

Goldstein JL, Brown MS. 2009. The LDL receptor. *Arterioscler Thromb Vasc Biol* **29**: 431–8.

Greenfeld CR, Pepling ME, Babus JK, Furth P a, Flaws J a. 2007. BAX regulates follicular endowment in mice. *Reproduction* **133**: 865–76.

Guicciardi ME, Gores GJ. 2009. Life and death by death receptors. *FASEB J* **23**: 1625–37.

Gwynne JT, Strauss JF. 1982. The role of lipoproteins in steroidogenesis and cholesterol metabolism in steroidogenic glands. *Endocr Rev* **3**: 299–329.

Haack TB, Hogarth P, Kruer MC, Gregory A, Wieland T, Schwarzmayr T, Graf E, Sanford L, Meyer E, Kara E, et al. 2012. Exome sequencing reveals de novo WDR45 mutations causing a phenotypically distinct, X-linked dominant form of NBIA. *Am J Hum Genet* **91**: 1144–9.

Hacker A, Capel B, Goodfellow P, Lovell-Badge R. 1995. Expression of Sry, the mouse sex determining gene. *Development* **121**: 1603–14.

Haider SG. 2004. Cell biology of Leydig cells in the testis. *Int Rev Cytol* **233**: 181–241.

Hailey DW, Rambold AS, Satpute-Krishnan P, Mitra K, Sougrat R, Kim PK, Lippincott-Schwartz J. 2010. Mitochondria supply membranes for autophagosome biogenesis during starvation. *Cell* **141**: 656–67.

Hakuno N, Koji T, Yano T, Kobayashi N, Tsutsumi O, Taketani Y, Nakane PK. 1996. Fas/APO-1/CD95 system as a mediator of granulosa cell apoptosis in ovarian follicle atresia. *Endocrinology* **137**: 1938–48.

Hale AN, Ledbetter DJ, Gawriluk TR, Rucker EB. 2013. Autophagy: regulation and role in development. *Autophagy* **9**: 951–72.

Hamasaki M, Furuta N, Matsuda A, Nezu A, Yamamoto A, Fujita N, Oomori H, Noda T, Haraguchi T, Hiraoka Y, et al. 2013. Autophagosomes form at ER-mitochondria contact sites. *Nature* **495**: 389–93.

Hardy MP, Zirkin BR, Ewing LL. 1989. Kinetic studies on the development of the adult population of Leydig cells in testes of the pubertal rat. *Endocrinology* **124**: 762–70.

Hassan SS, Romero R, Vidyadhari D, Fusey S, Baxter JK, Khandelwal M, Vijayaraghavan J, Trivedi Y, Soma-Pillay P, Sambarey P, et al. 2011. Vaginal progesterone reduces the rate of preterm birth in women with a sonographic short cervix: a multicenter, randomized, double-blind, placebo-controlled trial. *Ultrasound Obstet Gynecol* **38**: 18–31.

Hayashi-Nishino M, Fujita N, Noda T, Yamaguchi A, Yoshimori T, Yamamoto A. 2009. A subdomain of the endoplasmic reticulum forms a cradle for autophagosome formation. *Nat Cell Biol* **11**: 1433–7.

He C, Klionsky DJ. 2009. Regulation mechanisms and signaling pathways of autophagy. *Annu Rev Genet* **43**: 67–93.

He Y, Wu J, Dressman DC, Iacobuzio-Donahue C, Markowitz SD, Velculescu VE, Diaz LA, Kinzler KW, Vogelstein B, Papadopoulos N. 2010. Heteroplasmic mitochondrial DNA mutations in normal and tumour cells. *Nature* **464**: 610–4.

Hegele RA. 2009. Plasma lipoproteins: genetic influences and clinical implications. *Nat Rev Genet* **10**: 109–21.

Hennighausen L, Robinson GW, Wagner KU, Liu W. 1997. Prolactin signaling in mammary gland development. *J Biol Chem* **272**: 7567–9.

Hertig AT, Adams EC. 1967. Studies on the human oocyte and its follicle. *J Cell Biol* **34**: 647–75.

Hess R a, Renato de Franca L. 2005. History of the Sertoli Cell Discovery. In *Sertoli Cell Biology* (eds. M.K. Skinner and M.D. Griswold), pp. 3–13, Elsevier.

Hess RA, Renato de Franca L. 2008. Spermatogenesis and cycle of the seminiferous epithelium. *Adv Exp Med Biol* **636**: 1–15.

Hirota Y, Daikoku T, Tranguch S, Xie H, Bradshaw HB, Dey SK. 2010. Uterine-specific p53 deficiency confers premature uterine senescence and promotes preterm birth in mice. *J Clin Invest* **120**: 803–15.

Hirshfield AN. 1991. Development of follicles in the mammalian ovary. *Int Rev Cytol* **124**: 43–101.

Hirshfield AN, Midgley AR. 1978. Morphometric analysis of follicular development in the rat. *Biol Reprod* **19**: 597–605.

Horie K, Takakura K, Taii S, Narimoto K, Noda Y, Nishikawa S, Nakayama H, Fujita J, Mori T. 1991. The expression of c-kit protein during oogenesis and early embryonic development. *Biol Reprod* **45**: 547–52.

Hsieh M, Thao K, Conti M. 2011. Genetic dissection of epidermal growth factor receptor signaling during luteinizing hormone-induced oocyte maturation. *PLoS One* **6**: e21574.

Hsu SY, Lai RJ, Finegold M, Hsueh AJ. 1996. Targeted overexpression of Bcl-2 in ovaries of transgenic mice leads to decreased follicle apoptosis, enhanced folliculogenesis, and increased germ cell tumorigenesis. *Endocrinology* **137**: 4837–43.

Hsueh AJ, Billig H, Tsafriri A. 1994. Ovarian follicle atresia: a hormonally controlled apoptotic process. *Endocr Rev* **15**: 707–24.

Hu CL, Cowan RG, Harman RM, Porter DA, Quirk SM. 2001. Apoptosis of bovine granulosa cells after serum withdrawal is mediated by Fas antigen (CD95) and Fas ligand. *Biol Reprod* **64**: 518–26.

Huang EJ, Manova K, Packer AI, Sanchez S, Bachvarova RF, Besmer P. 1993. The murine steel panda mutation affects kit ligand expression and growth of early ovarian follicles. *Dev Biol* **157**: 100–9.

Huang L, Wang Z, Jiang Z, Hu M, Lin F, Zhang Q, Luo B, Hou Y, Zhao Y, Fan H, et al. 2013a. Specific Disruption of Tsc1 in Ovarian Granulosa Cells Promotes Ovulation and Causes Progressive Accumulation of Corpora Lutea. **8**.

Huang S, Jia K, Wang Y, Zhou Z, Levine B. 2013b. Autophagy genes function in apoptotic cell corpse clearance during C. elegans embryonic development. *Autophagy* **9**: 138–49.

Hughes T, Rusten TE. 2007. Origin and evolution of self-consumption: autophagy. *Adv Exp Med Biol* **607**: 111–8.

Huhtaniemi I, Pelliniemi LJ. 1992. Fetal Leydig cells: cellular origin, morphology, life span, and special functional features. *Proc Soc Exp Biol Med* **201**: 125–40.

Hung T-H, Hsieh T-T, Chen S-F, Li M-J, Yeh Y-L. 2013. Autophagy in the Human Placenta throughout Gestation. *PLoS One* **8**: e83475.

Huo L-J, Fan H-Y, Zhong Z-S, Chen D-Y, Schatten H, Sun Q-Y. 2004. Ubiquitin-proteasome pathway modulates mouse oocyte meiotic maturation and fertilization via regulation of MAPK cascade and cyclin B1 degradation. *Mech Dev* **121**: 1275–87.

Huo L-J, Yu L-Z, Liang C-G, Fan H-Y, Chen D-Y, Sun Q-Y. 2005. Cell-cycle-dependent subcellular localization of cyclin B1, phosphorylated cyclin B1 and p34cdc2 during oocyte meiotic maturation and fertilization in mouse. *Zygote* **13**: 45–53.

Huo L-J, Zhong Z-S, Liang C-G, Wang Q, Yin S, Ai J-S, Yu L-Z, Chen D-Y, Schatten H, Sun Q-Y. 2006. Degradation of securin in mouse and pig oocytes is dependent on ubiquitin-proteasome pathway and is required for proteolysis of the cohesion subunit, Rec8, at the metaphase-to-anaphase transition. *Front Biosci* **11**: 2193–202.

Huotari J, Helenius A. 2011. Endosome maturation. *EMBO J* **30**: 3481–500.

Hurst PR, Mora JM, Fenwick MA. 2006. Caspase-3, TUNEL and ultrastructural studies of small follicles in adult human ovarian biopsies. *Hum Reprod* **21**: 1974–80.

Hussein TS, Froiland DA, Amato F, Thompson JG, Gilchrist RB. 2005. Oocytes prevent cumulus cell apoptosis by maintaining a morphogenic paracrine gradient of bone morphogenetic proteins. *J Cell Sci* **118**: 5257–68.

Hutchison CA, Newbold JE, Potter SS, Edgell MH. 1974. Maternal inheritance of mammalian mitochondrial DNA. *Nature* **251**: 536–8.

Ichimura Y, Kominami E, Tanaka K, Komatsu M. 2008. Selective turnover of p62/A170/SQSTM1 by autophagy. *Autophagy* **4**: 1063–6.

Ishibashi S, Brown MS, Goldstein JL, Gerard RD, Hammer RE, Herz J. 1993. Hypercholesterolemia in low density lipoprotein receptor knockout mice and its reversal by adenovirus-mediated gene delivery. *J Clin Invest* **92**: 883–93.

Itakura E, Mizushima N. 2010. Characterization of autophagosome formation site by a hierarchical analysis of mammalian Atg proteins. *Autophagy* **6**: 764–76.

Jamieson S, Fuller PJ. 2012. Molecular pathogenesis of granulosa cell tumors of the ovary. *Endocr Rev* **33**: 109–44.

Jamin SP, Arango N a, Mishina Y, Hanks MC, Behringer RR. 2002. Requirement of Bmpr1a for Müllerian duct regression during male sexual development. *Nat Genet* **32**: 408–10.

Jégou B. 1992. The Sertoli cell in vivo and in vitro. *Cell Biol Toxicol* **8**: 49–54.

Jeyasuria P, Ikeda Y, Jamin SP, Zhao L, De Rooij DG, Themmen APN, Behringer RR, Parker KL. 2004. Cell-specific knockout of steroidogenic factor 1 reveals its essential roles in gonadal function. *Mol Endocrinol* **18**: 1610–9.

Jia S, Liu Z, Zhang S, Liu P, Zhang L, Lee SH, Zhang J, Signoretti S, Loda M, Roberts TM, et al. 2008. Essential roles of PI(3)K-p110beta in cell growth, metabolism and tumorigenesis. *Nature* **454**: 776–9.

Jiang P, Mizushima N. 2014. Autophagy and human diseases. *Cell Res* **24**: 69–79.

Jiang W, Napoli JL. 2013. The retinol dehydrogenase Rdh10 localizes to lipid droplets during acyl ester biosynthesis. *J Biol Chem* **288**: 589–97.

Jiménez LM, Binelli M, Bertolin K, Pelletier RM, Murphy BD. 2010. Scavenger receptor-B1 and luteal function in mice. *J Lipid Res* **51**: 2362–71.

Jing Y, Tang XM. 1995. Functional implication of autophagy in steroid-□secreting cells of the rat. *Anat Rec* **242**: 137–146.

Jing Y, Tang XM. 1999. The convergent point of the endocytic and autophagic pathways in leydig cells. *Cell Res* 243–253.

Jocelyn HD, Setchell BP. 1972. Regnier de Graaf on the human reproductive organs. An annotated translation of Tractatus de Virorum Organis Generationi Inservientibus (1668) and De Mulierub Organis Generationi Inservientibus Tractatus Novus (1962). *J Reprod Fertil Suppl* **17**: 1–222.

Johnson EE, Overmeyer JH, Gunning WT, Maltese WA. 2006. Gene silencing reveals a specific function of hVps34 phosphatidylinositol 3-kinase in late versus early endosomes. *J Cell Sci* **119**: 1219–32.

Johnson L, Thompson DL, Varner DD. 2008. Role of Sertoli cell number and function on regulation of spermatogenesis. *Anim Reprod Sci* **105**: 23–51.

Jones RL, Pepling ME. 2013. Role of the antiapoptotic proteins BCL2 and MCL1 in the neonatal mouse ovary. *Biol Reprod* **88**: 46.

Jost A, Vigier B, Prépin J, Perchellet JP. 1973. Studies on sex differentiation in mammals. *Recent Prog Horm Res* **29**: 1–41.

Joyce IM, Pendola FL, Wigglesworth K, Eppig JJ. 1999. Oocyte regulation of kit ligand expression in mouse ovarian follicles. *Dev Biol* **214**: 342–53.

Juhász G, Hill JH, Yan Y, Sass M, Baehrecke EH, Backer JM, Neufeld TP. 2008. The class III PI(3)K Vps34 promotes autophagy and endocytosis but not TOR signaling in Drosophila. *J Cell Biol* **181**: 655–66.

Kabeya Y, Mizushima N, Ueno T, Yamamoto A, Kirisako T, Noda T, Kominami E, Ohsumi Y, Yoshimori T. 2000. LC3, a mammalian homologue of yeast Apg8p, is localized in autophagosome membranes after processing. *EMBO J* **19**: 5720–8.

Kádasi A, Sirotkin A V, Maruniaková N, Nath S, Kolesárová A. 2012. The effect of rapamycin on secretory activity of the rabbit ovarian fragments. *J Microbiol Biotechnol food Sci* **1**: 488–497.

Kaipia A, Chun SY, Eisenhauer K, Hsueh AJ. 1996. Tumor necrosis factor-alpha and its second messenger, ceramide, stimulate apoptosis in cultured ovarian follicles. *Endocrinology* **137**: 4864–70.

Kang JS, Lee CJ, Lee JM, Rha JY, Song KW, Park MH. 2003. Follicular expression of c-Kit/SCF and inhibin-alpha in mouse ovary during development. *J Histochem Cytochem* **51**: 1447–58.

Kaplan DD, Meigs TE, Kelly P, Casey PJ. 2004. Identification of a role for beta-catenin in the establishment of a bipolar mitotic spindle. *J Biol Chem* **279**: 10829–32.

Kathiria AS, Butcher LD, Feagins LA, Souza RF, Boland CR, Theiss AL. 2012. Prohibitin 1 modulates mitochondrial stress-related autophagy in human colonic epithelial cells. *PLoS One* **7**: e31231.

Katritch V, Cherezov V, Stevens RC. 2013. Structure-function of the G protein-coupled receptor superfamily. *Annu Rev Pharmacol Toxicol* **53**: 531–56.

Kawamoto S, Niwa H, Tashiro F, Sano S, Kondoh G, Takeda J, Tabayashi K, Y JM. 2000. A novel reporter mouse strain that expresses enhanced green £ uorescent protein upon Cre-mediated recombination. **470**: 263–268.

Ke F, Voss A, Kerr JB, O'Reilly LA, Tai L, Echeverry N, Bouillet P, Strasser A, Kaufmann T. 2013. BCL-2 family member BOK is widely expressed but its loss has only minimal impact in mice. *Cell Death Differ* **20**: 183–183.

Kim J, Kundu M, Viollet B, Guan K-L. 2011. AMPK and mTOR regulate autophagy through direct phosphorylation of Ulk1. *Nat Cell Biol* **13**: 132–41.

Kim JM, Yoon YD, Tsang BK. 1999. Involvement of the Fas/Fas ligand system in p53-mediated granulosa cell apoptosis during follicular development and atresia. *Endocrinology* **140**: 2307–17.

Kim J-Y, Zhao H, Martinez J, Doggett TA, Kolesnikov A V, Tang PH, Ablonczy Z, Chan C-C, Zhou Z, Green DR, et al. 2013. Noncanonical autophagy promotes the visual cycle. *Cell* **154**: 365–76.

Kim Y, Kobayashi A, Sekido R, DiNapoli L, Brennan J, Chaboissier M-C, Poulat F, Behringer RR, Lovell-Badge R, Capel B. 2006. Fgf9 and Wnt4 act as antagonistic signals to regulate mammalian sex determination. *PLoS Biol* **4**: e187.

Kim Y-G, Kim JY, Mohan C, Lee GM. 2009. Effect of Bcl-xL overexpression on apoptosis and autophagy in recombinant Chinese hamster ovary cells under nutrient-deprived condition. *Biotechnol Bioeng* **103**: 757–66.

Klionsky DJ. 2000. Autophagy as a Regulated Pathway of Cellular Degradation. *Science (80-)* **290**: 1717–1721.

Klionsky DJ. 2008. Autophagy revisited: a conversation with Christian de Duve. *Autophagy* **4**: 740–3.

Klionsky DJ, Abdalla FC, Abeliovich H, Abraham RT, Acevedo-Arozena A, Adeli K, Agholme L, Agnello M, Agostinis P, Aguirre-Ghiso JA, et al. 2012. Guidelines for the use and interpretation of assays for monitoring autophagy. *Autophagy* **8**: 445–544.

Klionsky DJ, Emr SD. 2000. Autophagy as a regulated pathway of cellular degradation. *Science* **290**: 1717–21.

Kneitz B, Cohen PE, Avdievich E, Zhu L, Kane MF, Hou H, Kolodner RD, Kucherlapati R, Pollard JW, Edelmann W. 2000. MutS homolog 4 localization to meiotic chromosomes is required for chromosome pairing during meiosis in male and female mice. *Genes Dev* **14**: 1085–97.

Knudson CM, Tung KS, Tourtellotte WG, Brown GA, Korsmeyer SJ. 1995. Bax-deficient mice with lymphoid hyperplasia and male germ cell death. *Science* **270**: 96–9.

Ko C, Gieske MC, Al-Alem L, Hahn Y, Su W, Gong MC, Iglarz M, Koo Y. 2006. Endothelin-2 in ovarian follicle rupture. *Endocrinology* **147**: 1770–9.

Ko DC, Binkley J, Sidow A, Scott MP. 2003. The integrity of a cholesterol-binding pocket in Niemann-Pick C2 protein is necessary to control lysosome cholesterol levels. *Proc Natl Acad Sci U S A* **100**: 2518–25.

Koike M, Shibata M, Tadakoshi M, Gotoh K, Komatsu M, Waguri S, Kawahara N, Kuida K, Nagata S, Kominami E, et al. 2008. Inhibition of autophagy prevents hippocampal pyramidal neuron death after hypoxic-ischemic injury. *Am J Pathol* **172**: 454–69.

Kolmakova A, Wang J, Brogan R, Chaffin C, Rodriguez A. 2010. Deficiency of scavenger receptor class B type I negatively affects progesterone secretion in human granulosa cells. *Endocrinology* **151**: 5519–27.

Komatsu M, Waguri S, Ueno T, Iwata J, Murata S, Tanida I, Ezaki J, Mizushima N, Ohsumi Y, Uchiyama Y, et al. 2005. Impairment of starvation-induced and constitutive autophagy in Atg7-deficient mice. *J Cell Biol* **169**: 425–34.

Konishi I, Fujii S, Okamura H, Parmley T, Mori T. 1986. Development of interstitial cells and ovigerous cords in the human fetal ovary: an ultrastructural study. *J Anat* **148**: 121–35.

Kotani E, Sugimoto M, Kamata H, Fujii N, Saitoh M, Usuki S, Kubo T, Song K, Miyazaki M, Murakami K, et al. 1999. Biological roles of angiotensin II via its type 2 receptor during rat follicle atresia. *Am J Physiol* **276**: E25–33.

Kovács AL, Pálfia Z, Réz G, Vellai T, Kovács J. 2007. Sequestration revisited: integrating traditional electron microscopy, de novo assembly and new results. *Autophagy* **3**: 655–62.

Kovács J, Forgó V, Péczely P. 1992. The fine structure of the follicular cells in growing and atretic ovarian follicles of the domestic goose. *Cell Tissue Res* **267**: 561–9.

Kraemer FB, Shen W-J. 2002. Hormone-sensitive lipase: control of intracellular tri-(di-)acylglycerol and cholesteryl ester hydrolysis. *J Lipid Res* **43**: 1585–94.

Kroemer G, Levine B. 2008. Autophagic cell death: the story of a misnomer. *Nat Rev Mol Cell Biol* **9**: 1004–10.

Kuma A, Hatano M, Matsui M, Yamamoto A, Nakaya H, Yoshimori T, Ohsumi Y, Tokuhisa T, Mizushima N. 2004. The role of autophagy during the early neonatal starvation period. *Nature* **432**: 1032–6.

Kumar TR, Wang Y, Lu N, Matzuk MM. 1997. Follicle stimulating hormone is required for ovarian follicle maturation but not male fertility. *Nat Genet* **15**: 201–4.

Kurilo LF. 1981. Oogenesis in antenatal development in man. *Hum Genet* **57**: 86–92.

Lam GY, Cemma M, Muise AM, Higgins DE, Brumell JH. 2013. Host and bacterial factors that regulate LC3 recruitment to Listeria monocytogenes during the early stages of macrophage infection. *Autophagy* **9**: 985–95.

Lamb C a, Dooley HC, Tooze S a. 2013. Endocytosis and autophagy: Shared machinery for degradation. *Bioessays* **35**: 34–45.

Lapierre LR, Silvestrini MJ, Nuñez L, Ames K, Wong S, Le TT, Hansen M, Meléndez A. 2013. Autophagy genes are required for normal lipid levels in C. elegans. *Autophagy* **9**: 278–86.

Larsson NG, Oldfors A, Garman JD, Barsh GS, Clayton DA. 1997. Down-regulation of mitochondrial transcription factor A during spermatogenesis in humans. *Hum Mol Genet* **6**: 185–91.

Le JA, Wilson HM, Shehu A, Mao J, Devi YS, Halperin J, Aguilar T, Seibold A, Maizels E, Gibori G. 2012. Generation of mice expressing only the long form of the prolactin receptor reveals that both isoforms of the receptor are required for normal ovarian function. *Biol Reprod* **86**: 86.

Lee JW, Park S, Takahashi Y, Wang H-G. 2010. The association of AMPK with ULK1 regulates autophagy. *PLoS One* **5**: e15394.

Lei L, Spradling AC. 2013. Mouse primordial germ cells produce cysts that partially fragment prior to meiosis. *Development* **140**: 2075–81.

Lei ZM, Chegini N, Rao C V. 1991. Quantitative cell composition of human and bovine corpora lutea from various reproductive states. *Biol Reprod* **44**: 1148–56.

Lei ZM, Mishra S, Zou W, Xu B, Foltz M, Li X, Rao C V. 2001. Targeted disruption of luteinizing hormone/human chorionic gonadotropin receptor gene. *Mol Endocrinol* **15**: 184–200.

Lemon JG, Morton WR. 1968. Oogenesis in the golden hamster (Mesocricetus auratus). A study of the first meiotic prophase. *Cytogenetics* **7**: 376–89.

De Leon V, Johnson A, Bachvarova R. 1983. Half-lives and relative amounts of stored and polysomal ribosomes and poly(A) + RNA in mouse oocytes. *Dev Biol* **98**: 400–8.

Levine B, Kroemer G. 2008. Autophagy in the pathogenesis of disease. *Cell* **132**: 27–42.

Levine B, Mizushima N, Virgin HW. 2011. Autophagy in immunity and inflammation. *Nature* **469**: 323–35.

Leydig F. 1850. Zur Anatomie der mannlichen Geschlechtsorgane und Analdrusen der Saugerthiere. *Cell Biol Leydig Cells Testis* **2**: 1–57.

Li E. 2002. Chromatin modification and epigenetic reprogramming in mammalian development. *Nat Rev Genet* **3**: 662–73.

Li H, Zhu H, Xu CJ, Yuan J. 1998. Cleavage of BID by caspase 8 mediates the mitochondrial damage in the Fas pathway of apoptosis. *Cell* **94**: 491–501.

Li MWM, Xia W, Mruk DD, Wang CQF, Yan HHN, Siu MKY, Lui W-Y, Lee WM, Cheng CY. 2006a. Tumor necrosis factor {alpha} reversibly disrupts the blood-testis barrier and impairs Sertoli-germ cell adhesion in the seminiferous epithelium of adult rat testes. *J Endocrinol* **190**: 313–29.

Li W, Zou W, Yang Y, Chai Y, Chen B, Cheng S, Tian D, Wang X, Vale RD, Ou G. 2012. Autophagy genes function sequentially to promote apoptotic cell corpse degradation in the engulfing cell. *J Cell Biol* **197**: 27–35.

Li W-R, Chen L, Chang Z-J, Xin H, Liu T, Zhang Y-Q, Li G-Y, Zhou F, Gong Y-Q, Gao Z-Z, et al. 2011. Autophagic deficiency is related to steroidogenic decline in aged rat Leydig cells. *Asian J Androl* **13**: 881–8.

Li X-Y, Cui X-S, Kim N-H. 2006b. Transcription profile during maternal to zygotic transition in the mouse embryo. *Reprod Fertil Dev* **18**: 635–45.

Liang C, Feng P, Ku B, Dotan I, Canaani D, Oh B-H, Jung JU. 2006. Autophagic and tumour suppressor activity of a novel Beclin1-binding protein UVRAG. *Nat Cell Biol* **8**: 688–99.

Liang C, Lee J, Inn K, Gack MU, Li Q, Roberts EA, Vergne I, Deretic V, Feng P, Akazawa C, et al. 2008. Beclin1-binding UVRAG targets the class C Vps complex to coordinate autophagosome maturation and endocytic trafficking. *Nat Cell Biol* **10**: 776–87.

Lin D, Sugawara T, Strauss JF, Clark BJ, Stocco DM, Saenger P, Rogol A, Miller WL. 1995. Role of steroidogenic acute regulatory protein in adrenal and gonadal steroidogenesis. *Science* **267**: 1828–31.

Lin R-S, Jimenez-Movilla M, Dean J. 2014. Figla-Cre transgenic mice expressing myristoylated EGFP in germ cells provide a model for investigating perinatal oocyte dynamics. *PLoS One* **9**: e84477.

Lindsten T, Ross AJ, King A, Zong WX, Rathmell JC, Shiels HA, Ulrich E, Waymire KG, Mahar P, Frauwirth K, et al. 2000. The combined functions of proapoptotic Bcl-2 family members bak and bax are essential for normal development of multiple tissues. *Mol Cell* **6**: 1389–99.

Liu K, Czaja MJ. 2013. Regulation of lipid stores and metabolism by lipophagy. *Cell Death Differ* **20**: 3–11.

Liu K, Olofsson JI, Wahlberg P, Ny T. 1999. Distinct expression of gelatinase A [matrix metalloproteinase (MMP)-2], collagenase-3 (MMP-13), membrane type MMP 1 (MMP-14), and tissue inhibitor of MMPs type 1 mediated by physiological signals during formation and regression of the rat corpus luteum. *Endocrinology* **140**: 5330–8.

Liu L, Rajareddy S, Reddy P, Du C, Jagarlamudi K, Shen Y, Gunnarsson D, Selstam G, Boman K, Liu K. 2007. Infertility caused by retardation of follicular development in mice with oocyte-specific expression of Foxo3a. *Development* **134**: 199–209.

Lobascio AM, Klinger FG, De Felici M. 2007a. Isolation of apoptotic mouse fetal oocytes by AnnexinV assay. *Int J Dev Biol* **51**: 157–60.

Lobascio AM, Klinger FG, De Felici M, Farini D, De Felici M. 2007b. Analysis of programmed cell death in mouse fetal oocytes. *Reproduction* **134**: 241–52.

Lock R, Debnath J. 2008. Extracellular matrix regulation of autophagy. *Curr Opin Cell Biol* **20**: 583–8.

Loutradis D, Bletsa R, Aravantinos L, Kallianidis K, Michalas S, Psychoyos A. 1991. Preovulatory effects of the progesterone antagonist mifepristone (RU486) in mice. *Hum Reprod* **6**: 1238–40.

Lucin KM, O'Brien CE, Bieri G, Czirr E, Mosher KI, Abbey RJ, Mastroeni DF, Rogers J, Spencer B, Masliah E, et al. 2013. Microglial beclin 1 regulates retromer trafficking and phagocytosis and is impaired in Alzheimer's disease. *Neuron* **79**: 873–86.

Luo S-M, Ge Z-J, Wang Z-W, Jiang Z-Z, Wang Z-B, Ouyang Y-C, Hou Y, Schatten H, Sun Q-Y. 2013. Unique insights into maternal mitochondrial inheritance in mice. *Proc Natl Acad Sci U S A* **110**: 13038–43.

Lydon JP, DeMayo FJ, Conneely OM, O'Malley BW. 1996. Reproductive phenotpes of the progesterone receptor null mutant mouse. *J Steroid Biochem Mol Biol* **56**: 67–77.

Lydon JP, DeMayo FJ, Funk CR, Mani SK, Hughes AR, Montgomery CA, Shyamala G, Conneely OM, O'Malley BW. 1995. Mice lacking progesterone receptor exhibit pleiotropic reproductive abnormalities. *Genes Dev* **9**: 2266–78.

Lysiak JJ. 2004. The role of tumor necrosis factor-alpha and interleukin-1 in the mammalian testis and their involvement in testicular torsion and autoimmune orchitis. *Reprod Biol Endocrinol* **2**: 9.

Ma X, Dong Y, Matzuk MM, Kumar TR. 2004. Targeted disruption of luteinizing hormone beta-subunit leads to hypogonadism, defects in gonadal steroidogenesis, and infertility. *Proc Natl Acad Sci U S A* **101**: 17294–9.

Macintosh RL, Timpson P, Thorburn J, Anderson KI, Thorburn A, Ryan KM. 2012. Inhibition of autophagy impairs tumor cell invasion in an organotypic model. *Cell Cycle* **11**: 2022–9.

Maclean JA, Chen MA, Wayne CM, Bruce SR, Rao M, Meistrich ML, Macleod C, Wilkinson MF. 2005. Rhox: a new homeobox gene cluster. *Cell* **120**: 369–82.

MacLean JA, Hu Z, Welborn JP, Song H-W, Rao MK, Wayne CM, Wilkinson MF. 2013. The RHOX homeodomain proteins regulate the expression of insulin and other metabolic regulators in the testis. *J Biol Chem* **288**: 34809–25.

Maeda Y, Shiratsuchi A, Namiki M, Nakanishi Y. 2002. Inhibition of sperm production in mice by annexin V microinjected into seminiferous tubules: possible etiology of phagocytic clearance of apoptotic spermatogenic cells and male infertility. *Cell Death Differ* **9**: 742–9.

Magnus V. 1901. Ovariets betydning for svangerskabet med soerligt hensyn til corpus luteum. *Nor Mag Loegevidensk* **62**: 1138.

Maiuri MC, Zalckvar E, Kimchi A, Kroemer G. 2007. Self-eating and self-killing: crosstalk between autophagy and apoptosis. *Nat Rev Mol Cell Biol* **8**: 741–52.

Malassiné A, Frendo JL, Evain-Brion D. 2003. A comparison of placental development and endocrine functions between the human and mouse model. *Hum Reprod Update* **9**: 531–9.

Malpighi M. 1685. Praeclarissimo & eruditissimo Viro D. Jacobo sponio Medicinae doctor, & Lugdenensi anatomicl Accuatatissimo. *Philos Trans R Soc Lond B Biol Sci* **14**: 639–640.

Mammucari C, Milan G, Romanello V, Masiero E, Rudolf R, Del Piccolo P, Burden SJ, Di Lisi R, Sandri C, Zhao J, et al. 2007. FoxO3 controls autophagy in skeletal muscle in vivo. *Cell Metab* **6**: 458–71.

Mann JS, Kindy MS, Edwards DR, Curry TE. 1991. Hormonal regulation of matrix metalloproteinase inhibitors in rat granulosa cells and ovaries. *Endocrinology* **128**: 1825–32.

Manova K, Huang EJ, Angeles M, De Leon V, Sanchez S, Pronovost SM, Besmer P, Bachvarova RF. 1993. The expression pattern of the c-kit ligand in gonads of mice supports a role for the c-kit receptor in oocyte growth and in proliferation of spermatogonia. *Dev Biol* **157**: 85–99.

Martinez J, Almendinger J, Oberst A, Ness R, Dillon CP, Fitzgerald P, Hengartner MO, Green DR. 2011. Microtubule-associated protein 1 light chain 3 alpha (LC3)-associated phagocytosis is required for the efficient clearance of dead cells. *Proc Natl Acad Sci U S A* **108**: 17396–401.

Matsuda F, Inoue N, Maeda A, Cheng Y, Sai T, Gonda H, Goto Y, Sakamaki K, Manabe N. 2011. Expression and function of apoptosis initiator FOXO3 in granulosa cells during follicular atresia in pig ovaries. *J Reprod Dev* **57**: 151–8.

Matzuk M, Lamb D. 2002. Genetic dissection of mammalian fertility pathways. *Translocations* 23–25.

Matzuk MM, Lamb DJ. 2008. The biology of infertility: research advances and clinical challenges. *Nat Med* **14**: 1197–213.

Mayerhofer A. 2013. Human testicular peritubular cells: more than meets the eye. *Reproduction* **145**: R107–16.

May-Panloup P, Chrétien M-F, Savagner F, Vasseur C, Jean M, Malthièry Y, Reynier P. 2003. Increased sperm mitochondrial DNA content in male infertility. *Hum Reprod* **18**: 550–6.

Mazaud-Guittot S. 2011. Dissecting the phthalate-induced Sertoli cell injury: the fragile balance of proteases and their inhibitors. *Biol Reprod* **85**: 1091–3.

McClellan KA, Gosden R, Taketo T. 2003. Continuous loss of oocytes throughout meiotic prophase in the normal mouse ovary. *Dev Biol* **258**: 334–48.

McElreavey K, Vilain E, Abbas N, Herskowitz I, Fellous M. 1993a. A regulatory cascade hypothesis for mammalian sex determination: SRY represses a negative regulator of male development. *Proc Natl Acad Sci U S A* **90**: 3368–72.

McElreavey K, Vilain E, Cotinot C, Payen E, Fellous M. 1993b. Control of sex determination in animals. *Eur J Biochem* **218**: 769–83.

McEwan DG, Dikic I. 2011. The Three Musketeers of Autophagy: phosphorylation, ubiquitylation and acetylation. *Trends Cell Biol* **21**: 195–201.

McLaughlin E a, McIver SC. 2009. Awakening the oocyte: controlling primordial follicle development. *Reproduction* **137**: 1–11.

McLaughlin M, Patrizio P, Kayisli U, Luk J, Thomson TC, Anderson RA, Telfer EE, Johnson J. 2011. mTOR kinase inhibition results in oocyte loss characterized by empty follicles in human ovarian cortical strips cultured in vitro. *Fertil Steril* **96**: 1154–9.e1.

McLean DJ, Friel PJ, Pouchnik D, Griswold MD. 2002. Oligonucleotide microarray analysis of gene expression in follicle-stimulating hormone-treated rat Sertoli cells. *Mol Endocrinol* **16**: 2780–92.

Medema JP, Scaffidi C, Kischkel FC, Shevchenko A, Mann M, Krammer PH, Peter ME. 1997. FLICE is activated by association with the CD95 death-inducing signaling complex (DISC). *EMBO J* **16**: 2794–804.

Medvedev S, Pan H, Schultz RM. 2011. Absence of MSY2 in mouse oocytes perturbs oocyte growth and maturation, RNA stability, and the transcriptome. *Biol Reprod* **85**: 575–83.

Meidan R, Girsh E, Blum O, Aberdam E. 1990. In vitro differentiation of bovine theca and granulosa cells into small and large luteal-like cells: morphological and functional characteristics. *Biol Reprod* **43**: 913–21.

Meng X, Lindahl M, Hyvönen ME, Parvinen M, de Rooij DG, Hess MW, Raatikainen-Ahokas A, Sainio K, Rauvala H, Lakso M, et al. 2000. Regulation of cell fate decision of undifferentiated spermatogonia by GDNF. *Science* **287**: 1489–93.

Menke DB, Koubova J, Page DC. 2003. Sexual differentiation of germ cells in XX mouse gonads occurs in an anterior-to-posterior wave. *Dev Biol* **262**: 303–12.

Merz EA, Brinster RL, Brunner S, Chen HY. 1981. Protein degradation during preimplantation development of the mouse. *J Reprod Fertil* **61**: 415–8.

Miettinen HE, Rayburn H, Krieger M. 2001. Abnormal lipoprotein metabolism and reversible female infertility in HDL receptor (SR-BI)-deficient mice. *J Clin Invest* **108**: 1717–22.

De Miguel MP, Cheng L, Holland EC, Federspiel MJ, Donovan PJ. 2002. Dissection of the c-Kit signaling pathway in mouse primordial germ cells by retroviral-mediated gene transfer. *Proc Natl Acad Sci U S A* **99**: 10458–63.

Mirakhori F, Zeynali B, Tafreshi AP, Shirmohammadian A. 2013. Lithium induces follicular atresia in rat ovary through a GSK-3β/β-catenin dependent mechanism. *Mol Reprod Dev* **80**: 286–96.

Mizushima N. 2009. *Methods for monitoring autophagy using GFP-LC3 transgenic mice.* 1st ed. Elsevier Inc.

Mizushima N, Jung CH, Ro S-H, Cao J, Otto NM, Kim D-H. 2010. mTOR regulation of autophagy. *FEBS Lett* **584**: 1287–1295.

Mizushima N, Yamamoto A. 2004. In vivo analysis of autophagy in response to nutrient starvation using transgenic mice expressing a fluorescent autophagosome marker. *Mol Biol Cell* **15**: 1101–1111.

Modi DN, Sane S, Bhartiya D. 2003. Accelerated germ cell apoptosis in sex chromosome aneuploid fetal human gonads. *Mol Hum Reprod* **9**: 219–25.

Molyneaux KA, Zinszner H, Kunwar PS, Schaible K, Stebler J, Sunshine MJ, O'Brien W, Raz E, Littman D, Wylie C, et al. 2003. The chemokine SDF1/CXCL12 and its receptor CXCR4 regulate mouse germ cell migration and survival. *Development* **130**: 4279–86.

Monastyrska I, Rieter E, Klionsky DJ, Reggiori F. 2009. Multiple roles of the cytoskeleton in autophagy. *Biol Rev Camb Philos Soc* **84**: 431–48.

Moor RM. 1968. Effect of Embryo on Corpus Luteum Function. *J Anim Sci* **27**: 97–118.

Morales C, Clermont Y. 1993. Structural changes in teh Seroli cell during the cycle of the seminiferous epithelium. In *The Sertoli Cell* (eds. D.L. Russell and M.D. Griswold), pp. 305–239, Cache River Press, Clearwater, FL.

Moreau K, Renna M, Rubinsztein DC. 2013. Connections between SNAREs and autophagy. *Trends Biochem Sci* **38**: 57–63.

Morita Y, Perez GI, Maravei D V, Tilly KI, Tilly JL. 1999. Targeted expression of Bcl-2 in mouse oocytes inhibits ovarian follicle atresia and prevents spontaneous and chemotherapy-induced oocyte apoptosis in vitro. *Mol Endocrinol* **13**: 841–50.

Mukumoto S, Mori K, Ishikawa H. 1995. Efficient induction of superovulation in adult rats by PMSG and hCG. *Exp Anim* **44**: 111–8.

Murphy BD. 2000. Models of luteinization. *Biol Reprod* **63**: 2–11.

Murray SA, Morgan JL, Kane C, Sharma Y, Heffner CS, Lake J, Donahue LR. 2010. Mouse gestation length is genetically determined. *PLoS One* **5**: e12418.

Na G, Bridges PJ, Koo Y, Ko C. 2008. Role of hypoxia in the regulation of periovulatory EDN2 expression in the mouse. *Can J Physiol Pharmacol* **86**: 310–9.

Nair U, Jotwani A, Geng J, Gammoh N, Richerson D, Yen W-L, Griffith J, Nag S, Wang K, Moss T, et al. 2011. SNARE proteins are required for macroautophagy. *Cell* **146**: 290–302.

Nakae J, Barr V, Accili D. 2000. Differential regulation of gene expression by insulin and IGF-1 receptors correlates with phosphorylation of a single amino acid residue in the forkhead transcription factor FKHR. *EMBO J* **19**: 989–96.

Nakagawa A, Shiratsuchi A, Tsuda K, Nakanishi Y. 2005. In vivo analysis of phagocytosis of apoptotic cells by testicular Sertoli cells. *Mol Reprod Dev* **71**: 166–77.

Nakanishi Y, Shiratsuchi A. 2004. Phagocytic removal of apoptotic spermatogenic cells by Sertoli cells: mechanisms and consequences. *Biol Pharm Bull* **27**: 13–6.

Nakatogawa H, Suzuki K, Kamada Y, Ohsumi Y. 2009. Dynamics and diversity in autophagy mechanisms: lessons from yeast. *Nat Rev Mol Cell Biol* **10**: 458–67.

Nelson SE, Gibori G, Hunzicker-Dunn M. 1992a. The cAMP-dependent signalling cascade in the two luteal cell types of the pregnant rat corpus luteum. *Mol Cell Endocrinol* **85**: 195–203.

Nelson SE, McLean MP, Jayatilak PG, Gibori G. 1992b. Isolation, characterization, and culture of cell subpopulations forming the pregnant rat corpus luteum. *Endocrinology* **130**: 954–66.

Nezis IP, Shravage B V, Sagona AP, Lamark T, Bjørkøy G, Johansen T, Rusten TE, Brech A, Baehrecke EH, Stenmark H. 2010. Autophagic degradation of dBruce controls DNA fragmentation in nurse cells during late Drosophila melanogaster oogenesis. *J Cell Biol* **190**: 523–31.

Nielsen R, Courtoy PJ, Jacobsen C, Dom G, Lima WR, Jadot M, Willnow TE, Devuyst O, Christensen EI. 2007. Endocytosis provides a major alternative pathway for lysosomal biogenesis in kidney proximal tubular cells. *Proc Natl Acad Sci U S A* **104**: 5407–12.

Nishimura Y, Yoshinari T, Naruse K, Yamada T, Sumi K, Mitani H, Higashiyama T, Kuroiwa T. 2006. Active digestion of sperm mitochondrial DNA in single living sperm revealed by optical tweezers. *Proc Natl Acad Sci U S A* **103**: 1382–7.

Niwa H, Yamamura K, Miyazaki J. 1991. Efficient selection for high-expression transfectants with a novel eukaryotic vector. *Gene* **108**: 193–9.

Noda T, Matsunaga K, Taguchi-Atarashi N, Yoshimori T. 2010. Regulation of membrane biogenesis in autophagy via PI3P dynamics. *Semin Cell Dev Biol* **21**: 671–6.

Noda T, Suzuki K, Ohsumi Y. 2002. Yeast autophagosomes: de novo formation of a membrane structure. *Trends Cell Biol* **12**: 231–5.

Nowak MA, Boerlijst MC, Cooke J, Smith JM. 1997. Evolution of genetic redundancy. *Nature* **388**: 167–71.

O'Shaughnessy PJ, Monteiro A, Fowler PA, Morris I. 2014. Identification of Leydig cell-specific mRNA transcripts in the adult rat testis. *Reproduction*.

Oakley OR, Frazer ML, Ko C. 2011. Pituitary-ovary-spleen axis in ovulation. *Trends Endocrinol Metab* **22**: 345–52.

Oberstein A, Jeffrey PD, Shi Y. 2007. Crystal structure of the Bcl-XL-Beclin 1 peptide complex: Beclin 1 is a novel BH3-only protein. *J Biol Chem* **282**: 13123–32.

Oczypok EA, Oury TD, Chu CT. 2013. It's a Cell-Eat-Cell World. *Am J Pathol* **182**: 612–622.

Ogren L, Southard JN, Colosi P, Linzer DI, Talamantes F. 1989. Mouse placental lactogen-I: RIA and gestational profile in maternal serum. *Endocrinology* **125**: 2253–7.

Oh S-Y, Choi S-J, Kim KH, Cho EY, Kim J-H, Roh C-R. 2008. Autophagy-related proteins, LC3 and Beclin-1, in placentas from pregnancies complicated by preeclampsia. *Reprod Sci* **15**: 912–20.

Ohinata Y, Payer B, O'Carroll D, Ancelin K, Ono Y, Sano M, Barton SC, Obukhanych T, Nussenzweig M, Tarakhovsky A, et al. 2005. Blimp1 is a critical determinant of the germ cell lineage in mice. *Nature* **436**: 207–13.

Ohsaki Y, Suzuki M, Fujimoto T. 2014. Open questions in lipid droplet biology. *Chem Biol* **21**: 86–96.

Ost A, Svensson K, Ruishalme I, Brännmark C, Franck N, Krook H, Sandström P, Kjolhede P, Strålfors P. 2010. Attenuated mTOR signaling and enhanced autophagy in adipocytes from obese patients with type 2 diabetes. *Mol Med* **16**: 235–46.

Packer AI, Hsu YC, Besmer P, Bachvarova RF. 1994. The ligand of the c-kit receptor promotes oocyte growth. *Dev Biol* **161**: 194–205.

Palanisamy GS, Cheon Y-P, Kim J, Kannan A, Li Q, Sato M, Mantena SR, Sitruk-Ware RL, Bagchi MK, Bagchi IC. 2006. A novel pathway involving progesterone receptor, endothelin-2, and endothelin receptor B controls ovulation in mice. *Mol Endocrinol* **20**: 2784–95.

Pan H, O'brien MJ, Wigglesworth K, Eppig JJ, Schultz RM. 2005. Transcript profiling during mouse oocyte development and the effect of gonadotropin priming and development in vitro. *Dev Biol* **286**: 493–506.

Papaioannou MD, Pitetti J-L, Ro S, Park C, Aubry F, Schaad O, Vejnar CE, Kühne F, Descombes P, Zdobnov EM, et al. 2009. Sertoli cell Dicer is essential for spermatogenesis in mice. *Dev Biol* **326**: 250–9.

Parma P, Radi O, Vidal V, Chaboissier MC, Dellambra E, Valentini S, Guerra L, Schedl A, Camerino G. 2006. R-spondin1 is essential in sex determination, skin differentiation and malignancy. *Nat Genet* **38**: 1304–9.

Parzych KR, Klionsky DJ. 2013. An Overview of Autophagy: Morphology, Mechanism, and Regulation. *Antioxid Redox Signal*.

Pauli SA, Tang H, Wang J, Bohlen P, Posser R, Hartman T, Sauer M V, Kitajewski J, Zimmermann RC. 2005. The vascular endothelial growth factor (VEGF)/VEGF receptor 2 pathway is critical for blood vessel survival in corpora lutea of pregnancy in the rodent. *Endocrinology* **146**: 1301–11.

Pavlok A, Lucas-Hahn A, Niemann H. 1992. Fertilization and developmental competence of bovine oocytes derived from different categories of antral follicles. *Mol Reprod Dev* **31**: 63–7.

Payne CJ. 2013. Cycling to and from a stem cell niche: the temporal and spatial odyssey of mitotic male germ cells. *Int J Dev Biol* **57**: 169–77.

Peluso JJ, England-Charlesworth C, Bolender DL, Steger RW. 1980. Ultrastructural alterations associated with the initiation of follicular atresia. *Cell Tissue Res* **211**: 105–15.

Pepling ME, Spradling AC. 1998. Female mouse germ cells form synchronously dividing cysts. *Development* **125**: 3323–8.

Pepling ME, Spradling AC. 2001. Mouse ovarian germ cell cysts undergo programmed breakdown to form primordial follicles. *Dev Biol* **234**: 339–51.

Pescador N, Soumano K, Stocco DM, Price CA, Murphy BD. 1996. Steroidogenic acute regulatory protein in bovine corpora lutea. *Biol Reprod* **55**: 485–91.

Pesce M, De Felici M. 1994. Apoptosis in mouse primordial germ cells: a study by transmission and scanning electron microscope. *Anat Embryol (Berl)* **189**: 435–40.

Peters H, Levy E, Crone M. 1965. Oogenesis in rabbits. *J Exp Zool* **158**: 169–179.

Petersen C, Soder O. 2006. The sertoli cell--a hormonal target and “super” nurse for germ cells that determines testicular size. *Horm Res* **66**: 153–61.

Petherick KJ, Williams AC, Lane JD, Ordóñez-Morán P, Huelsken J, Collard TJ, Smartt HJM, Batson J, Malik K, Paraskeva C, et al. 2013. Autolysosomal β-catenin degradation regulates Wnt-autophagy-p62 crosstalk. *EMBO J* **32**: 1903–16.

Petiot A, Faure J, Stenmark H, Gruenberg J. 2003. PI3P signaling regulates receptor sorting but not transport in the endosomal pathway. *J Cell Biol* **162**: 971–9.

Pfeiffer MJ, Siatkowski M, Paudel Y, Balbach ST, Baeumer N, Crosetto N, Drexler HCA, Fuellen G, Boiani M. 2011. Proteomic analysis of mouse oocytes reveals 28 candidate factors of the “reprogrammome”. *J Proteome Res* **10**: 2140–53.

Pierson R, Stephanson R. 2010. Imagining reproduction in science and history. *J Med Humanit* **31**: 1–9.

Pikó L, Clegg KB. 1982. Quantitative changes in total RNA, total poly(A), and ribosomes in early mouse embryos. *Dev Biol* **89**: 362–78.

Piras A, Gianetto D, Conte D, Bosone A, Vercelli A. 2011. Activation of autophagy in a rat model of retinal ischemia following high intraocular pressure. *PLoS One* **6**: e22514.

Popa SM, Clifton DK, Steiner RA. 2008. The role of kisspeptins and GPR54 in the neuroendocrine regulation of reproduction. *Annu Rev Physiol* **70**: 213–38.

Qu X, Yu J, Bhagat G. 2003. Promotion of tumorigenesis by heterozygous disruption of the beclin 1 autophagy gene. *J Clin …* **112**: 1809–1820.

Quirk SM, Cowan RG, Joshi SG, Henrikson KP. 1995. Fas antigen-mediated apoptosis in human granulosa/luteal cells. *Biol Reprod* **52**: 279–87.

Rabinovitch M. 1995. Professional and non-professional phagocytes: an introduction. *Trends Cell Biol* **5**: 85–7.

Rajagopalan-Gupta RM, Lamm ML, Mukherjee S, Rasenick MM, Hunzicker-Dunn M. 1998. Luteinizing hormone/choriogonadotropin receptor-mediated activation of heterotrimeric guanine nucleotide binding proteins in ovarian follicular membranes. *Endocrinology* **139**: 4547–55.

Rantanen A, Jansson M, Oldfors A, Larsson NG. 2001. Downregulation of Tfam and mtDNA copy number during mammalian spermatogenesis. *Mamm Genome* **12**: 787–92.

Ratts VS, Flaws JA, Kolp R, Sorenson CM, Tilly JL. 1995. Ablation of bcl-2 gene expression decreases the numbers of oocytes and primordial follicles established in the post-natal female mouse gonad. *Endocrinology* **136**: 3665–8.

Ravikumar B, Moreau K, Jahreiss L, Puri C, Rubinsztein DC. 2010. Plasma membrane contributes to the formation of pre-autophagosomal structures. *Nat Cell Biol* **12**: 747–57.

Al Rawi S, Louvet-Vallée S, Djeddi A, Sachse M, Culetto E, Hajjar C, Boyd L, Legouis R, Galy V. 2011. Postfertilization autophagy of sperm organelles prevents paternal mitochondrial DNA transmission. *Science* **334**: 1144–7.

Reddy P, Adhikari D, Zheng W, Liang S, Hämäläinen T, Tohonen V, Ogawa W, Noda T, Volarevic S, Huhtaniemi I, et al. 2009. PDK1 signaling in oocytes controls reproductive aging and lifespan by manipulating the survival of primordial follicles. *Hum Mol Genet* **18**: 2813–24.

Reddy P, Liu L, Adhikari D, Jagarlamudi K, Rajareddy S, Shen Y, Du C, Tang W, Hämäläinen T, Peng SL, et al. 2008. Oocyte-specific deletion of Pten causes premature activation of the primordial follicle pool. *Science* **319**: 611–3.

Reichman-Fried M, Minina S, Raz E. 2004. Autonomous modes of behavior in primordial germ cell migration. *Dev Cell* **6**: 589–96.

Reynier P, May-Panloup P, Chrétien MF, Morgan CJ, Jean M, Savagner F, Barrière P, Malthièry Y. 2001. Mitochondrial DNA content affects the fertilizability of human oocytes. *Mol Hum Reprod* **7**: 425–9.

Reynolds LP, Grazul-Bilska AT, Killilea SD, Redmer DA. 1994. Mitogenic factors of corpora lutea. *Prog Growth Factor Res* **5**: 159–75.

Reynolds LP, Grazul-Bilska AT, Redmer DA. 2000. Angiogenesis in the corpus luteum. *Endocrine* **12**: 1–9.

Reynolds LP, Grazul-Bilska AT, Redmer DA. 2002. Angiogenesis in the female reproductive organs: pathological implications. *Int J Exp Pathol* **83**: 151–63.

Rhéaume E, Lachance Y, Zhao HF, Breton N, Dumont M, de Launoit Y, Trudel C, Luu-The V, Simard J, Labrie F. 1991. Structure and expression of a new complementary DNA encoding the almost exclusive 3 beta-hydroxysteroid dehydrogenase/delta 5-delta 4-isomerase in human adrenals and gonads. *Mol Endocrinol* **5**: 1147–57.

Ricciotti E, FitzGerald GA. 2011. Prostaglandins and inflammation. *Arterioscler Thromb Vasc Biol* **31**: 986–1000.

Richards JS. 2005. Ovulation: new factors that prepare the oocyte for fertilization. *Mol Cell Endocrinol* **234**: 75–9.

Richards JS, Russell DL, Ochsner S, Hsieh M, Doyle KH, Falender AE, Lo YK, Sharma SC. 2002. Novel signaling pathways that control ovarian follicular development, ovulation, and luteinization. *Recent Prog Horm Res* **57**: 195–220.

Richardson BE, Lehmann R. 2010. Mechanisms guiding primordial germ cell migration: strategies from different organisms. *Nat Rev Mol Cell Biol* **11**: 37–49.

Ricken AM, Traenkner A, Merkwitz C, Hummitzsch K, Grosche J, Spanel-Borowski K. 2007. The short prolactin receptor predominates in endothelial cells of micro- and macrovascular origin. *J Vasc Res* **44**: 19–30.

Riedlinger G, Okagaki R, Wagner K-U, Rucker EB, Oka T, Miyoshi K, Flaws J a, Hennighausen L. 2002. Bcl-x is not required for maintenance of follicles and corpus luteum in the postnatal mouse ovary. *Biol Reprod* **66**: 438–44.

Rigotti A, Trigatti BL, Penman M, Rayburn H, Herz J, Krieger M. 1997. A targeted mutation in the murine gene encoding the high density lipoprotein (HDL) receptor scavenger receptor class B type I reveals its key role in HDL metabolism. *Proc Natl Acad Sci U S A* **94**: 12610–5.

Ro S-H, Jung CH, Hahn WS, Xu X, Kim Y-M, Yun YS, Park J-M, Kim KH, Seo M, Ha T-Y, et al. 2013. Distinct functions of Ulk1 and Ulk2 in the regulation of lipid metabolism in adipocytes. *Autophagy* **9**: 2103–14.

Roa J, Garcia-Galiano D, Varela L, Sánchez-Garrido MA, Pineda R, Castellano JM, Ruiz-Pino F, Romero M, Aguilar E, López M, et al. 2009. The mammalian target of rapamycin as novel central regulator of puberty onset via modulation of hypothalamic Kiss1 system. *Endocrinology* **150**: 5016–26.

Robker RL, Richards JS. 1998. Hormone-induced proliferation and differentiation of granulosa cells: a coordinated balance of the cell cycle regulators cyclin D2 and p27Kip1. *Mol Endocrinol* **12**: 924–40.

Rode L, Langhoff-Roos J, Andersson C, Dinesen J, Hammerum MS, Mohapeloa H, Tabor A. 2009. Systematic review of progesterone for the prevention of preterm birth in singleton pregnancies. *Acta Obstet Gynecol Scand* **88**: 1180–9.

Rodgers RJ, Irving-Rodgers HF. 2010. Morphological classification of bovine ovarian follicles. *Reproduction* **139**: 309–18.

Rodrigues P, Limback D, McGinnis LK, Plancha CE, Albertini DF. 2009. Multiple mechanisms of germ cell loss in the perinatal mouse ovary. *Reproduction* **137**: 709–20.

Röhrl C, Stangl H. 2013. HDL endocytosis and resecretion. *Biochim Biophys Acta* **1831**: 1626–33.

Rosales-Torres AM, Alonso I, Vergara M, Romano MC, Castillo-Juárez H, Avalos A, Rosado A, Gutiérrez CG. 2010. Vascular endothelial growth factor isoforms 120, 164 and 205 are reduced with atresia in ovarian follicles of sheep. *Anim Reprod Sci* **122**: 111–7.

Rosales-Torres AM, Avalos-Rodríguez A, Vergara-Onofre M, Hernández-Pérez O, Ballesteros LM, García-Macedo R, Ortíz-Navarrete V, Rosado A. 2000. Multiparametric study of atresia in ewe antral follicles: histology, flow cytometry, internucleosomal DNA fragmentation, and lysosomal enzyme activities in granulosa cells and follicular fluid. *Mol Reprod Dev* **55**: 270–81.

Rosenfeld CS, Wagner JS, Roberts RM, Lubahn DB. 2001. Intraovarian actions of oestrogen. *Reproduction* **122**: 215–26.

Row PE, Reaves BJ, Domin J, Luzio JP, Davidson HW. 2001. Overexpression of a rat kinase-deficient phosphoinositide 3-kinase, Vps34p, inhibits cathepsin D maturation. *Biochem J* **353**: 655–61.

Rubinstein L, Forbes TR. 1963. Maintenance of pregnancy with subcutaneous pellets of progesterone in ovariectomized mice. *Proc Soc Exp Biol Med* **113**: 1043–6.

Ruck A, Attonito J, Garces KT, Núnez L, Palmisano NJ, Rubel Z, Bai Z, Nguyen KCQ, Sun L, Grant BD, et al. 2011. The Atg6/Vps30/Beclin 1 ortholog BEC-1 mediates endocytic retrograde transport in addition to autophagy in C. elegans. *Autophagy* **7**: 386–400.

Rucker EB, Dierisseau P, Wagner KU, Garrett L, Wynshaw-Boris a, Flaws J a, Hennighausen L. 2000. Bcl-x and Bax regulate mouse primordial germ cell survival and apoptosis during embryogenesis. *Mol Endocrinol* **14**: 1038–52.

Rudraraju N, Baltz JM. 2009. Amino acid carryover in the subzonal space of mouse fertilized ova affects subsequent transport kinetics. *Zygote* **17**: 281–7.

Ryter SW, Cloonan SM, Choi AMK. 2013. Autophagy: a critical regulator of cellular metabolism and homeostasis. *Mol Cells* **36**: 7–16.

Saitou M, Barton SC, Surani MA. 2002. A molecular programme for the specification of germ cell fate in mice. *Nature* **418**: 293–300.

Sakamaki K, Yoshida H, Nishimura Y, Nishikawa S, Manabe N, Yonehara S. 1997. Involvement of Fas antigen in ovarian follicular atresia and luteolysis. *Mol Reprod Dev* **47**: 11–8.

Salo AL, Randall CL, Becker HC. 1996. Effect of acute ethanol and cocaine administration on gestation days 14-17 in mice. *Alcohol* **13**: 369–75.

Salvador LM, Maizels E, Hales DB, Miyamoto E, Yamamoto H, Hunzicker-Dunn M. 2002. Acute signaling by the LH receptor is independent of protein kinase C activation. *Endocrinology* **143**: 2986–94.

Santos HB, Thomé RG, Arantes FP, Sato Y, Bazzoli N, Rizzo E. 2008. Ovarian follicular atresia is mediated by heterophagy, autophagy, and apoptosis in Prochilodus argenteus and Leporinus taeniatus (Teleostei: Characiformes). *Theriogenology* **70**: 1449–60.

Sanz E, Evanoff R, Quintana A, Evans E, Miller JA, Ko C, Amieux PS, Griswold MD, McKnight GS. 2013. RiboTag analysis of actively translated mRNAs in Sertoli and Leydig cells in vivo. ed. S. Schlatt. *PLoS One* **8**: e66179.

Sathananthan AH, Ng SC, Edirisinghe R, Ratnam SS, Wong PC. 1986. Human sperm-egg interaction in vitro. *Gamete Res* **15**: 317–326.

Sathananthan AH, Ratnam SS, Ng SC, Tarín JJ, Gianaroli L, Trounson A. 1996. The sperm centriole: its inheritance, replication and perpetuation in early human embryos. *Hum Reprod* **11**: 345–56.

Sato M, Kimura T, Kurokawa K, Fujita Y, Abe K, Masuhara M, Yasunaga T, Ryo A, Yamamoto M, Nakano T. 2002. Identification of PGC7, a new gene expressed specifically in preimplantation embryos and germ cells. *Mech Dev* **113**: 91–4.

Sato M, Sato K. 2011. Degradation of paternal mitochondria by fertilization-triggered autophagy in C. elegans embryos. *Science* **334**: 1141–4.

Sato M, Sato K. 2013. Dynamic regulation of autophagy and endocytosis for cell remodeling during early development. *Traffic* **14**: 479–86.

Schlatt S, de Kretser DM, Loveland KL. 1996. Discriminative analysis of rat Sertoli and peritubular cells and their proliferation in vitro: evidence for follicle-stimulating hormone-mediated contact inhibition of Sertoli cell mitosis. *Biol Reprod* **55**: 227–35.

Schmahl J, Kim Y, Colvin JS, Ornitz DM, Capel B. 2004. Fgf9 induces proliferation and nuclear localization of FGFR2 in Sertoli precursors during male sex determination. *Development* **131**: 3627–36.

Schöler HR, Ruppert S, Suzuki N, Chowdhury K, Gruss P. 1990. New type of POU domain in germ line-specific protein Oct-4. *Nature* **344**: 435–9.

Schwarze PE, Seglen PO. 1985. Reduced autophagic activity, improved protein balance and enhanced in vitro survival of hepatocytes isolated from carcinogen-treated rats. *Exp Cell Res* **157**: 15–28.

Seki Y, Yamaji M, Yabuta Y, Sano M, Shigeta M, Matsui Y, Saga Y, Tachibana M, Shinkai Y, Saitou M. 2007. Cellular dynamics associated with the genome-wide epigenetic reprogramming in migrating primordial germ cells in mice. *Development* **134**: 2627–38.

Sekido R, Bar I, Narváez V, Penny G, Lovell-Badge R. 2004. SOX9 is up-regulated by the transient expression of SRY specifically in Sertoli cell precursors. *Dev Biol* **274**: 271–9.

Sengupta A, Molkentin JD, Yutzey KE. 2009. FoxO transcription factors promote autophagy in cardiomyocytes. *J Biol Chem* **284**: 28319–31.

Sertoli E. 1865. Dell' esistenza de particolari cellule ramifacte nei cnalicoli sminiferi del testicolo umano. *Morgagni* **7**: 31–40.

Shaha C, Tripathi R, Mishra DP. 2010. Male germ cell apoptosis: regulation and biology. *Philos Trans R Soc Lond B Biol Sci* **365**: 1501–15.

Shaid S, Brandts CH, Serve H, Dikic I. 2013. Ubiquitination and selective autophagy. *Cell Death Differ* **20**: 21–30.

Shapiro-Mendoza C, Lackritz E. 2012. Epidemiology of late and moderate preterm birth. *Semin Fetal Neonatal ….*

Shen H-M, Codogno P. 2011. Autophagic cell death: Loch Ness monster or endangered species? *Autophagy* **7**: 457–65.

Shen S, Kepp O, Kroemer G. 2012. The end of autophagic cell death? *Autophagy* **8**: 1–3.

Shibata M, Yoshimura K, Furuya N, Koike M, Ueno T, Komatsu M, Arai H, Tanaka K, Kominami E, Uchiyama Y. 2009. The MAP1-LC3 conjugation system is involved in lipid droplet formation. *Biochem Biophys Res Commun* **382**: 419–23.

Shibata M, Yoshimura K, Tamura H, Ueno T, Nishimura T, Inoue T, Sasaki M, Koike M, Arai H, Kominami E, et al. 2010. LC3, a microtubule-associated protein1A/B light chain3, is involved in cytoplasmic lipid droplet formation. *Biochem Biophys Res Commun* **393**: 274–9.

Shimizu S, Kanaseki T, Mizushima N, Mizuta T, Arakawa-Kobayashi S, Thompson CB, Tsujimoto Y. 2004. Role of Bcl-2 family proteins in a non-apoptotic programmed cell death dependent on autophagy genes. *Nat Cell Biol* **6**: 1221–8.

Shimshek DR, Kim J, Hübner MR, Spergel DJ, Buchholz F, Casanova E, Stewart AF, Seeburg PH, Sprengel R. 2002. Codon-improved Cre recombinase (iCre) expression in the mouse. *Genesis* **32**: 19–26.

Shin S-W, Shimizu N, Tokoro M, Nishikawa S, Hatanaka Y, Anzai M, Hamazaki J, Kishigami S, Saeki K, Hosoi Y, et al. 2013. Mouse zygote-specific proteasome assembly chaperone important for maternal-to-zygotic transition. *Biol Open* **2**: 170–82.

Shin S-W, Tokoro M, Nishikawa S, Lee H-H, Hatanaka Y, Nishihara T, Amano T, Anzai M, Kato H, Mitani T, et al. 2010. Inhibition of the ubiquitin-proteasome system leads to delay of the onset of ZGA gene expression. *J Reprod Dev* **56**: 655–63.

Shitara H, Kaneda H, Sato A, Inoue K, Ogura A, Yonekawa H, Hayashi JI. 2000. Selective and continuous elimination of mitochondria microinjected into mouse eggs from spermatids, but not from liver cells, occurs throughout embryogenesis. *Genetics* **156**: 1277–84.

Shpilka T, Weidberg H, Pietrokovski S, Elazar Z. 2011. Atg8: an autophagy-related ubiquitin-like protein family. *Genome Biol* **12**: 226.

Signorelli P, Avagliano L, Virgili E, Gagliostro V, Doi P, Braidotti P, Bulfamante GP, Ghidoni R, Marconi AM. 2011. Autophagy in term normal human placentas. *Placenta* **32**: 482–5.

Singh AP, Maerzke S, von Deimling O, Raman R, Sperling K, Neitzel H. 1993. Oocytes from pachytene to dictyotene can easily be analysed in neonatal rodents. *Chromosome Res* **1**: 209–13.

Singh R, Kaushik S, Wang Y, Xiang Y, Novak I, Komatsu M, Tanaka K, Cuervo AM, Czaja MJ. 2009a. Autophagy regulates lipid metabolism. *Nature* **458**: 1131–5.

Singh R, Xiang Y, Wang Y, Baikati K, Cuervo AM, Luu YK, Tang Y, Pessin JE, Schwartz GJ, Czaja MJ. 2009b. Autophagy regulates adipose mass and differentiation in mice. *J Clin Invest* **119**: 3329–39.

Smith BE, Braun RE. 2012. Germ Cell Migration Across Sertoli Cell Tight Junctions. *Science* **338**: 798–802.

Smith MF, McIntush EW, Smith GW. 1994. Mechanisms associated with corpus luteum development. *J Anim Sci* **72**: 1857–72.

Snowden T, Acharya S, Butz C, Berardini M, Fishel R. 2004. hMSH4-hMSH5 recognizes Holliday Junctions and forms a meiosis-specific sliding clamp that embraces homologous chromosomes. *Mol Cell* **15**: 437–51.

Snyder BW, Beecham GD, Schane HP. 1984. Inhibition of ovulation in rats with epostane, an inhibitor of 3 beta-hydroxysteroid dehydrogenase. *Proc Soc Exp Biol Med* **176**: 238–42.

Soares MJ, Colosi P, Talamantes F. 1982. The development and characterization of a homologous radioimmunoassay for mouse placental lactogen. *Endocrinology* **110**: 668–70.

Steinberger A, Steinberger E. 1971. Replication pattern of Sertoli cells in maturing rat testis in vivo and in organ culture. *Biol Reprod* **4**: 84–7.

Stocco C, Telleria C, Gibori G. 2007. The molecular control of corpus luteum formation, function, and regression. *Endocr Rev* **28**: 117–49.

Stocco DM, Clark BJ. 1996. Role of the steroidogenic acute regulatory protein (StAR) in steroidogenesis. *Biochem Pharmacol* **51**: 197–205.

Stone D, Hechter O. 1954. Role of the steroidogenic acute regulatory protein (StAR) in steroidogenesis. *Arch Biochem Biophys* **51**: 457–69.

Su Y-Q, Wu X, O'Brien MJ, Pendola FL, Denegre JN, Matzuk MM, Eppig JJ. 2004. Synergistic roles of BMP15 and GDF9 in the development and function of the oocyte-cumulus cell complex in mice: genetic evidence for an oocyte-granulosa cell regulatory loop. *Dev Biol* **276**: 64–73.

Subramanian K, Balch WE. 2008. NPC1/NPC2 function as a tag team duo to mobilize cholesterol. *Proc Natl Acad Sci U S A* **105**: 15223–4.

Suh N, Baehner L, Moltzahn F, Melton C, Shenoy A, Chen J, Blelloch R. 2010. MicroRNA function is globally suppressed in mouse oocytes and early embryos. *Curr Biol* **20**: 271–7.

Sui X, Kong N, Zhu M, Wang X, Lou F, Han W, Pan H. 2014. Cotargeting EGFR and autophagy signaling: A novel therapeutic strategy for non-small-cell lung cancer. *Mol Clin Oncol* **2**: 8–12.

Sun Q, Westphal W, Wong KN, Tan I, Zhong Q. 2010. Rubicon controls endosome maturation as a Rab7 effector. *Proc Natl Acad Sci U S A* **107**: 19338–43.

Sun Q-Y, Miao Y-L, Schatten H. 2009. Towards a new understanding on the regulation of mammalian oocyte meiosis resumption. *Cell Cycle* **8**: 2741–7.

Sutovsky P, Moreno RD, Ramalho-Santos J, Dominko T, Simerly C, Schatten G. 1999. Ubiquitin tag for sperm mitochondria. *Nature* **402**: 371–2.

Sutovsky P, Moreno RD, Ramalho-Santos J, Dominko T, Simerly C, Schatten G. 2000. Ubiquitinated sperm mitochondria, selective proteolysis, and the regulation of mitochondrial inheritance in mammalian embryos. *Biol Reprod* **63**: 582–90.

Sutovsky P, Navara CS, Schatten G. 1996. Fate of the sperm mitochondria, and the incorporation, conversion, and disassembly of the sperm tail structures during bovine fertilization. *Biol Reprod* **55**: 1195–205.

Takahashi Y, Coppola D, Matsushita N, Cualing HD, Sun M, Sato Y, Liang C, Jung JU, Cheng JQ, Mulé JJ, et al. 2007. Bif-1 interacts with Beclin 1 through UVRAG and regulates autophagy and tumorigenesis. *Nat Cell Biol* **9**: 1142–51.

Takahashi Y, Meyerkord CL, Hori T, Runkle K, Fox TE, Kester M, Loughran TP, Wang H-G. 2011. Bif-1 regulates Atg9 trafficking by mediating the fission of Golgi membranes during autophagy. *Autophagy* **7**: 61–73.

Tam PP, Snow MH. 1981. Proliferation and migration of primordial germ cells during compensatory growth in mouse embryos. *J Embryol Exp Morphol* **64**: 133–47.

Tamanini C, De Ambrogi M. 2004. Angiogenesis in developing follicle and corpus luteum. *Reprod Domest Anim* **39**: 206–16.

Tang XM, Hui-xin Z, Jing Y. 1992. Leydig Cells a Normal Cell Model of Cellular Autophagy. *Acta Biol Exp Sin*.

Tanwar PS, Kaneko-Tarui T, Zhang L, Rani P, Taketo MM, Teixeira J. 2010. Constitutive WNT/beta-catenin signaling in murine Sertoli cells disrupts their differentiation and ability to support spermatogenesis. *Biol Reprod* **82**: 422–32.

Tanwar PS, Kaneko-Tarui T, Zhang L, Teixeira JM. 2012. Altered LKB1/AMPK/TSC1/TSC2/mTOR signaling causes disruption of Sertoli cell polarity and spermatogenesis. *Hum Mol Genet* **21**: 4394–405.

Teglund S, McKay C, Schuetz E, van Deursen JM, Stravopodis D, Wang D, Brown M, Bodner S, Grosveld G, Ihle JN. 1998. Stat5a and Stat5b proteins have essential and nonessential, or redundant, roles in cytokine responses. *Cell* **93**: 841–50.

Teixeira J, He WW, Shah PC, Morikawa N, Lee MM, Catlin EA, Hudson PL, Wing J, Maclaughlin DT, Donahoe PK. 1996. Developmental expression of a candidate müllerian inhibiting substance type II receptor. *Endocrinology* **137**: 160–5.

Thompson WE, Ramalho-Santos J, Sutovsky P. 2003. Ubiquitination of prohibitin in mammalian sperm mitochondria: possible roles in the regulation of mitochondrial inheritance and sperm quality control. *Biol Reprod* **69**: 254–60.

Thomson TC, Johnson J. 2010. Inducible somatic oocyte destruction in response to rapamycin requires wild-type regulation of follicle cell epithelial polarity. *Cell Death Differ* **17**: 1717–27.

Thoresen SB, Pedersen NM, Liestøl K, Stenmark H. 2010. A phosphatidylinositol 3-kinase class III sub-complex containing VPS15, VPS34, Beclin 1, UVRAG and BIF-1 regulates cytokinesis and degradative endocytic traffic. *Exp Cell Res* **316**: 3368–78.

Thumm M, Egner R, Koch B, Schlumpberger M, Straub M, Veenhuis M, Wolf DH. 1994. Isolation of autophagocytosis mutants of Saccharomyces cerevisiae. *FEBS Lett* **349**: 275–80.

Tilly JL, Billig H, Kowalski KI, Hsueh AJ. 1992. Epidermal growth factor and basic fibroblast growth factor suppress the spontaneous onset of apoptosis in cultured rat ovarian granulosa cells and follicles by a tyrosine kinase-dependent mechanism. *Mol Endocrinol* **6**: 1942–50.

Tilly JL, Tilly KI. 1995. Inhibitors of oxidative stress mimic the ability of follicle-stimulating hormone to suppress apoptosis in cultured rat ovarian follicles. *Endocrinology* **136**: 242–52.

Tingen CCM, Bristol-gould SKS, Kiesewetter SSE, Wellington JTJ, Shea L, Woodruff TTK. 2009. Prepubertal primordial follicle loss in mice is not due to classical apoptotic pathways. *Biol Reprod* **25**: 16–25.

Tobin AB, Butcher AJ, Kong KC. 2008. Location, location, location...site-specific GPCR phosphorylation offers a mechanism for cell-type-specific signalling. *Trends Pharmacol Sci* **29**: 413–20.

Tomizuka K, Horikoshi K, Kitada R, Sugawara Y, Iba Y, Kojima A, Yoshitome A, Yamawaki K, Amagai M, Inoue A, et al. 2008. R-spondin1 plays an essential role in ovarian development through positively regulating Wnt-4 signaling. *Hum Mol Genet* **17**: 1278–91.

Trigatti B, Rayburn H, Viñals M, Braun A, Miettinen H, Penman M, Hertz M, Schrenzel M, Amigo L, Rigotti A, et al. 1999. Influence of the high density lipoprotein receptor SR-BI on reproductive and cardiovascular pathophysiology. *Proc Natl Acad Sci U S A* **96**: 9322–7.

Tsai RY. 2005. Sertoli Cell Biology. *Vitr Cell Dev Biol* **41**: 177.

Tsuda M, Sasaoka Y, Kiso M, Abe K, Haraguchi S, Kobayashi S, Saga Y. 2003. Conserved role of nanos proteins in germ cell development. *Science* **301**: 1239–41.

Tsukada M, Ohsumi Y. 1993. Isolation and characterization of autophagy-defective mutants of Saccharomyces cerevisiae. *FEBS Lett* **333**: 169–74.

Tsukamoto S, Kuma A, Mizushima N. 2008a. The role of autophagy during the oocyte-to-embryo transition. *Autophagy* **4**: 1076–8.

Tsukamoto S, Kuma A, Murakami M, Kishi C, Yamamoto A, Mizushima N. 2008b. Autophagy is essential for preimplantation development of mouse embryos. *Science* **321**: 117–20.

Tuloup-Minguez V, Hamaï A, Greffard A, Nicolas V, Codogno P, Botti J. 2013. Autophagy modulates cell migration and β1 integrin membrane recycling. *Cell Cycle* **12**: 3317–28.

Udy GB, Towers RP, Snell RG, Wilkins RJ, Park SH, Ram P a, Waxman DJ, Davey HW. 1997. Requirement of STAT5b for sexual dimorphism of body growth rates and liver gene expression. *Proc Natl Acad Sci U S A* **94**: 7239–44.

Vagner-Capodano AM, Hartung M, Stahl A. 1987. Nucleolus, nucleolar chromosomes, and nucleolus-associated chromatin from early diplotene to dictyotene in the human oocyte. *Hum Genet* **75**: 140–6.

Vaskivuo TE, Anttonen M, Herva R, Billig H, Dorland M, te Velde ER, Stenbäck F, Heikinheimo M, Tapanainen JS. 2001. Survival of human ovarian follicles from fetal to adult life: apoptosis, apoptosis-related proteins, and transcription factor GATA-4. *J Clin Endocrinol Metab* **86**: 3421–9.

Vassart G, Pardo L, Costagliola S. 2004. A molecular dissection of the glycoprotein hormone receptors. *Trends Biochem Sci* **29**: 119–26.

Vasudevan S, Seli E, Steitz JA. 2006. Metazoan oocyte and early embryo development program: a progression through translation regulatory cascades. *Genes Dev* **20**: 138–46.

Velentzas AD, Nezis IP, Stravopodis DJ, Papassideri IS, Margaritis LH. 2007. Mechanisms of programmed cell death during oogenesis in Drosophila virilis. *Cell Tissue Res* **327**: 399–414.

Virgo BB, Bellward GD. 1974. Serum progesterone levels in the pregnant and postpartum laboratory mouse. *Endocrinology* **95**: 1486–90.

De Vries SS, Baart EB, Dekker M, Siezen A, de Rooij DG, de Boer P, te Riele H. 1999. Mouse MutS-like protein Msh5 is required for proper chromosome synapsis in male and female meiosis. *Genes Dev* **13**: 523–31.

Wagner KU, Wall RJ, St-Onge L, Gruss P, Wynshaw-Boris A, Garrett L, Li M, Furth PA, Hennighausen L. 1997. Cre-mediated gene deletion in the mammary gland. *Nucleic Acids Res* **25**: 4323–30.

Walther TC, Farese R V. 2009. The life of lipid droplets. *Biochim Biophys Acta* **1791**: 459–66.

Wang C, Liu Z, Huang X. 2012a. Rab32 is important for autophagy and lipid storage in Drosophila. *PLoS One* **7**: e32086.

Wang H, Xie H, Dey SK. 2008. Loss of cannabinoid receptor CB1 induces preterm birth. *PLoS One* **3**: e3320.

Wang RC, Wei Y, An Z, Zou Z, Xiao G, Bhagat G, White M, Reichelt J, Levine B. 2012b. Akt-mediated regulation of autophagy and tumorigenesis through Beclin 1 phosphorylation. *Science* **338**: 956–9.

Wang S, Kou Z, Jing Z, Zhang Y, Guo X, Dong M, Wilmut I, Gao S. 2010. Proteome of mouse oocytes at different developmental stages. *Proc Natl Acad Sci U S A* **107**: 17639–44.

Wassarman PM, Litscher ES. 2012. Influence of the zona pellucida of the mouse egg on folliculogenesis and fertility. *Int J Dev Biol* **56**: 833–9.

Watari H, Blanchette-Mackie EJ, Dwyer NK, Glick JM, Patel S, Neufeld EB, Brady RO, Pentchev PG, Strauss JF. 1999. Niemann-Pick C1 protein: obligatory roles for N-terminal domains and lysosomal targeting in cholesterol mobilization. *Proc Natl Acad Sci U S A* **96**: 805–10.

Wei Q, Yokota C, Semenov M V, Doble B, Woodgett J, He X. 2007. R-spondin1 is a high affinity ligand for LRP6 and induces LRP6 phosphorylation and beta-catenin signaling. *J Biol Chem* **282**: 15903–11.

Weidberg H, Shvets E, Shpilka T, Shimron F, Shinder V, Elaza Z. 2010. LC3 and GATE-16/GABARAP subfamilies are both essential yet act differently in autophagosome biogenesis. *EMBO J* **29**: 1792–802.

Whitaker M. 2008. Calcium signalling in early embryos. *Philos Trans R Soc Lond B Biol Sci* **363**: 1401–18.

Winiwarter H de. 1920. Couche corticale definitive au hile de l'ovarie et pseudo-neoformation ovulaire. *Ann la Société Entomol Fr Rev d'entomologie générale appliquée* **83**: 1406–8.

Xie Z, Nair U, Klionsky DJ. 2008. Atg8 controls phagophore expansion during autophagosome formation. *Mol Biol Cell* **19**: 3290–8.

Xiong W, Chen Y, Wang H, Wang H, Wu H, Lu Q, Han D. 2008. Gas6 and the Tyro 3 receptor tyrosine kinase subfamily regulate the phagocytic function of Sertoli cells. *Reproduction* **135**: 77–87.

Xiong W, Wang H, Wu H, Chen Y, Han D. 2009. Apoptotic spermatogenic cells can be energy sources for Sertoli cells. *Reproduction* **137**: 469–79.

Xu Y, Her C. 2013. VBP1 facilitates proteasome and autophagy-mediated degradation of MutS homologue hMSH4. *FASEB J* **27**: 4799–810.

Xu Y-N, Shen X-H, Lee S-E, Kwon J-S, Kim D-J, Heo Y-T, Cui X-S, Kim N-H. 2012. Autophagy influences maternal mRNA degradation and apoptosis in porcine parthenotes developing in vitro. *J Reprod Dev* **58**: 576–84.

Yamaji M, Seki Y, Kurimoto K, Yabuta Y, Yuasa M, Shigeta M, Yamanaka K, Ohinata Y, Saitou M. 2008. Critical function of Prdm14 for the establishment of the germ cell lineage in mice. *Nat Genet* **40**: 1016–22.

Yamashita Y, Shimada M. 2012. The release of EGF domain from EGF-like factors by a specific cleavage enzyme activates the EGFR-MAPK3/1 pathway in both granulosa cells and cumulus cells during the ovulation process. *J Reprod Dev* **58**: 510–4.

Yan C, Wang P, DeMayo J, DeMayo FJ, Elvin JA, Carino C, Prasad S V, Skinner SS, Dunbar BS, Dube JL, et al. 2001. Synergistic roles of bone morphogenetic protein 15 and growth differentiation factor 9 in ovarian function. *Mol Endocrinol* **15**: 854–66.

Yang T, Espenshade PJ, Wright ME, Yabe D, Gong Y, Aebersold R, Goldstein JL, Brown MS. 2002. Crucial step in cholesterol homeostasis: sterols promote binding of SCAP to INSIG-1, a membrane protein that facilitates retention of SREBPs in ER. *Cell* **110**: 489–500.

Yang Y, Hu L, Zheng H, Mao C, Hu W, Xiong K, Wang F, Liu C. 2013. Application and interpretation of current autophagy inhibitors and activators. *Acta Pharmacol Sin* **34**: 625–35.

Yao P-L, Lin Y-C, Sawhney P, Richburg JH. 2007. Transcriptional regulation of FasL expression and participation of sTNF-alpha in response to sertoli cell injury. *J Biol Chem* **282**: 5420–31.

Yefimova MG, Messaddeq N, Harnois T, Meunier A-C, Clarhaut J, Noblanc A, Weickert J-L, Cantereau A, Philippe M, Bourmeyster N, et al. 2013. A chimerical phagocytosis model reveals the recruitment by Sertoli cells of autophagy for the degradation of ingested illegitimate substrates. *Autophagy* **9**: 653–66.

Yen W-L, Shintani T, Nair U, Cao Y, Richardson BC, Li Z, Hughson FM, Baba M, Klionsky DJ. 2010. The conserved oligomeric Golgi complex is involved in double-membrane vesicle formation during autophagy. *J Cell Biol* **188**: 101–14.

Yi Y-C, Chen M-J, Ho JY-P, Guu H-F, Ho ES-C. 2007. Mitochondria transfer can enhance the murine embryo development. *J Assist Reprod Genet* **24**: 445–9.

Yoshida H, Takakura N, Kataoka H, Kunisada T, Okamura H, Nishikawa SI. 1997. Stepwise requirement of c-kit tyrosine kinase in mouse ovarian follicle development. *Dev Biol* **184**: 122–37.

Yoshida K, Kondoh G, Matsuda Y, Habu T, Nishimune Y, Morita T. 1998. The mouse RecA-like gene Dmc1 is required for homologous chromosome synapsis during meiosis. *Mol Cell* **1**: 707–18.

Yoshida S, Sukeno M, Nakagawa T, Ohbo K, Nagamatsu G, Suda T, Nabeshima Y. 2006. The first round of mouse spermatogenesis is a distinctive program that lacks the self-renewing spermatogonia stage. *Development* **133**: 1495–505.

Youle RJ, Narendra DP. 2011. Mechanisms of mitophagy. *Nat Rev Mol Cell Biol* **12**: 9–14.

Young ARJ, Narita M, Ferreira M, Kirschner K, Sadaie M, Darot JFJ, Tavaré S, Arakawa S, Shimizu S, Watt FM, et al. 2009. Autophagy mediates the mitotic senescence transition. *Genes Dev* **23**: 798–803.

Young JM, McNeilly AS. 2010. Theca: the forgotten cell of the ovarian follicle. *Reproduction* **140**: 489–504.

Yu YS, Sui HS, Han Z Bin, Li W, Luo MJ, Tan JH. 2004. Apoptosis in granulosa cells during follicular atresia: relationship with steroids and insulin-like growth factors. *Cell Res* **14**: 341–6.

Yue Z, Jin S, Yang C, Levine AJ, Heintz N. 2003. Beclin 1, an autophagy gene essential for early embryonic development, is a haploinsufficient tumor suppressor. *Proc Natl Acad Sci U S A* **100**: 15077–82.

Zarnescu O. 2004. Ultrastructural observations of previtellogenic ovarian follicles of dove. *Zygote* **12**: 285–92.

Zeng X, Overmeyer JH, Maltese W a. 2006. Functional specificity of the mammalian Beclin-Vps34 PI 3-kinase complex in macroautophagy versus endocytosis and lysosomal enzyme trafficking. *J Cell Sci* **119**: 259–70.

Zhang FP, Poutanen M, Wilbertz J, Huhtaniemi I. 2001. Normal prenatal but arrested postnatal sexual development of luteinizing hormone receptor knockout (LuRKO) mice. *Mol Endocrinol* **15**: 172–83.

Zhang Y, Goldman S, Baerga R, Zhao Y, Komatsu M, Jin S. 2009. Adipose-specific deletion of autophagy-related gene 7 (atg7) in mice reveals a role in adipogenesis. *Proc Natl Acad Sci U S A* **106**: 19860–5.

Zhang Y, Wang F, Han L, Wu Y, Li S, Yang X, Wang Y, Ren F, Zhai Y, Wang D, et al. 2011. GABARAPL1 negatively regulates Wnt/β-catenin signaling by mediating Dvl2 degradation through the autophagy pathway. *Cell Physiol Biochem* **27**: 503–12.

Zhou Q, Li H, Xue D. 2011a. Elimination of paternal mitochondria through the lysosomal degradation pathway in C. elegans. *Cell Res* **21**: 1662–9.

Zhou W, Wang G, Small CL, Liu Z, Weng CC, Yang L, Griswold MD, Meistrich ML. 2011b. Gene expression alterations by conditional knockout of androgen receptor in adult Sertoli cells of Utp14b jsd/jsd (jsd) mice. *Biol Reprod* **84**: 400–8.

Zhu BT, Conney AH. 1998. Functional role of estrogen metabolism in target cells: review and perspectives. *Carcinogenesis* **19**: 1–27.

Zhu J-H, Horbinski C, Guo F, Watkins S, Uchiyama Y, Chu CT. 2007. Regulation of autophagy by extracellular signal-regulated protein kinases during 1-methyl-4-phenylpyridinium-induced cell death. *Am J Pathol* **170**: 75–86.

Van Zutphen T, Todde V, de Boer R, Kreim M, Hofbauer HF, Wolinski H, Veenhuis M, van der Klei IJ, Kohlwein SD. 2014. Lipid droplet autophagy in the yeast Saccharomyces cerevisiae. *Mol Biol Cell* **25**: 290–301.

Vita

Thomas Raymond Gawriluk

Education

2006 B.S. in Honors Biology at the University of Illinois at Urbana-Champaign
2007 Began graduate school in Genetics at Texas A&M University
2008 Transferred to Biology at the University of Kentucky
2013 Frontiers in Reproduction at Marine Biological Laboratory, Woods Hole, MA

Scholastic Honors

2012 Gertrude Flora Ribble Fellowship
2010 Preparing Future Faculty Certificate
2009 President of the Biology Graduate Student Association

Publications

Peer Refereed

1. Hale A. N., Ledbetter D. J., **Gawriluk T. R.**, Rucker III E. B. Autophagy: Regulation and Role in Development. Autophagy 9:7 951-72, 2013.

2. D.J. Klinonsky, … **T. R. Gawriluk** … and B. Zuckerbraun (1042 authors), Guidelines for the use and interpretation of assays for monitoring autophagy. Autophagy 8:4, 1-100, 2012.

3. **Gawriluk T. R.**, Hale A. N., Flaws J. A., Dillon C. P., Green D. R., and Rucker III E. B. Autophagy is a cell survival program for female germ cells in the murine ovary. Reproduction 141:759-765, 2011.

4. M. A. Renshaw, **T. R. Gawriluk** and J. R. Gold. *Characterization of red drum (Sciaenops ocellatus) microsatellite markers in spotted sea trout*. North American Aquaculture 71:374-379, 2009.

BOOK CHAPTERS

1. Rucker E. B., Hale A. N., **Gawriluk T. R.,** Ledbetter D. J. Altering autophagy: mouse models of human disease. <u>Autophagy – A Double-Edged Sword – Cell Survival or Death?</u> ISBN 978-953-51-1062-0.